| 1. Report No. | 2. Government Accession No. | 3. Recipient's Catalog No. |
|---|---|---|
| 4. Title and Subtitle<br>Vehicular Traffic Flow Theory and Tunnel Traffic Flow Measurements | | 5. Report Date<br>June, 1971<br>6. Performing Organization Code<br>TEC |
| 7. Author(s) G. Chin, L. Jordan, D. Kahn, S. Morin, P. Yoh | | 8. Performing Organization Report No.<br>DOT-TSC-71-7 |
| 9. Performing Organization Name and Address<br>Transportation Systems Center<br>55 Broadway<br>Cambridge, Mass. 02142 | | 10. Work Unit No.<br>OS-12<br>11. Contract or Grant No.<br>13. Type of Report and Period Covered<br>Technical Report |
| 12. Sponsoring Agency Name and Address<br>Office of the Secretary<br>U.S. Department of Transportation<br>Washington, D.C. | | 14. Sponsoring Agency Code<br>R1070 |

15. Supplementary Notes Traffic flow measurements taken with the cooperation of the Massachusetts Turnpike Authority, Tunnel Division.

16. Abstract

Vehicular traffic flow has been investigated theoretically and experimentally in order that peak hour collective traffic flow dynamics be understood and that the peak hour flow through the Callahan Tunnel be improved by means of traffic flow control and modification. Two theoretical models are suggested, the finite reaction time model and the asymmetrical response model, as predictive of observed traffic density dynamics, wave growth and asymmetry. Experimentally, a traffic flow profile of capacities, vehicle speeds and traffic densities in the Callahan Tunnel has been obtained, and relationships between slowdown wave phenomena and traffic flow, determined. Based on these, it is suggested that traffic flow may be improved with traffic flow modification procedures.

17. Key Words
- Traffic Flow
- Tunnel Traffic
- Congestion
- Airport Access

18. Distribution Statement
Unclassified-Unlimited

| 19. Security Classif. (of this report) | 20. Security Classif. (of this page) | 21. No. of Pages | 22. Price |
|---|---|---|---|
| Unclassified | Unclassified | 221 | |

## TABLE OF CONTENTS

## TABLE OF CONTENTS (Cont.)

## PREFACE

The different traffic handling capabilities of seemingly similar roadways has puzzled road designers and traffic planners. Why are some roads able to carry 2000 vehicles per hour per lane while other similar roads, can carry considerably less? Why does traffic run relatively smoothly over certain roads while on others it is largely of a stop and go type? The answers to such questions could help in finding ways to alleviate some of the existing traffic jams. An understanding of what causes the roadway to have low flow rates may lead to improvements of existing roadways and to better designs for future roadways.

This report presents a discussion of some of the short term solutions to the general problem of traffic congestion. It is certainly true that a complete solution to the traffic congestion problem must involve some sort of reorientation from the private vehicle mode to public transportation. Possibilities range from an automatic guideway system with its several-fold increase in roadway capacity; to a traffic network plan with traffic responsive go-no-go indicators or to a mixed-modal route structure which is a function of such things as trip purpose, trip length, and population density. That a fully satisfactory solution to the future and even present situation requires such a comprehensive study is evident, however, it is also evident that many of the immediate problems are not going to wait until such studies are implemented. Since an understanding of roadway capacity can help to bring improvements now, these short term solutions to traffic congestion which can be obtained and implemented now, must not be disregarded because they do not solve the problem completely.

In this report, which covers the work and results obtained by the Modeling and Analysis Group of the Transportation Systems Center during the five month period from August 1970 to December 1970, the development of a theory which accounts for driver re-

action response within the framework of continuum theory is outlined. This theory is based on a suggestion from R. Foote of the Port Authority of New York, that the strength of the driver's response is likely to be different in an accelerating maneuver than it is in a decelerating maneuver and that therefore, more than just one flow and speed concentration curve exists. Roadway capacity then becomes a rather strong function of the quantity of acceleration maneuvers likely to occur (whether these maneuvers are due to road design or to prevailing traffic conditions).

Another theory within the continuum model is also developed to account for the finite reaction time of drivers. A flow or speed concentration relationship becomes meaningful only when the finite time of propagation of information is included. The implications of these *retarded solutions* for roadway capacity are the occurrence of growing waves whenever the concentration reaches a critical value. Since driver reaction times are functions of traffic conditions as well as road design and road peripherals, the occurrence of growing waves and the resultant traffic stoppages will be influenced by road design and density control procedures.

While experiments specifically designed to test the theories would have been preferable (say, by the use of specifically designed test tracks), this was not possible in this project. Instead, experiments were made on traffic flow in tunnels. Data was taken on traffic in one lane of the Callahan Tunnel in Boston, Massachusetts, and in addition, some data taken by the Port Authority of New York personnel of the Holland Tunnel was used.

Actually, there were two purposes in taking the tunnel data. The first was the opportunity the tunnel affords for interpretation and understanding of the basic process of traffic dynamics. This is so because of the nearly controlled conditions that exist inside the tunnel system where lane changing is minimal so that a single lane of traffic under various density conditions can be observed to yield relationships between traffic density, speed,

flow and wave phenomena. The knowledge of such relationships is important to the understanding of roadway capacity and the factors which tend to reduce such capacity, and affords a partial verification of the theories.

The second purpose is that the tunnel roadway is an airport access route (to Boston's Logan International Airport) whose optimal utilization is of interest to the U. S. Department of Transportation. By taking data of traffic flow and concentration, any naturally occurring bottlenecks which impede tunnel throughput could be found and a recommendation of a density control system for increasing the throughput could be made. In this latter effort, however, only partial success was obtained due to the short five-month span of the study and the detailed traffic control system recommendation must be deferred to a later date (when the study is resumed).

## LIST OF ILLUSTRATIONS

## LIST OF ILLUSTRATIONS (Continued)

## LIST OF ILLUSTRATIONS (Continued)

## LIST OF ILLUSTRATIONS (Continued)

## LIST OF ILLUSTRATIONS (Continued)

## LIST OF ILLUSTRATIONS (Continued)

## LIST OF ILLUSTRATIONS (Continued)

## LIST OF ILLUSTRATIONS (Continued)

## LIST OF ILLUSTRATIONS (Continued)

## LIST OF ILLUSTRATIONS (Continued)

## LIST OF ILLUSTRATIONS (Continued)

## LIST OF ILLUSTRATIONS (Continued)

## LIST OF ILLUSTRATIONS (Continued)

## LIST OF ILLUSTRATIONS (Continued)



## TABLES

# SECTION 1
# INTRODUCTION

## 1.1 THEORY

Theoretical work in traffic flow dynamics has generally taken one of three approaches, a deterministic continuum approach, a statistical kinetic theory approach and a car-following theory approach (refs. 1 through 16). Each of these approaches has its advocates and each has its own range of applicability. For example, the continuum approach cannot be expected to yield a valid description of *rarefied* traffic flow. In a continuum, a well defined density function is assumed to exist and vehicle displacements and densities are considered collectively, rather than individually. Where independent individual vehicle manuevers predominate, the concept of a continuum is meaningless. When, however, as in dense traffic flow, collective interactions predominate, and the distance over which individual vehicles influence each other is small compared with the distance over which traffic densities and flows are described, the continuum theory becomes a potentially useful approach.

The statistical distribution function or Boltzmann equation method should also be applicable to the dense traffic situation. It should also be applicable to light traffic conditions since a velocity distribution function rather than average macroscopic quantities are described by the method. That is, the Boltzmann equation describes the space and time evolutions of the distribution function itself, giving the law for the change of the distribution function due to individual vehicle interactions. In fact, the Boltzmann equation approach does seem to describe light traffic conditions adequately. However, somewhat surprisingly the method, at least to date, does not seem appropriate for a dense traffic description. This is in contrast to the situation in the classical application of the Boltzmann equation to the kinetic theory of gases where the continuum or dense case (dense in the sense that we have been using the term) is well described, being just

the zero order approximation solution of the Boltzmann equation. This comes about quite naturally: The Boltzmann equation describes the non-steady state, and the zero order approximation is just the steady state solution where collisions between molecules do not alter the distribution function. The form of this collision term is obtained by recourse to physical laws of molecular interaction (e.g., the force between molecules depends only on their mutual separation) and then it is found that this interaction term contributes nothing to the space and time evolution of the distribution function when this distribution is of a particular form (Maxwellian or Equilibrium). That is, collisions do not change this particular distribution function. Entropy considerations then show that in fact such a distribution is approached in the gas. The space and time dependence of this distribution is determined solely by the space and time dependence of those macroscopic quantities which are conserved in elastic collisions between molecules (number, momentum and energy); thus the *natural* appropriateness of the Boltzmann equation for a correct description of continuum gas dynamics.

In the vehicular traffic problem, however, the form for the interaction term is difficult to obtain as no well defined physical mutual interaction law between vehicles has been established. Without this there is no counterpart for the Maxwellian or Equilibrium distribution function for traffic flow and hence no means for obtaining a collective flow or continuum solution of traffic flow from the Boltzmann equation. However, since the Boltzmann approach inherently <u>is</u> capable of yielding such continuum solutions, further effort in this area is probably worthwhile.

Finally, the car-following theories have been used extensively and successfully in describing the acceleration response of interacting vehicles. The acceleration response is generally a function of the relative velocity and distance of the interacting vehicles. Stability criteria between vehicles have also been established. However, the car-following theories are limited

in that they are true microscopic theories dealing with individual vehicles, and therefore unable to predict such well known and important observed collective behavior as the propagation of travelling waves of constant flow and constant density. As these phenomena often have profound effects on traffic movement, their absence in the car-following theories constitutes a serious limitation. On the other hand, it should be noted that the use of car-following theories together with the continuum approach, particularly as a taking off point for the continuum theory, has proven particularly useful.

The two approaches outlined in this report have their origin in car-following theory. This theoretical work is reported in Section 2.

## 1.2 EXPERIMENT

Experimental work in traffic flow has covered a wide range of objectives, from two car piano wire tests designed to establish a car following law, to aerial photography of multi-lane freeways and arterial networks to determine overall traffic patterns and relationships; from intensive studies on simple roadways to extensive work on complex road systems (refs. 17 through 22). For an understanding of the traffic dynamics of a stream of heavy traffic flow, one of the simplest types of roadways was studied: the single lane no-passing tunnel roadway; in particular, one lane of the Callahan Tunnel in Boston, as well as one lane of the Holland Tunnel in New York. The New York data was given to us by the Port Authority of New York, while the Callahan data was obtained by observation.

In addition to this fundamental understanding of traffic flow dynamics, sufficient tunnel traffic data was sought to also allow a recommendation of a specific traffic control system for improving the tunnel throughput. However, as explained in the Preface of this report, this was not possible in the limited time allotted to the project. Nonetheless, we have obtained data which we feel is directly related to throughput improvement and these results are reported in Section 4.

With the full cooperation of the Division of Tunnels, Massachusetts Turnpike Authority, traffic flow data was taken on some 6600 vehicles in the Callahan Tunnel during the month of November (1970) on fifteen different occasions. For each run, two observation stations were established which enclosed various sections of interest within the tunnel. At each station the observers were equipped with either a Hewlett Packard strip chart recorder model number 320 or a Sanborn strip chart recorder model number 299. Electrically connected to the recorder was a device which produced different length lines on the chart paper whenever any one of four buttons was depressed; the buttons were labelled *Bus*, *Car*, *Taxi*, or *Truck*. The line markings on the chart paper

thus gave the time of arrival and departure in the section as well as vehicle identification. The vehicle identification was necessary in order that the time of entrance into the first station and the time of departure from the exit station for any particular vehicle be known. This was insured through pattern recognition performed on the two strip charts taken as a pair. While lane changing inside the tunnel is minimal, it does occur often enough that such a procedure was found to be necessary.

In addition to the four-button device, an external 60-Hertz timer was connected to the Sanborn 299 (the Hewlett Packard had its own internal 60-Hertz timer). These separate timing markers insured against improper or inconsistent chart speeds. Accurate measurements were thereby obtained for the times of entrance and exit of a particular vehicle in a given tunnel section and from these measurements we derived such quantities as flow, density, speed and transit time under both steady state conditions and during the passage of a shock wave. The experimental results are reported in Section 4.

# SECTION 2
# CONTINUUM TRAFFIC FLOW THEORY

## 2.1 INTRODUCTION

In this section, the progress which has been made in our theoretical investigations of traffic flow dynamics is outlined. The studies made deal exclusively with single-lane, no-passing traffic of the type encountered in either lane of the Callahan Tunnel.

The starting point for any macroscopic study of single-lane traffic is the continuity equation which relates the traffic concentration k (vehicles/unit length) and the traffic flow q (vehicles/unit time passing a point on the roadway). This equation is given as follows:

$$\frac{\partial}{\partial t} k(x,t) + \frac{\partial}{\partial x} q(x,t) = 0 \qquad (2.1)$$

In Eq. (2.1), k and q are functions of the time (t) and the distance (x) measured along the roadway from some arbitrary point. The function q (x,t) is defined in terms of the concentration k (x,t) and the traffic speed V (x,t) by the relation

$$q(x,t) = k(x,t)\ V(x,t) \qquad (2.2)$$

Equation (2.1) simply states that the time rate of change in the number of cars on a stretch of road is equal to the difference between the number of cars entering and the number of cars leaving that stretch of road per unit time. In order to solve Eq. (2.1) for the concentration, an equation of state relating q to k must first be postulated. For a spatially homogeneous roadway (i.e., a roadway whose physical characteristics do not change appreciably with distance x), the most general form of such an equation of state is

$$q(x,t) = q(k, k_t, k_x, k_{tt}, k_{xx}, \ldots) \qquad (2.3)$$

where the subscripts "t" and "x" denote partial differentiation with respect to time and distance, respectively. In what follows two models of the form given in Eq. (2.3) will be developed. Some quantitative results will be derived from these models, and some possibilities for future research will be suggested.

## 2.2 DRIVER RESPONSE TIME

To develop an equation of state of the type (2.3), first consider some aspects of the discrete or microscopic theory of traffic flow. Much research has been done on the car-following approach to traffic dynamics (refs. 11 through 16, and 23). This approach is based upon the experimentally observed fact that in single-lane traffic a driver's acceleration appears to be proportional to his speed relative to the driver ahead of him, after a certain delay time $\tau$ has elapsed. Quantitatively, this fact is expressed by the following differential difference equation

$$\frac{d^2 x_n(t+\tau)}{dt^2} = \lambda \left[ \frac{d\, x_{n-1}(t)}{dt} - \frac{d\, x_n(t)}{dt} \right] \tag{2.4}$$

where $x_n$ denotes the position along the roadway of the nth car. The delay time $\tau$ is the time it takes a driver to react psychologically and physiologically to an acceleration or deceleration of the car ahead of him. Typically, $\tau$ is on the order of one second. The parameter $\lambda$ appearing in Eq. (2.4) measures the strength of the driver's response to a given acceleration or deceleration of the car ahead and is generally assumed to be a function of the distance between the lead car and the following car. For example, one widely used model is based upon the assumption that $\lambda$ is inversely proportional to the driver's headway. With this assumption, Eq. (2.4) becomes

$$\frac{d^2}{dt^2} x_n(t+\tau) = \frac{C\left[\frac{d\, x_{n-1}(t)}{dt} - \frac{d\, x_n(t)}{dt}\right]}{x_{n-1}(t) - x_n(t)} \tag{2.5}$$

where C is some constant. Equation 2.5 can be integrated once to yield the following relationship:

$$V_n(t+\tau) = C \ln \left\{\left[x_{n-1}(t) - x_n(t)\right] k_j\right\} \tag{2.6}$$

where $V_n$ is the velocity of the nth car and $k_j$ is a constant identified as the jam concentration of the road (bumper to bumper traffic).

In the past, researchers have used relationships of the type given in Eq. (2.6) to suggest equations of state for use in the macroscopic approach to traffic flow. For example, if the macroscopic flow velocity $V(x,t)$ is identified with $V_n(t+\tau)$ and the concentration $k(x,t)$ with $\left[x_{n-1}(t) - x_n(t)\right]^{-1}$, Eq. (2.6) becomes

$$V(x,t) = C \ln \left[k_j/k(x,t)\right] \tag{2.7}$$

If Eq. (2.7) is now combined with Eq. (2.2), we obtain the following equation of state:

$$q(x,t) = C\, k(x,t) \ln \left[k_j/k(x,t)\right] \tag{2.8}$$

Equation (2.8) has in fact been used as a model of traffic flow by many researchers. It has been found to be quite useful in describing moderate to heavy traffic. In light traffic ($k \to 0$), this logarithmic model is of course inadequate since according to Eq. (2.7), $V \to \infty$ as $k \to 0$.

One serious objection which can be made to the derivation of Eq. (2.7) is that the driver reaction time $\tau$ was dropped in making the transition to the macroscopic formulation. To investigate the effects of this delay time upon the propagation of concentration or density waves in a stream of traffic, Eq. (2.7) is rewritten as:

$$V(x,t) = C \ln \left[k_j/k(x,t-\tau)\right] \tag{2.9}$$

Finally, combining Eqs. (2.9) and (2.2), the following equation of state is obtained:

$$q(x,t) = C\, k(x,t) \ln \left[k_j/k(x,t-\tau)\right] \tag{2.10}$$

Equation (2.10) can now be substituted into the continuity equation (2.1) to study the dynamics of concentration waves in traffic. Unfortunately, the resulting differential equation (when viewed as an equation for $k(x,t)$) is of infinite order owing to the time delay which makes $q(x,t)$ a function of both $k(x,t)$ and $k(x,t-\tau)$. To make the equation manageable while maintaining at least the qualitative effects of the time delay, instead of Eq. (2.10), an approximate equation of state obtained by expanding (2.10) in a power series in $\tau$, keeping only the first two terms is used:

$$q(x,t) = C\, k(x,t) \ln \left[k_j/k(x,t)\right] + C\, \tau \frac{\partial k(x,t)}{\partial t} \tag{2.11}$$

Substituting the approximate equation of state (2.11) into the continuity equation (2.1), the following equation of motion is obtained:

$$\frac{\partial k}{\partial t} + C \ln\left(k_j/ek\right)\frac{\partial k}{\partial x} + C\, \tau \frac{\partial^2 k}{\partial x \partial t} = 0 \tag{2.12}$$

where the k's are all evaluated at the same time t.

Before proceeding with solutions of this equation of motion, it is well to point out that this type of analysis in which the finite reaction $\tau$ is taken into account is applicable to other car-following models as well. The car-following model given by Eq. (2.5) yielded the log function given by Eq. (2.6). Other car-following models yield different functions. For example, when $\lambda$ in Eq. (2.4) is proportional to the inverse square of the driver's headway, instead of the logarithmic function given by Eq. (2.10), the following equation of state is obtained:

$$q(x,t) = k(x,t)\ U_f\left[1-k(x,t-\tau)/k_j\right] \tag{2.13}$$

(in which the velocity and concentration are linearly related). The constant $U_f$ is the free speed (the speed at zero concentration). Then, expanding in a power series in $\tau$, instead of Eq. (2.11), the following approximate equation of state is obtained:

$$\begin{aligned} q(x,t) &= k(x,t)\ U_f\left[1-k(x,t)/k_j\right] \\ &\quad + k(x,t)\ U_f\ \tau\frac{\partial k}{\partial t} \Big/ k_j \end{aligned} \tag{2.14}$$

which when substituted into the continuity equation (2.1) yields the equation of motion:

$$\frac{\partial k}{\partial t} + U_f\ \frac{\partial k}{\partial x}\left(1-2k/k_j\right) + \frac{U_f\ \tau k}{k_j}\left[\frac{\partial^2 k}{\partial x \partial t} + \frac{1}{k}\ \frac{\partial k}{\partial t}\ \frac{\partial k}{\partial x}\right] = 0 \tag{2.15}$$

as compared to the equation of motion for the log model given in Eq. (2.12). In general, with the function in Eq. (2.14) given by the inverse m power of the driver's space headway, the approximate equation of motion turns out to be:

$$\begin{aligned} &\frac{\partial k}{\partial t} + U_f\ \frac{\partial k}{\partial x}\left[1-mk^{(m-1)}/k_j^{(m-1)}\right] \\ &\quad + \frac{(m-1)U_f\ k^{(m-1)}\tau}{k_j^{(m-1)}}\left[\frac{\partial^2 k}{\partial t \partial x} + \frac{(m-1)}{k}\ \frac{\partial k}{\partial t}\ \frac{\partial k}{\partial x}\right] = 0,\ m>1 \end{aligned} \tag{2.16}$$

which is derived, as before, by expanding the equation of state in a power series in the reaction time $\tau$. This reduces to the linear case, Eq. (2.15) when m=2.

For the heavy traffic conditions of interest here, the last term in Eq. (2.16) or Eq. (2.15) can probably be neglected compared with the others. However, as only the log model will be used in this analysis, other models will not be pursued further,

it being sufficient to have shown how the finite reaction time may be used to obtain the appropriate equations of motion for other car-following models.

Returning to the equation of motion given by Eq. (2.12), we first examine the propagation of small amplitude (linear) density waves. Assume that $k(x,t)$ is given by

$$k = k_o + h_o \exp\left[i(\alpha x - \omega t)\right] \tag{2.17}$$

where $k_o$ and $h_o$ are constants and $k_o >> h_o$, ($k_o$ representing the steady state density and $h_o$ representing the amplitude of the perturbed density). Substituting Eq. (2.17) into Eq. (2.12) and ignoring terms of order $h_o^2$ and higher, we obtain the following "dispersion relation" between $\alpha$ and $\omega$:

$$-i\omega + ib\alpha + C\tau\alpha\omega = 0, \quad b = C \ln\left[k_j/ek_o\right] \tag{2.18}$$

Rewriting Eq. (2.18), we obtain

$$\omega = \frac{b\alpha - iC\tau\alpha^2 b}{1 + C^2\tau^2\alpha^2} \tag{2.19}$$

From Eq. (2.19), (using Eq. (2.17) with $\omega=\omega_1+i\omega_2$), it can immediately be concluded that density perturbations dissipate in time if $b>0$ (Im $\omega<0$) and grow in time if $b<0$ (Im $\omega>0$). We note that $b>0$ for $0<k_o<k_j/e$ and that $b<0$ for $k_j/e<k_o\leq k_j$. The parameter $k_m=k_j/e$ is in fact the density associated with maximum flow along the roadway. Equation (2.19) predicts that for $k_o>k_m$, density disturbances will grow into stoppage waves (jam concentration) as a result of finite driver reaction time. This phenomenon is familiar to most drivers. If, in a long line of traffic, one driver brakes suddenly (without actually stopping), and then speeds up again, there very often results an actual stoppage of cars further on down the line due to the fact that a driver requires a finite time to react to the actions of the car ahead of him. If he is sufficiently close to the lead car (small headway

and hence large concentration), and the lead car brakes sharply, he may during the time $\tau$ approach so close to the lead car ($k \to k_j$) that he is forced to brake to a complete stop even though the lead car did not actually stop.

To illustrate graphically how density perturbations can grow into stoppage waves, the full quasi-linear differential equation (2.12) is solved numerically as an initial value problem. Assuming that for t=0, k(x,0) is given by:

$$k(x,0) = k_o + k_1 \exp\left[-x^2/\sigma^2\right] \tag{2.20}$$

The distribution (2.20) is designed to simulate a long line of traffic of uniform density $k_o$ which contains a "hump" of peak density $k_o+k_1$ and which is approximately $2\sigma$ long. In Figures 2.1 through 2.6 we have plotted k(x,t) for t = 0, 2, 4, 6, 8, and 10, for $k_o$ = 130/mi, $k_1$ = 30/mi and $\sigma = 5C\tau$. The concentration is plotted as a function of $x/C\tau$. The jam concentration $k_j$ was 208/mi while $k_m$ was 77/mi so that $k_o > k_m$. The sequence of graphs clearly shows that the initial density perturbation centered at x=0 produces a virtual traffic stoppage upstream 10 delay time units later (k = 203/mi $\doteq k_j$ for $t = 10\tau$ and $x = -4\ C\tau$).

It must be stressed once again that Eq. (2.12) is based upon the approximate equation of state (2.11) and not upon the more exact Eq. (2.10). Nonetheless, even this approximate theory does predict the growth of density waves and the associated traffic stoppages. Further work is indicated. One possibility would be to retain another term in the series expansion in $\tau$. If this is done we obtain ($t_o\ \tau^2$):

$$q(x,t) = C\,k(x,t)\,\ln\left[k_j/k(x,t)\right] + C\,\tau\,\frac{\partial k}{\partial t} - \frac{\tau^2}{2}\,C\,\frac{\partial^2 k}{\partial t^2} \tag{2.21}$$

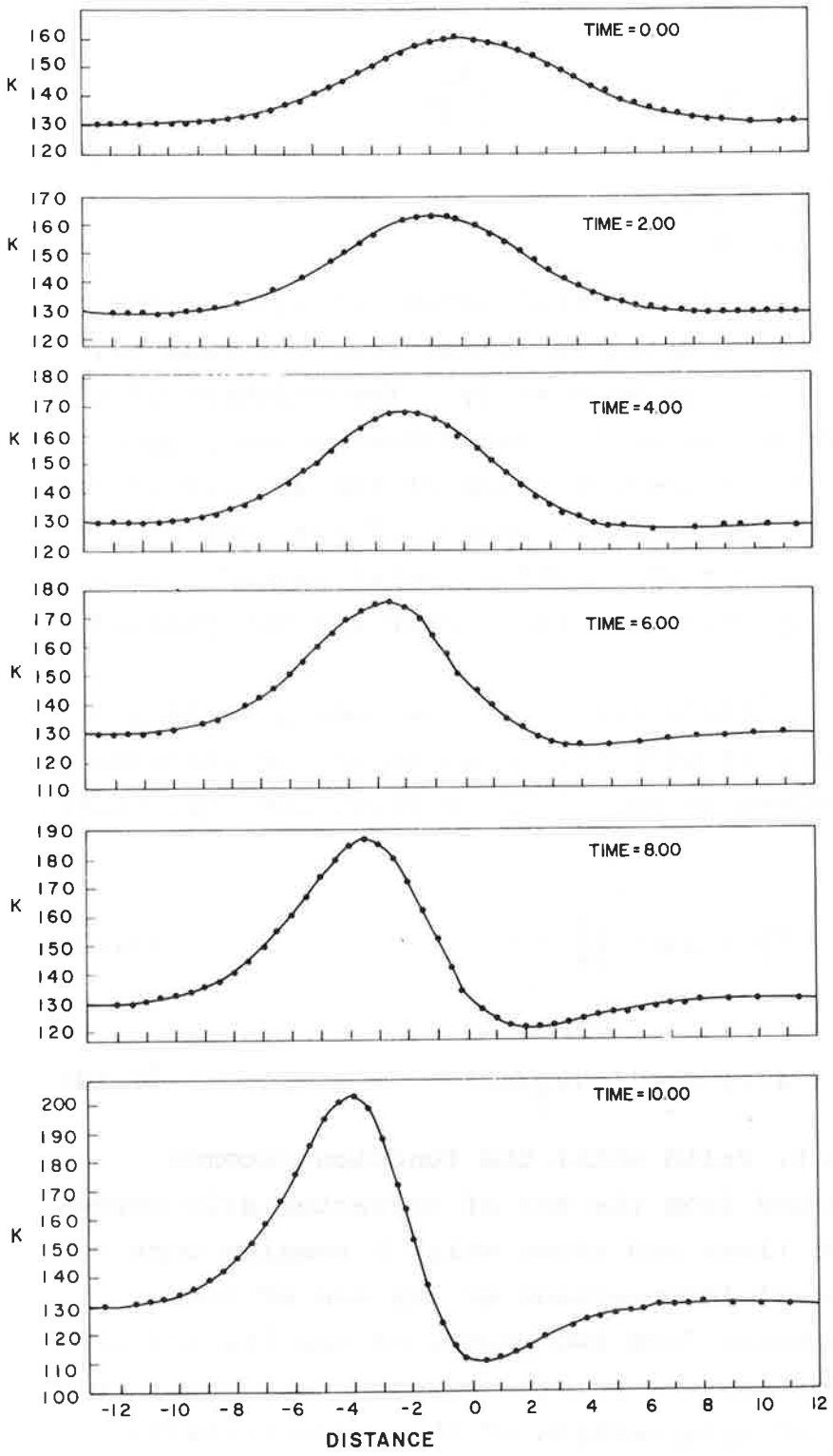


Figures 2.1. to 2.6.- The concentration $k(x,t)$ is plotted as a function of the normalized distance $x/c\tau$ for the normalized times 0, 2, 4, 6, 8 and $10\tau$ units. The average density $k_o$ = 130 vehicles/mile; the perturbation density $k_1$ = 30 vehicles/mile; the jam density $k_j$ = 208 vehicles/mile; the density at which flow is maximum $k_m$ = 77 vehicles/mile; and $\sigma = 5c\tau$

for the equation of state for high densities. The equation of motion for this case is then:

$$\frac{\partial k}{\partial t} + C\,\frac{\partial k}{\partial x}\,\ln\,(k_j/ek) + C\,\tau\,\frac{\partial^2 k}{\partial t \partial x} - \frac{C\,\tau^2}{2}\,\frac{\partial^3 k}{\partial t^2 \partial x} = 0 \tag{2.22}$$

If this is analyzed for small amplitude waves, it again shows that for $k>k_m$ the waves grow until jam conditions are reached, though at a different rate than previously. The solution of the full quasi-linear equation, as an initial value problem, however, requires, in addition to the specification of the density at t=0, the value of the initial time rate of change of the density, $(\partial k/\partial t)_{t=0}$. It was decided that solutions which depended upon $(\partial k/\partial t)$ were overly restrictive and the matter was not pursued further.

Before leaving this finite reaction time model, it is instructive to also compare it with the usual theory of instantaneous response, (equivalent to Eq. (2.12) without its last term). This may be written as

$$\frac{\partial k}{\partial t} + a(k)\,\frac{\partial k}{\partial x} = 0 \tag{2.23}$$

where

$$a(k) = C\,\ln(k_j/ek) \tag{2.24}$$

A solution of Eq. (2.23), valid until the function becomes irregular, may be obtained from the set of characteristic curves which are here straight lines and along which k remains constant. By considering the time of intersection of any two of these characteristic lines issuing from two points on the initial line t=0, and taking the limit as the points approach each other, we obtain for the time $t_o$ of intersection of the characteristic lines the equation:

$$t_o(x) = -1 \Big/ \frac{da}{dk} \cdot \frac{dk}{dx} \qquad (2.25)$$

Assuming the same initial Gaussian density distribution as given by Eq. (2.20), this becomes:

$$t_o = -\frac{\sigma^2}{2k_1 C}\left[k_o \exp(x^2/\sigma^2) + k_1\right] \Big/ x \qquad (2.26)$$

where $k_o$ (=130 vehicles/mile) is the average density, $k_1$ (=30 vehicles/mile) is the perturbed density, $\sigma$ (=5 C$\tau$) is the initial Gaussian distribution parameter and $k_j$ (=208 vehicles/mile) is the jam density.

In order to find the time at which the solution becomes irregular, that is, the time at which the shock first forms, we use the above values and find the extreme of $t_o$; the resulting equation is

$$\frac{2x^2}{25} - 1 = \frac{3}{13} \Big/ \exp(x^2/25) \qquad (2.27)$$

which has solutions $x_o = \pm 3.7601$ which are the spatial points of the initial line t=0 through which the characteristic lines first intersect. Actually, the negative solution is the physically meaningful one, and using this, we obtain for the normalized time of onset of the shock and associated density, the following values: $t_o(x_o) = 28.684$, $k = 147.042$ vehicles per mile. The point at which the shock first occurs is obtained from the general trajectory equation:

$$x_s = x_o + a(k)t \qquad (2.28)$$

which yields a value of -22.496 for this point, $x_s$. Thus, the wave traveling to the left, first becomes multi-valued at time $t_o(x_o)$=28.685 delay time units at which time it has reached the spatial point $x_s$=-22.496 C$\tau$ units upstream. This evolvement of the initial density perturbation is shown in figures 2.7 through 2.10 which graphically illustrate the formation of the dis-

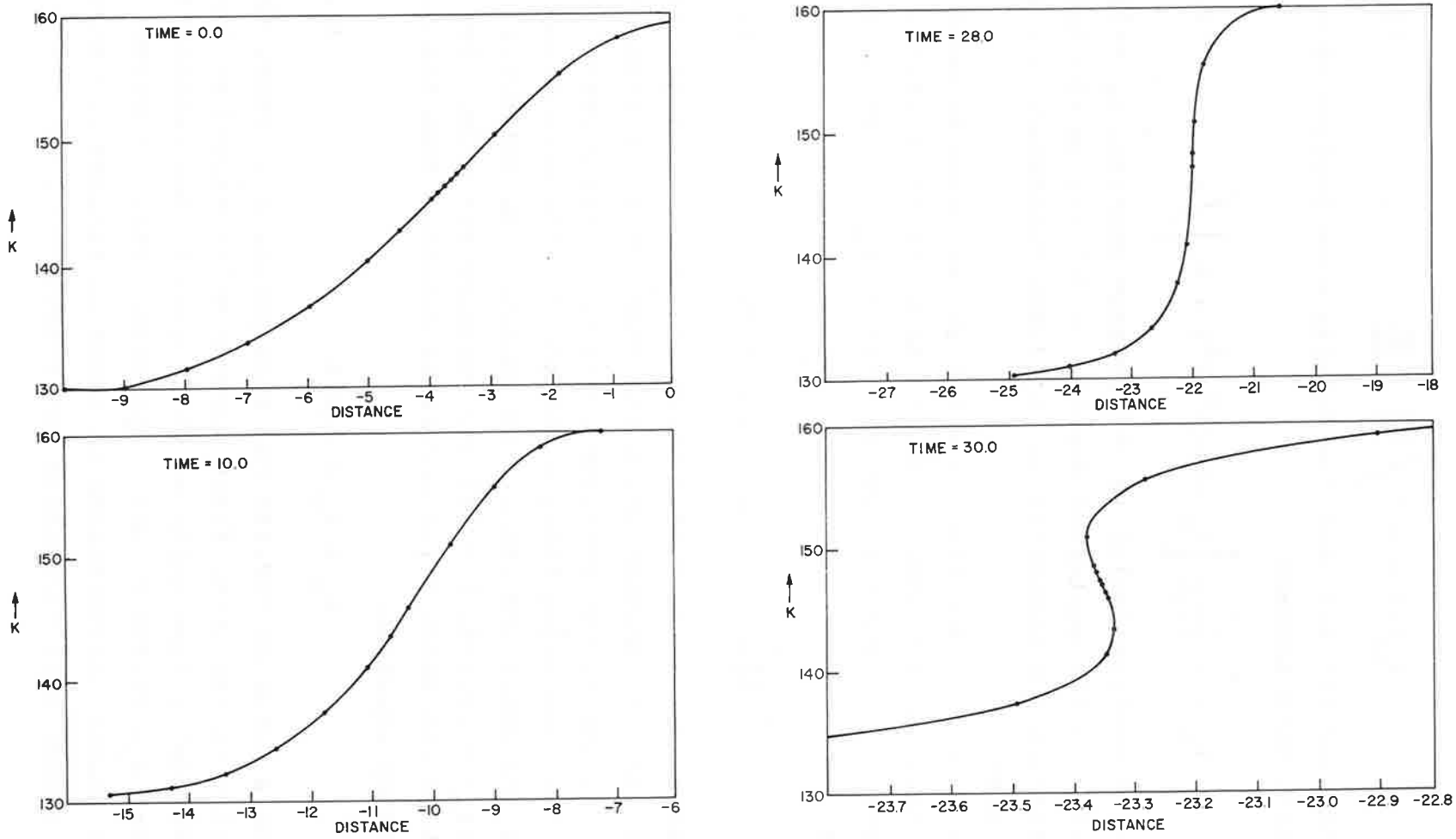


Figures 2.7. to 2.10. - The concentration k(x,t) is plotted as a function of the normalized distance x/cτ for the normalized times 0, 10, 28, and 30τ units. The numerical values of the parameters are the same as in Figures 2.1. to 2.6.

continuity and eventual multivaluedness of the function. Thus Eq. (2.23), which describes instantaneous response, predicts that an initial Gaussian density perturbation centered at x=0 will travel upstream with constant density amplitude but with an ever increasing density gradiant until the density becomes a point function and finally multivalued.

Eq. (2.12), which takes into account the finite time of reaction of response, on the other hand, predicts that the initial Gaussian perturbation centered at x=0 will grow in amplitude until jam conditions are reached. (This happens in about a third the time and in about a sixth the distance of where the shock first forms under the instantaneous theory.)

The main thrust of the finite reaction time theory then is the inevitable growth of a density perturbation in an overdense traffic situation ($k>k_m$) until a stoppage occurs and the impossibility, therefore of stable driving conditions under such traffic densities. Of course stoppages do not always occur under these conditions in real world traffic situations. This is because there is a constant readjustment of driving conditions as an initial density perturbation grows and travels upstream. That is, unlike the theory, where an initial density perturbation is allowed to take its inevitable course according to the equation of motion, in the real world situation, drivers are continuously adjusting their driving which acts to prevent the density perturbation from growing to the ultimate jam condition. They are not always successful.

## 2.3 ASYMMETRY OF DRIVER RESPONSE

The second theoretical model is an attempt to take into account the fact that a driver tends to respond more strongly to a deceleration than to an acceleration of the lead car. This phenomenon is familiar to most of us and arises simply as a result of our highly developed self-preservation instincts. To incor-

porate this asymmetry of a driver's response into a dynamic theory of traffic flow, we begin by proposing a new car-following model which is given as follows:

$$\frac{d^2x_n(t+\tau)}{dt^2} = \frac{C_1\left[\frac{dx_{n-1}(t)}{dt} - \frac{dx_n(t)}{dt}\right]}{x_{n-1}(t) - x_n(t)} \tag{2.29}$$

for $\frac{d}{dt}(X_{n-1} - x_n) > 0$ and

$$\frac{d^2x_n(t+\tau)}{dt^2} = \frac{C_2\left[\frac{dx_{n-1}(t)}{dt} - \frac{dx_n(t)}{dt}\right]}{x_{n-1}(t) - x_n(t)} \tag{2.30}$$

for $\frac{d}{dt}(x_{n-1} - x_n) < 0$

and where $C_2 > C_1$

This new model has two response constants $C_1$ and $C_2$. The response constant for decreasing headway ($C_2$) is greater than the response constant for increasing headway ($C_1$). (A similar model was suggested by Newell (refs. 3 and 24).) Following the procedure outlined in Sec. 2.2, the following macroscopic relationship between $V(x,t)$ and $k(x,t)$ (ignoring the delay time $\tau$) is obtained:

$$V = C_1 \ln(k_j/k)\left[1-\theta(\dot{k})\right] + C_2 \ln(k_j/k)\,\theta(\dot{k}) \tag{2.31}$$

where $\dot{k} = \partial k/\partial t$ and $\theta(x)$ is defined by

$$\theta(x) = \begin{cases} 0, & x<0 \\ 1, & x>0 \end{cases} \tag{2.32}$$

Combining Eqs. (2.31), (2.32), and (2.2) with the continuity equation (2.1) we obtain essentially two continuity equations which are:

$$\frac{\partial k}{\partial t} + C_1 \ln(k_j/ek)\frac{\partial k}{\partial x} = 0, \quad \dot{k}<0 \tag{2.33}$$

and

$$\frac{\partial k}{\partial t} + C_2 \ln(k_j/ek) \frac{\partial k}{\partial x} = 0, \quad \dot{k}>0 \tag{2.34}$$

Differential equations of this type, $\frac{\partial k}{\partial t} + a(k) \frac{\partial k}{\partial x} = 0$, have been extensively studied (ref. 25) and admit of implicit solutions of the following form:

$$k(x,t) = \phi\left[x-ta(k)\right] \tag{2.35}$$

where $k(x,o) = \phi(x)$ as discussed previously. Equation (2.35) represents a nonlinear wave. The speed of propagation is given by $a(k)$. Applying these results to Eqs. (2.33) and (2.34) shows that, in traffic, there are actually two wave speeds, $a_1(k)$ and $a_2(k)$, which are given by

$$a_{1,2} = C_{1,2} \ln(k_j/ek) \tag{2.36}$$

Notice that $a_2>a_1$. Consequently, a deceleration wave ($\dot{k}>0$) travels more rapidly than an acceleration wave ($\dot{k}<0$). This phenomenon has been experimentally observed by several investigators. Other consequences of this model that may be emphasized are that the velocities and flows are multivalued functions of concentration, and specifically, that

$$V_2/V_1 = q_2/q_1 = q_{2max}/q_{1max} = C_2/C_1>1 \tag{2.37}$$

where

$$q_{imax} = C_i k_j/e, \quad i = 1,2 \tag{2.38}$$

We thus see that the wave speeds, the flows, the velocities, the velocities at maximum flows and the maximum flows are all different in accelerating and decelerating traffic. Some of these phenomena have been observed in the Holland Tunnel traffic data which will be reported on in the next Section and which may help explain the apparent failure of theoretical q-k curves, in which $q = f(k)$, to adequately account for the observed flow-concentration relationship.

We feel that this two-state theory should be developed further, perhaps in conjunction with the driver reaction model, to produce more realistic models of traffic flow. One possibility would be simply to combine finite time dependence and concentration gradient dependence into one theory. For example, the velocity at time t may be written as some function of the concentration and concentration gradient at an earlier time:

$$V(x,t) = F\left[k(x,t-\tau),\ \dot{k}(x,t-\tau)\right] \qquad (2.39)$$

where the precise functional dependence on k may or may not be logarithmic, and the functional dependence on k may be continuous or it may take on only one of two values as before. We could then expand k and $\dot{k}$ in a power series in $\tau$ to obtain an approximate representation for the velocity and then proceed as before to obtain the equation of motion and its solutions.

Whether this or some other method is used, however, it is believed that the observed phenomenon of asymmetry and the existence of a finite reaction time are sufficiently important to warrant their inclusion in any realistic theory of collective traffic flow.

# SECTION 3
# ANALYSIS OF TRAFFIC FLOW DATA FROM THE HOLLAND TUNNEL IN NEW YORK CITY SHOWING A SLOWDOWN WAVE

## 3.1 INTRODUCTION

The Holland Tunnel traffic flow data which we shall discuss was made available to us by R. Foote of the Port Authority of New York.

Transducers which generated this data were pairs of photocells situated 13 feet apart at a given observer station. The data was taken in March, 1964, in the fast lane of the Holland Tunnel South Tube, at observer stations 4 and 5 which enclosed a section of roadway 483 feet long ending at the foot of the upgrade. Figure 3.1, from articles by Foote and Crowley (refs. 26 and 27), shows a layout of the Holland Tunnel and the locations of stations 4 and 5. From the raw data consisting of the arrival and departure times of each vehicle at the two fixed points monitored by the pair of photocells, various parameters of the traffic flow were computed by the Port Authority of New York. These are the time and space headways, the velocity at a given station, the acceleration, the density associated with a vehicle, and the flow. (The procedure for obtaining these parameters is described in Ref. 28.) This data is analyzed below.

## 3.2 ARRIVAL TIME AND SPACE-TIME GRAPHS

At 4502 seconds (or 1 1/4 hr.) after the beginning of the recording of this set of data a slowdown (or stoppage) wave appears to have arrived at station 5; the following and all subsequent analyses will largely be confined to this portion of the data. Figure 3.2 shows for this period a plot of the arrival time of a vehicle at stations 4 and 5 versus the vehicle number. The graph shows a discrete curve for the upstream observer at station 4 and a similar curve displaced in time for the downstream observer at station 5. The horizontal separation of the curves is

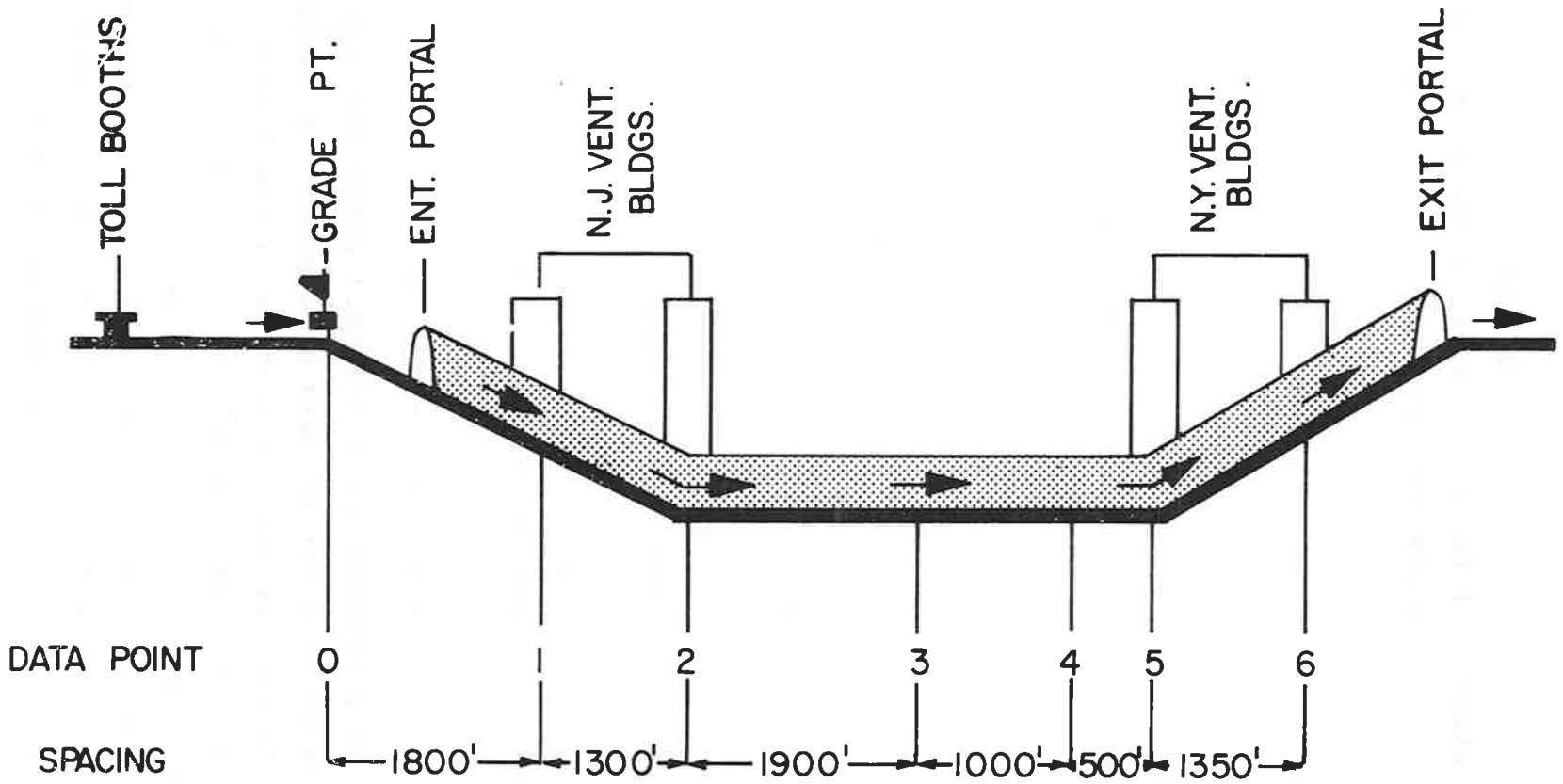


Figure 3.1.- Location of data points. Holland Tunnel-South Tube. (From Foote and Crowley, "Developing density controls for improved traffic operations" New York Port Authority, Report TBR 4-65, August 1965.)

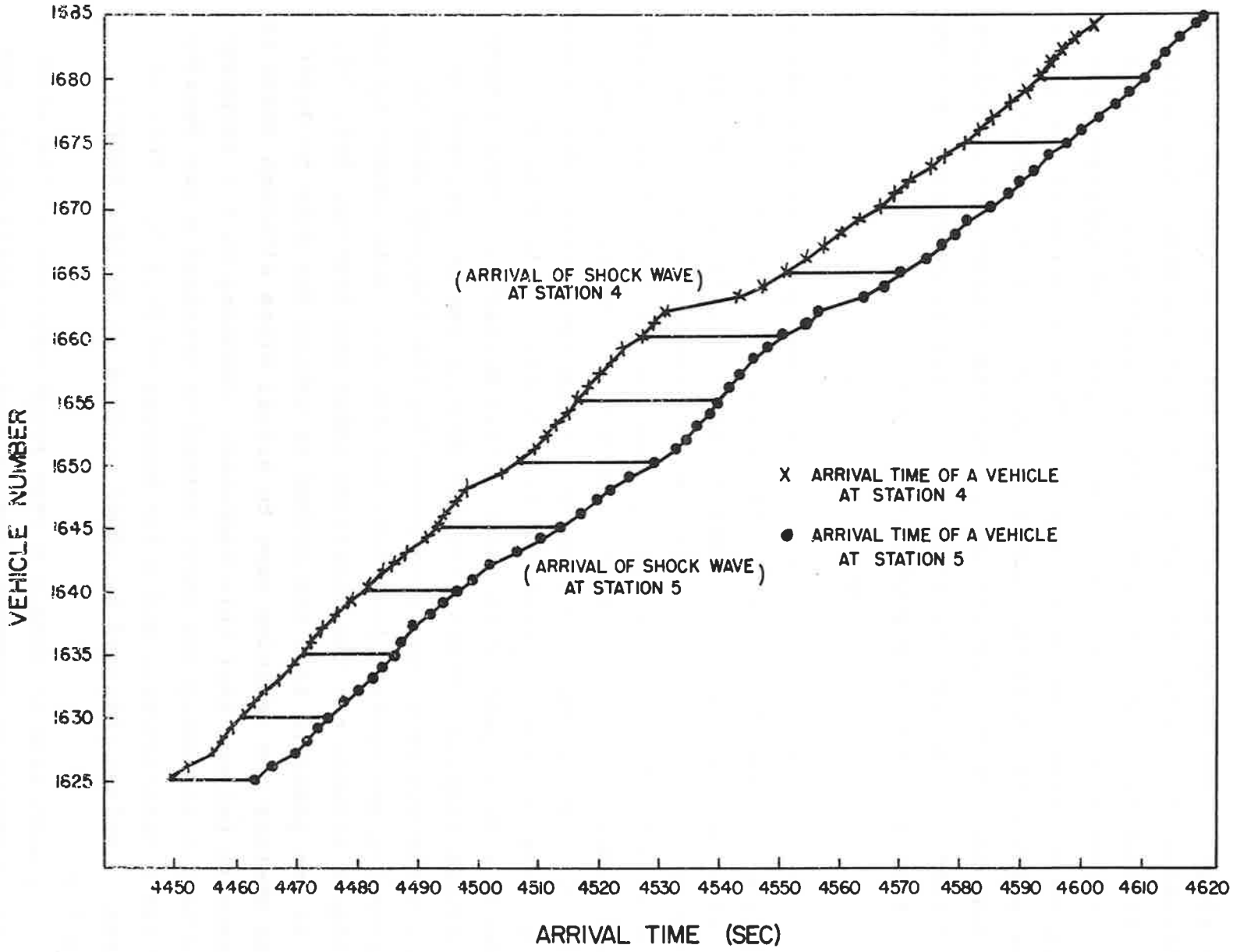


Figure 3.2.- Arrival times of vehicles at stations 4 and 5 vs vehicle number.

indicative of the transit time experienced by individual drivers; the slope of the curves indicates the vehicular flow rates at the observation stations. If horizontal lines are drawn connecting the arrival times of vehicles at the two stations (as shown in the figure) then at any given time the number of intersections that these lines make with a vertical line position at the given time point will yield the number of vehicles in the section of roadway between the two stations. The time headway of a vehicle is defined as the time of arrival of a vehicle at a station minus the arrival time of the preceding vehicle.

$$HWT_i = T_i - T_{i-1} \qquad (3.1)$$

Inspection of Figure 3.2 shows that the time headways at station 5 increased sharply beginning with vehicle number 1643. Since the slope of the curve is proportional to the flow, we see that a wave of attenuated flow (lower slope) reached station 5 at around 4504 seconds. This is followed by a period of relatively lower flow. A similar attenuation of flow occurred later at station 4, at around 4533 seconds. It is conjectured that a wave of attenuated flow has traveled from stations 5 to 4 in 29 seconds with a speed of 16 ft/sec (11.4 miles/hr). When a wave of actual stoppage occurs, the jam density can be computed by taking the number of vehicles passed by the stoppage wave in traversing two spatial locations and dividing this number by the distance between the two locations (Edie and Baverez, Ref. 29). It is not possible from the method of taking the data to determine whether the vehicles came to actual stops although there is reason to believe that this happened. Assuming that a stoppage did happen and using the above method we obtained a jam density of 218.6 vehicles/mile and a jam headway of 24.2 ft. This is close to values obtained by other studies on Holland Tunnel traffic.

We wish also to obtain a very rough estimate of the width of the slowdown or stoppage density wave. We shall assume the

wave to have a uniform, time invariant width w and a jam density $k_j$. Outside the spatial interval where the density is $k_j$ let the density have a spatially uniform value k. Consider the stoppage wave to be entirely inside the section between locations 4 and 5. Then

$$k_j w + k(D-w) = N \qquad (3.2)$$

where $k_j w$ is the number of vehicles in the portion of the roadway occupied by the stoppage wave and k(D-w) is the number of vehicles in the remaining portion, and N is the total number of vehicles in the roadway. From the procedure described in the preceding paragraph we obtain a jam density $k_j$ = 0.0414 veh/ft; the average density k = 0.0135 veh/ft, and the distance D between locations 4 and 5 is 483 feet. From the data we have also N = 11. Then using the above equation we obtain a stoppage wave width of 161.3 ft. (one third the length of the section) within which are 6.7 vehicles. While this shock wave width calculation is a rough estimate since the actual wave is not uniform in space and also may change in time, it does give a good indication of the severity of the shock wave causing degradation of the flow in the tunnel.

Another way of plotting the data is given in Figure 3.3 where the arrival time of vehicles at stations 4 and 5 are displayed in a space time diagram. Connecting lines are drawn between the space-time points of each vehicle at locations 4 and 5 -- the slope of these lines then gives the average speed of the vehicle in travelling between 4 and 5. The number of vehicles in the section between the two stations can be determined graphically at any time by drawing a vertical straight line through the time point and counting the number of intersections that the connecting lines make with this vertical line. Traffic slowdown shows up in this type of diagram in the slopes becoming less steep. This is observed beginning approximately with car number 1643 at 4504 seconds and continues until approximately 4535 seconds when the

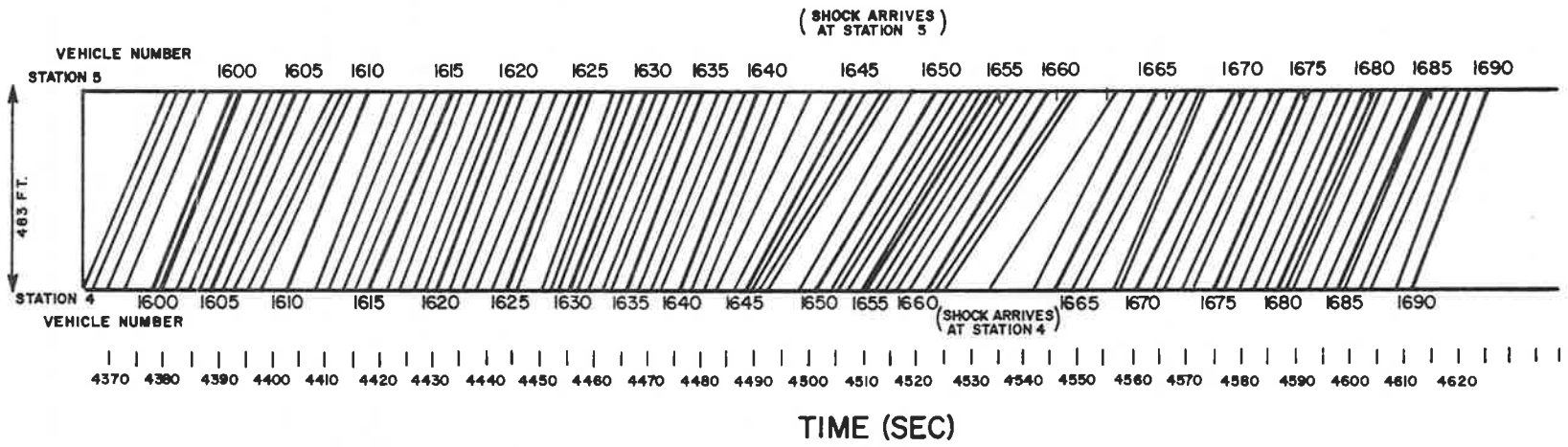


Figure 3.3.- Space vs time diagram of vehicles passing through stations 4 and 5.

slopes increase again to their normal values following the passage of the shock wave. Either type of graph, Figure 3.2 or Figure 3.3, then, can be used for analysis of the slowdown. If, in addition, the stretch of roadway were monitored by a number of observers, the actual trajectory of the shock wave could be traced in the flattening of the slope of the connecting lines.

## 3.3 TIME AND SPACE HEADWAYS

In Figure 3.4a and 3.4b are shown the vehicular flow, defined as 1/time headway, versus time at stations 5 and 4. This presentation shows the onset of attenuated flow but, as expected with individual vehicles, there is considerable scatter. Similar scatter appears in the vehicular density data. In order to obtain smooth curves, running averages were taken over groups of 5 vehicles for the various traffic parameters. The average value versus the time of passage of the middle vehicle in the group of five is plotted. In Figures 3.5, 3.6, and 3.7 are shown running averages of vehicular density, speed and flow versus time.

The average density plotted in Figure 3.5 is given by the equation

$$\bar{k} = 5280 \Big/ \left( \sum_{i=1}^{N} (HWT)_i \Big/ N \right) \tag{3.3}$$

where the space headway in feet is

$$(HWF)_i = (HWT)_i \, V_i \tag{3.4}$$

$HWT_i$ is the time headway in seconds and $V_i$ is the speed of the $i^{th}$ vehicle in feet per second. N is 5, the number of vehicles in the group. $\bar{k}$ is given in number of vehicles per mile (5280 being the conversion factor).

The vehicular space mean speed in Figure 3.6 is given by the equation

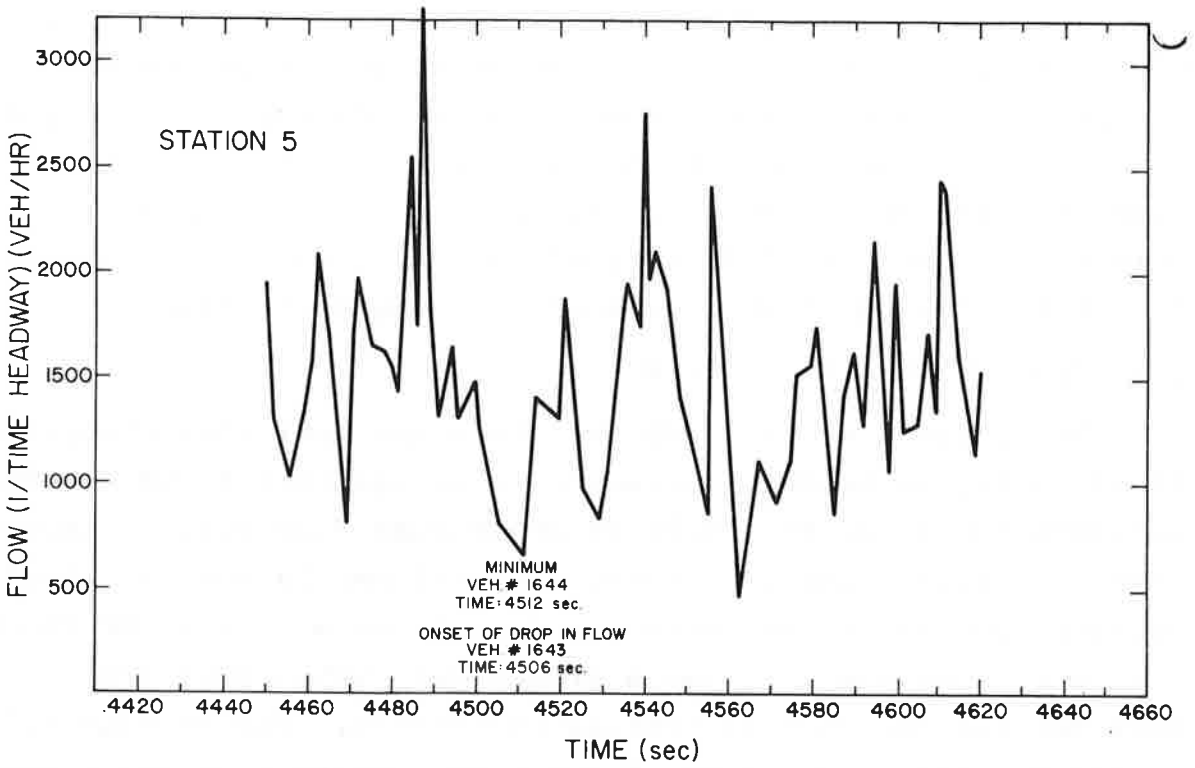


Figure 3.4a.- Vehicular flow (1/time headway) vs time. Station 5

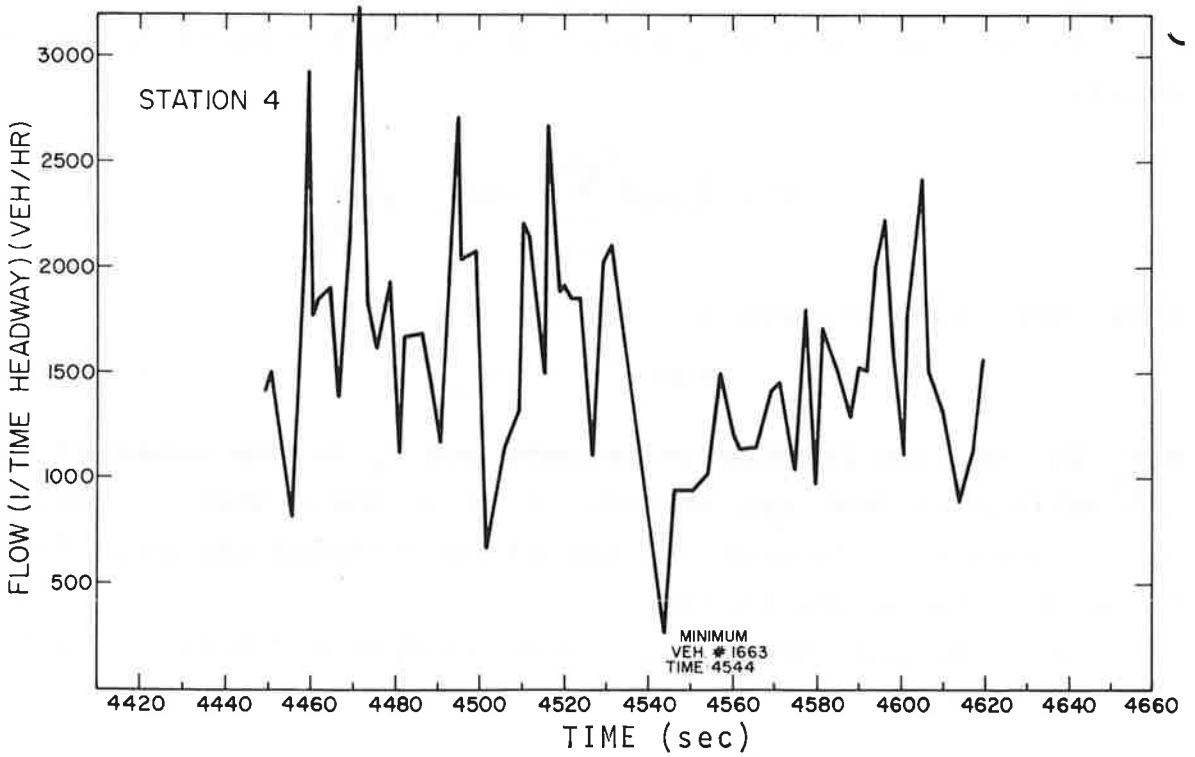


Figure 3.4b.- Vehicular flow (1/time headway) vs time. Station 4

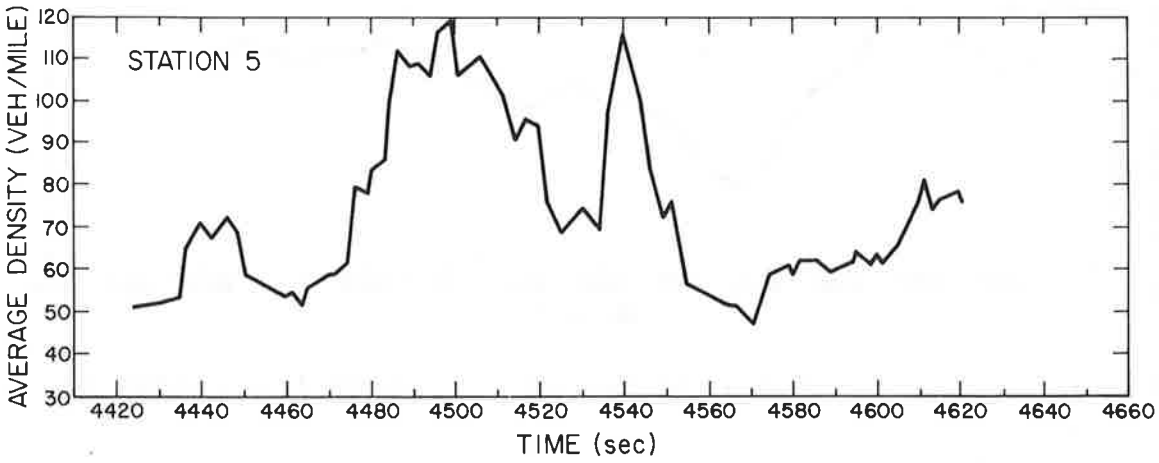


Figure 3.5a.- Average vehicular density vs time. Station 5.

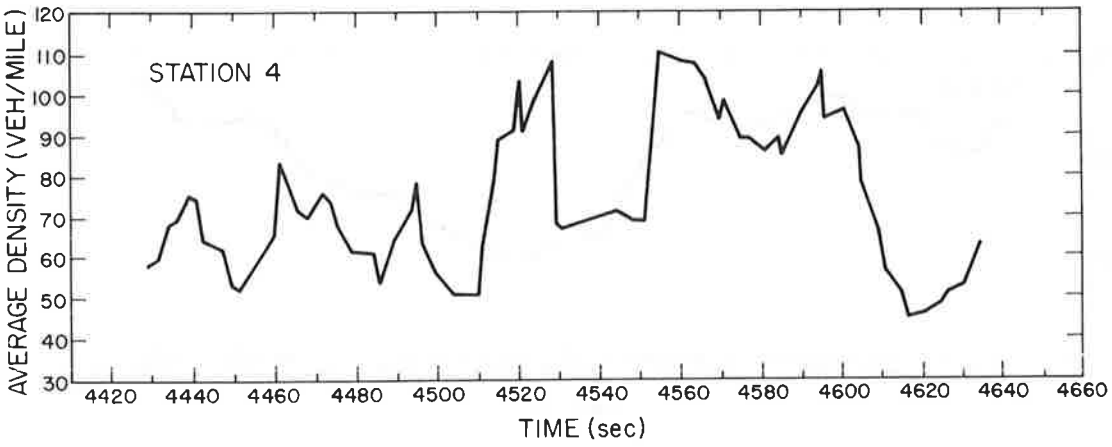


Figure 3.5b.- Average vehicular density vs time. Station 4.

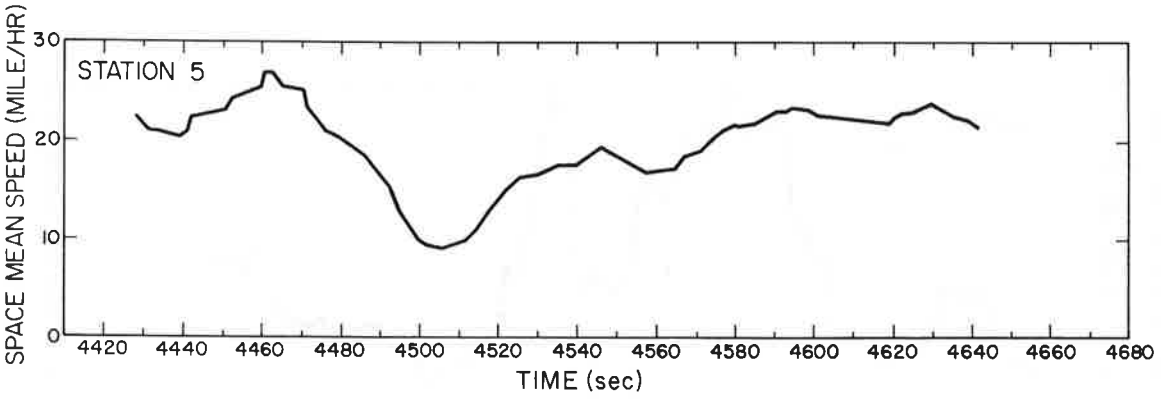


Figure 3.6a.- Vehicular space mean speed vs time. Station 5.

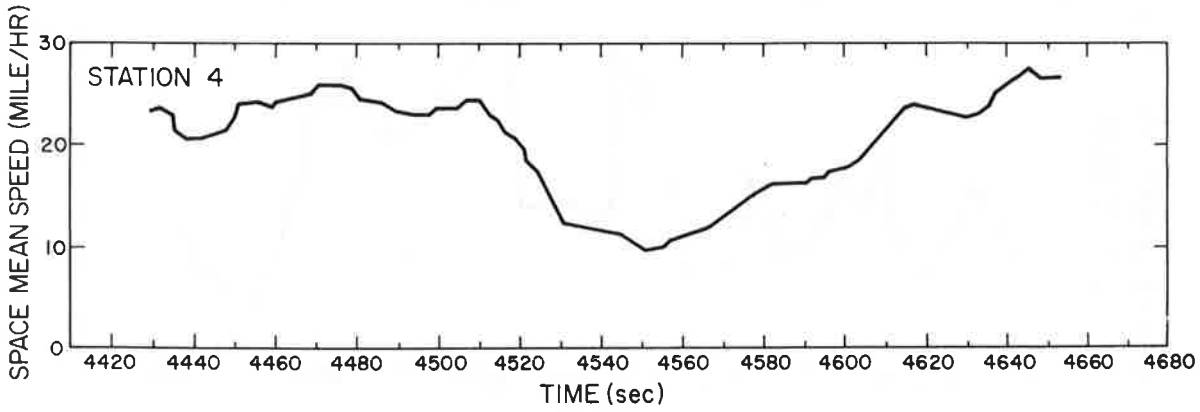


Figure 3.6b.- Vehicular space mean speed vs time. Station 4.

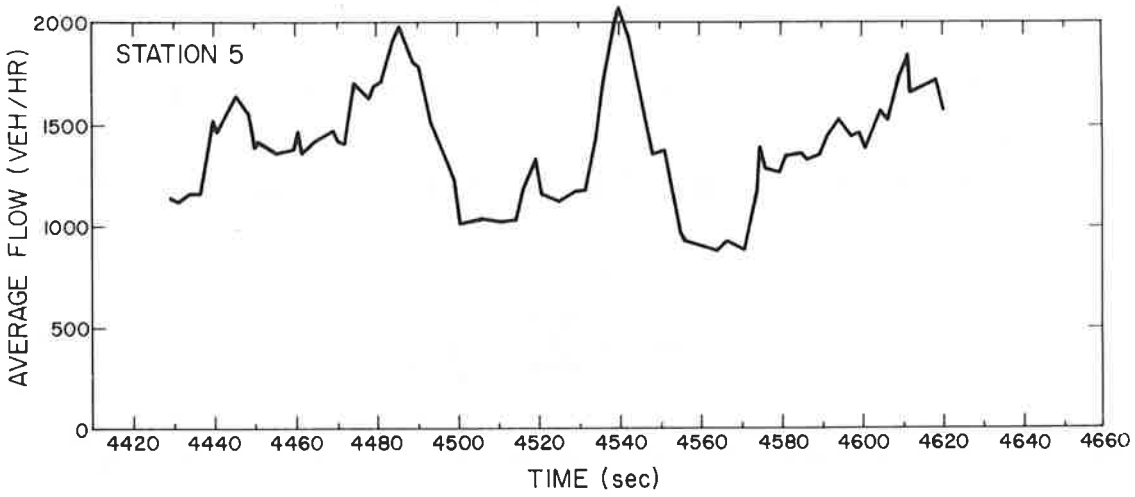


Figure 3.7a.- Average vehicular flow vs time. Station 5.

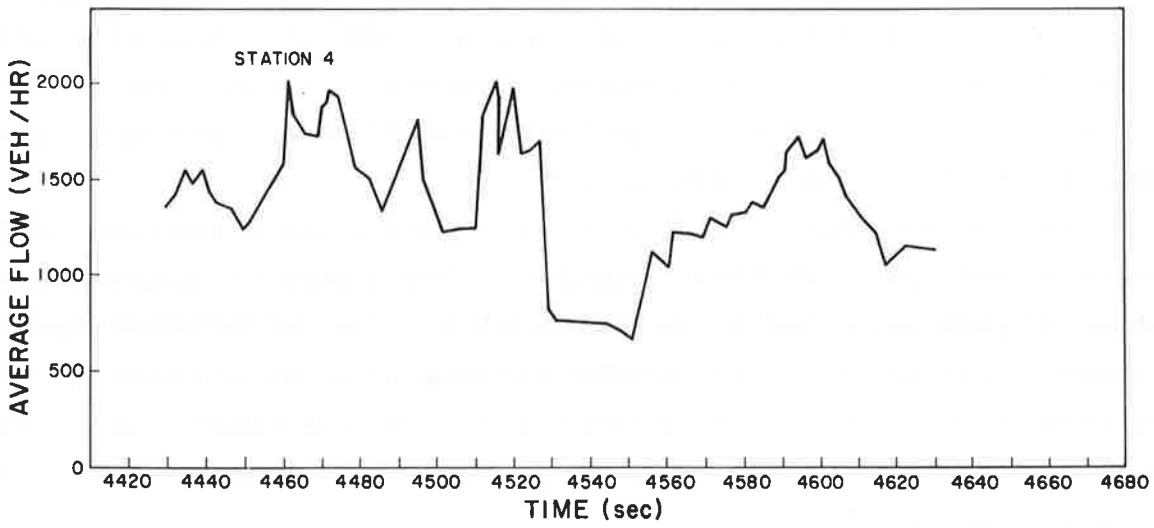


Figure 3.7b.- Average vehicular flow vs time. Station 4.

$$\bar{V} = 0.6818\ N / \sum_{i=1}^{N} (1/V_i) \qquad (3.5)$$

where 0.6818 is a conversion factor which yields $\bar{V}$ in miles per hour.

The average vehicular flow in Figure 3.7 is given by the equation

$$\bar{Q} = 3600\ N / \sum_{i=1}^{N} HWT_i \qquad (3.6)$$

where 3600 is the conversion factor which yields $\bar{Q}$ in number of vehicles per hour. The above procedure for obtaining average values is not the only possible one. A discussion of various methods for obtaining relationships between traffic flow, concentration and speed and methods of taking averages is given later and in Ref. 30.

Inspection of the average density and speed at stations 4 and 5, Figures 3.5 and 3.6, shows, as expected, a decrease in speed accompanying an increase in the density. The minimum average speed occurred at station 5 at 4506 sec. and at station 4 at 4551 sec. The time interval between the two times being 45 sec. The minimum speed is less than 10 miles per hour and is less than half of ordinary speeds.

We may consider the flow at a location as a product of the density and speed at that location. The times of minimum average flow, Figure 3.7a and b, coincide with those of minimum speed, Figures 3.6a and b. The second minimum flow at station 5, occurring at time 4560 sec, Figure 3.7a, on the other hand, appears to be partly due to the minimum in vehicular density at the time (see Figure 3.5a).

In general, the figures may be looked at in pairs, for example 3.6a and 3.6b, and as a sequence, for example, 3.5a, 3.6a, and 3.7a. As pairs, we obtain a qualitative understanding of the

effects of the stoppage wave as it propagates upstream from station 5 to station 4. In the pair 3.6a and 3.6b, for example, we see that the low velocity condition appears first at station 5, then at a later time at station 4 as the shock wave travels upstream from station 5 to station 4. Similarly in the pair 3.7a and 3.7b we see the effects of the shock wave in the reduced flow it causes at station 5 and later at station 4. In Figure 3.7a, the first flow minimum is the one associated with the shock wave. The second flow minimum is simply due to a reduced density at constant velocity. The figures when viewed as a sequence on the other hand, give (qualitatively) the relationship between the density, flow and speed at any one station. For example, in the sequence 3.5a, 3.6a, and 3.7a we see the high densities, and corresponding low flows and low speeds associated with the shock wave as it passes station 5. Similarly, though with somewhat more ambiguity, the sequence 3.5b, 3.6b, and 3.7b depict conditions at station 4.

## 3.4 Q-K CURVE

At this point it is interesting to digress for a moment from just the slowdown period and see what the general conditions were like when the data was taken and how the slowdown period fits into the total period. This is best done with a flow-density curve. The flow-density relationship, obtained from the data of the entire hour-and-a-half run, is shown in Figures 3.8a and 3.8b in which the average flow is plotted against the average density (30 second averages). Several things may be noted from this overview, first, we see that the general traffic level during the run was only moderately heavy, for the most part lying below maximum flow. Apparently the one slowdown period observed in this run occurred against a background of only moderately heavy traffic, triggered perhaps by an abnormally high flow rate preceding the slow down.

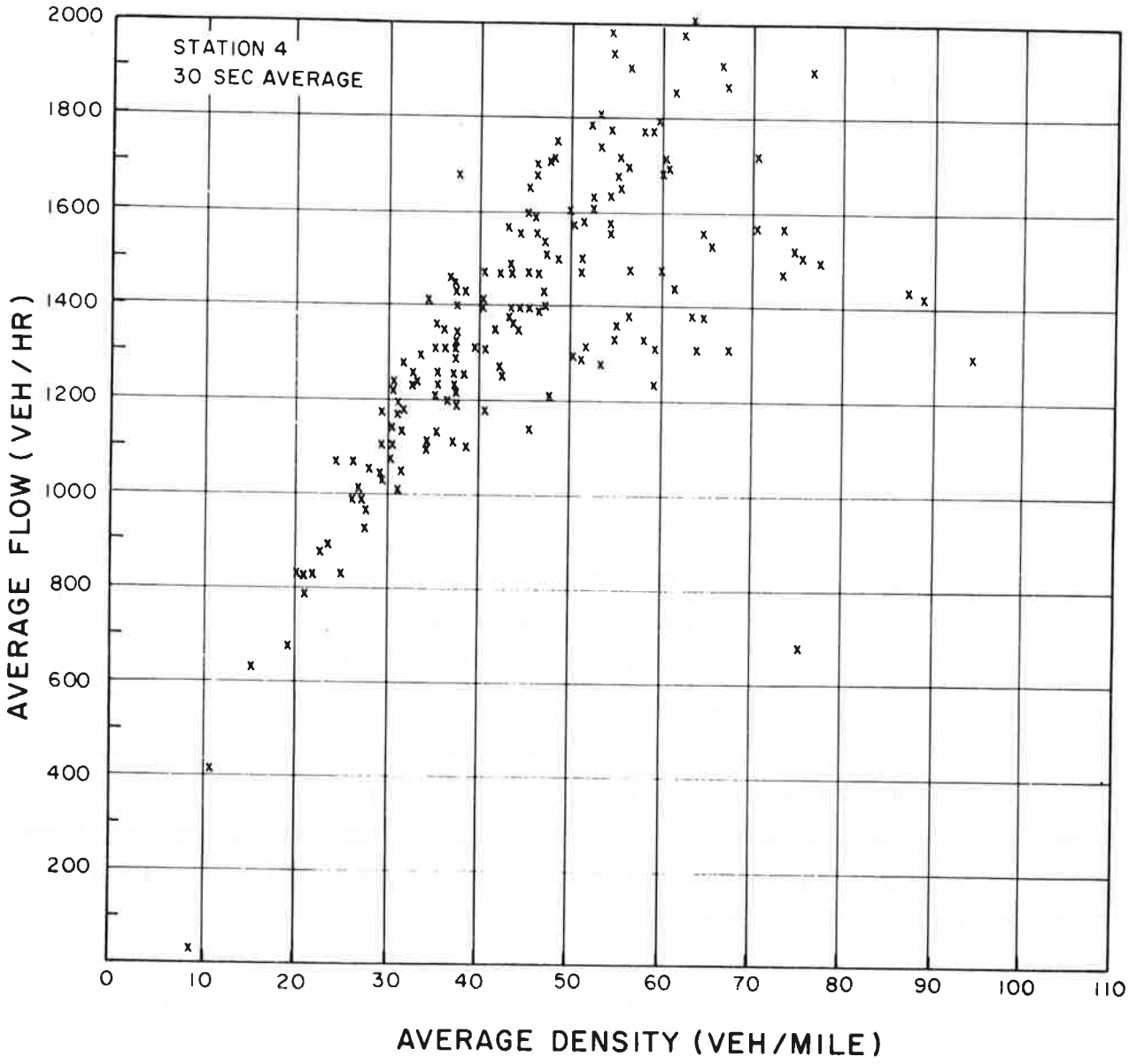


Figure 3.8a.- Average flow vs average density (averaged over 30 seconds). Station 4.

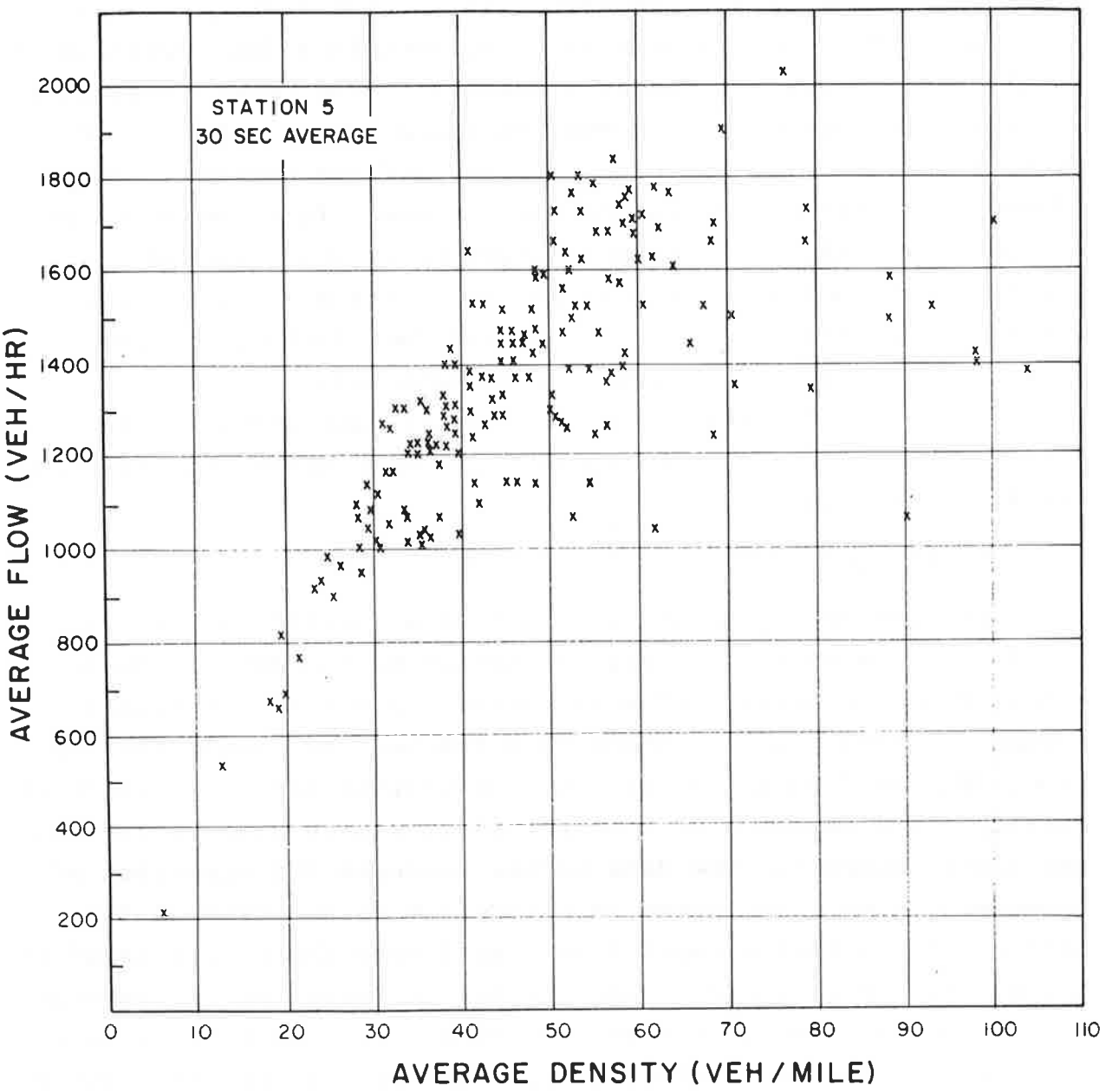


Figure 3.8b.- Average flow vs average density (averaged over 30 seconds).

There is a greater scatter in the points around maximum flow compared with that at the lower densities. This is probably indicative of relatively unstable conditions there and the existence of a multivalued Q-k relationship. We further note the greater scatter and greater number of high density points at station 5 (Figure 3.8b) compared with station 4 (Figure 3.8a). This conforms to the pattern expected from locations upstream of a bottleneck (Ref. 14) (as is station 5). The observed scatter and larger densities here undoubtedly are due to a number of small shocks forming at the bottleneck and the observed lower flows due to the corresponding congestions. It is believed that the one large shock or slowdown observed in this run had its origin at the bottleneck, traveled back to station 5 and was sufficiently strong to arrive some 500 feet further upstream to station 4 as shown in Figures 3.2 through 3.7.

It is now of interest to examine the flow and speed in somewhat more detail as a function not only of density, but also of its first derivative.

## 3.5 EVIDENCE OF ASYMMETRICAL RESPONSE

The flow and speed are examined as a function of density for the case when the density is increasing and decreasing in time. From the average flow and density plots for station 5 around the time when the shock wave reached and passed the station, (Figure 3.5a and 3.7a), we have plotted the flow versus the density for a sequence of time points in Figure 3.9. Arrows in the lines connecting the data points indicate the direction of increasing time. The curve in Figure 3.9 is composed of two parts. First, that segment from 1 to 3 when there is a trend of increasing density, i.e., when the density wave approaches station 5, and secondly, that segment from 3 to 5 when there is a trend of decreasing density, i.e., when the density wave passed station 5. The illustration shows that for the same value of

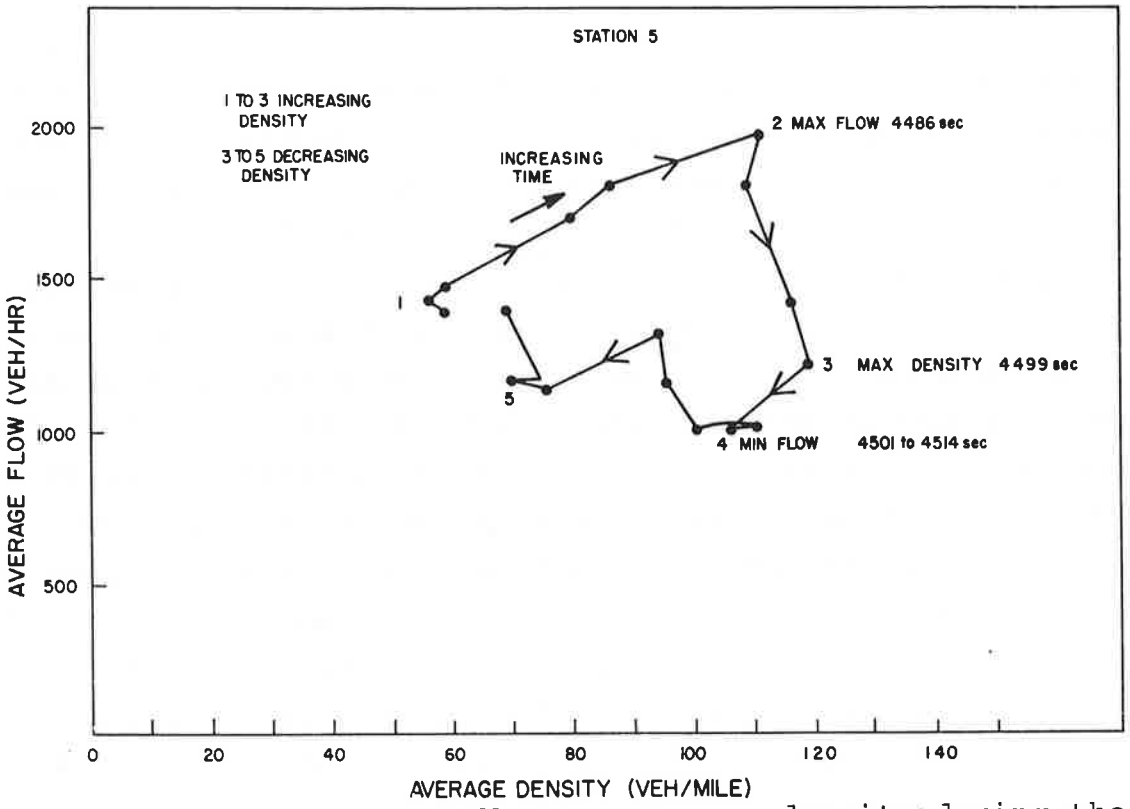


Figure 3.9.- Average flow vs average density during the time when a shock wave passes station 5. Data plotted for a sequence of time points.

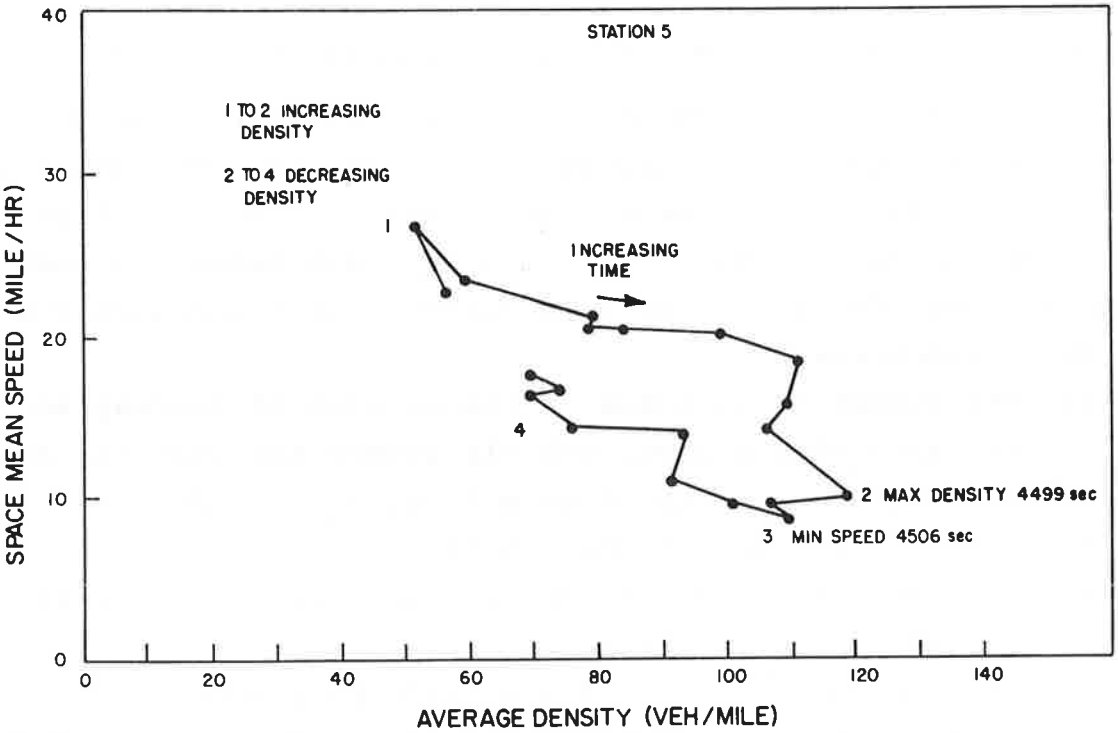


Figure 3.10.- Average speed vs average density during the time when a shock wave passes station 5.

density there is a larger flow for the case of increasing density in comparison with the flow for the case of decreasing density. A similar plot for the space mean speed versus the average density is given in Figure 3.10. This figure shows that there is a larger speed for increasing density in comparison with the speed for decreasing density. This behavior is consistent with the flow, speed and density relationships expected when two kinds of acceeration response strengths exist, (Figures 3.11 and 3.12). The average driver finding himself in increasing traffic density has a stronger magnitude of deceleration response in comparison to the magnitude of acceleration response of a driver who finds himself in decreasing traffic density. This asymmetrical behavior might help explain the large scatter and multi-valuedness mentioned previously in connection with flow-density relations in Figures 3.8a and 3.8b. In any case, it is evident that such asymmetrical behavior does occur and Figures 3.9 and 3.10 indicate qualitative agreement with theory, predicting higher flow and speeds when the density is increasing.

## 3.6 TRAFFIC PARAMETERS PERTAINING TO A LENGTH OF ROADWAY

In addition to the time and space headway calculations of flow, speed, and density we may also consider, as Greenberg did (Ref. 31), the traffic parameters pertaining to the length of roadway between the two stations where the data was taken. A computer program has been developed for this purpose which computes the following parameters:

(1) The number of vehicles in the section of roadway at the time when a given vehicle enters the section, $N_i$.

(2) The average density at this time, $k_i = N_i / D$.

(3) The transit time of the vehicle, $T_i$.

(4) The flow at the end of the section averaged over the transit time, $Q_i = N_i/T_i$.

(5) The average velocity of a vehicle in traversing the section of roadway, $V_i = D/T_i$. (D is the length of the section.)

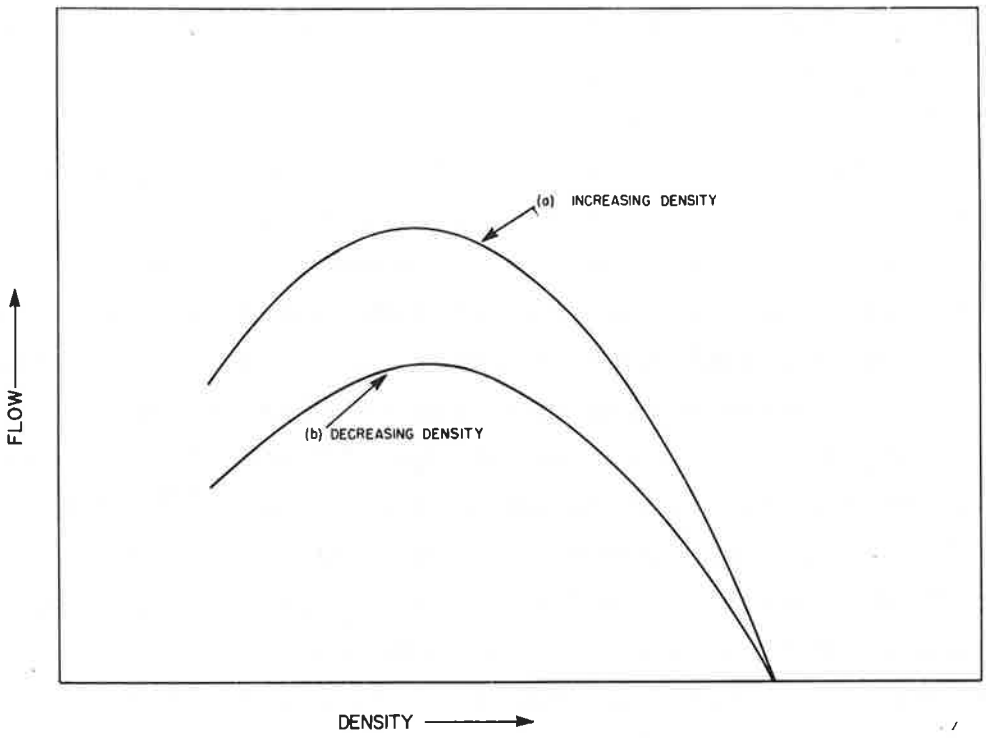


Figure 3.11.- Schematic of theoretical flow vs density curves assuming different response strengths for increasing and decreasing density.

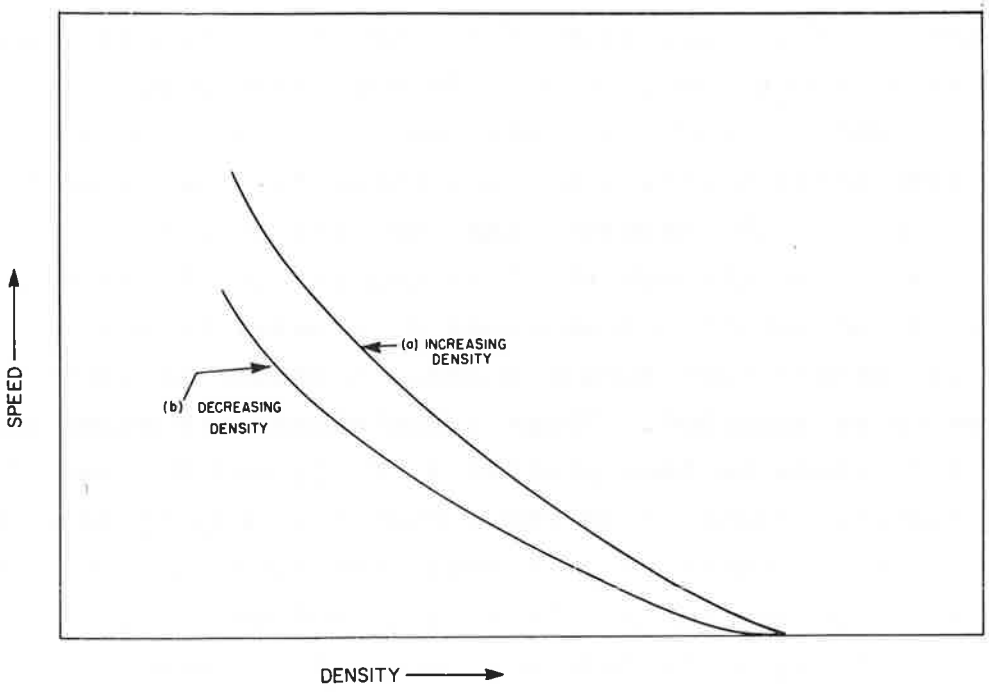


Figure 3.12.- Schematic of theoretical flow vs density curves assuming different response strengths for increasing and decreasing density.

In Figures 3.13a and b are shown the number of vehicles in the section of roadway between the time when the $i^{th}$ vehicle entered the section and the time when it left the section. Figure 3.13c shows the change in number of vehicles in the section during the time of transit of the $i^{th}$ vehicle. These graphs are useful for finding correlations between any increase in the number of vehicles in the section and the transit time and flow through the section. When the number of vehicles in the section increases due to the shock wave during the transit time of the $i^{th}$ vehicle (Figure 3.13), the transit time of the $i^{th}$ vehicle increases (Figure 3.14) and the flow associated with the $i^{th}$ vehicle decreases (Figure 3.15). However, it should be pointed out that while it is meaningful to relate $N_i$ to $T_i$ and $Q_i$ when the number of vehicles in the section does not change greatly during the time interval of transit, a degree of ambiguity does exist when a large change occurs. When a large change in the number of vehicles in a section occurs, the intervals of integration -- the spatial length between the stations and the time of transit -- set a limit on the resolution of the traffic parameters and the relationships among them. A vehicle may enter a section at a time when there are very few vehicles in the section and encounter a shock wave after travelling, say, three fourths through the section. Most of the transit time then may be due to the slowdown in travelling through the last quarter of the section. Nonetheless, we can obtain correlations of general trends of the traffic parameters even though a certain amount of imprecision will have to be accepted. These correlations are shown in Figures 3.13 to 3.16 where we have plotted N, T, Q, and V versus the vehicle number. Figure 3.14 shows that the transit time between stations 4 and 5 starts to rise beginning with the time vehicle #1643 arrives at station 5. This is indeed the first vehicle where the flow begins to fall at station 5. Figure 3.13a shows, correspondingly, that the number of vehicles in the section of roadway begins to increase at this time. The figures also show

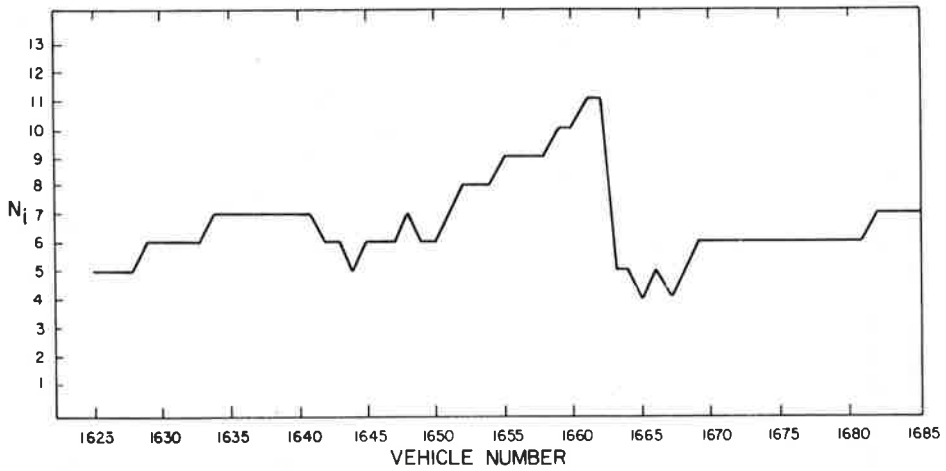


Figure 3.13a.- $N_i$, Number of vehicles in section of roadway between stations 4 and 5 at the time when the $i^{th}$ vehicle reaches station 4 vs vehicle number

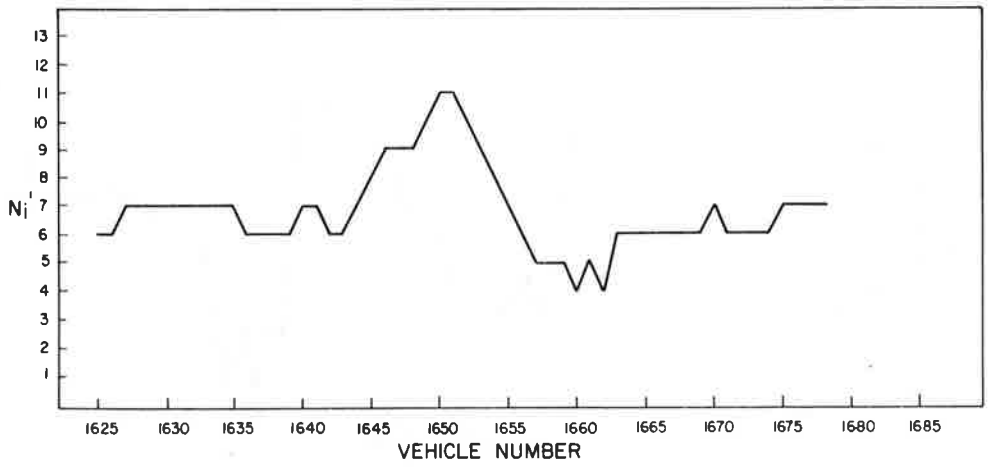


Figure 3.13b.- $N_i$, Number of vehicles in section of roadway between stations 4 and 5 at the time when the $i^{th}$ vehicle reaches station 5 vs vehicle number

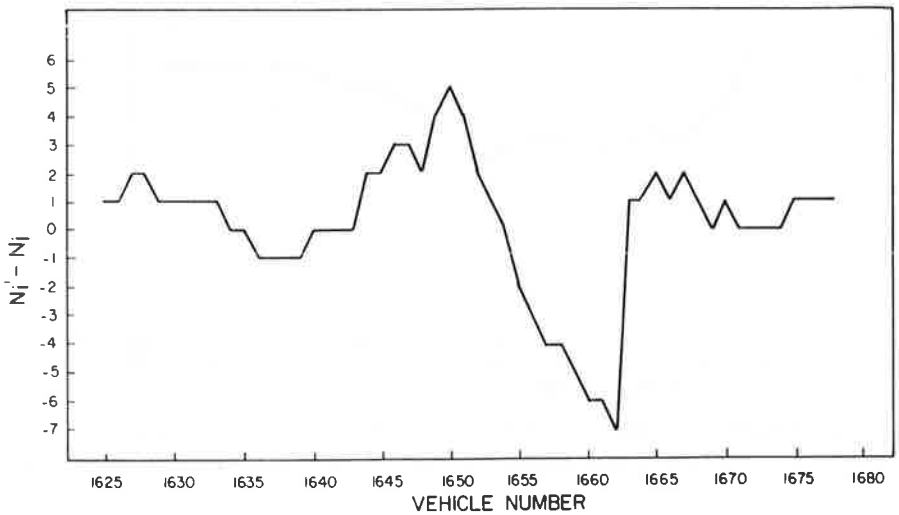


Figure 3.13c.- Change in number of vehicles in roadway during transit of $i^{th}$ vehicle from 4 to 5 vs vehicle number.

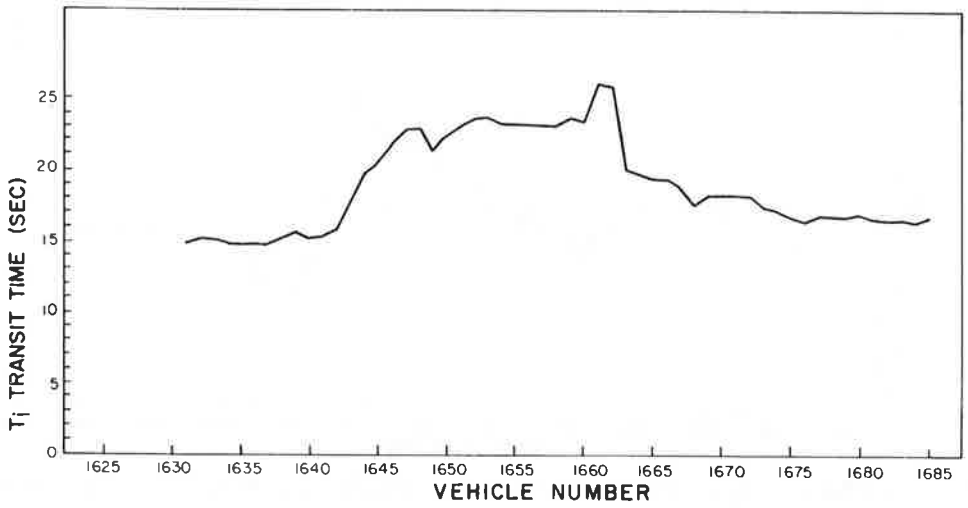


Figure 3.14.- $T_i$, Transit time of $i^{th}$ vehicle traveling from stations 4 to 5 vs vehicle number.

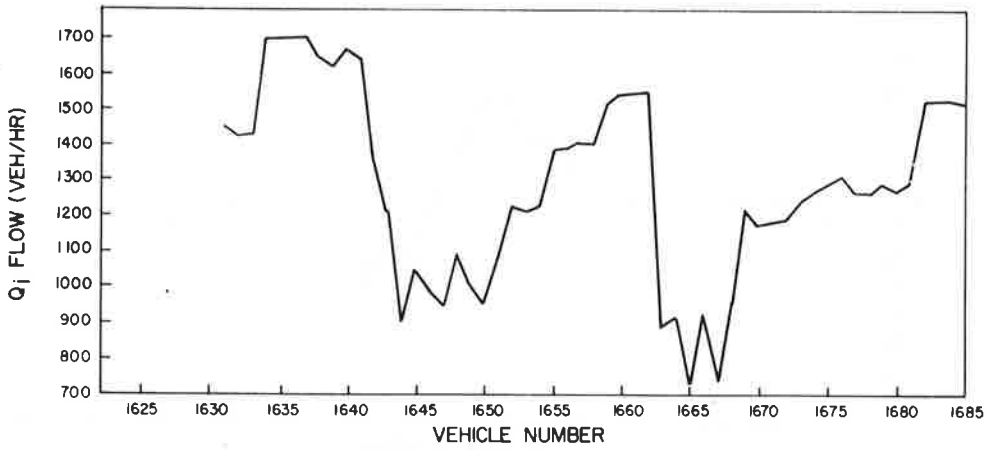


Figure 3.15.- $Q_i$, Flow at station 5 averaged over the transit time of the $i^{th}$ vehicle vs vehicle number.

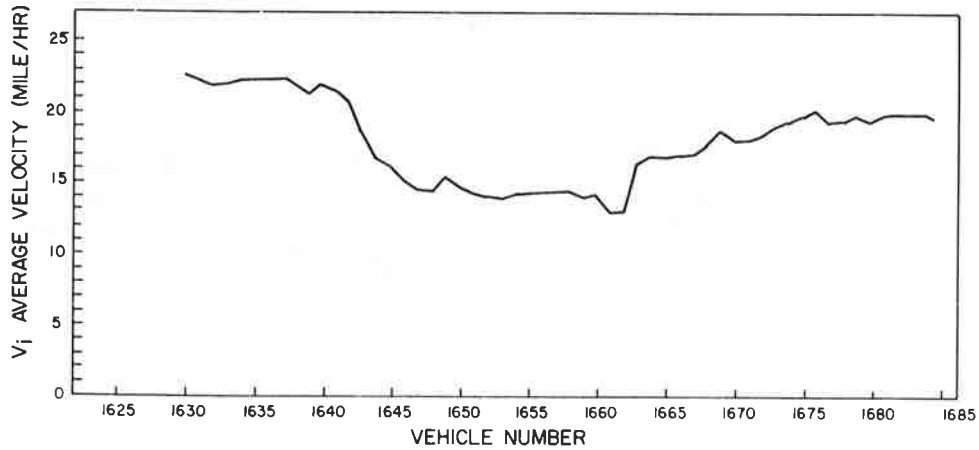


Figure 3.16.- $V_i$, Average velocity of the $i^{th}$ vehicle in traveling from stations 4 to 5 vs vehicle number.

that after a maximum number of eleven vehicles in the section is reached, there is a subsequent rarefaction down to 4 vehicles. This effect is also seen in Figure 3.15 where there are two flow minima; the first is associated with the increase in transit time, while the second is associated with the rarefaction in vehicle number which followed the number build up. Whether or not this rarefaction with its resultant overcorrection of the high density situation, is a common occurrence after such a density build-up, is not known and would require a more extensive study.

In addition to this set of graphs in which the section traffic parameters were plotted against the vehicle number in order to show the relationship between number build up, transit time and flow of individual vehicles traversing the section, these section traffic parameters can also be plotted against time. This would show the relations between the parameters at any given time and might therefore, be somewhat more useful for the implementation of a real time control system. These plots of number of vehicles, transit time, average speed and average flow versus time are shown in Figures 3.17 through 3.20. Figure 3.17 shows the number of vehicles in the section at the time a vehicle enters that section versus the time of entry, i.e., versus the time at which the vehicle reaches station 4. We see that the number of vehicles in the section begins to rise substantially at around time 4500 seconds. Now the $i^{th}$ vehicle traverses the section in a time of transit $T_i$, and the question arises as to what is the meaningful time against which this transit time should be plotted. For example, if we plotted the transit time at the time of entry into the section, then when a shock wave passes the exit station and travels towards the point of entry, it would appear as if the transit time increased before the density began to build up. This is because the transit time becomes lengthened as the vehicle encounters a shock somewhere within the section and this lengthened transit time would appear to occur before the density build-up if plotted at a time earlier

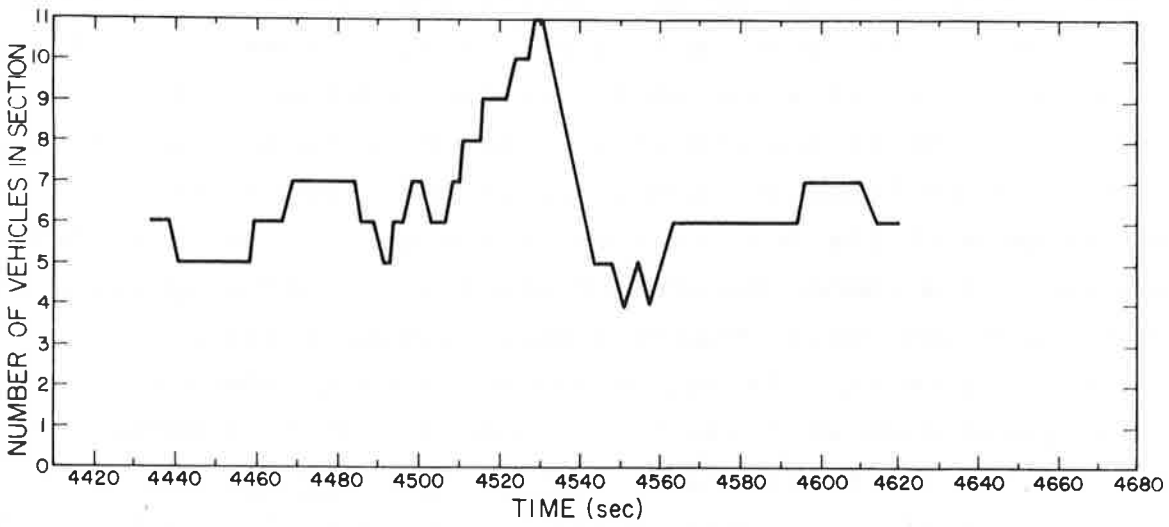


Figure 3.17.- Number of vehicles in section of roadway between stations 4 and 5 vs time.

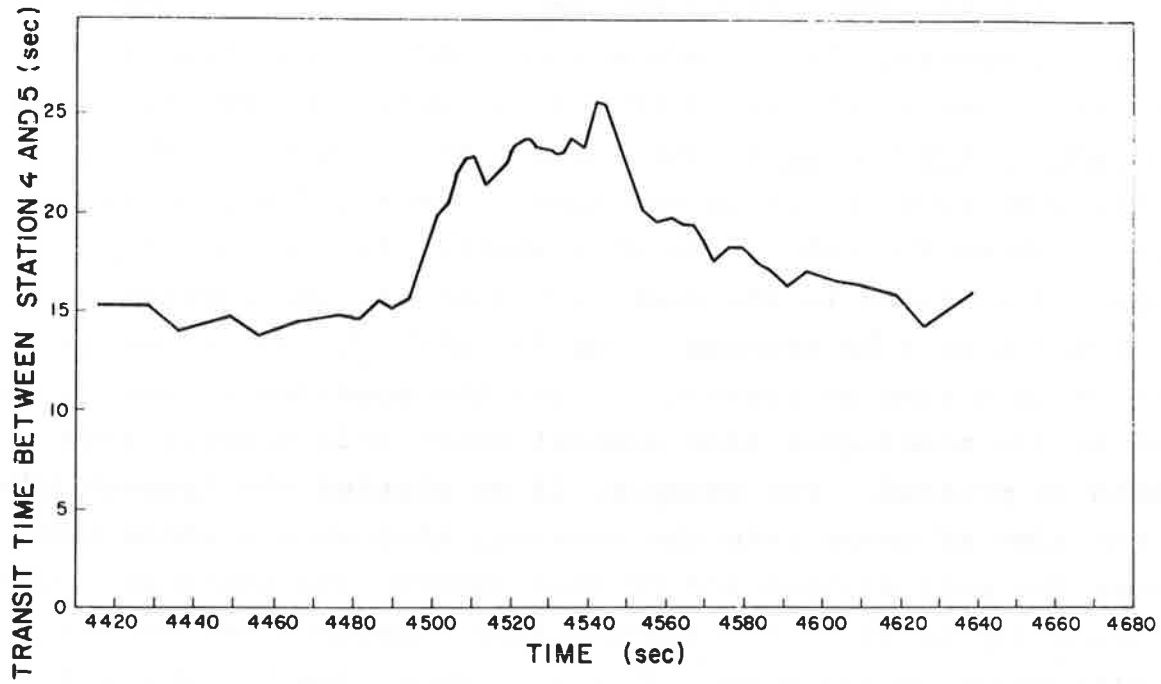


Figure 3.18.- Transit of vehicle between stations 4 and 5 vs middle of transit time.

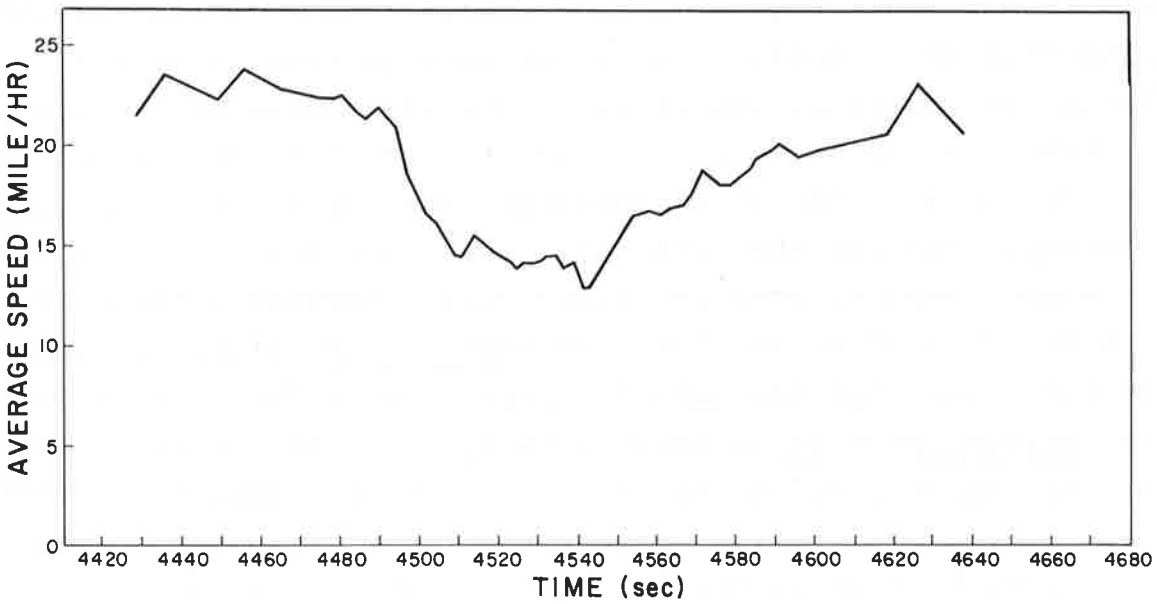


Figure 3.19.- Average speed during the transit of a vehicle between stations 4 and 5 vs the middle of the transit time.

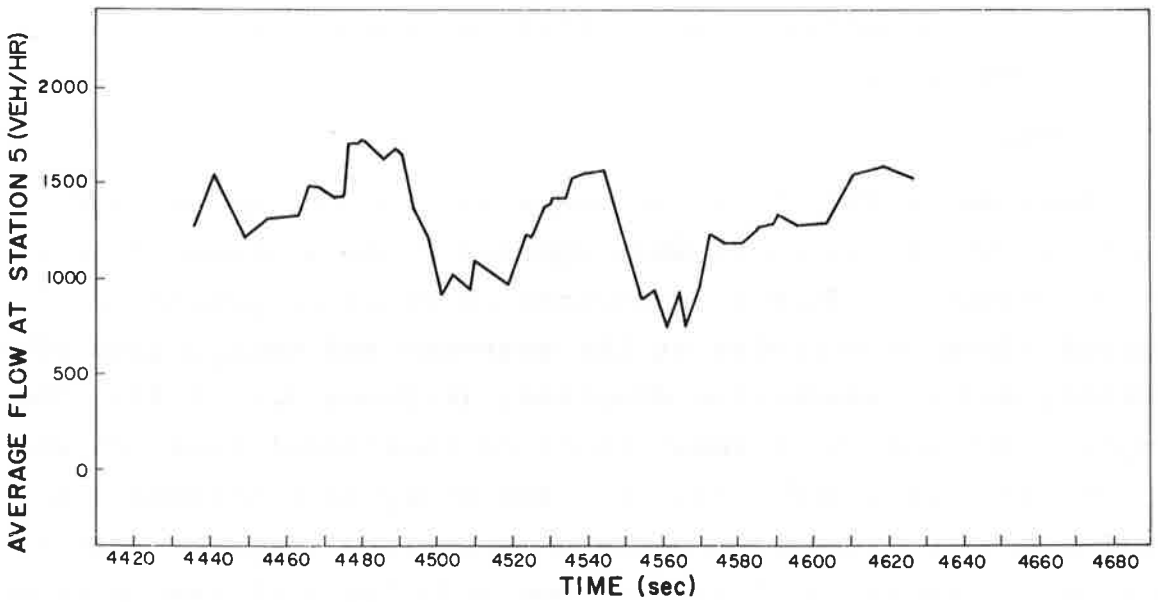


Figure 3.20.- Flow at station 5 averaged over the transit time of a vehicle vs the middle of the transit time.

than when the shock entered the section. One alternative would be to plot the transit time at the average time of transit through the section. While this is still imprecise since we do not know exactly at what time and at what distance through the section the vehicle first encounters the shock, it should yield reasonable results for sections, like the one here, which are not too long. This is done in Figure 3.18. Comparing this figure with Figure 3.17 we see that the transit time rises at about the same time that the number of vehicles in the section rises. The average velocity in traversing the section, which is inversely proportional to the transit time, is shown to correspondingly decrease at this time (Figure 3.19). Finally, in Figure 3.20 where we have plotted the flow at station 5, averaged over the transit time of the $i^{th}$ vehicle, versus the middle of the transit time, we find the same two flow minima as previously seen in Figure 3.15 where flow was plotted as a function of vehicle number. The first flow minimum which occurs at around 4500 seconds is related to the reduced speed in the congestion while the second minimum is due to the rarefaction in the number of vehicles which followed the initial section congestion as discussed previously.

## 3.7 SUMMARY

Data on traffic flow through a section of the Holland Tunnel in New York, shows what appears to be a slowdown wave in the section. This was examined by means of graphs of arrival times of vehicles at the entrance and exit points of the section, and by space-time diagrams, (Figures 3.2, 3.3). The graphs displayed the transit times of individual vehicles as well as the flow rates and densities, and analysis confirmed the existence of a slowdown wave which travelled upstream from the exit to the entrance of the section (483 feet) in twenty nine seconds with a speed of 16 feet per second (11.4 miles/hour). From the slowdown, a jam density of 218.6 vehicles/mile and a

jam headway of 24.2 feet were computed as well as a shock width of 161.3 feet which contained 6.7 vehicles.

This confirmation of the slowdown wave and analysis of its properties was followed by a study of the relationship between flow, density, speed and transit time, immediately preceding, during and following the slowdown. For this purpose, average flow, density, and space mean speed measured at the entrance and exit points and defined in terms of time and space headways were plotted against time by using running averages over groups of five vehicles. The graphs (Figures 3.5 through 3.7) showed the effects of the slowdown wave (effects such as low velocity and low flow) appearing first at the exit station and later at the entrance point. They also showed the low flow, low velocity, high density relationship that prevailed at each of the stations during the passage of the wave.

These graphs were supplemented with a general flow-density curve (Q-k curve, Figure 3.8), which showed a pattern consistant with that obtained previously for conditions upstream of a bottleneck for station 5 (exit point).

The graphs were also supplemented by curves of flow, number of vehicles, transit time and speed versus both vehicle number and time, (Figures 3.13 through 3.20). In these, the flow, density and speed were defined in terms of the length of the section (Greenberg method). This type of analysis of the slowdown yielded such quantities as the change in the number of vehicles in the section during the transit time of a particular vehicle, the transit time, and average velocity of the vehicle through the section as a function of vehicle number and time, and the flow averaged over the transit time as a function of vehicle number and time. The efficiency of these different methods for analysis of traffic flow were discussed particularly in regards to the amount of precision that can be expected in establishing correlations between density build up, lengthened transit time, reduced velocity and reduced flow during the passage of the slowdown wave.

Finally, we presented some evidence for an asymmetrical acceleration response during the passage of the shock wave. Plotting average flow and speed versus density for a sequence of times when the density was increasing and when the density was decreasing, it was found that for the same value of density there is a larger flow and a higher velocity when the density is increasing in time than when it is decreasing. This is in agreement with theory as discussed in Section 2.

# SECTION 4
# TRAFFIC FLOW ANALYSIS OF CALLAHAN TUNNEL

## 4.1 INTRODUCTION

This Section is a report on measurements of traffic flow through the Callahan tunnel in Boston. The Callahan is one of two tunnels in Boston which connect the city with East Boston and Logan International Airport. The other is the Sumner tunnel which carries traffic in the opposite direction, from East Boston and the airport into the city. Together the two tunnels handle approximately 70,000 vehicles on their four lanes in a normal 24-hour period, the peak traffic flow for each tunnel being typically between 2850 and 2900 vehicles per hour. This traffic is made up predominately of passenger cars with truck and bus traffic constituting a small percentage of the total traffic. The truck and bus traffic in the *truck lane* of the Callahan measured 11 percent of the total vehicular traffic in that lane (only 0.62 percent were buses). This may be contrasted with the traffic in the Holland tunnel (cf. Section 3) where trucks and buses make up a much larger portion of the total traffic. The Holland tunnel differs from the Callahan in another way which may be important: In the Holland tunnel the toll booths are on the entrance side of the tunnel while in the Callahan they are on the exit side. In the jargon of mathematical theory, it can be said that different boundary conditions exist and that the optimum densities, flow and speeds would be different for the different tunnels even though one dynamical theory of traffic flow may apply to both roadways. The data supported this, the numerical values did differ, but the basic relationships remained the same.

The question arose on the best way to take the data for the program. Unlike the New York studies conducted by the Port Authority itself, our work was in *somebody else's* tunnel. Although complete cooperation, encouragement and help were accorded by the Massachusetts Turnpike Authority, there were still some

selfimposed constraints; such as, for example, not breaking up the roadway, which the installation of accurate automatic sensors such as the photoelectric cells and induction loops used in New York might require. For this reason and also because this part of the study was to be only the first phase (the so called "manual" phase), we performed the measurements without the aid of such automatic sensing equipment. Nonetheless, a reasonably high degree of accuracy was needed to derive flow, speeds, and densities from the measurements. To achieve the required degree of accuracy a number of previous schemes were investigated. One such was an early method used by the Port Authority of New York in which 15-second time slots were delineated and the number and types of vehicles passing the observer in that time slot were recorded. This method is subject to a maximum error of a half minute which occurs when only one vehicle appears in the 15-second time slot. For a mile long tunnel with typical transit times of two minutes or so, there could be as high as 25 percent errors. Even though the likelihood of such errors was small because most measurements would be taken during the high density peak hours, the few times when low density measurements would be needed made it desirable to look for an alternative method.

The method chosen simply produced a continuous time history of the arrival and departure times of vehicles entering and leaving the tunnel section under observation. This was done with the aid of two strip-chart recorders (Sanborn 299 and Hewlett Packard 320) and two *car identification* boxes as shown in Figure 4.1, (see also Section 1, paragraph 1.2). The recorders had 60 Hz timers so that inconsistent or inaccurate chart speeds would be known and could be compensated. (It turned out that in a half hour run the chart speed typically, would be off by a minute or so, though this would vary from run to run.) With this independent check of the times, and with the vehicle identifications, it was possible to obtain the transit times of individual vehicles with sufficient accuracy to derive all the quantities

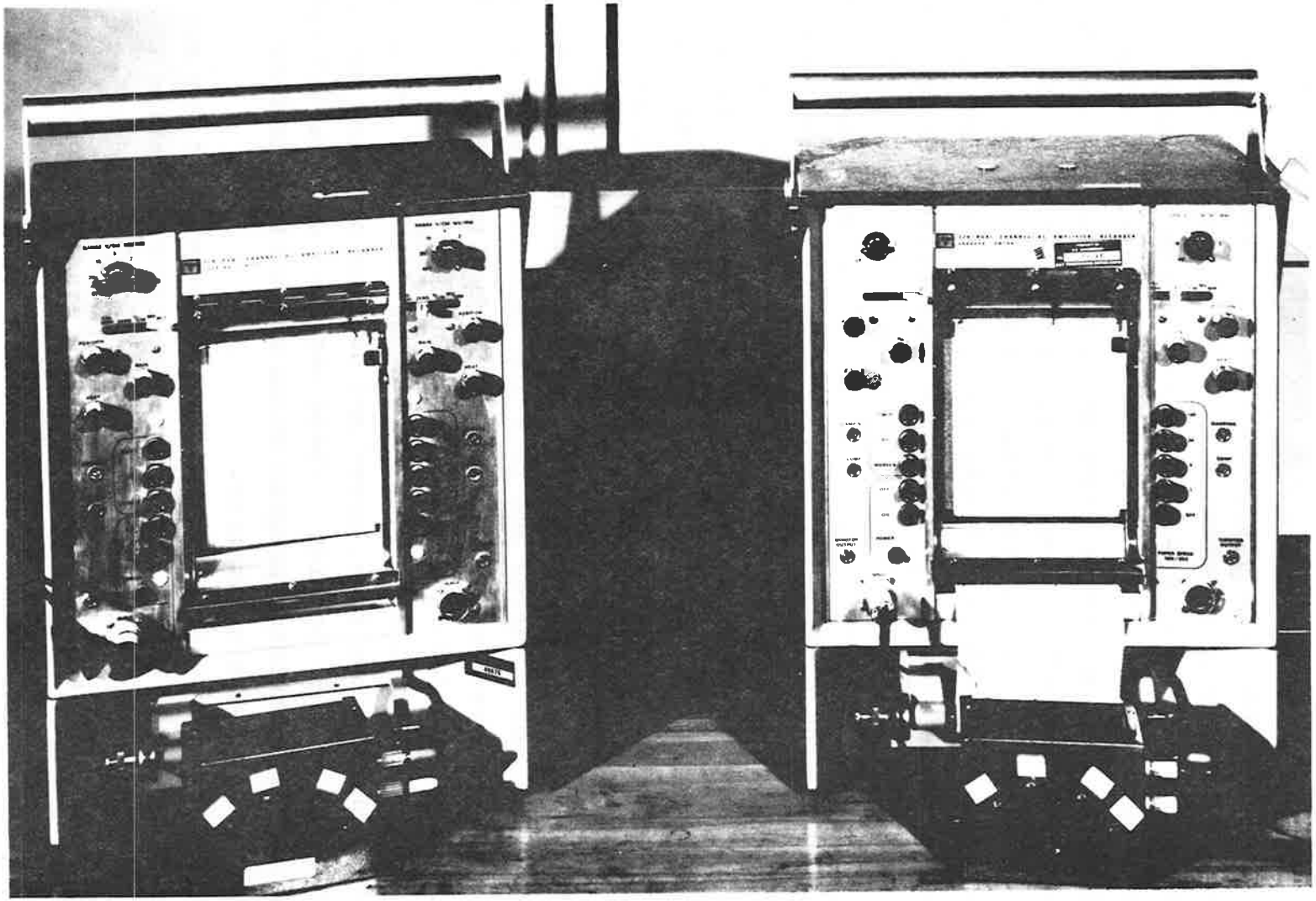

Figure 4.1. - Photograph of vehicle identification boxes and strip chart recorder.

that would be of interest in the different experiments that were planned under both high and low density conditions.

The measurements were all taken from the catwalk by two or more researchers stationed along the walk. The observation stations are shown in Figure 4.2. At each of these stations the observer was equipped with the strip chart recorder, the vehicle identification box, the 60 Hz timer and a synchronized stop watch. At the synchronized start time, the researchers would cause the pen of the timer to record this time on the chart paper and the taking of data would begin. As the front bumper of a vehicle passed in front of the observer and the appropriate button on his vehicle identification box was depressed, the time would be recorded on the chart paper (which was moving with a speed of a 5mm/sec.) as a line mark of one of four possible lengths, denoting a car, bus, taxi or truck. This enabled the determination of the transit time of any particular vehicle since a pattern recognition could be made from the recordings taken at the entrance and exit stations. For example, a car followed by a truck, two cars, a taxi, three cars and a bus might be one pattern appearing on both chart papers. This would pretty much assure us that a lane-change had not occurred and that the vehicle whose time we had recorded on entering the section was indeed the same vehicle whose time was recorded on leaving the section.

From this raw data of arrival and departure times of vehicles we obtained the various flow, speed and density averages shown in the figures of this Section. These averages were calculated with the aid of a computer program which was written to both calculate and plot the quantities.

Two experiments were performed in the tunnel. In one experiment it was desired to obtain a tunnel traffic profile to determine the degree of homogeneity of the roadway and to see if a single flow-concentration relation and a single tunnel capacity could be defined. In fact, the data showed that it was not possible to define a single capacity for the tunnel; rather, several

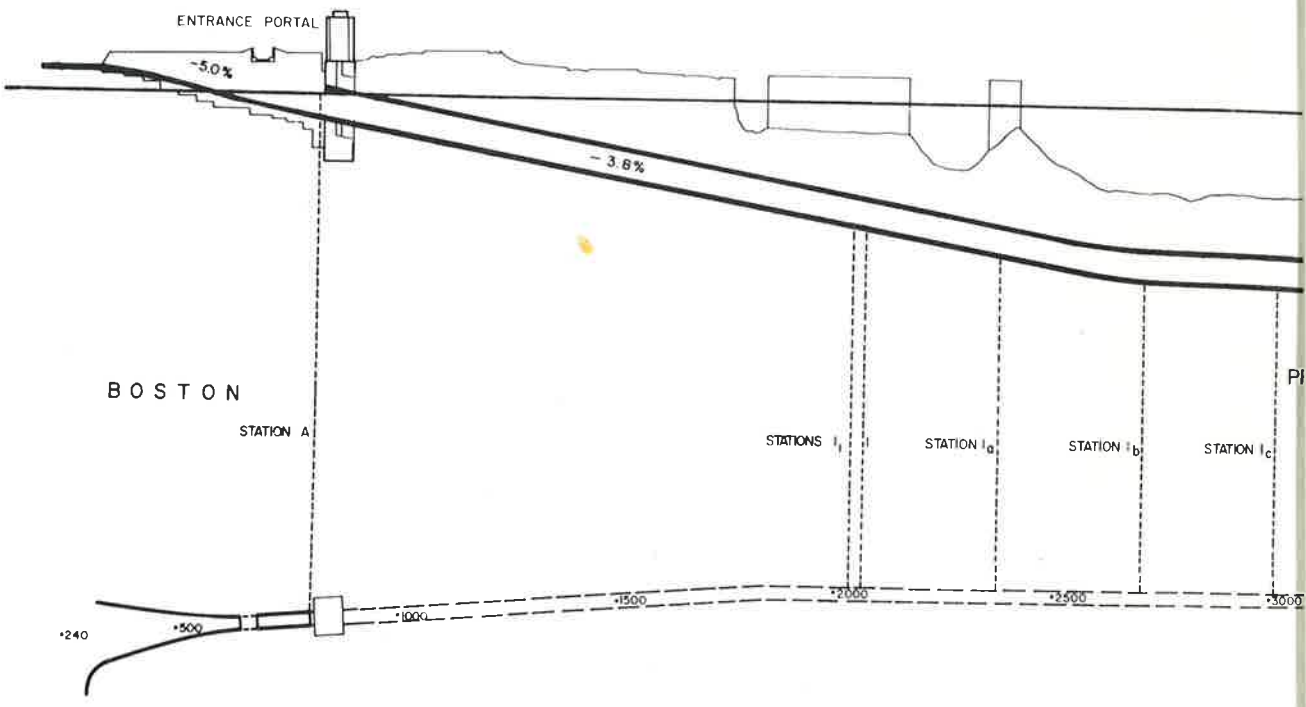
ENTRANCE PORTAL
-5.0%
-3.6%
BOSTON
STATION A
STATIONS
STATION
STATION
STATION
STATION
+240
+500
+1000
+1500
+2000
+2500
+3000

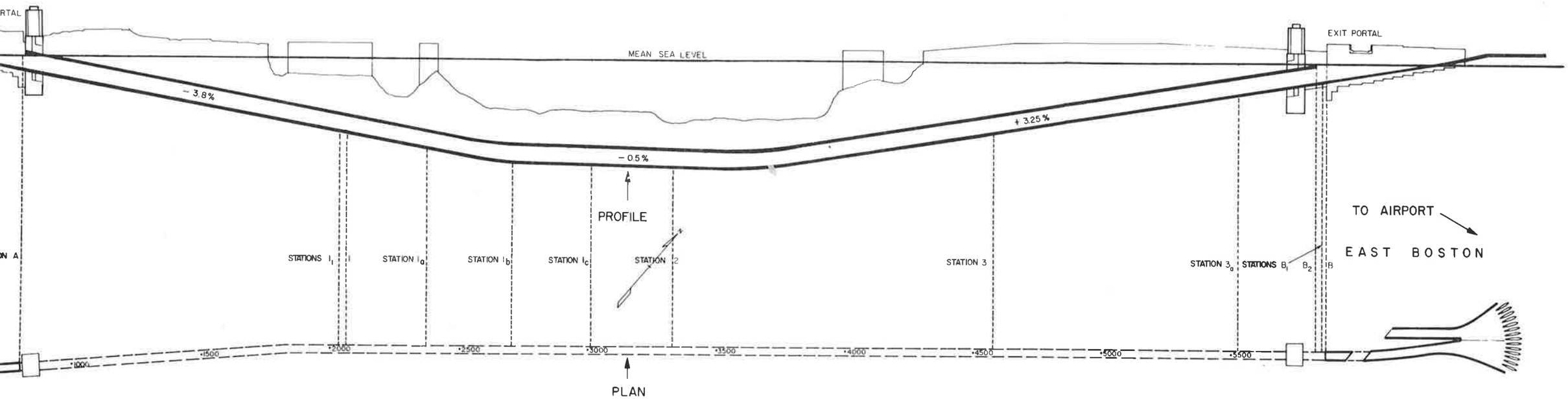
RTAL
MEAN SEA LEVEL
EXIT PORTAL
- 3.8%
+ 3.25%
- 0.5%
PROFILE
TO AIRPORT
EAST BOSTON
ON A
STATIONS $I_1$
STATION $I_a$
STATION $I_b$
STATION $I_c$
STATION $I_2$
STATION 3
STATION $3_a$
STATIONS $B_1$
$B_2$
B
1000
1500
2000
2500
3000
3500
4000
4500
5000
5500
PLAN

capacities were found to exist which were different for the different sections of the tunnel. This fact is important for the implementation of an effective control system for the tunnel. If the section capacities differ, then the flow, speed, and density readings from one section of the tunnel would require different control procedures than from another. Readings of high densities from a low capacity section would require different control procedures than the same readings from a high capacity section; worse yet, a control based on one density reading for the tunnel as a whole could lead to an unexpected and deleterious response. A traffic flow profile of the Callahan tunnel therefore was considered to be an important and necessary precursor to the implementation of a system to control the tunnel throughput. These profile measurements, however, probably should be supplemented with data taken simultaneously at a larger number of stations than was possible in our experiments. This is possible, practically, only by the installation of some form of automatic data-taking equipment.

While most of the data was taken during the peak hours where control is most likely to be used, in a second experiment, some low density data was taken to "fill out" the Q-K curve. This allowed examination of the flow-concentration relation as a whole. The analysis also includes a discussion of the effect of shock waves on the flow-concentration relation, the relationship between flow, speed, and density with and without a shock present, and the shape and continuity of the curve near the transition flows when the densities are just below and just above optimum.

The traffic flow profile is discussed first, in paragraph 4.2. This is followed by an analysis of slowdown waves in paragraph 4.3. In paragraph 4.4 there is a discussion of the flow-density and velocity-density relations as measured and these are compared to the case when the observed shock waves have been removed from the data.

## 4.2 TRAFFIC FLOW PROFILE

### 4.2.1 Introduction

The Callahan conveniently separates into three sections as far as traffic flow within the tunnel is concerned. These sections are the beginning section which covers the distance between the entrance portal and station 1, located before the foot of the downgrade, the center section which is between station 1 and station 3, and the end section which is between station 3 and the exit portal, B (see Figure 4.2). Within the center section, the roadway between stations 2 and 3 encloses the foot of the upgrade, generally considered a bottleneck in the tunnel.

The traffic flow through these sections is examined by comparing minute average maximum flows; Q-K curves, V-K curves; and section densities and section speeds. It is found, in general, that the beginning section has the highest capacity, the middle section the lowest; that the speeds are greatest in the beginning section and that they increase there, as expected, with decreasing density; that the speeds are lowest in the middle section and increase there only somewhat with decreasing density; that the speeds pick up again in the end section and remain relatively constant, almost independent of density there. The implications of these findings will be discussed.

### 4.2.2 Definitions

The following quantities are used in the profile analysis:

$N_i$ - Section vehicle number. This is the number of vehicles in the section of roadway between two observer locations in the tunnel at the time when the $i^{th}$ vehicle entered the section.

$T_i$ - Transit time between two stations. This is the time required for a vehicle to travel from one observer location to another.

$V_i$ - Average speed of a vehicle travelling between two stations. This is given by $V_i = D/T_i$ where D is the distance between the two locations and $T_i$ is the transit time.

$Q_i$ - Flow average over the transit time. This is given by $Q_i = N_i/T_i$. It is the flow at the exit of the section being observed.

$K_i$ - Average density in a section. This is given by $K_i = N_i/D$.

$\bar{Q}_K$ - Mean flow for a given density. When data points of $Q_i$ versus $K_i$ are plotted, the values of $K_i$ are discrete in magnitude since the number of vehicles in the section is an integer. We compute the mean value of the flow for all the data points having the same value of density.

$$\bar{Q}_K = \sum_{j=1}^{m} Q_K(j)/m \tag{4.1}$$

where j indicates the $j^{th}$ data point and m is the number of data points for a given density. In order to have some measure of the scatter around the mean flow, we define a standard deviation,

$$\sigma = \left[ \frac{\sum_{j=1}^{m} \left[ \bar{Q}_K - Q_K(j) \right]^2}{m} \right]^{1/2} \tag{4.2}$$

In the graphs a vertical line of length $2\sigma$ ($\pm\sigma$) has been drawn through the mean flow points $\bar{Q}_K$.

$\bar{V}_K$ - Mean speed for a given density.

$\bar{T}_N$ - Mean transit time for a given section vehicle number.

In concluding this section it should be stressed that the observation techniques employed in the Callahan tunnel are such that only the average density and the average speed over an observed section can be obtained but not the density, speed, and acceleration at a single spatial point in the tunnel.

### 4.2.3 Sections of Tunnel

Figure 4.2 shows a side and top view of the Callahan tunnel. The entrance portal is at A and the exit portal is at B. Measured from a zero reference point where the Callahan tunnel property

begins, the distances at the various observation stations are given in Table 4.1. Also given are the normalized distances measured from station A.

TABLE 4.1 LOCATION OF OBSERVATION STATIONS

| Station | Normalized Distance (feet) |
|---|---|
| A---------801--(Entrance Portal)---------- | 0 |
| $1_1$--------2035---------- | 1234 |
| 1---------2060--(Boston Guard Booth)---------- | 1259 |
| $1_a$--------2370---------- | 1569 |
| $1_b$--------2706---------- | 1905 |
| $1_c$--------3010---------- | 2209 |
| 2---------3325--(Center Guard Booth)---------- | 2524 |
| 3---------4585--(East Boston Guard Booth)---------- | 3784 |
| $3_a$--------5536---------- | 4735 |
| $B_2$--------5843---------- | 5042 |
| $B_1$--------5864---------- | 5063 |
| B---------5870--(Exit Portal)---------- | 5069 |

In Table 4.2, for convenience, are listed the runs taken and some of their characteristics. Runs 7, 11, and 12 are not included as the data from these runs were not usable for a variety of reasons such as the timer not working.

### 4.2.4 Capacity Profile

First a profile of the flow capacity of the Callahan including the locations of lowest flow capacity is obtained. To determine this, ideally there should be observers stationed along the tunnel taking simultaneous measurements. This was impractical due to limitations on equipment amd manpower availability. Instead, approximations of these simultaneous measurements, with several runs taken on different days are used. This was done if the times of these runs were approximately the same, falling between 4:15 pm and 5:00 pm and if the minute flows when averaged over the entire

TABLE 4.2 LIST OF DATA RUNS AND SOME CHARACTERISTICS

| RUN NO. | DATE TAKEN (1970) | TIME TAKEN | LENGTH OF RUN (MIN) | SECTION MEASURED | SECTION DISTANCE (FT.) | AVERAGE MINUTE FLOWS | AVERAGE SPEED mph |
|---|---|---|---|---|---|---|---|
| 1 | 11/9 | 2:45PM | 20 | $A-B_1$ | 5063 | 13.7 | 19.4 |
| 2 | 11/9 | 3:10 " | 20 | $A-B_1$ | 5063 | 14.8 | 22.8 |
| 3 | 11/12 | 4:15 " | 21 | $1_1-3$ | 2550 | 21.6 | 13.6 |
| 4 | 11/13 | 4:25 " | 36 | 2-3 | 1260 | 21.8 | 17.1 |
| 5 | 11/12 | 4:50 " | 22 | $1_1-3$ | 2550 | 22.8 | 14.0 |
| 8 | 11/16 | 4:20 " | 36 | $3-B_1$ | 1279 | 21.7 | 15.4 |
| 9 | 11/19 | 4:15 " | 36 | 1-2 | 1265 | 22.9 | 12.2 |
| 10 | 11/17 | 4:15" | 37 | A-1 | 1259 | 22.6 | 23.3 |
| 13 | 11/24 | 10:30AM | 30 | 2-3 | 1260 | 10.9 | 40.0 |
| 14 | 11/25 | 4:00PM | 15 | $3_a-B_2$ | 307 | 22.2 | 18.4 |
| 15 | 11/25 | 4:50 " | 15 | $3_a-B_2$ | 307 | 22.9 | 19.4 |

run were approximately the same, falling within the range of 22 to 23 vehicles per minute. It is believed that this approximation should give the relative section capacities correctly, however, they should be verified by simultaneous measurements in future work.

The next question that comes up concerns itself with types of averages that should be taken. For example, it would be desirable to compare section densities and speeds. For this purpose two types of averages were considered. In the first type the average of the density, $K_i$, or the average of the speed, $V_i$ is computed over the entire run; and in the second type, a time-weighted density and a time weighted speed is taken. The second type of average is physically more meaningful since theoretically during a stoppage, vehicles may be stationary in a section for a long time so that the time weight of this density or speed should be taken into account.

These time weighted averages are shown in Figures 4.3a and 4.3b. In Figure 4.3a the section density is plotted for the different sections in the tunnel. The arrows on the lines in the figure indicate the spatial extent between the two observers for each run. For example, in run number 10 one observer was at station A and the other at station 1, the distance between them being 1259 feet.

The plot clearly shows the vehicle density in the tunnel to be higher in the middle section of the tunnel than in the beginning and end sections. In the beginning section, covering the distance between the entrance portal and about 2/3 through the downgrade portion, the observed section density is seen to be considerably lower than that in the middle part of the tunnel. The section density in the last quarter of the tunnel decreases again somewhat from the high values found in the middle. This asymmetry in the measured densities in the different parts of the tunnel should be reflected in the speeds with which vehicles traverse these different sections. Such was found to be the case.

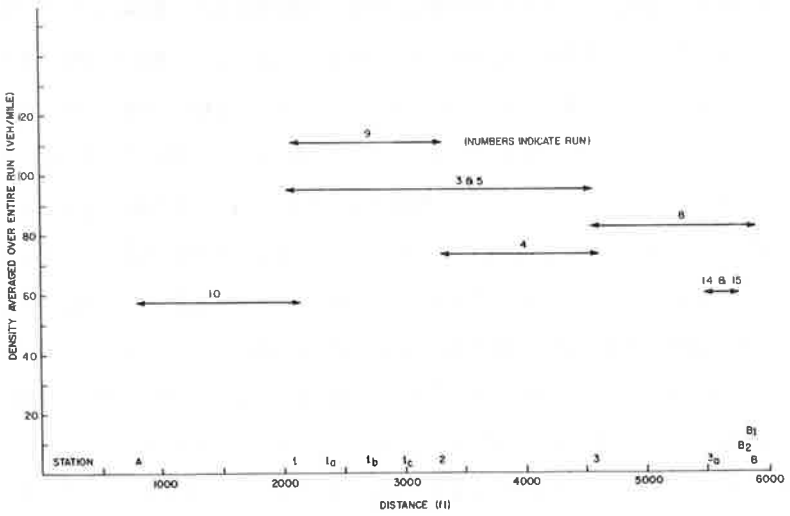


Figure 4.3a.- Section density averaged over entire runs vs. spatial extent of each section.

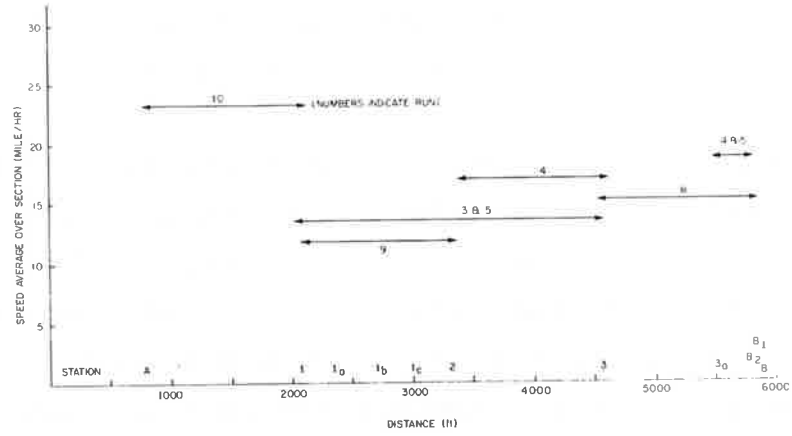


Figure 4.3b.- Section speed averaged over entire run vs. spatial extent of each section.

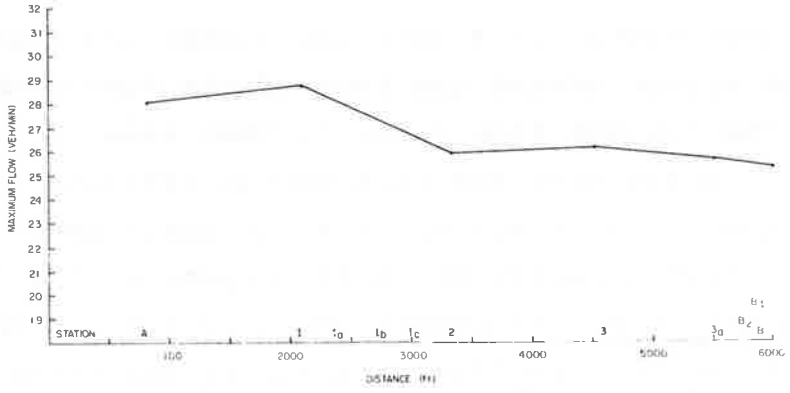


Figure 4.3c.- Maximum one minute flow vs. observation location.

Figure 4.3b shows the time-averaged section speed averaged over the entire run versus the spatial extent of the corresponding section. The plot shows the average section speed to be highest in the beginning section of the tunnel and that the speed drops sharply near the foot of the downgrade and remains low until well into the upgrade, increasing somewhat toward the exit portal. Taking the two figures together, the general trend of density is seen as varying inversely with the speed. A driver upon entering the tunnel soon finds himself in a relatively low density situation, travelling at a nice clip; on reaching the end of the downgrade however, he finds himself in a much more dense traffic situation and travelling at much slower speeds (often having to decelerate rapidly to adjust to the situation, as observed from the catwalk); finally, the driver finds he can begin to pick up a little speed as he gets well into the final quarter of the tunnel where the density of traffic becomes somewhat less than in the center of the tunnel.

The maximum flow at each of these observation stations was determined by taking the data from each run and subdividing the time during the run into one minute intervals. The flow during the minute intervals at the two observation stations were then determined and the maximum minute flow was recorded. For each station a mean value of the maximum minute flows was computed by averaging over all similar runs. The result is shown in Figure 4.3c. The maximum flow capacity increases slightly as one proceeds from the entrance portal at A into the tunnel and then decreases sharply at the region around the foot of the downgrade (around station $l_b$). The maximum flow capacity then remains constant until it decreases slightly near the exit portal (Station B). It thus appears that the Callahan tunnel is a non-homogeneous roadway with a traffic flow capacity which is largest in the first quarter of the tunnel where the speeds are also highest and the densities lowest; the traffic flow capacity of the tunnel decreases sharply near the foot of the downgrade and remains relatively

constant except for a slight decrease in the last quarter. The graphs show, then, that an effective bottleneck exists beyond the downgrade section where the capacity drops rapidly, the density rises, and the speed falls.

This information on the capacities of the various sections is essential for assigning proper weight to sensor-measured densities and speeds when these are to be used in determining certain controls on input traffic.

### 4.2.5 Q-K Relations

In addition to having these section density, speed, and maximum flow plots to determine the relative magnitudes of the different section speeds, densities and flows, it is also important to obtain the individual Q-K and V-K relations for each section. With these relations it could be seen directly whether the flows and speeds for the individual sections were occurring for densities below or above optimum, and if these relationships between flow, speed and density were functionally the same in the different sections. This is important in establishing the different sensitivities of the sections to imposed changes in density and flow. If the density in a section consistently measures well below $k_m$, then the section obviously can handle a higher input of vehicles without causing unstable traffic flow; on the other hand for a section in which the flows are consistently around the transition point, even slight increases in density could make the traffic unstable; similarly if the speed varies only slightly with density in one section while it does so rapidly in another, changing the density will have different effects on the speeds in the two sections. It is well to compare the different sections, bearing in mind, however, that the sections are not independent but form a coupled system. The different Q-K curves are shown in Figures 4.4 through 4.11.

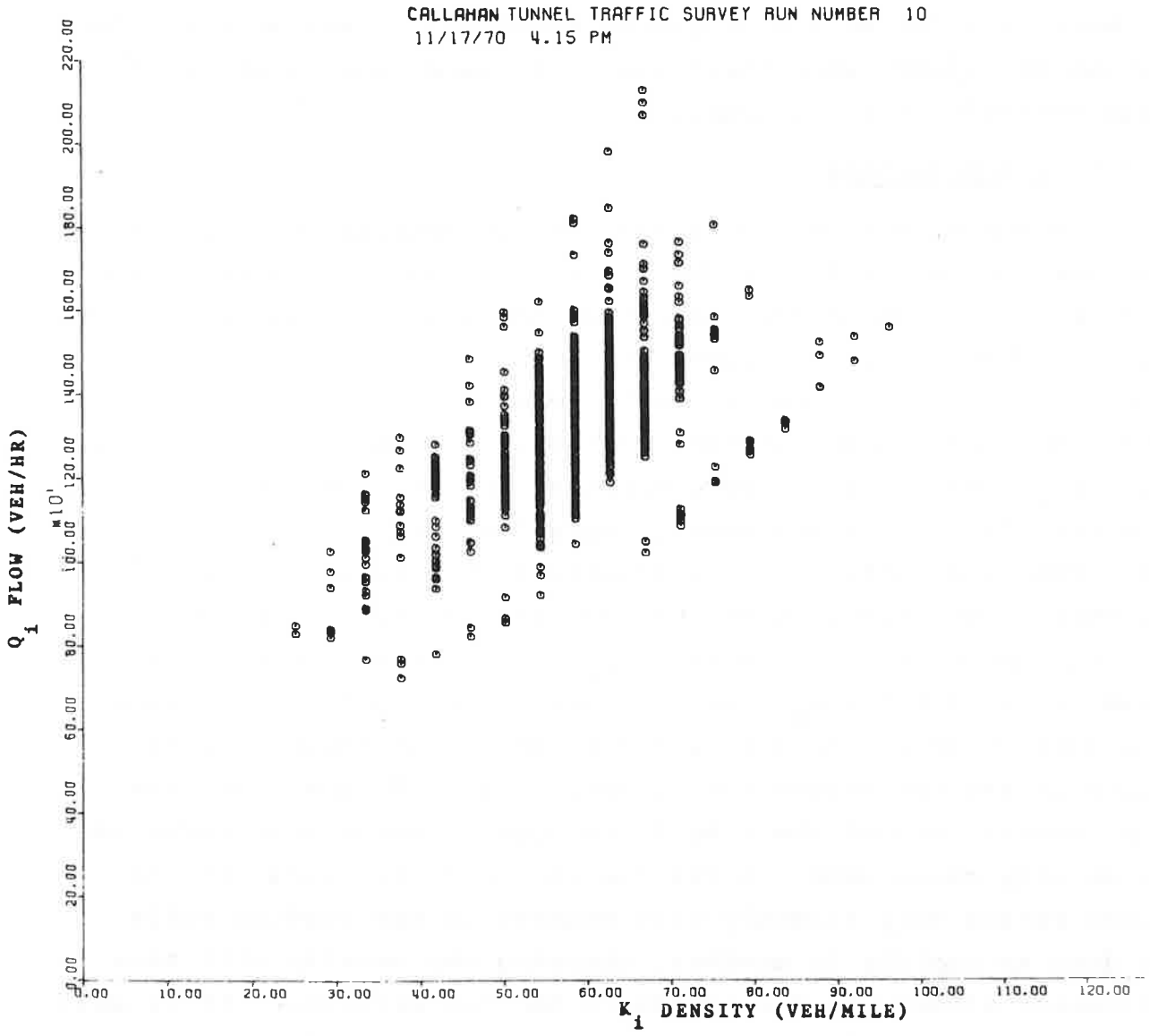


Figure 4.4a.- Run #10: Flow averaged over the transit time, $Q_i$, vs average section density, $K_i$, stations A to 1. Distance of 1259 ft.

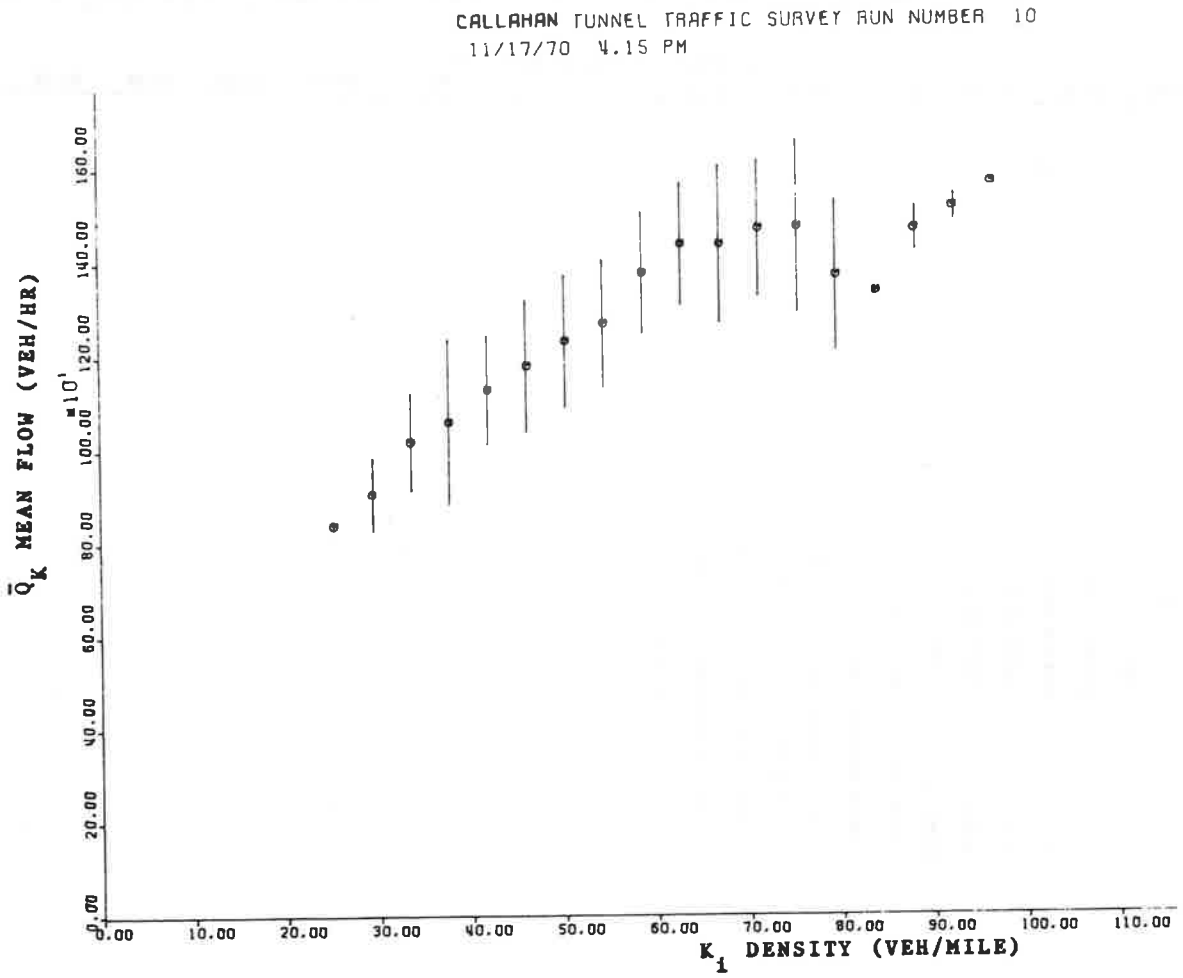


Figure 4.4b.- Run #10: Mean flow for a given section density, $\bar{Q}_K$, vs the density, $K_i$, stations A to 1. Distance of 1259 ft.

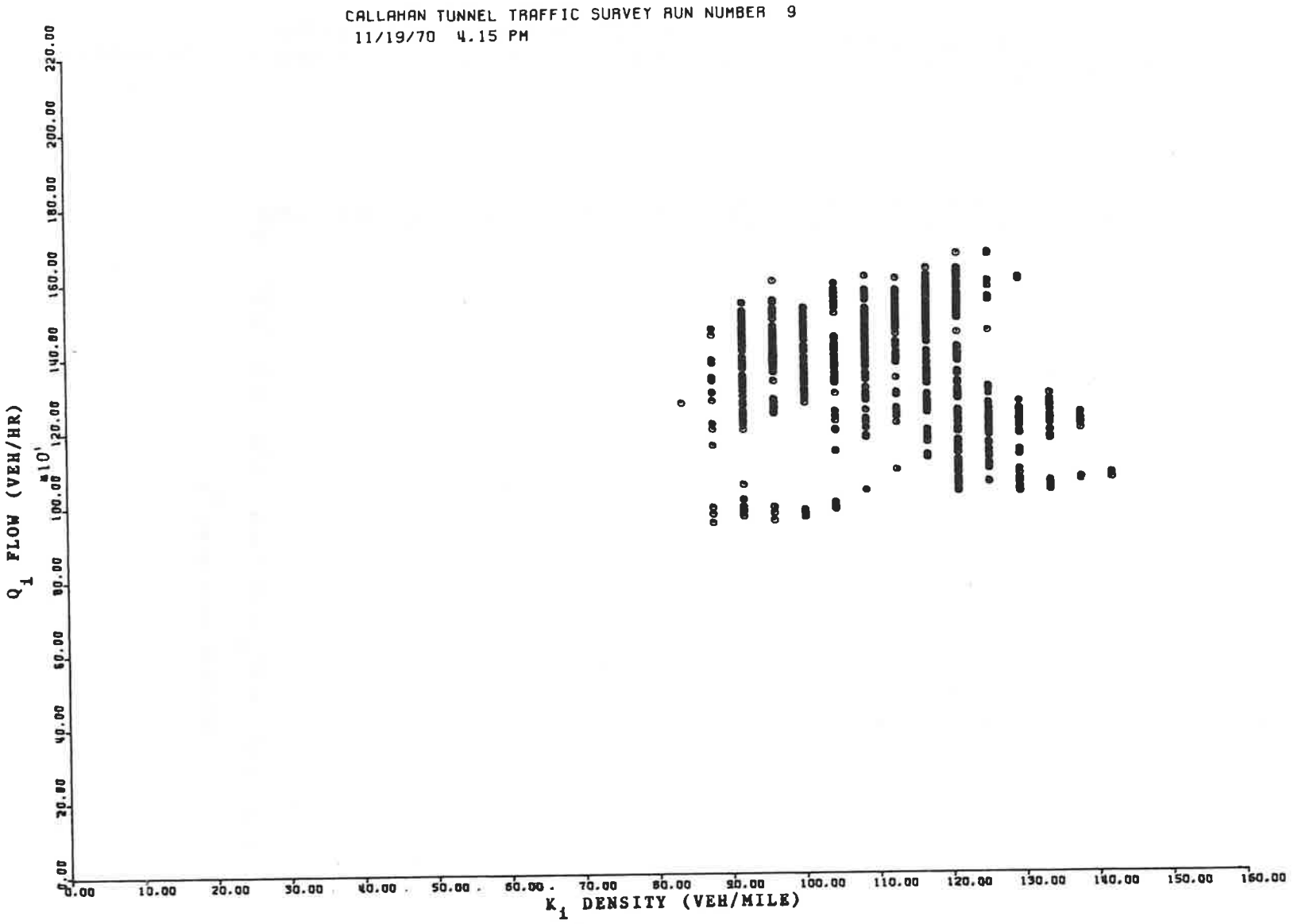


Figure 4.5a.- Run #9: Flow averaged over the transit time $Q_i$, vs average section density, $K_i$, stations 1 to 2. Distance of 1265 ft.

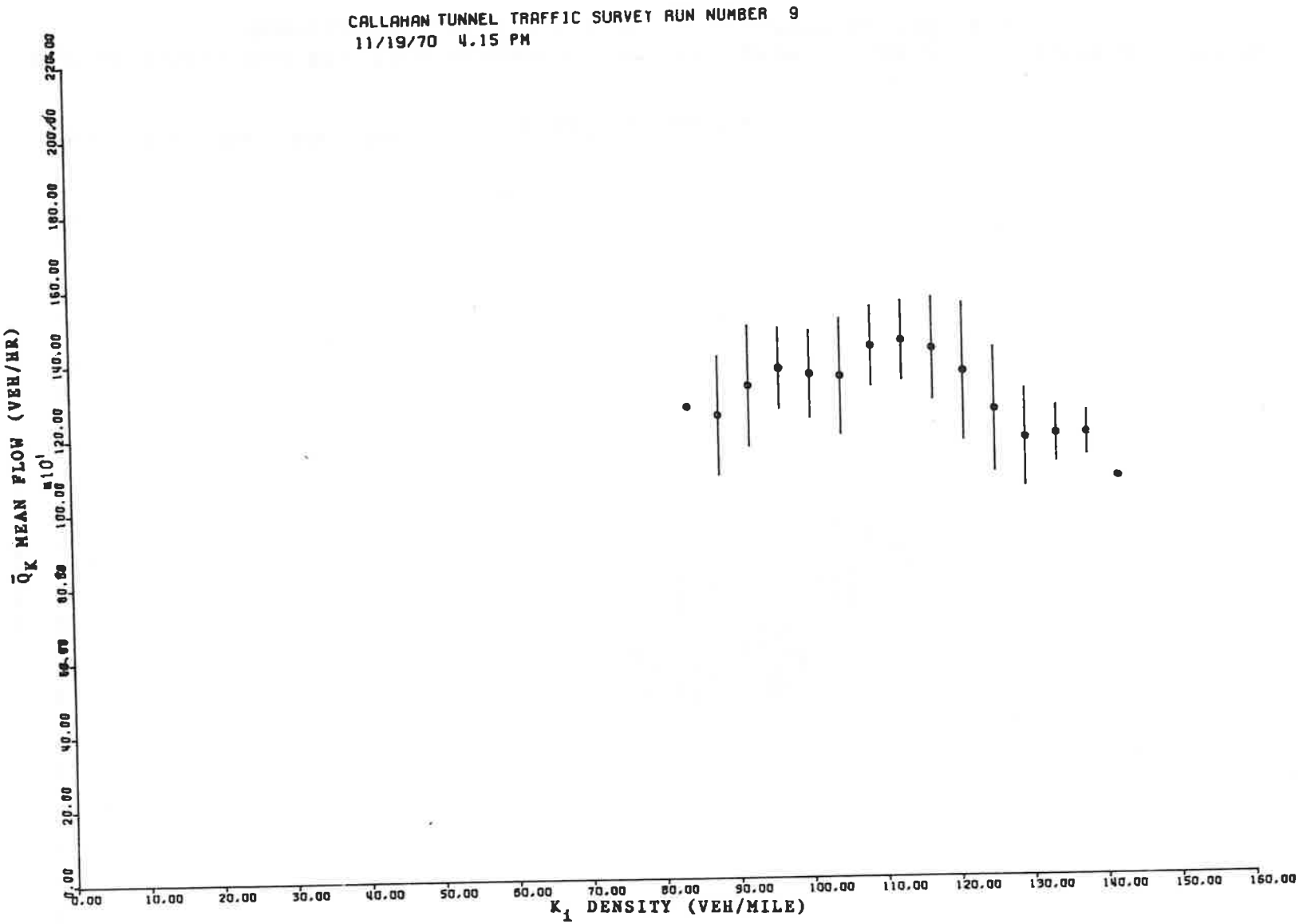


Figure 4.5b.- Run #9: Mean flow for a given section density, $\bar{Q}_K$, vs the density, $K_i$, stations 1 to 2. Distance of 1265 ft.

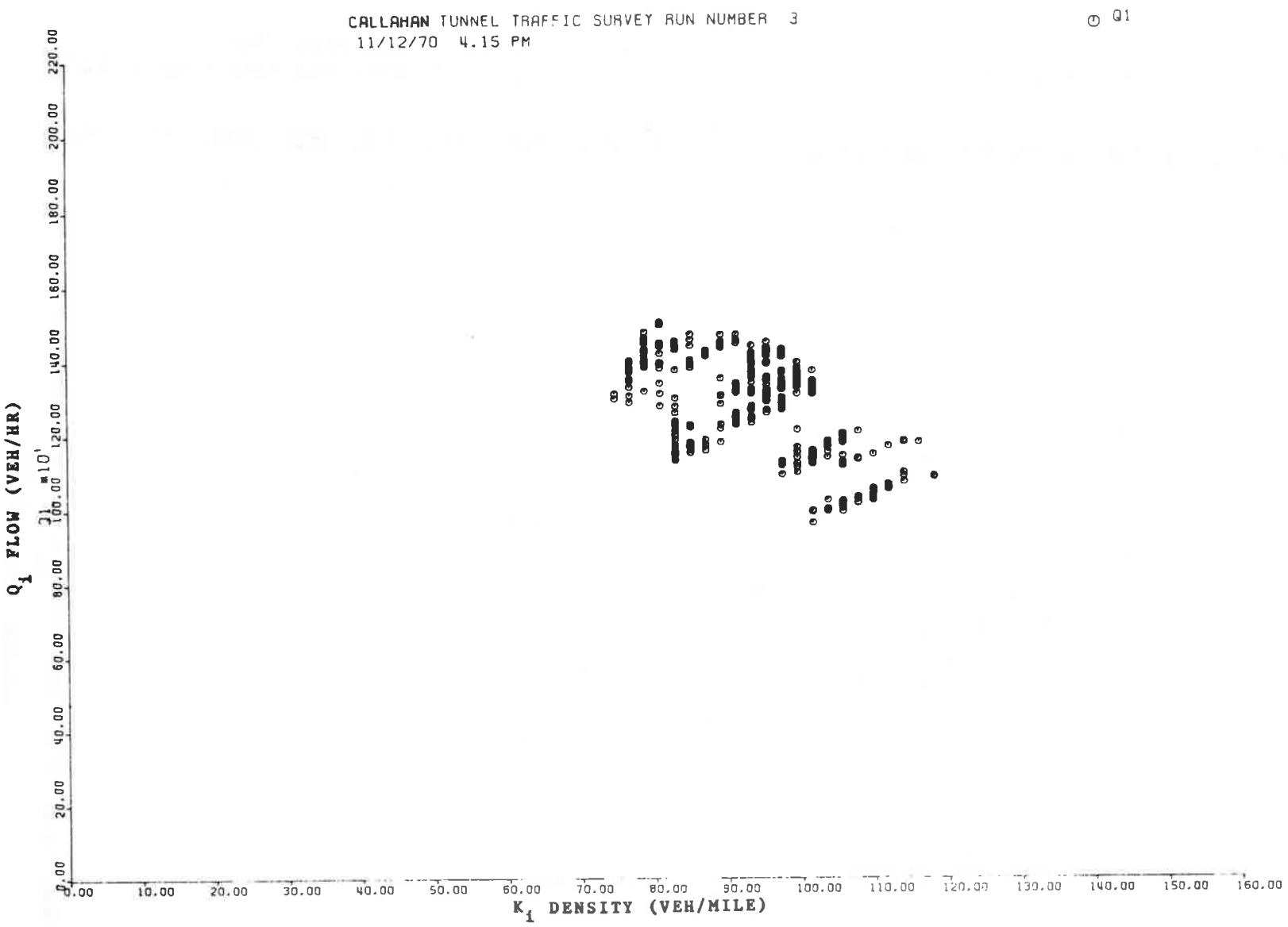


Figure 4.6a.- Run #3: Flow averaged over the transit time $Q_i$, vs average section density, $K_i$, stations 1 to 3. Distance of 2550 ft.

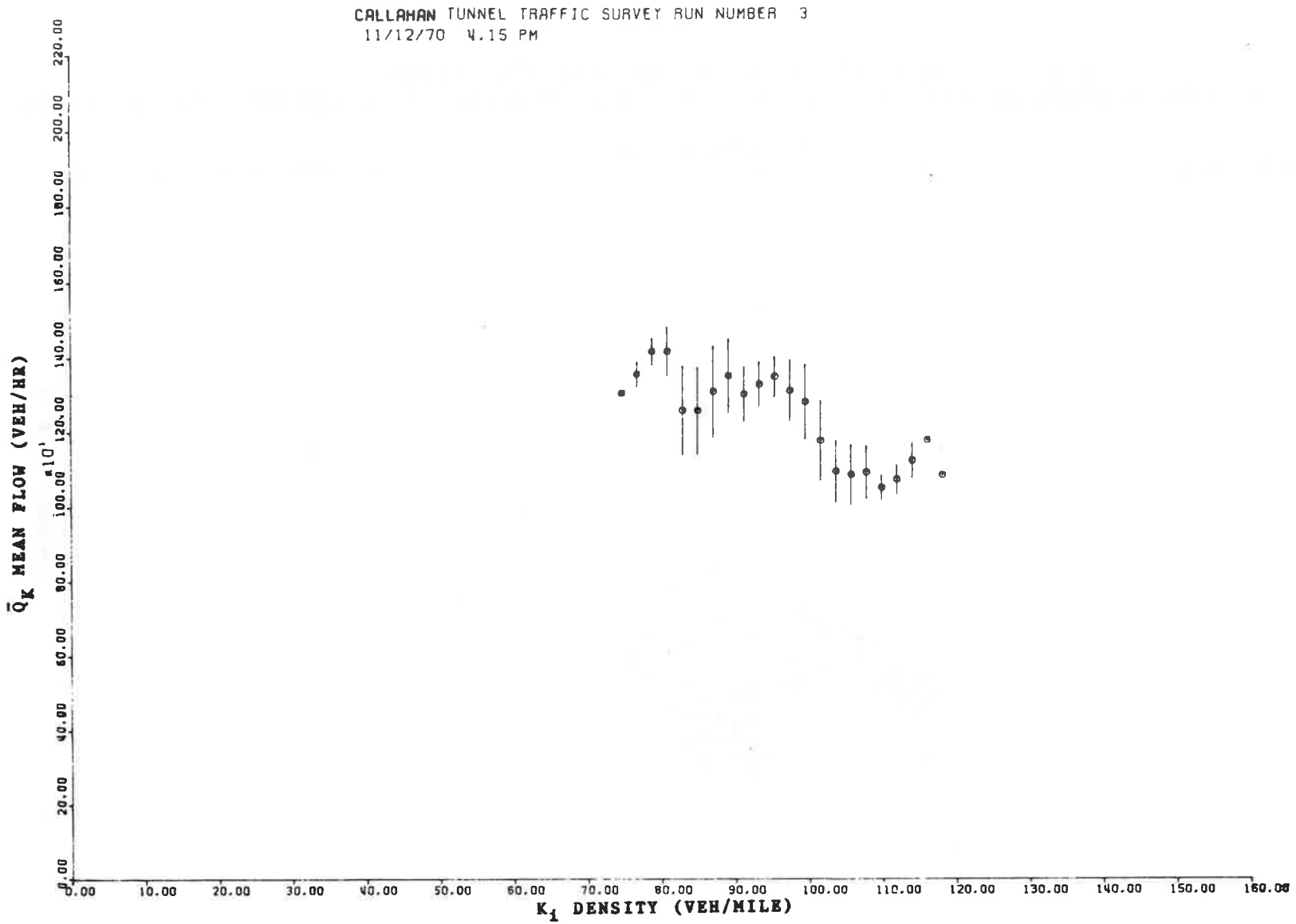


Figure 4.6b.- Run #3: Mean flow for a given section density, $\bar{Q}_K$, vs the density $K_i$, stations 1 to 3. Distance of 2550 ft.

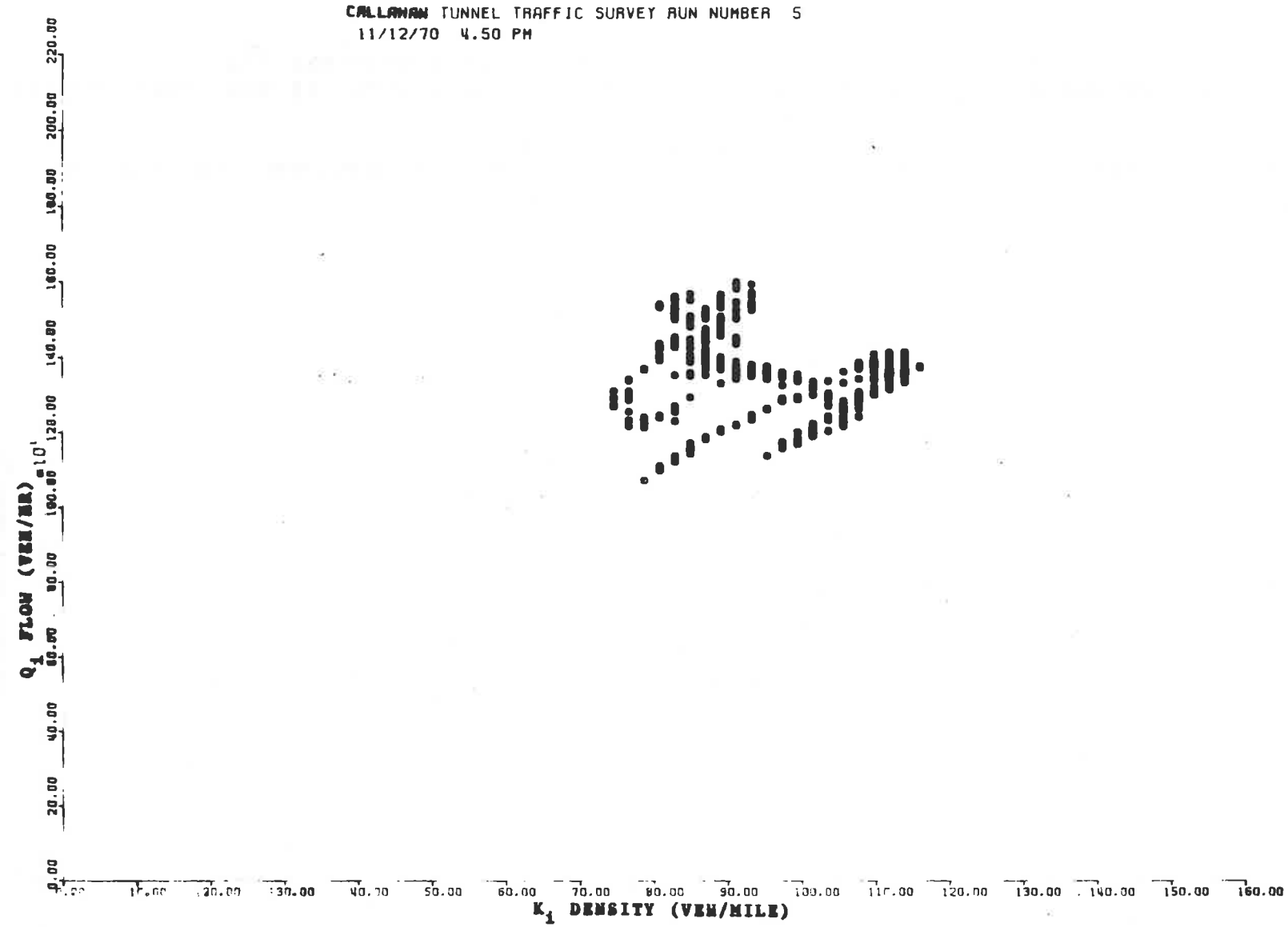


Figure 4.7a.- Run #5: Flow averaged over the transit time, $Q_i$, vs average section density, $K_i$, stations 1 to 3. Distance of 2550 ft.

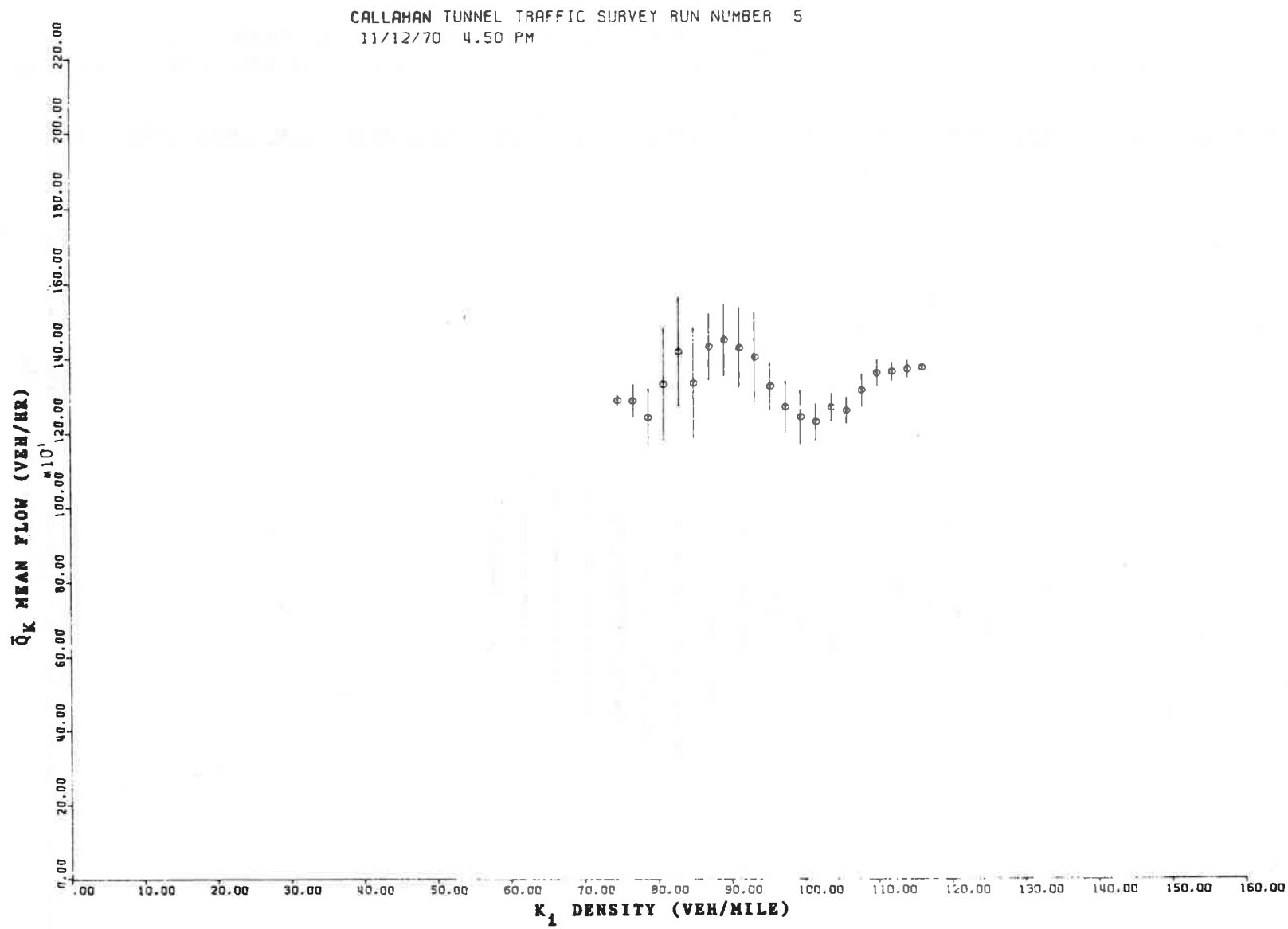


Figure 4.7b.- Run #5: Mean flow for a given section density, $\bar{Q}_K$, vs. the density, $K_i$, stations 1 to 3. Distance of 2250'.

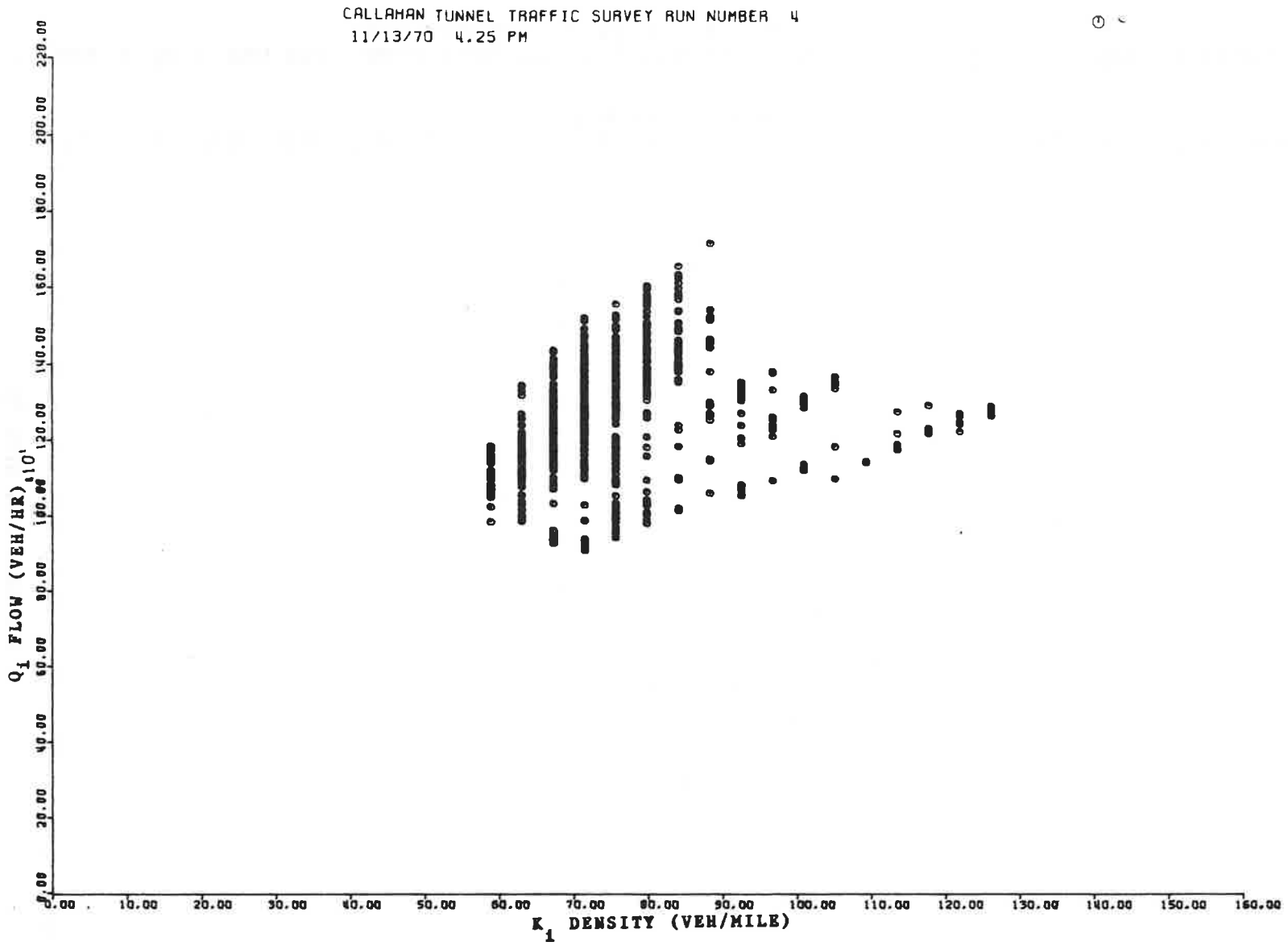


Figure 4.8a.- Run #4: Flow averaged over the transit time, $Q_i$, vs. averaged section density $K_i$, stations 2 to 3. Distance of 1260'.

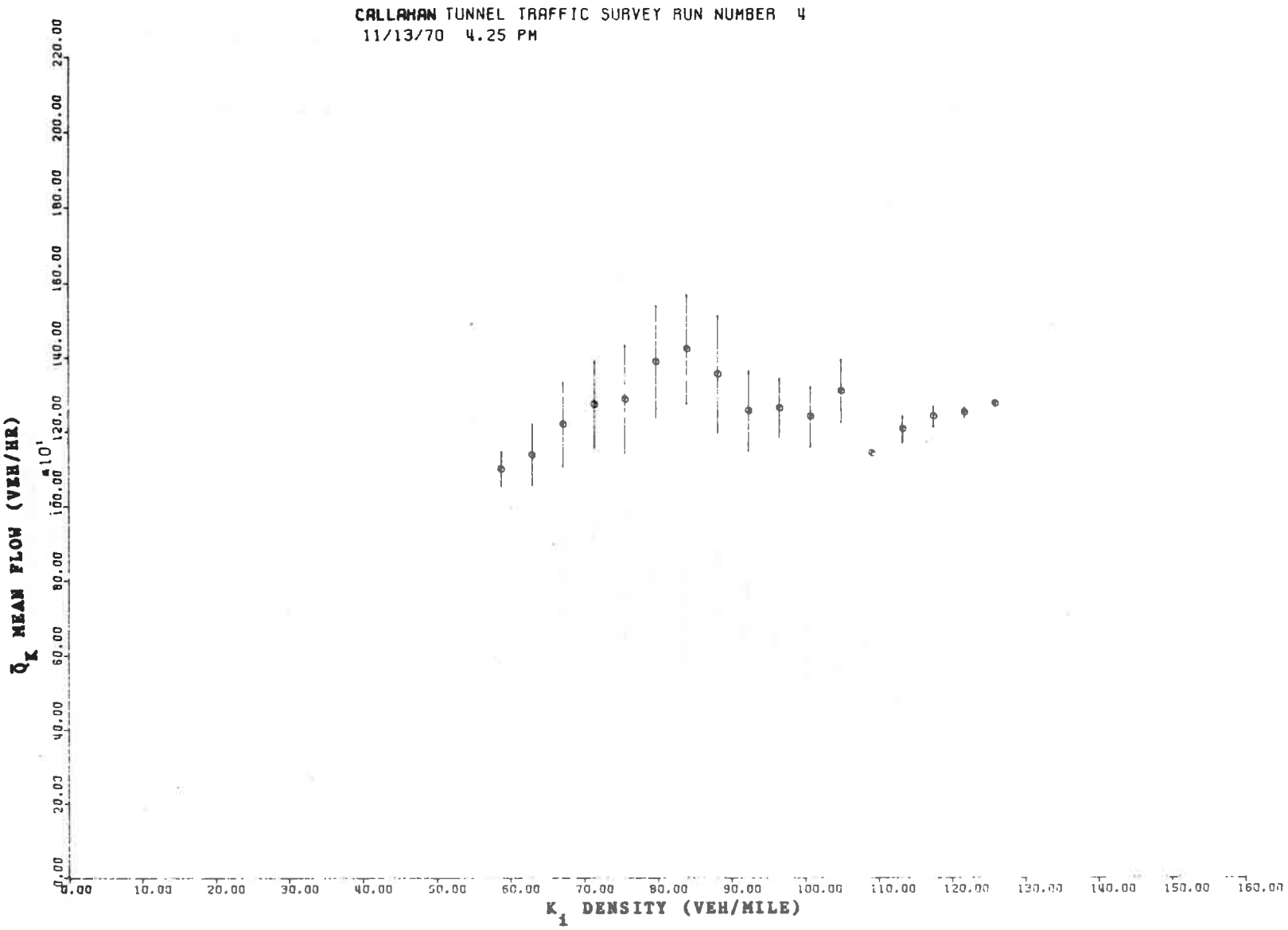


Figure 4.8b.- Run #4: Mean flow for a given section density, $\bar{Q}_k$, vs. the density, $K_i$, stations 2 to 3. Distance of 1260'.

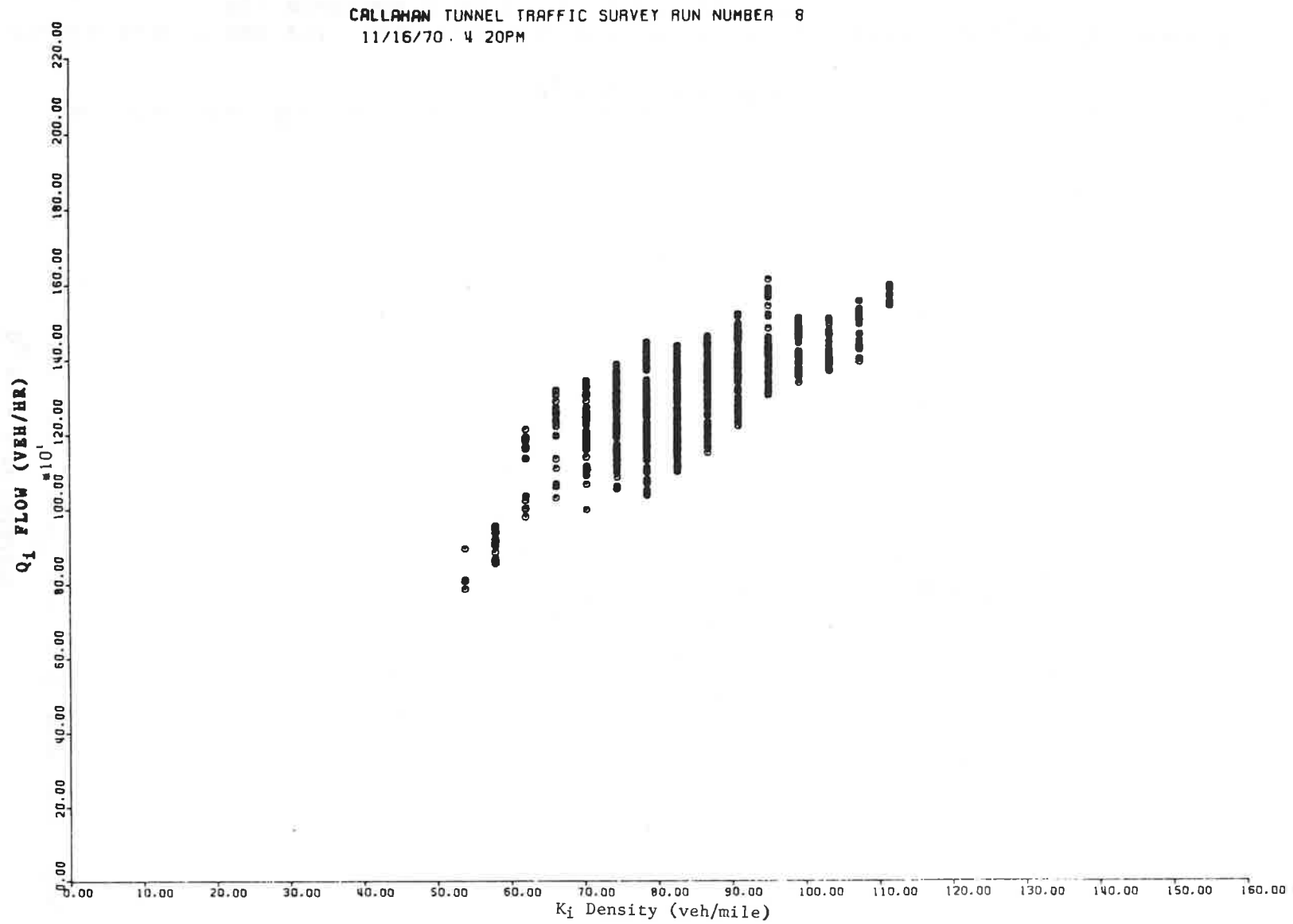


Figure 4.9a.- Run #8: Flow averaged over the transit time, $Q_i$, vs. average density, $K_i$, stations 3 to $B_1$. Distance of 1279'.

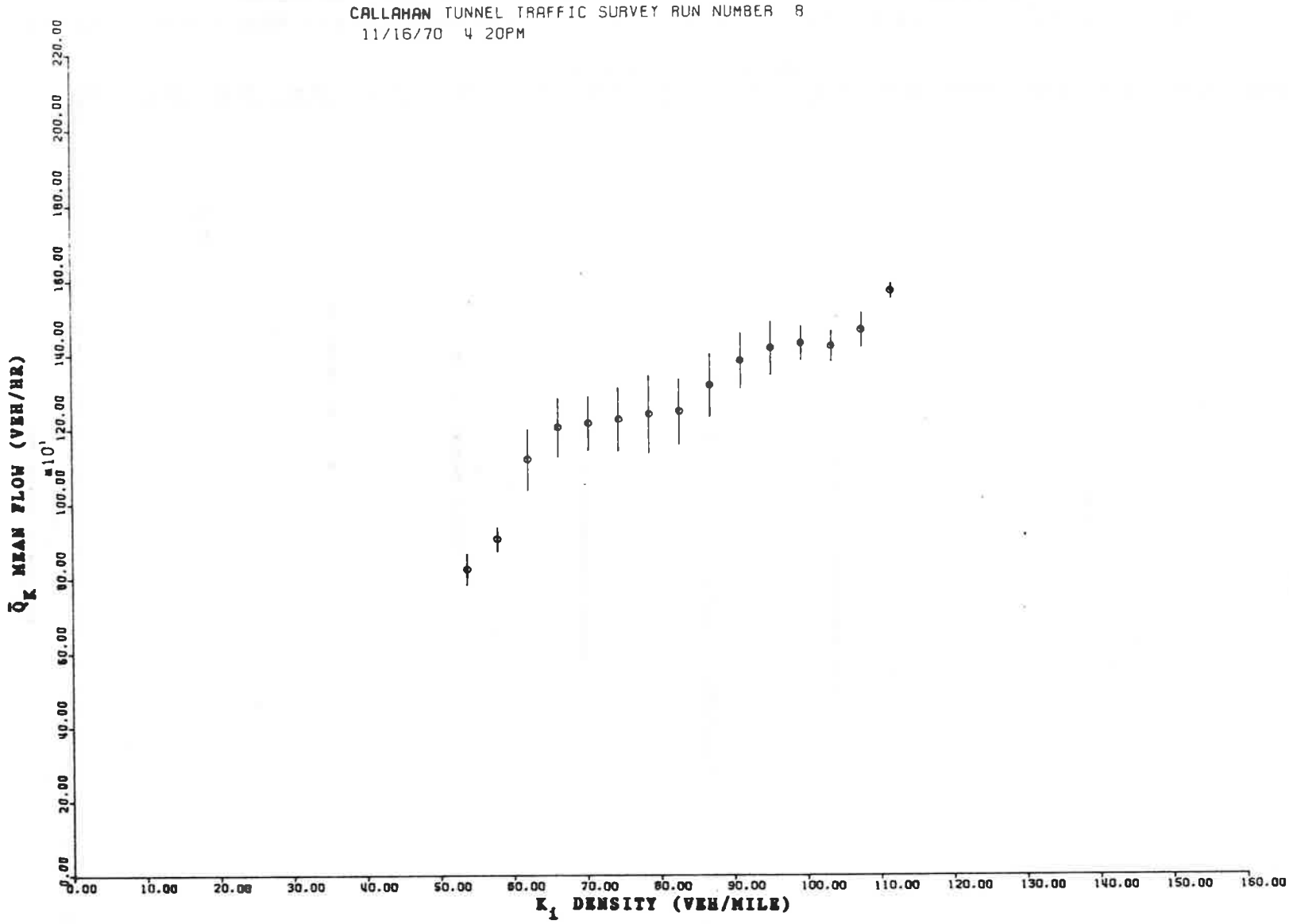


Figure 4.9b.- Run #8: Mean flow for a given section density, $\bar{Q}_k$, vs. the density, $K_i$, stations 3 to $B_1$. Distance of 1279'.

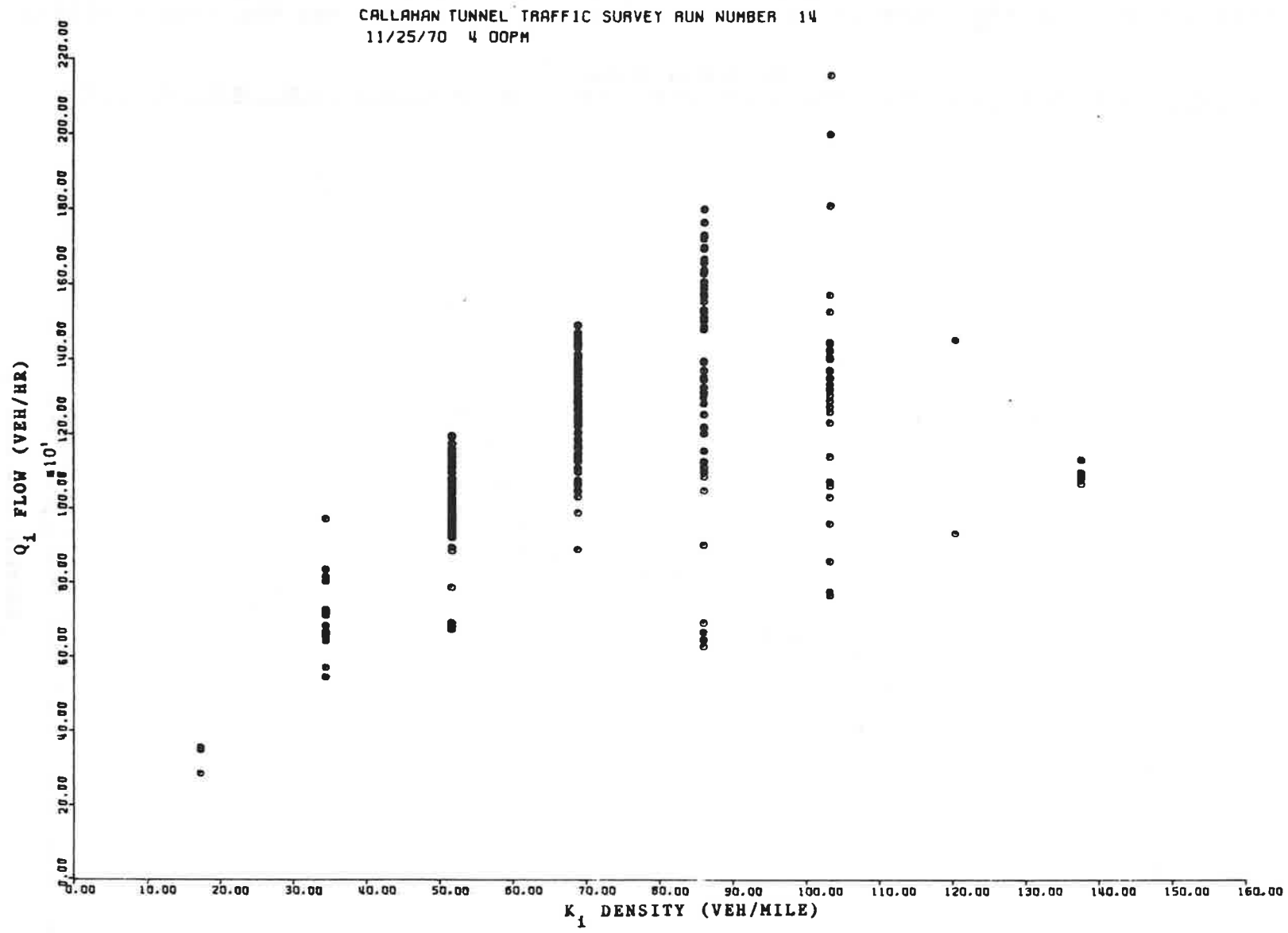


Figure 4.10a.- Run #14: Flow averaged over the transit time, $Q_i$, vs. average section density, $K_i$, stations $3_a$ to $B_2$. Distance of 307.3'.

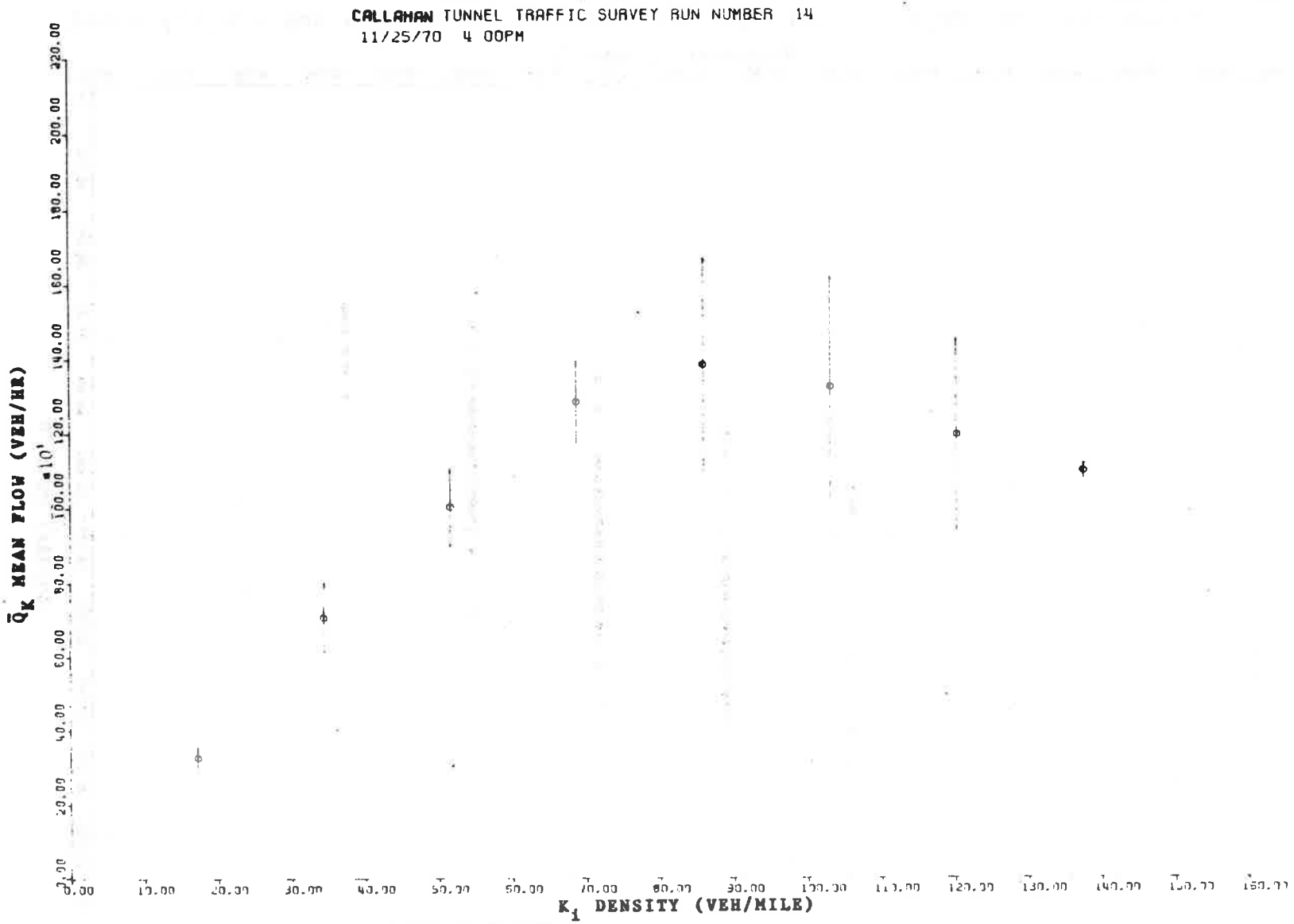


Figure 4.10b.- Run #14: Mean flow for a given section density, $\bar{Q}_k$, vs. the density $K_i$ stations $3_a$ to $B_2$. Distance of 307.3'.

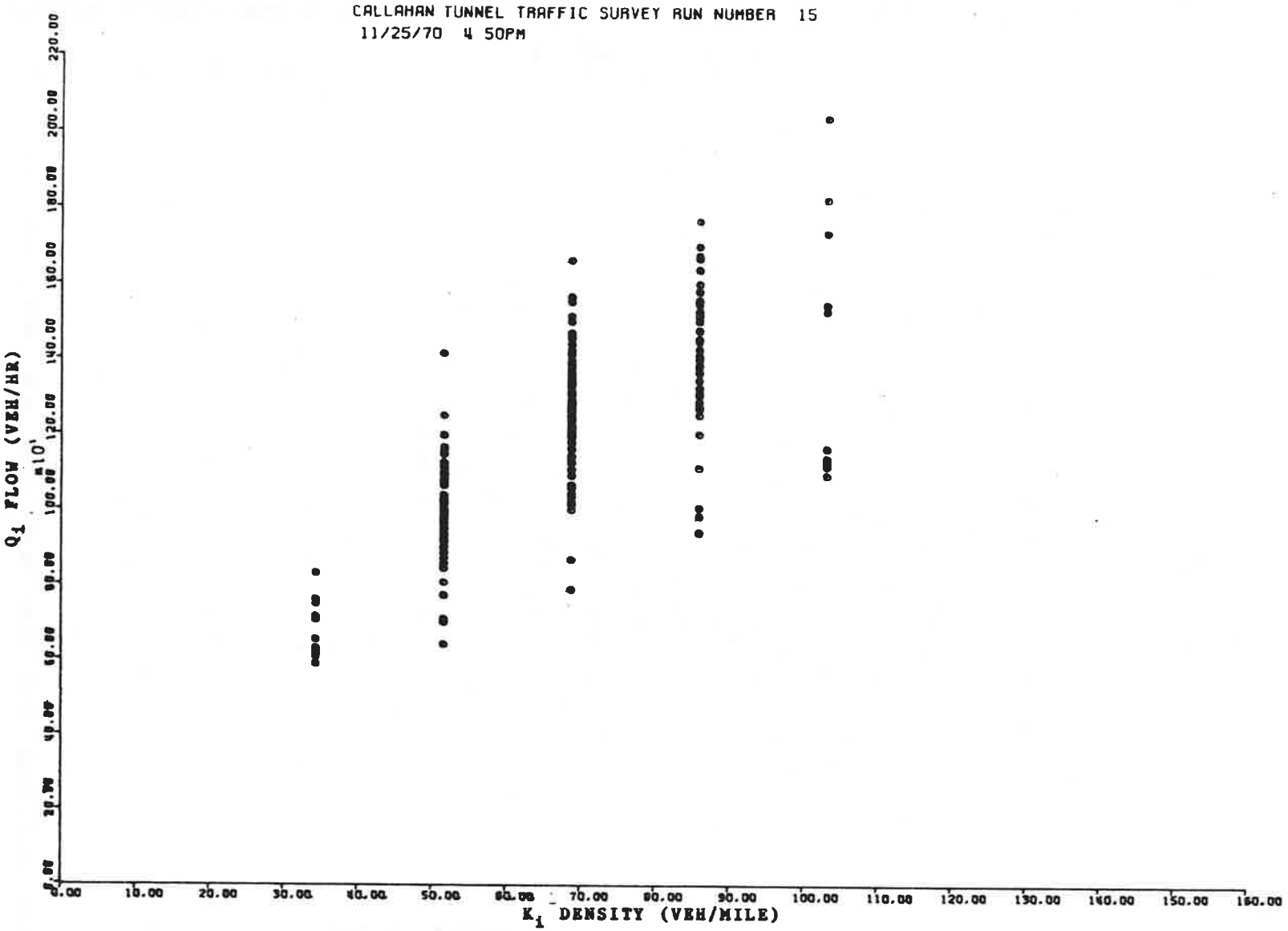


Figure 4.11a.- Run #15: Flow averaged over the transit time, $Q_i$, vs. average section, density, $K_i$, station $3_a$ to $B_2$. Distance of 307.3

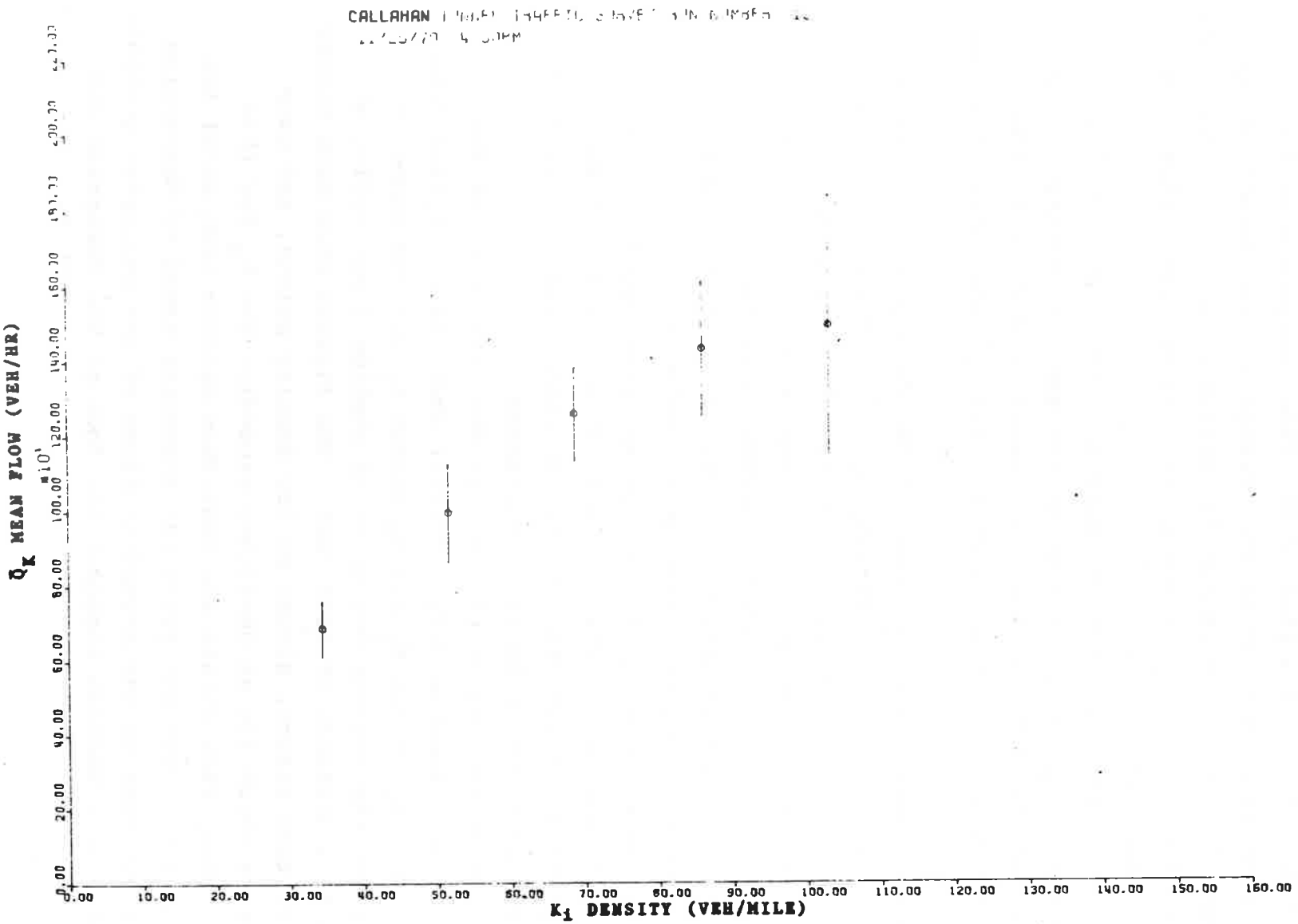


Figure 4.11b.- Run #15: Mean flow for a given section density $\bar{Q}_k$, vs. the density, $K_i$, stations $3_a$ to $B_2$.

Figure 4.4a gives a plot of the flow averaged over the transit time as a function of the average section density $K_i$ for run number 10. This run is for the beginning section of the tunnel extending from the entrance portal at A to station number 1, a total distance of 1259 feet.

Figure 4.4b gives, for the same run, the mean flow for a given density, $\bar{Q}_K$, as a function of the section density $K_i$; the vertical line through the mean flow point extends $\pm\sigma$ in length, $\sigma$ being the standard deviation of the flow points having the same density.

These figures show that most of the data points lie to the left of an optimum section density $k_m \simeq 75$ vehicles per mile, that the flows are generally rising and the section may be characterized as non-congested and even under-utilized. Physically, this section is on a 3.8 percent downgrade; the entrance portion of the section accepts vehicles which have slowed down or have come to a complete stop at the entrance to the tunnel. The result is a number of large gaps and high speeds as the vehicles get into the section. There is a bend in the road at the very end of this section which may contribute to a slowing down there as the next section is entered.

This next section of the tunnel, the first half of the middle section, shows a very different character. Figures 4.5a and 4.5b show $Q_i$ versus $K_i$ and $\bar{Q}_K$ versus $K_i$ for run number 9 which is for the section beginning at station 1 and ending at station 2, a distance of 1265 feet. The figures show much higher densities than before, almost no low density points, and many data points which lie at densities exceeding the $k_m$ for this section. Many flow points are less than optimum because of the high densities. The Q-K curve has a greater trend of descending flows in contrast to the ascending flows of the beginning section. Physically this section includes the foot of the downgrade and

most of the *straightaway*. It must absorb the low density high speed vehicles from the downgrade and is unable to do so without experiencing congestion and slowdowns.

It is interesting to speculate that the functional relationship between flow and density itself may be different in the two sections. In the first section the $k_m$ is around 75 vehicles/mile, while in the second a much larger $k_m$ seems to exist (if it did not, then the high densities experienced would undoubtedly lead to extremely low flows). The "optimum" density for this section may be as high as 110 vehicles/mile. Of course, the concept of an optimum density must be questioned as this assumes that one maximum flow exists for one value of the density. As we have seen (Section 2) flow is at least a function of $\dot{k}$, the time derivative of the density, as well as the density itself, and therefore a single valued relationship between flow and density does not exist. But whether a single optimum density is considered as only an ideal or not, it is clear that the functional relation between flow and density must be different in the two sections when based on the density alone. A comparison of Figures 4.4 and 4.5 for the two sections, in fact, suggests that this is the case.

The full middle section, from station 1 to 3, is covered in the next two figures (Figures 4.6 and 4.7) in which $Q_i$ and $\overline{Q}_K$ versus $K_i$ are plotted for runs number 3 and number 5.

The figures show a character similar to run number 9 which was for just the first half of the middle section, but somewhat less extreme. There are still a substantial number of data points for large densities, not too many instances of low density, and generally decreasing rather than increasing flows as also occurred in run number 9. The degree to which these occur over the full middle section, however, is less severe.

The second half of the middle section by itself is shown in Figures 4.8a and 4.8b. The Q-K curves in this case are for run number 4. We note that the curves are now much less extreme than run number 9 suggesting that the downgrade portion of the middle section (run number 9) is most congested, while the upgrade portion of the middle section (this run) is becoming less so. While a considerable number of data points still lie at larger densities, they are much fewer than in runs 9,3 and 5. The congestion is decreasing and the flow increasing as the end section is approached. However, note that even here as in runs numbers 9, 3 and 5, there are few or no flows exceeding 1600 vehicles/mile while there are over 30 such data points for run number 10. This corroborates Figure 4.3c which showed that the beginning section had the largest maximum flow.

As we approach the last quarter of the tunnel, again a different character of the flow-density relation emerges. This is run number 8 shown in Figures 4.9a and b which covers stations 3 to the exit portal and is on the upgrade. Here the flow increases with density with no obvious turning to lower flows. This type of behavior resembles that at the beginning section, run number 10. Runs 14 and 15, Figures 4.10 and 4.11, taken in the last 300 feet of this section, further show this reverting of the flow-density relation to that of the beginning section, (the greater spread in flows in 14 and 15 is due to the shorter section and hence shorter averaging time there). In general then, it appears that the congestion which appeared in the second quarter of the tunnel has mostly dissipated by this fourth quarter, and the flows begin to resemble those at the beginning of the tunnel.

It is interesting to point out here that the shape of the Q-K curve in run number 8 (end section), approximates that coming from a location downstream of the upgrade bottleneck,

resembling the data of Edie and Foote for a similar location in the Lincoln tunnel in New York (ref. 20).

It may be noted that a bottleneck, other than the congestion in the middle sections of the tunnel, does show up in the data quite clearly in run number 14. Every once in awhile a back up from the toll booths occurs, and this shows up as a shock wave producing a number of low flow points at high densities, as seen towards the end of run number 14. (See Figure 4.10.)

4.2.6 V-K Relations

This profile of the tunnel can now be supplemented with a brief comparison of the velocity-density relations (V-K relations) for the different sections. These are plotted in Figures 4.12 to 4.19, where both $V_i$, the time weighted average speed of a vehicle traversing the section and $\overline{V}_K$, the mean of the values of $V_i$ for a given $K_i$ are plotted as a function of $K_i$.

In glancing at Figures 4.12 through 4.19, it can be learned that the greatest spread in speeds occurs at the beginning section (run number 10, Figure 4.12) where the speeds vary from about 35 mph to 16 mph over a density range of about 30 vehicles/mile to 90 vehicles/mile (vpm). This variation is in reasonable agreement with the theoretical logarithmic V-K relation discussed in Section 2. The wide variation in densities is probably caused by the ease with which gaps may form at the entrance to this section, as discussed before: The wide speed variation with density is a result of the low densities present here (where the speeds vary more strongly with density) and the physical ease with which vehicles may speed down the downgrade when the density permits. Vehicular traffic in this section, then, while having the widest variation in speeds and one of the widest variations in density of all the sections, very rarely finds itself "crawling" because of congested conditions - in agreement with our findings previously.

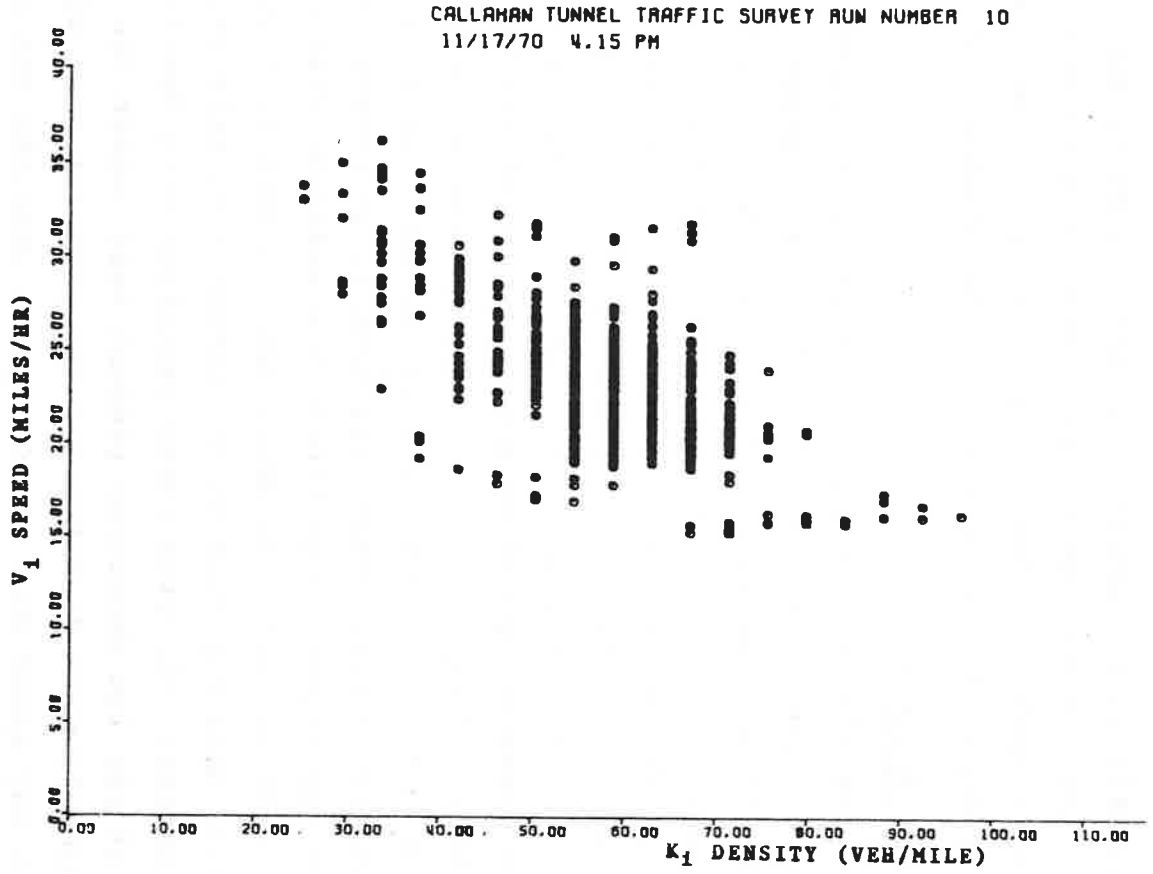


Figure 4.12a.- Run #10: Average speed over a Section, $V_i$, vs. section density, $K_i$, stations A to 1. Distance of 1259'.

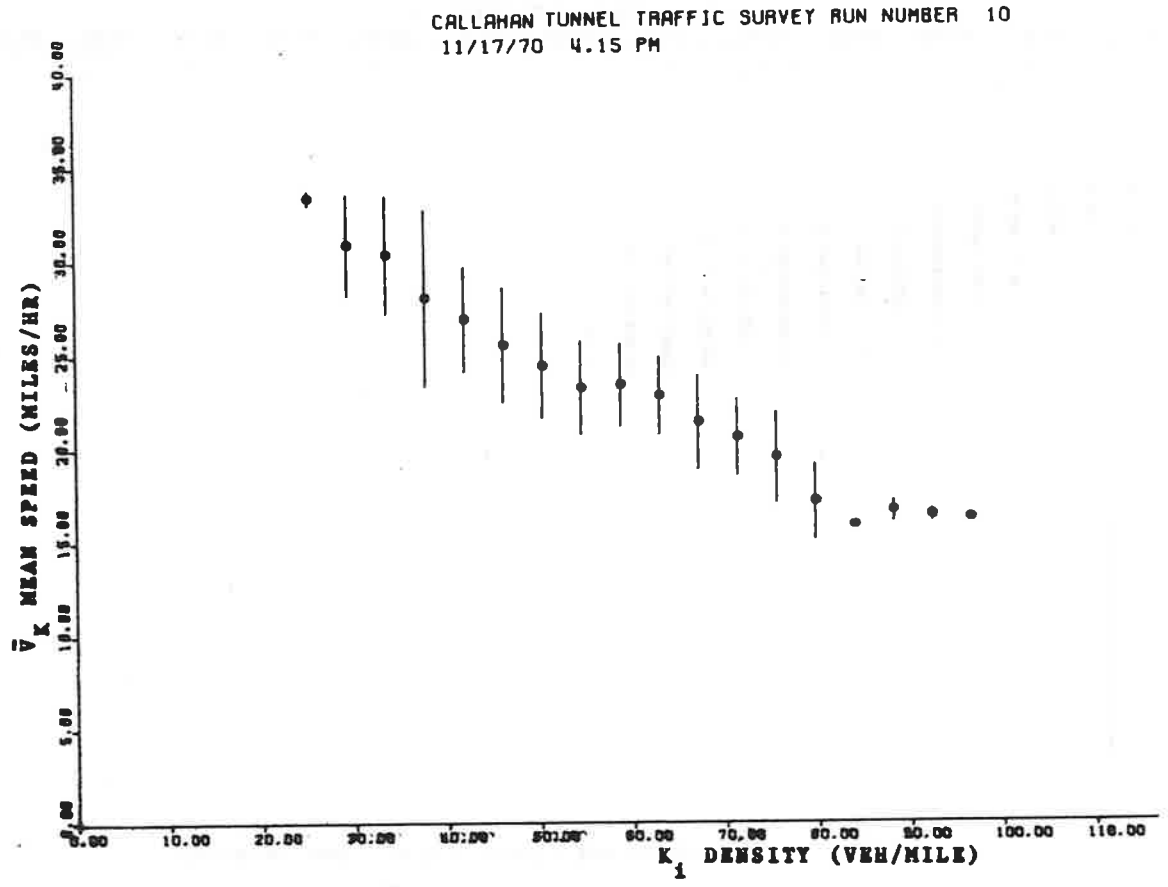


Figure 4.12b.- Run #10: Mean speed for a given density, $\bar{V}_k$, vs. the density $K_i$, stations A to 1. Distance of 1259'.

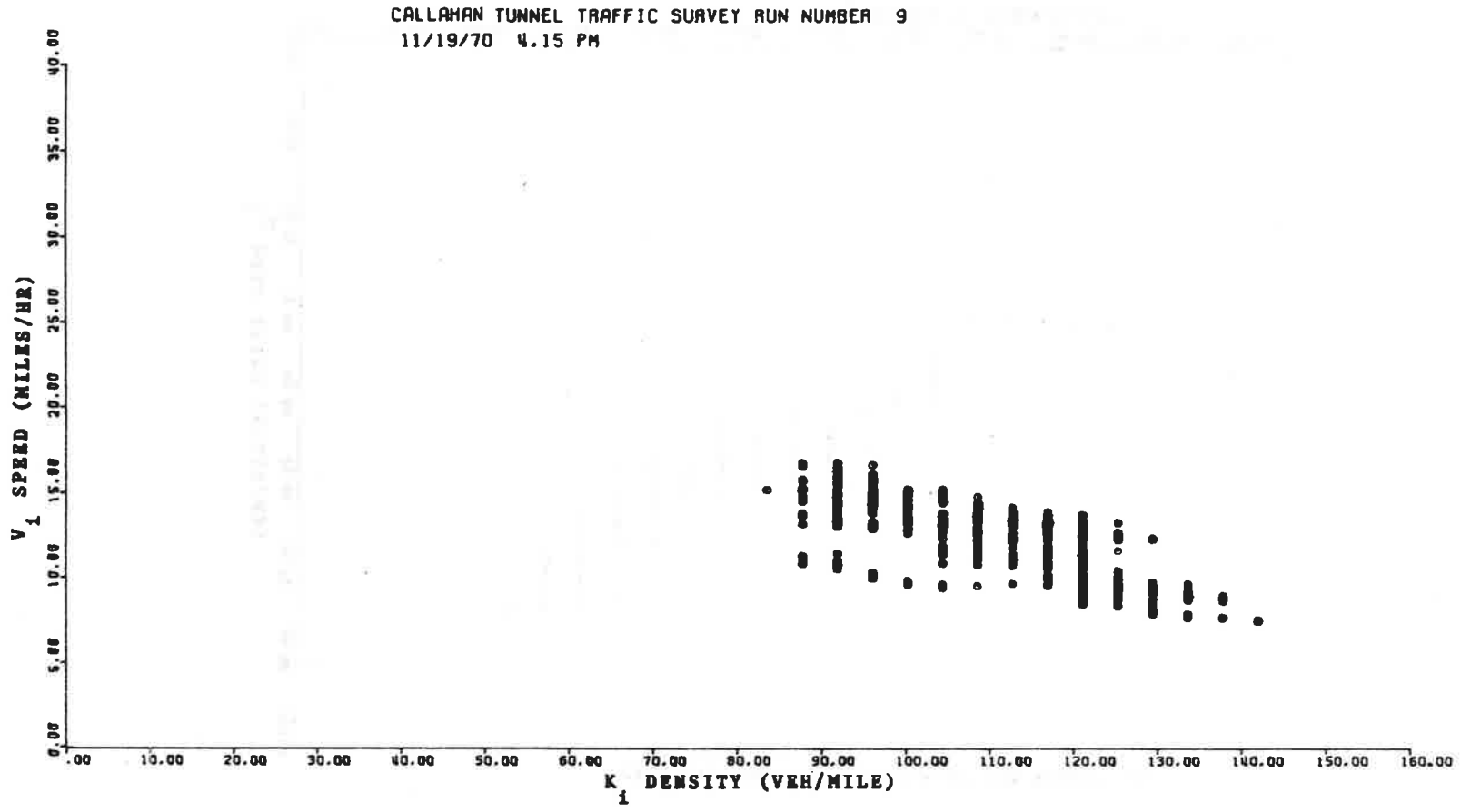


Figure 4.13a.- Run #9: Average speed over a section $V_i$, vs. section density $K_i$, stations 1 to 2. Distance of 1265'.

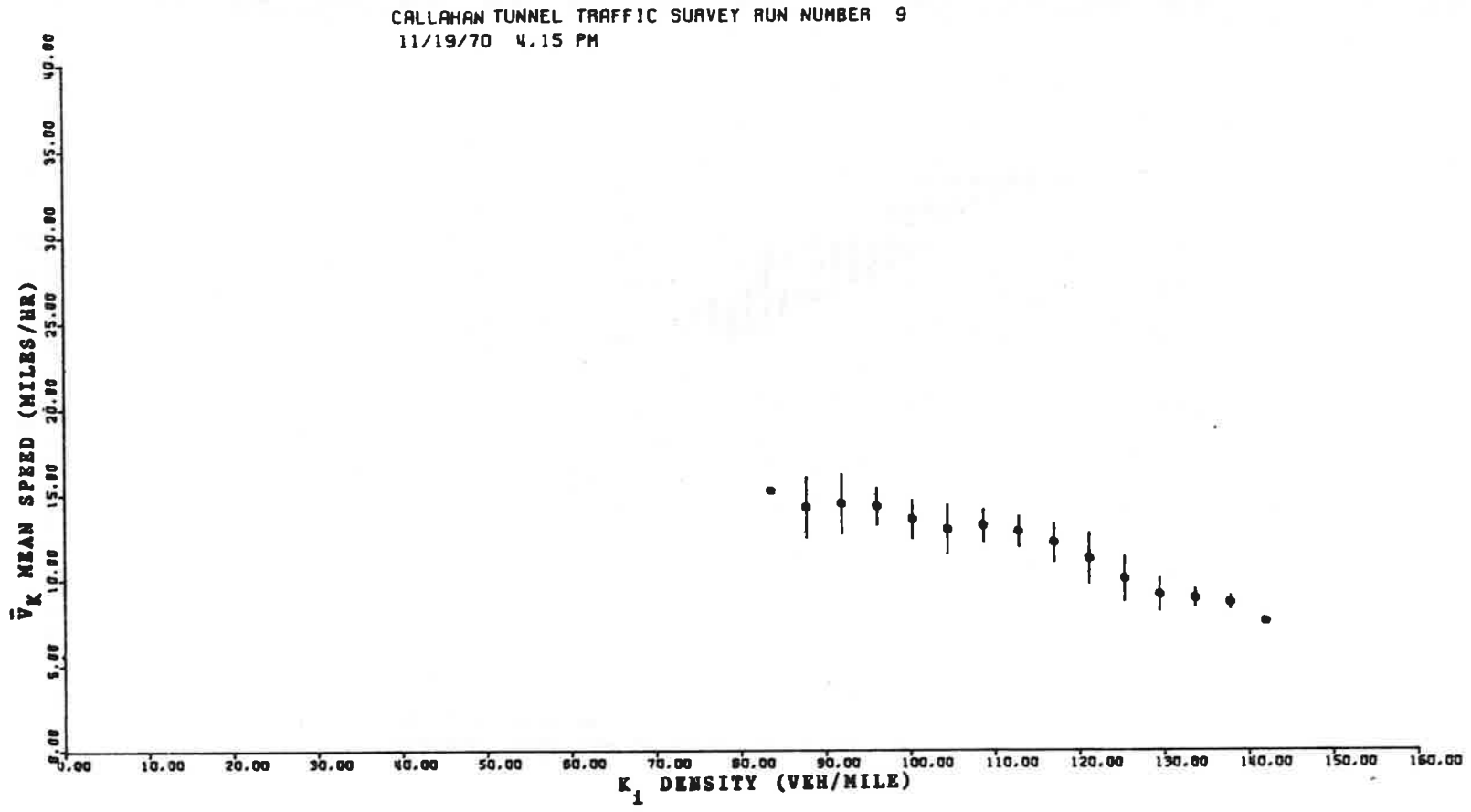


Figure 4.13b.- Run #9: Mean speed for a given density, $\bar{V}_k$, vs. the density $K_i$, Stations 1 to 2. Distance of 1265'.

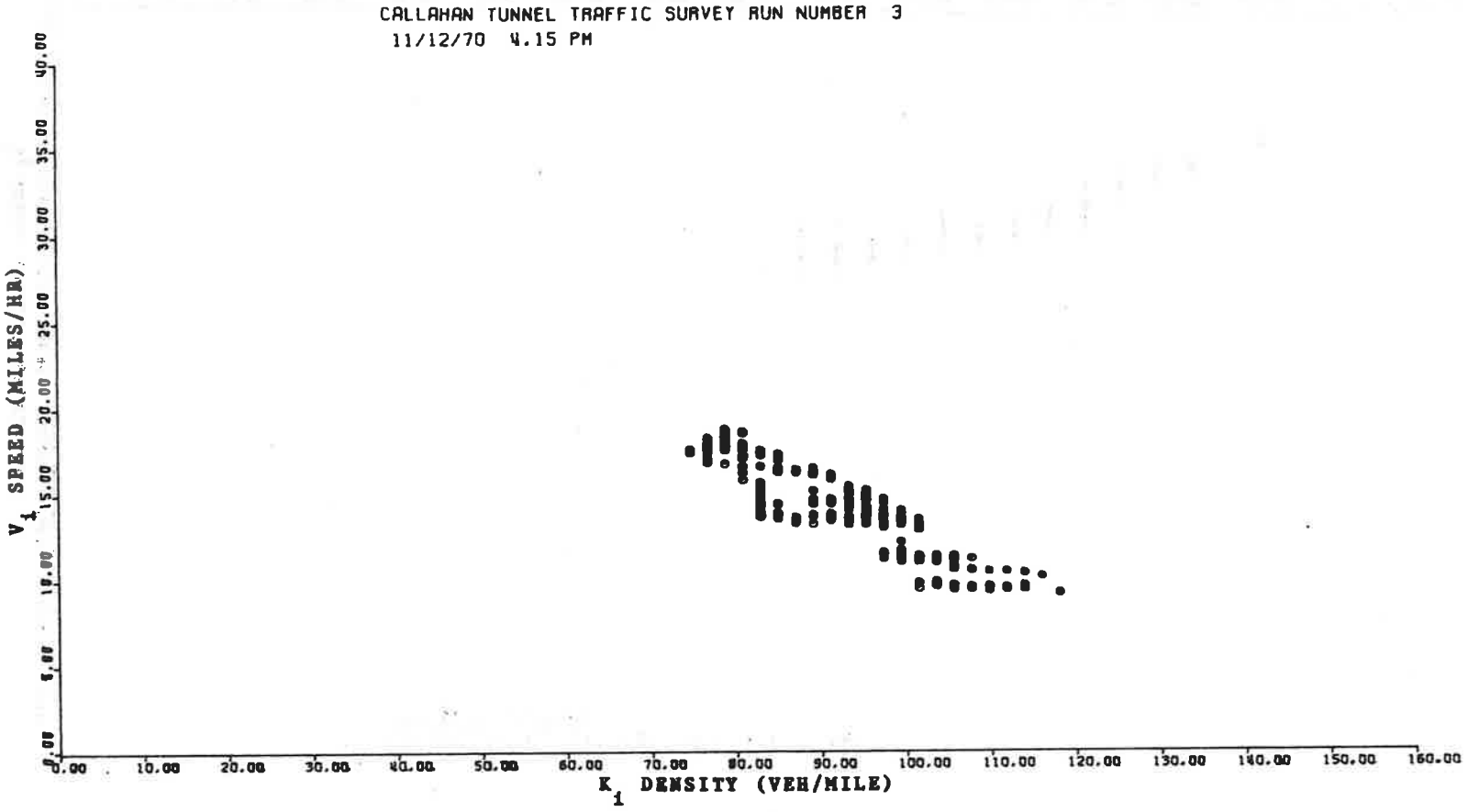


Figure 4.14a.- Run #3: Average speed over a section $V_i$, vs. section density $K_i$, Stations 1 to 3. Distance of 2550'.

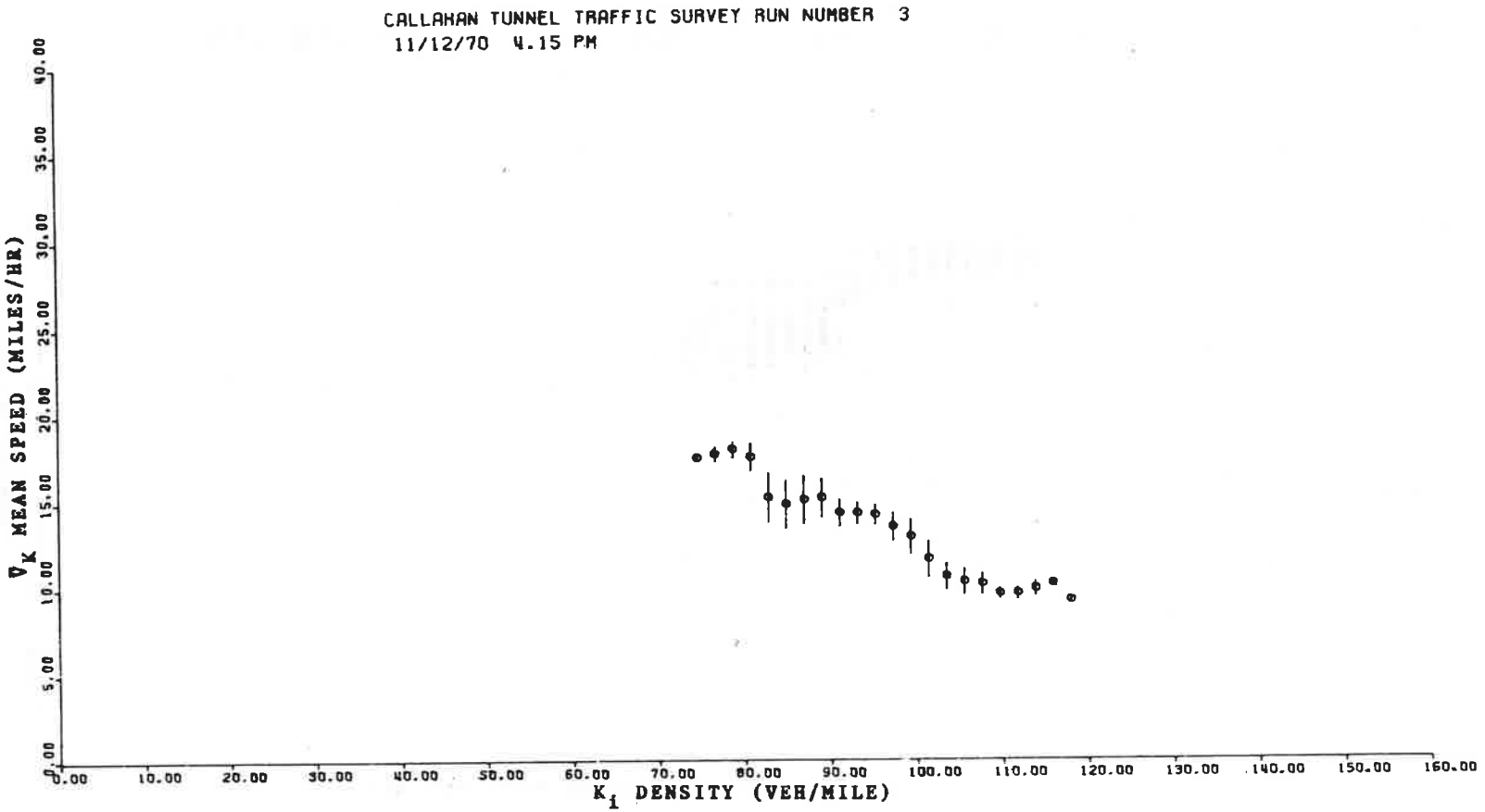


Figure 4.14b.- Run #3: Mean speed for a given density, $\bar{V}_k$, vs. the density $K_i$, Station 1 to 3. Distance of 2550'.

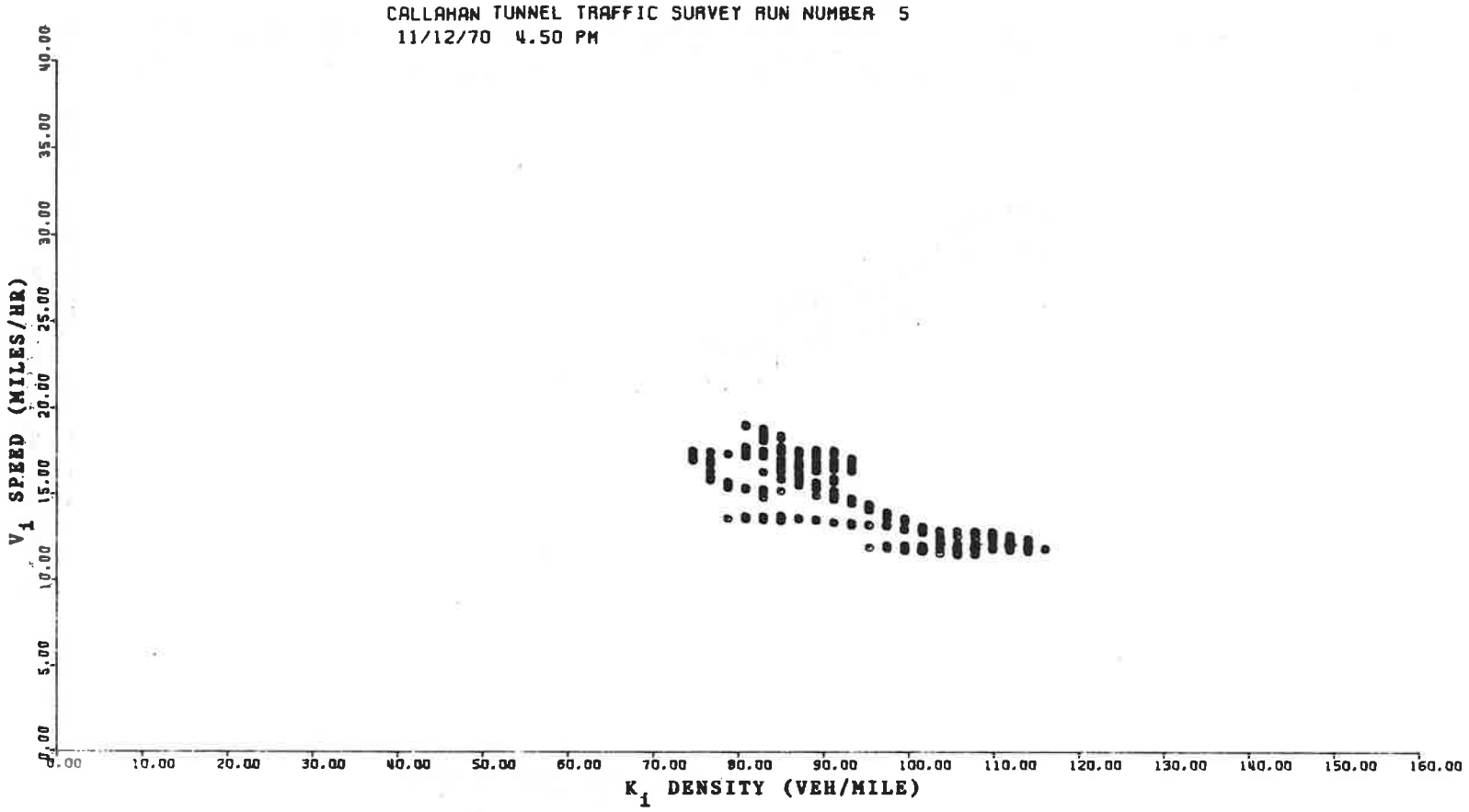


Figure 4.15a.- Run #5: Average speed over a section $\overline{V}_i$, vs. section density, $K_i$, Stations 1 to 3. Distance of 2550.

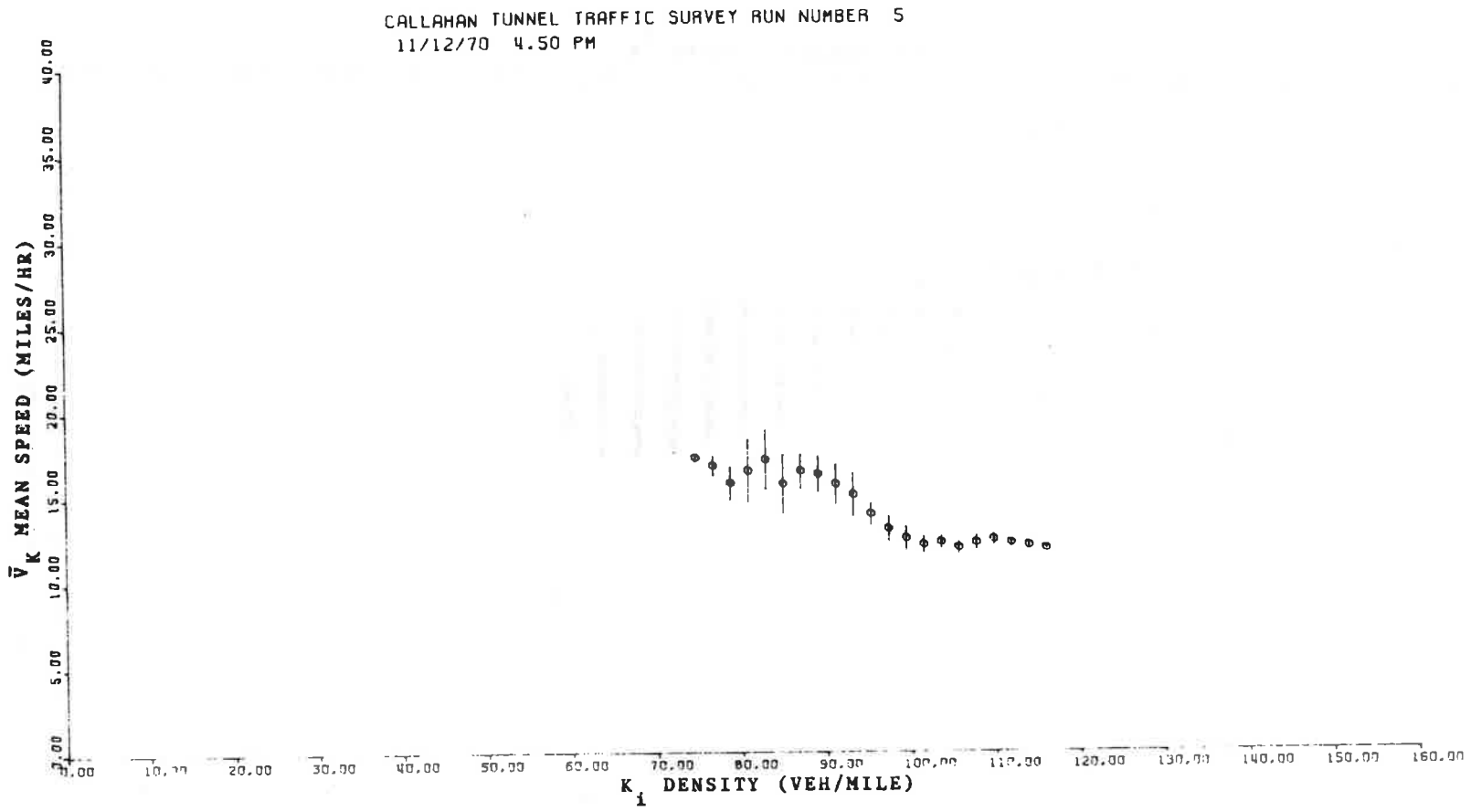


Figure 4.15b.- Run #5: Mean speed for a given density, $\bar{V}_k$, vs. section density $K_i$ Stations 1 to 3. Distance of 2550'.

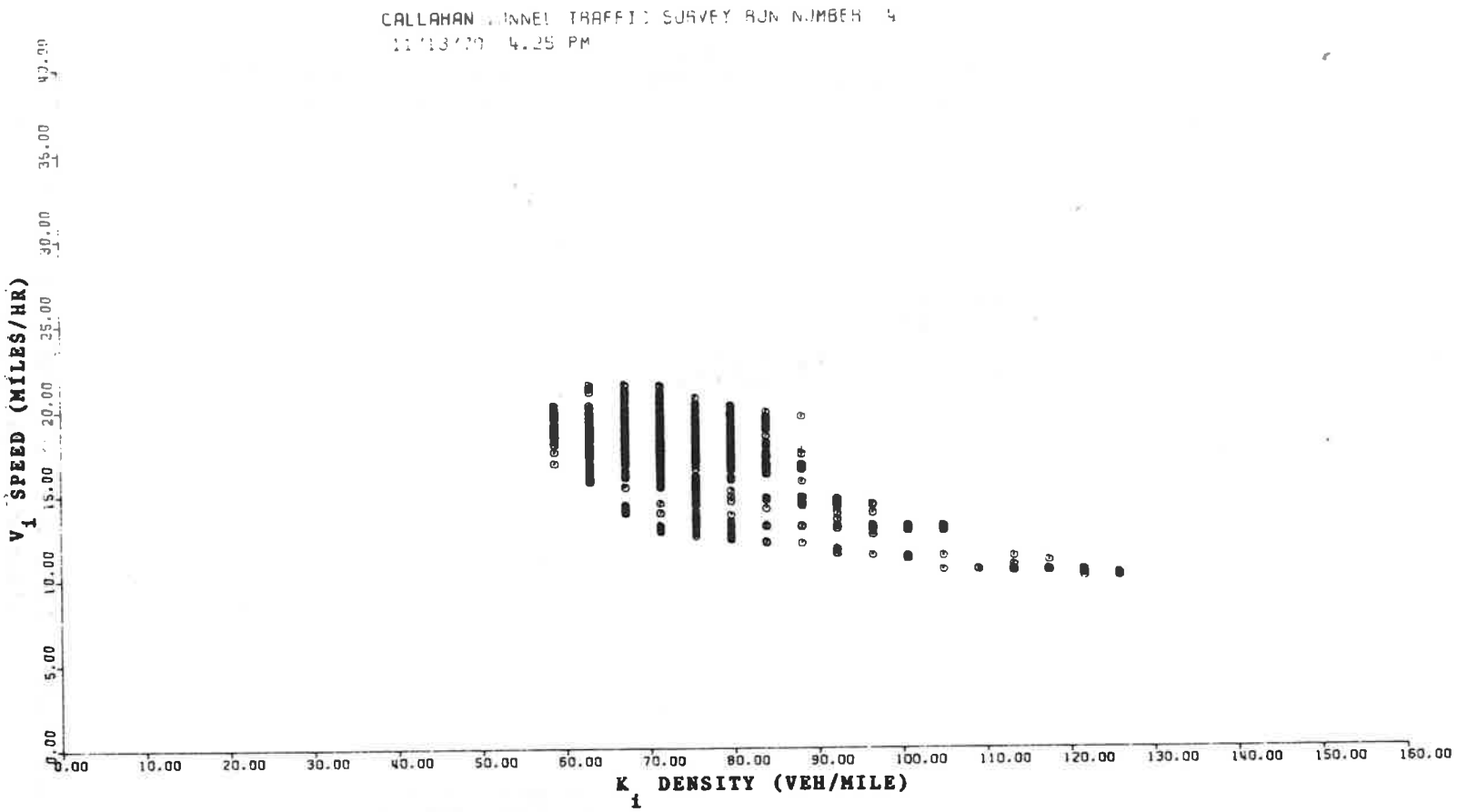


Figure 4.16a.- Run #4: Average speed over a section, $V_i$, vs. section density, $K_i$, Stations 2 to 3. Distance of 1260'.

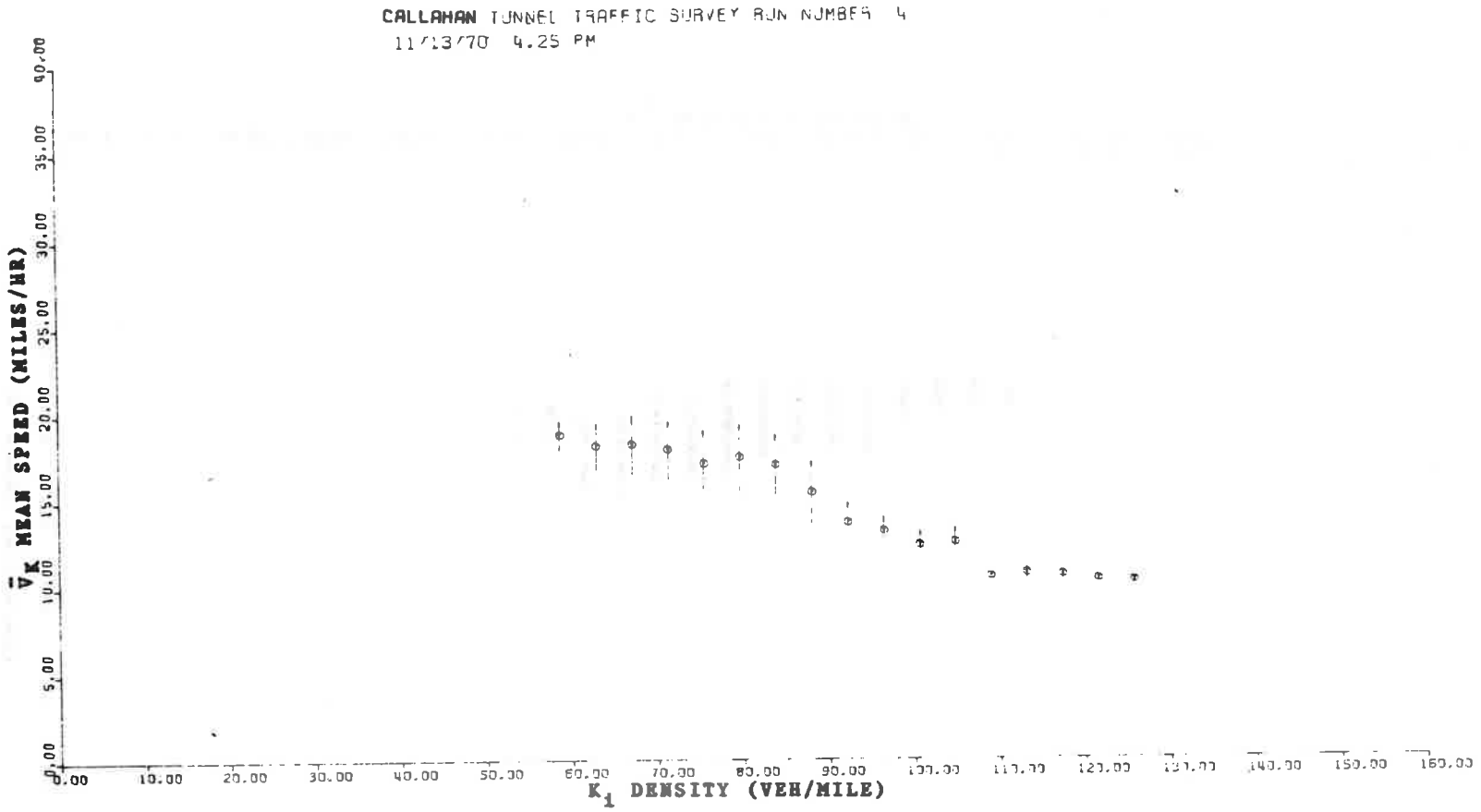


Figure 4.16b.- Run #4: Mean speed for a given density, $\bar{V}_k$, vs. section density, $K_i$, Stations 2 to 3. Distance of 1260'.

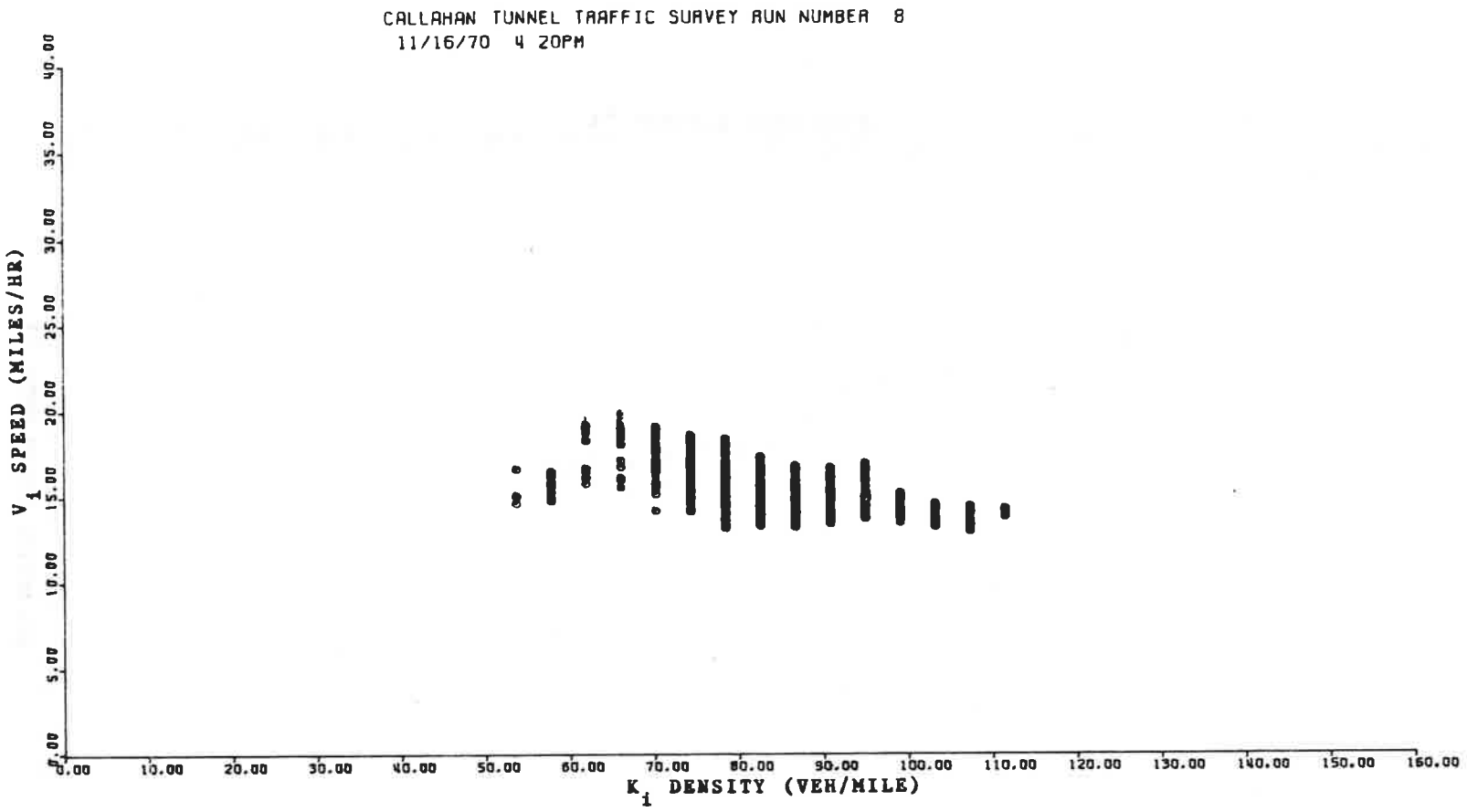


Figure 4.17a.- Run #8: Average speed over a section, $V_i$, vs. section density, Ki, Stations 3 to $B_1$. Distance of 1279'.

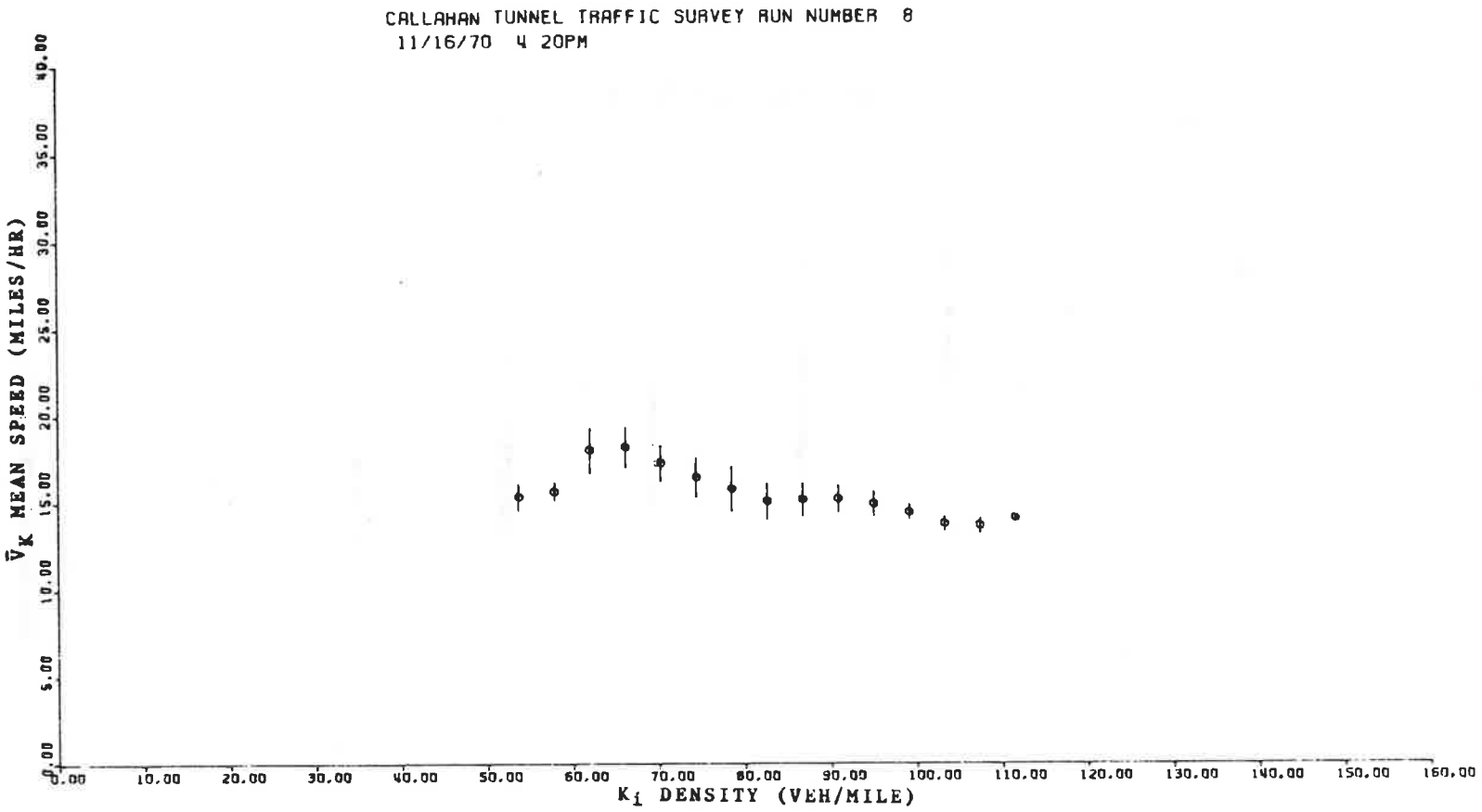


Figure 4.17b.- Run #8: Mean speed for a given density, $\bar{V}_k$, vs. section density, $K_i$, Stations 3 to $B_1$. Distance of 1279'.

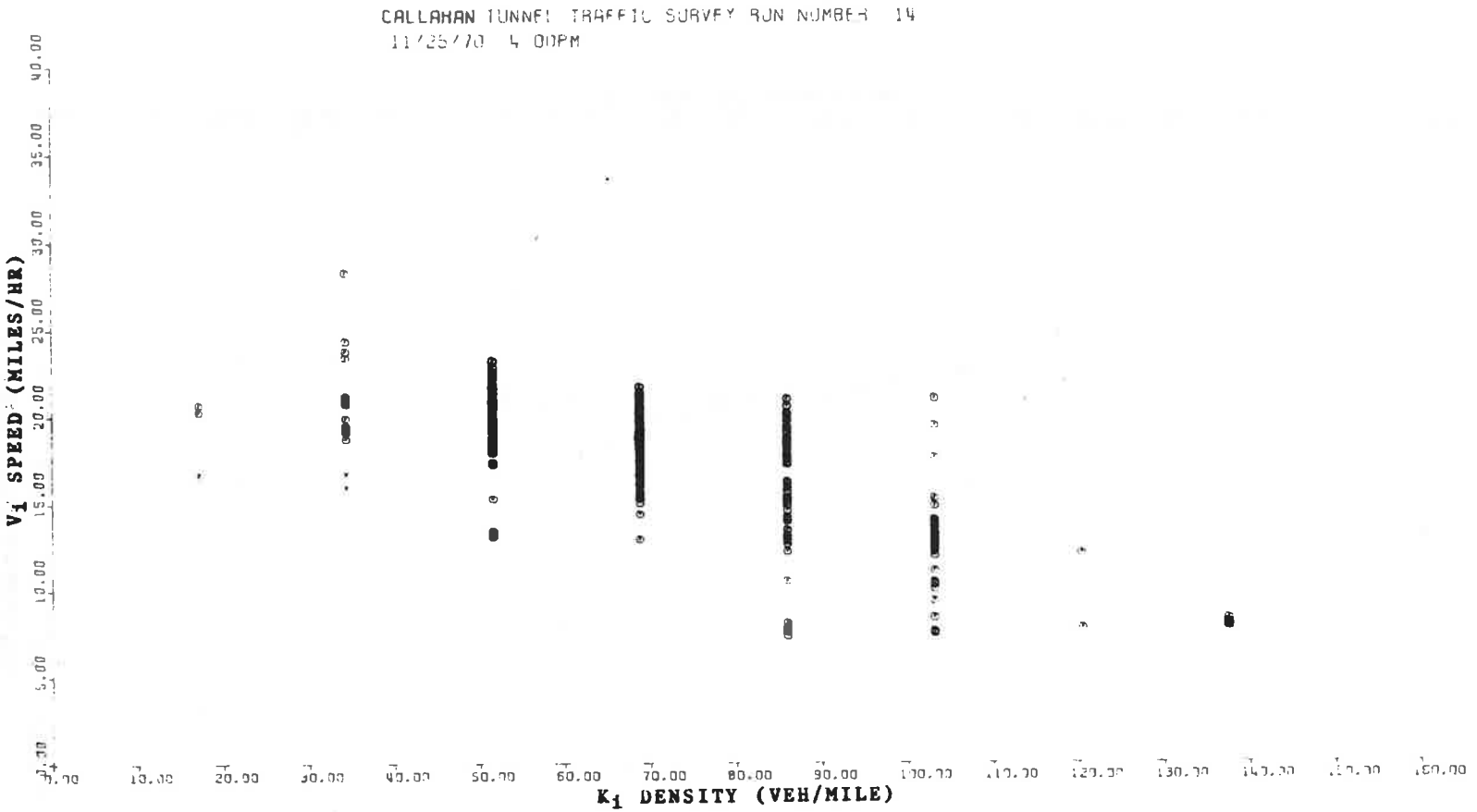


Figure 4.18a.- Run #14: Average speed over a section $V_i$, vs. section density, $K_i$, Stations 3a to $B_2$. Distance of 307.3'.

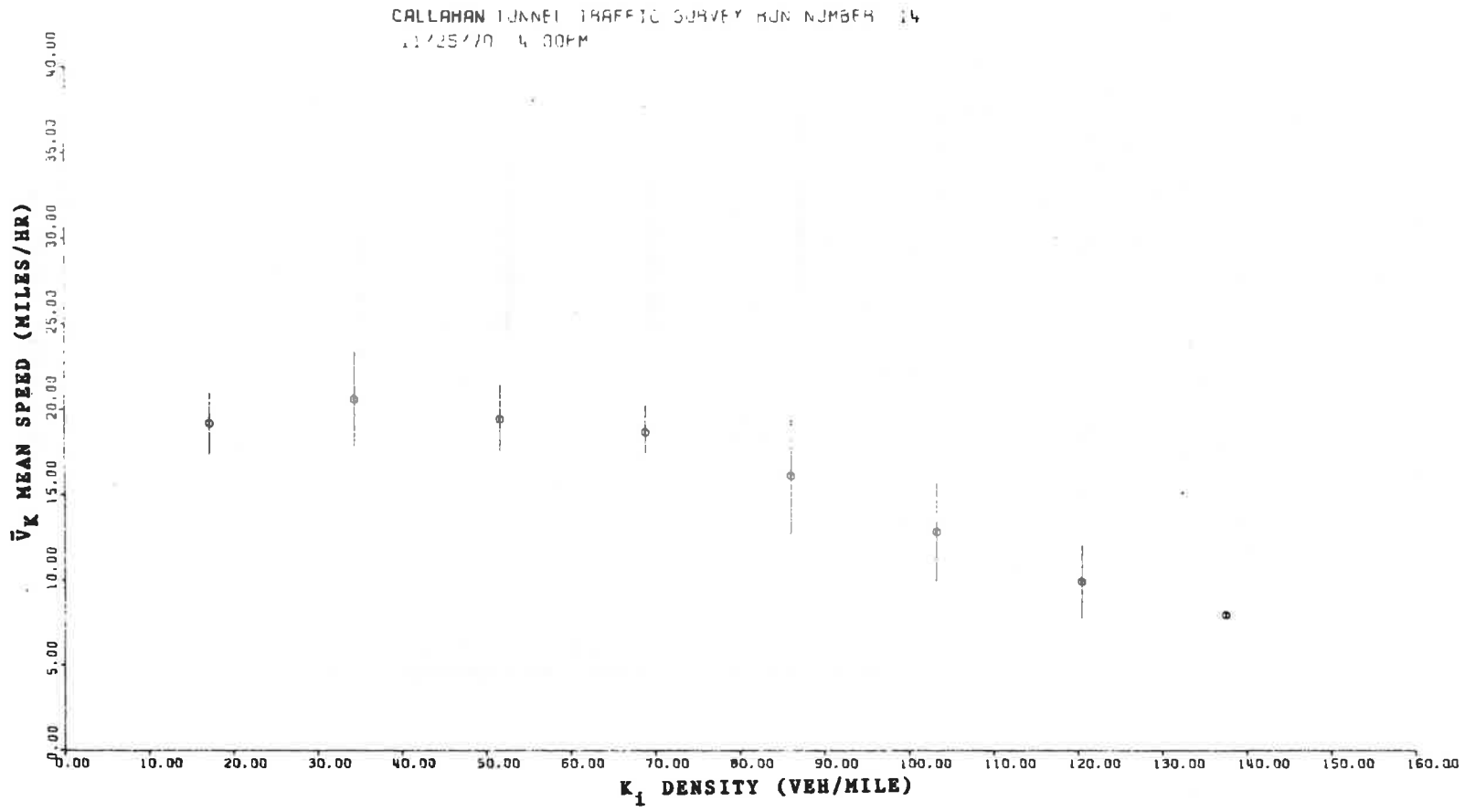


Figure 4.18b.- Run #14: Mean speed for a given density $\bar{V}_k$, vs. section density, $K_i$, Station 3a to $B_2$. Distance of 307.3'.

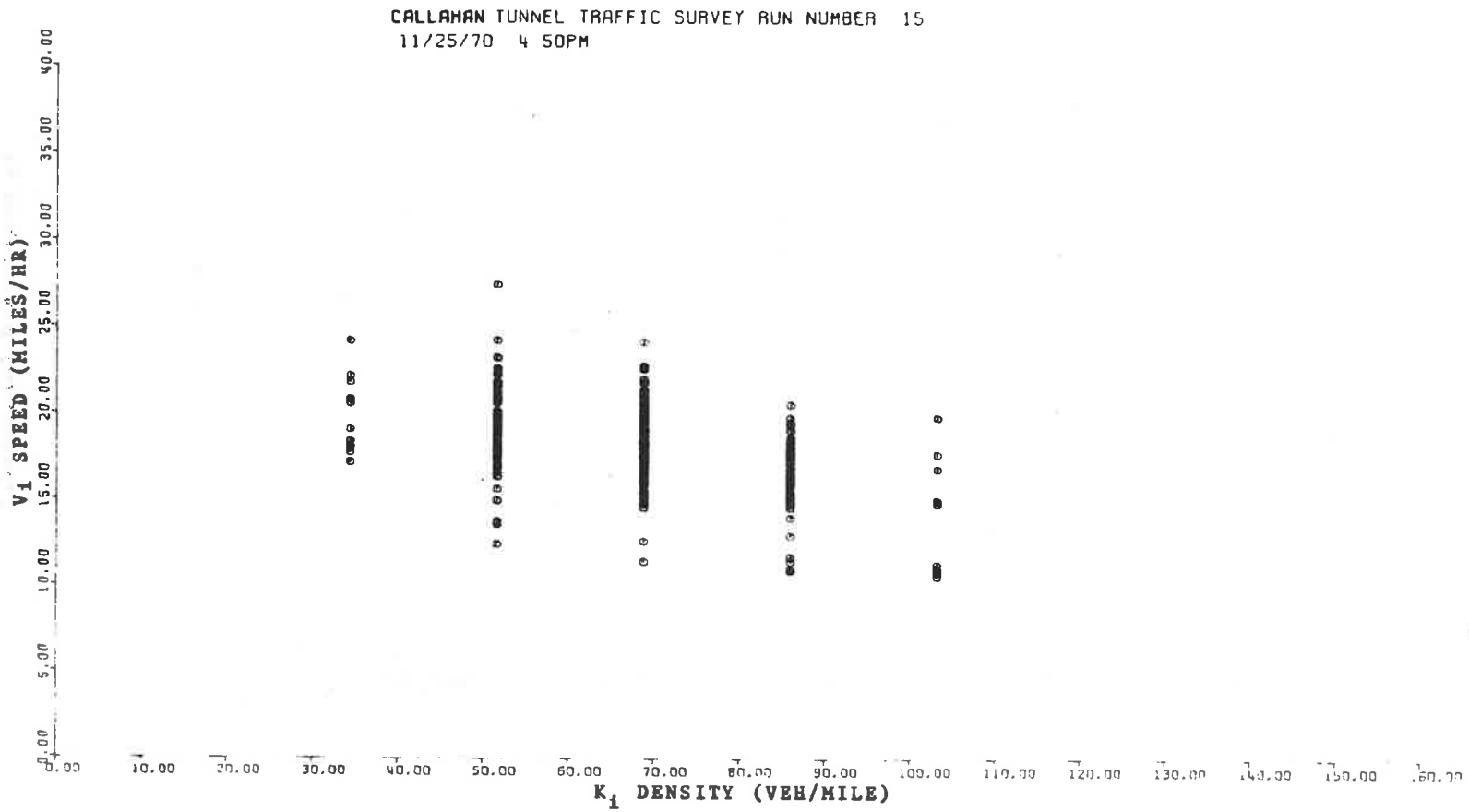


Figure 4.19a.- Run #15: Average speed over a section, $V_i$, vs. section density, $K_i$, Station 3a to $B_2$. Distance of 307.3'.

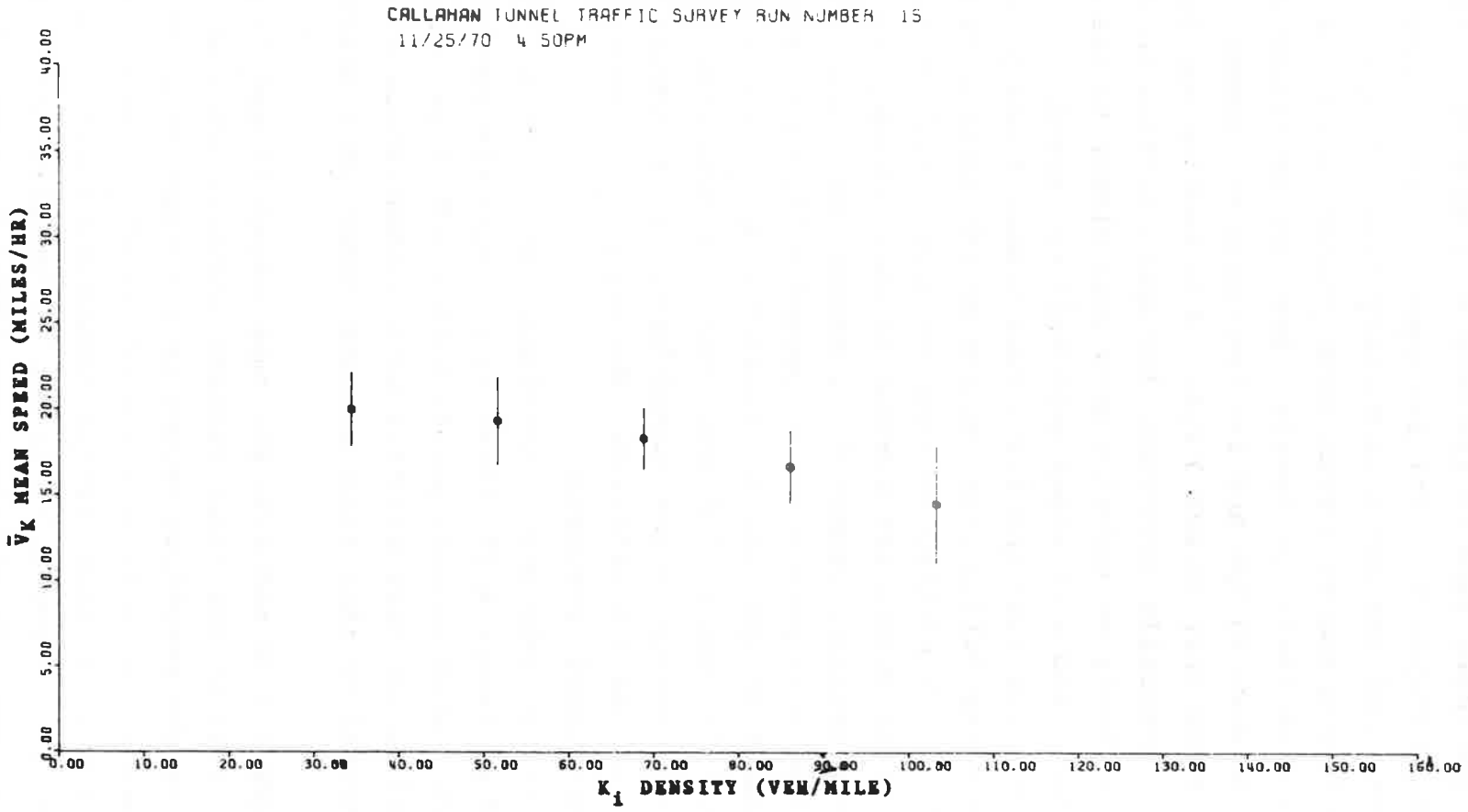


Figure 4.19b.- Run #15: Mean speed for a given density $\bar{V}_k$, vs. section density, $K_i$, Station 3a to $B_2$. Distance of 307.3'.

On the other hand in the very next section of the tunnel, as shown in Figure 4.12 for run number 9, the driver finds that an almost equal variation in density takes place at much higher density levels and with much lower speeds, which vary only slightly from their low levels. Here the densities vary approximately between 85 vpm and 140 vpm while the speeds vary somewhere between only 15 and 7 mph. This section may be characterized as a generally congested, low speed section in which a driver is likely to travel a good deal closer to his neighbors than before, and with about only half the speed.

In Figures 4.14 and 4.15, runs number 3 and 5 are plotted which show the full center section of the tunnel; in Figure 4.16, run number 4 is plotted showing the second half of the center section. The curves are similar to that for the first half of the middle section, Figure 4.13, except that there are a number of lower density points in the second half, down from about 85 vpm to about 60 vpm, and the densities do not go as high, down from about 140 vpm to 120 vpm. There is also less variation of speed with density in the second half. In agreement with the analysis of the Q-K relations, the congestion seems to be easing up and the speed increasing.

As the vehicle enters the final section of the tunnel, run number 8 of Figure 4.17, there is a relatively constant speed. There are few or no data points with speeds less than 12 mph and the speed varies only slightly with concentration of vehicles. The traversal of this final section occurs at a relatively steady pace.

Figures 4.18 and 4.19 for runs number 14 and 15 show the last 300 feet of the final section. These curves are somewhat similar to the preceding except that a wider range of density points occur. This is partly a result of the relatively short section being measured and the consequent shorter averaging time, resulting in a curve which is not as "smoothed out" as the longer section curves. In addition, run number 14 shows the back-up

from the toll booth mentioned previously. This is evident in Figure 4.18 from the number of high density and low speed data points which are present. A back-up did occur in run number 15 as well (Figure 4.19), but it was much less severe as is evident in the more restricted range of data points for this run as compared to the previous one.

### 4.2.7 Traffic Flow Profile Summary

With the aid of these velocity - density (V-K) and flow-density (Q-K) relations, Figures 4.12 through 4.19 and 4.4 through 4.11 respectively, and with the average density, average speed and the maximum flow curves, Figure 4.3, the following peak hour profile emerges:

The highest average speeds occur in the first 1200 feet or so of the tunnel, which is the downgrade portion. This average speed was 23 mph. The range of speeds however, also happened to be greatest in this section of the tunnel, ranging approximately from 34 mph down to 16 mph.

The density here averaged 58 vpm, the range of densities was about 60 vpm, from 30 vpm to 90 vpm, an average range for all the sections. The range of flows, on the other hand, was higher than usual, as might be expected from the large speed variations and only average density variations, going from approximately 1750 to 1000 vph. The maximum minute average flow was also highest in this section going from a high of 1680 vph at the entrance portal to a high of 1725 at station 1 located just before the foot of the downgrade.

Thus this section may be characterized as a high speed and high flow capacity section that is relatively erratic with some very large speed and flow variations. There appears to be an optimum density at around 75 vpm which means the traffic is operating, on the average, well below optimum in this section.

The next section of the tunnel from station 1 to station 2 which includes the foot of the downgrade, may be characterized as a very slow and very dense section. The average speed in this section is 12 mph which is only half that in the first section and the speed range goes from about 16 mph to 7 mph, again only about half that of the previous section. The average density is around 110 vpm and the range of densities goes from 85 vpm to 140 vpm. On the other hand the flows are still relatively high, ranging from about 1600 vph to 1000 vph, though most of these flows probably represent an upper limit with very little or no excess capacity available as occurred in the previous section. This lack of excess capacity is seen from the fact that the average and optimum densities are the same and from the shape of the Q-K curve which shows mainly decreasing flows.

The capacity in this section has sharply deteriorated from that in the first, the minute average maximum flows going from 1725 vph at the beginning of the section (at station 1) to only 1560 vph at the end of the section (at station 2), and the traffic is relatively slow and congested.

The next section from station 2 to station 3 which includes the foot of the upgrade has a higher average speed, around 17 mph, which is about half-way between the speeds of the first and second sections. The speed varies between about 19 and 10 mph and the section doesn't have the low speeds (around 7-9 mph) which the previous section had. The density is also sharply lower in this section, the average here being about 75 vpm and the range being between 60 and 120 vpm. Again the higher densities around 130 vpm, prevalent in the previous section, are absent here, and the absence in the previous section of low values of density, around 70 vpm, are present here.

The flow range is comparable, between 1650 and 1000 vph, but unlike the previous section, the maximum minute average flow is relatively constant at around 1560 vph. This means that the flow coming from the previous section is easily absorbed and congestion does not form.

Finally, as the vehicle proceeds it enters the end section defined by station 3 and the exit portal. Here the speeds are essentially the same as in the previous section. The average speed slightly less (15 mph instead of 17 mph) but fewer lower speeds are present. Similarly the average density is a little higher here but there are less high density points here than there were in the previous section. The range of flows is slightly greater, from 1575 to 900 vph, and the maximum minute average is 1575 vph at station 3 and 1520 at the exit portal compared to about 1560 vph in the previous section.

Thus it appears that the transition into this section is relatively smooth. However, the presence of the toll booths some 700 feet beyond the exit portal and a rather sharp bend in the roadway there, does lead to the occurrence of slow downs every once in a while which are related to toll booth backups. Some of these slowdowns were evident in the curves presented of the last 300 feet of the section (runs 14 and 15) and will be discussed further when the flow with and without shocks is analyzed.

Clearly then, the Callahan tunnel is a non-homogenious roadway with different section capacities, different average section speeds and average densities, different *ranges* of the speed and density in the sections, and different section susceptibility to the occurrence of shock waves. It has been shown in the past (ref. 20) that the restriction of traffic input can result in an increase in traffic throughput. The data suggests that such a control system may indeed be effective in improving flow in the middle tunnel section; but final justification of this conclusion and an explicit control system recommendation would have to depend on more extensive data measurements taken simultaneously at a number of points all along the roadway.

## 4.3 ANALYSIS OF SLOWDOWN WAVES

### 4.3.1 Introduction

Attention is now turned to an analysis of prominent slowdowns which occurred during the runs. The analysis is similar to that employed in studying the slowdown in the Holland tunnel given in Section 3. The analysis will be an attempt to locate the wave, follow its progress from a downstream station as it propagates against the traffic to the upstream station, determine its speed of propagation, determine its spatial extent and determine its adverse effects of the traffic by comparing the vehicular flows, speeds and densities both before and during the presence of the wave phenomenon. This is done generally with the aid of seven types of plots: (1) A plot of the arrival times of vehicles reaching each of the two stations making up a section (2) A space time plot for the visualization of changing vehicular speeds as the wave propagates into the traffic stream (3),(4) A set of figures showing the change in vehicular flow, (5) speed, (6) transit time and (7) density as the wave passes through.

### 4.3.2 Run Number 4 - Middle Section, Second Half

A severe slowdown occurred between stations 2 and 3 during run number 4 where the vehicular speeds averaged only about half their normal speeds. The first figure, 4.20, shows the vehicle arrival times at the two stations preceding, during, and after the passage of the shock wave. The upper curve is that for the upstream observer at station 2 while the lower curve is for the downstream observer at station 3. The two curves are displaced in time, the displacement being equal to the transit time of a vehicle and shown as a horizontal line on the figure. The figure shows the change in the flow rates of the vehicles at the observation stations as a change in the slope of the upstream and downstream curves. As the flow decreases, the slope flattens out and the arrival of a shock or slowdown wave is seen as a decreasing

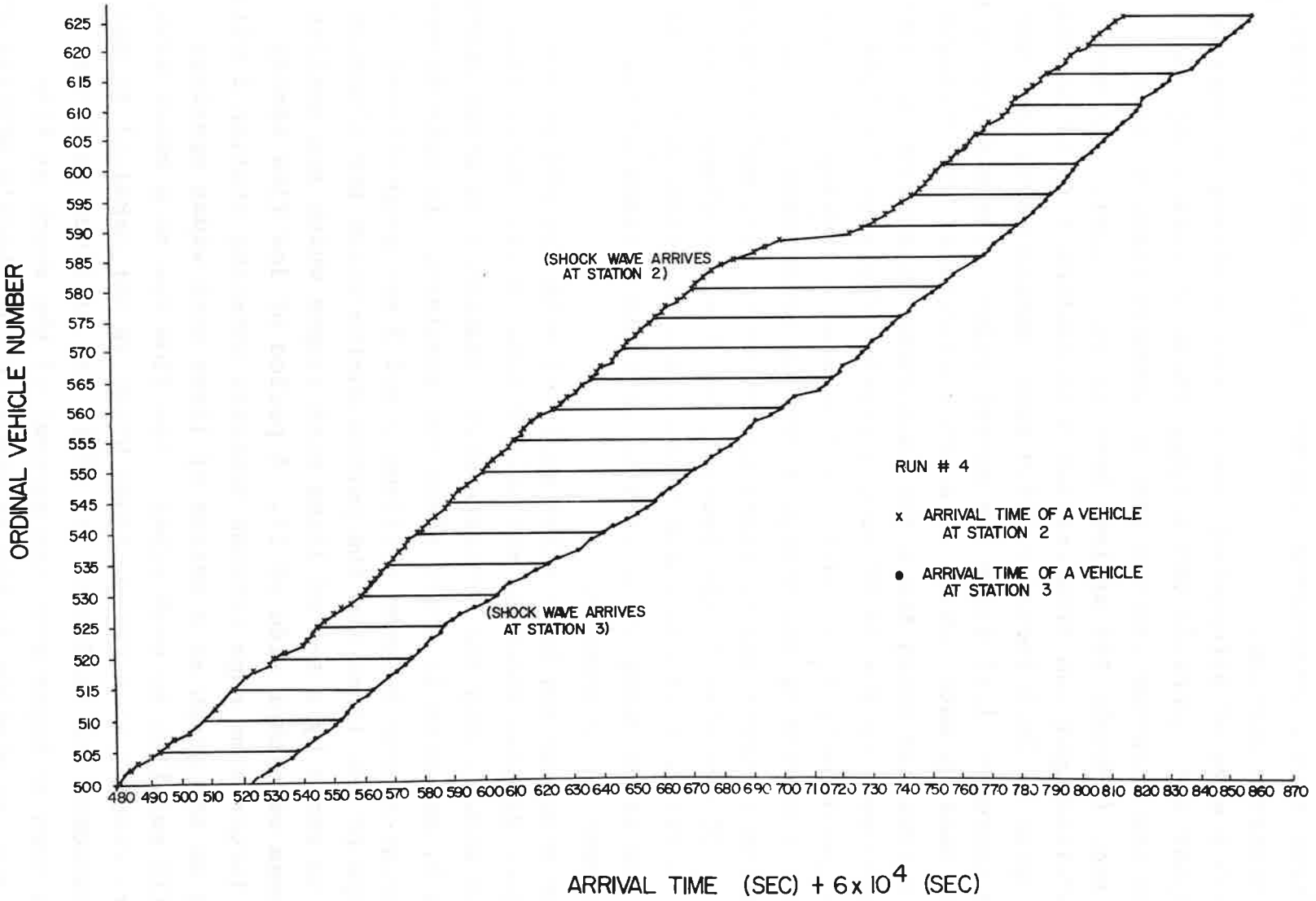


Figure 4.20.- Run #4: Arrival times of vehicles at stations 2 and 3 vs. ordinal vehicle number.

slope first at the downstream station and then some time later, at the upstream station.

Such a wave of attenuated flow is seen arriving at station 3 at 60,599 sec. (vehicle 528 arrives there at this time) and reaching the upstream station some 87 seconds later at time 60,686 sec. (vehicle 584 arrives here at this time). The wave has travelled upstream from station 3 to station 2 in 87 seconds with a speed of 14.5 feet/sec. (9.9 mph), during which time the density increased 1.67 times its normal value. The width of this slowdown density wave, which is another measure of its strength, may be calculated using the method described in Section 3. With an average density K = 74.98 vpm, a section distance D = 1260 feet, a jam density $K_j$ = 234.7 vpm (computed by taking the number of vehicles passed by the stoppage wave in traversing the two observation stations and dividing by the distance), and a maximum number of 30 vehicles in the section, we obtain a stoppage wave width w = 397 feet within which there are approximately 18 vehicles. The *shock delay time*, (the shock width divided by the shock speed) is 27 seconds.

The stoppage may be further analyzed with the aid of the space time diagram shown in the next figure, 4.21. Here, distance is shown along the ordinate where station 3 is shown above station 2, and time is shown along the abscissa. In this diagram the average speeds between stations 2 and 3 are proportional to the slope of the lines and the period during which the slowdown occurs is shown by a set of lines with slopes which are smaller than those on either side of it. A period of low flow simply due to larger time gaps between vehicles entering station 2 will show up on the graph as a series of lines with wider spacings but still parallel to each other. Low flow due to a shock wave, however, results in a set of lines which is not parallel to the sets preceding and following it. This set of lines in Figure 4.21 is seen to begin with the arrival of the shock at time 60,600 sec. at station 3, and to end with the shock's arrival at station 2 at time 60,690 sec.

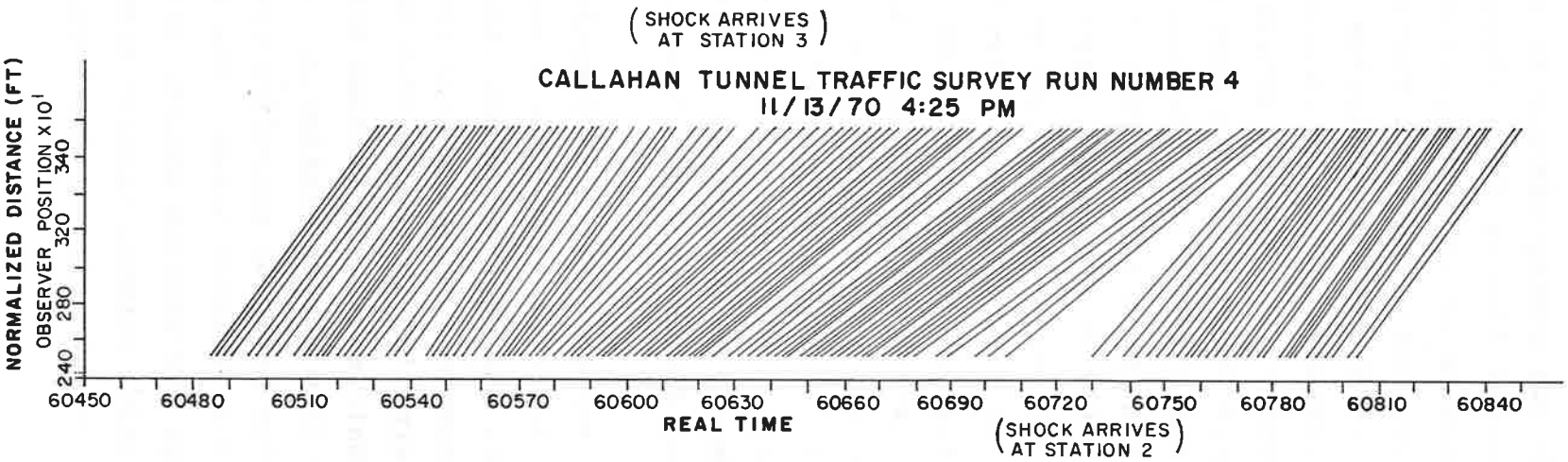


Figure 4.21. - Run #4: Space vs. time diagram of vehicles passing through stations 2 and 3.

The slowdown stands out pretty clearly in the next set of graphs showing the vehicular flow as the reciprocal of the time headway plotted as a function of time, Figures 4.22a and 4.22b. This flow is averaged over some number of vehicles (here seven vehicles). The arrival of the shock at station 2, Figure 4.22a is shown as a dramatic decrease in the average flow beginning at about 60,690 sec. and lasting for about a minute until the time 60,750 sec. This dramatic decrease in the flow appears to have been preceded by a general rise in the flow rate which began around 60,200 sec. and continued to rise until the severe drop in flow occurred. Similarly at station 3, Figure 4.22b there is a sharp drop in flow beginning at time 60,600 sec. which is preceded by a general rise in flow between the times 60,050 sec, and 60,400 sec. While further evidence will be needed, this general rise in the flow input preceding the sharp drop, may be one condition which precedes some shocks and which may be used to predict the occurrence of certain types of stoppages.

In this case the higher flows preceding the sharp reduction are not due to higher densities but rather to higher speeds as will be seen below in the discussion of Figure 4.23, and Figure 4.25.

In Figure 4.23 the average vehicular density is plotted as a function of time. We see that except for a small build-up near the beginning of the run, the density remains more or less uniform throughout the 36-minute run except near the time 60,600 sec. when there is a sharp rise in the traffic density. This rapid accumulation of vehicles in the section coincides with the rapid drop of vehicular flow across station 3. However, we note the absence of any density build-up preceding its sharp rise.

Figure 4.24 shows the relation between the time it takes the vehicle to travel through the section and the section density. We see a very close relation between transit time and density with a mild increase in transit time at the beginning of the run

to correspond with the increased traffic density there, and the sharp rise in the transit time beginning at 60,600 sec. coinciding with the sharp increase in density at that time.

Figure 4.25 shows the average velocity of a vehicle in the section to have decreased at the same times that the density increased, moderately at the beginning of the run and strongly later on at time 60,600 sec. There is also a higher than average velocity preceding its sharp drop, and it appears that this accounts for the increased flow that preceded the shock.

Finally, we show in Figure 4.26 the flow at station 3 averaged over the transit time of a vehicle and contrast this flow with that shown in Figure 4.22b in which a different flow average was used. We see that the drop in flow around the time 60,600 sec. is much less pronounced in this transit time averaging than it was in Figure 4.22b, where the average was over seven vehicles. This example points out the important role the choice of averaging can play in studying traffic flow phenomena. The averaging time based on the transit time here is so long that if it had been used, the stoppage might have been missed.

### 4.3.3 Run Number 9 - Middle Section, First Half

Run number 9 covered the section between stations 1 and 2. At least one shock occurred in this section during the run. Another was a general congestion with no clear return to a non-congested condition within the period that data was taken. These two conditions for run number 9 are shown in the next set of figures 4.27 through 4.33. Figures 4.27a and 4.27b show the arrival time graph from which are calculated the onset of the shock and its speed. The same conditions are shown in a space time plot in Figures 4.28a and 4.28b. The relationship between flow, density, vehicle transit time and speed are shown in Figures 4.29-4.32, and finally a different flow average versus time plot in Figure 4.33.

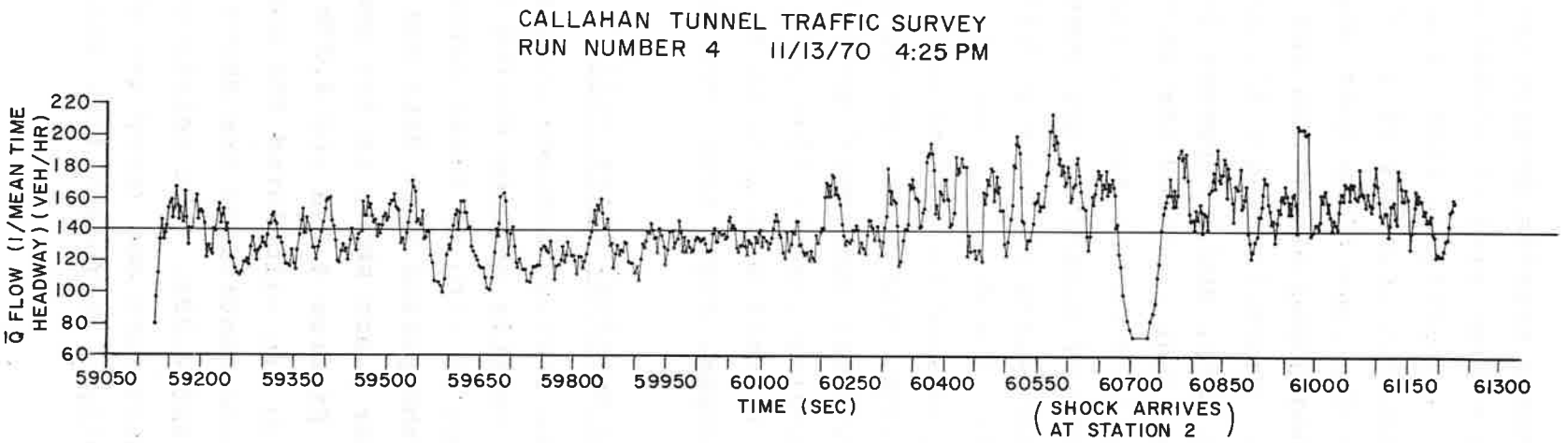


Figure 4.22a. - Run #4: $\bar{Q}$, Vehicular flow (1/mean time headway averaged over 7 vehicles) vs. time. Station 2.

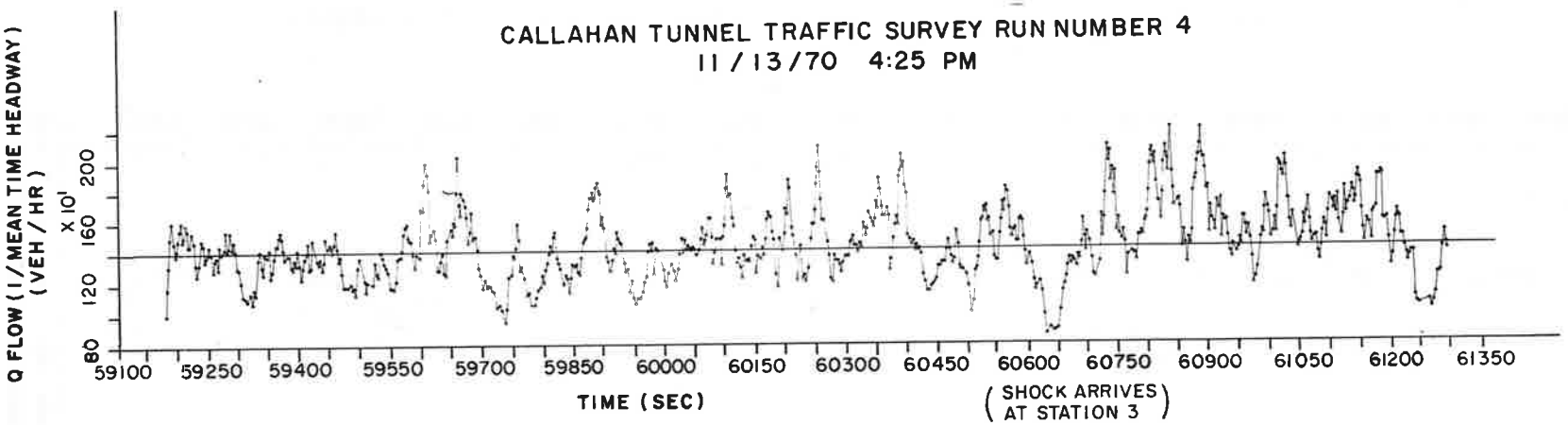


Figure 4.22b. - Run #4: $\bar{Q}$, Vehicular flow (1/mean time headway averaged over 7 vehicles) vs. time. Station 3.

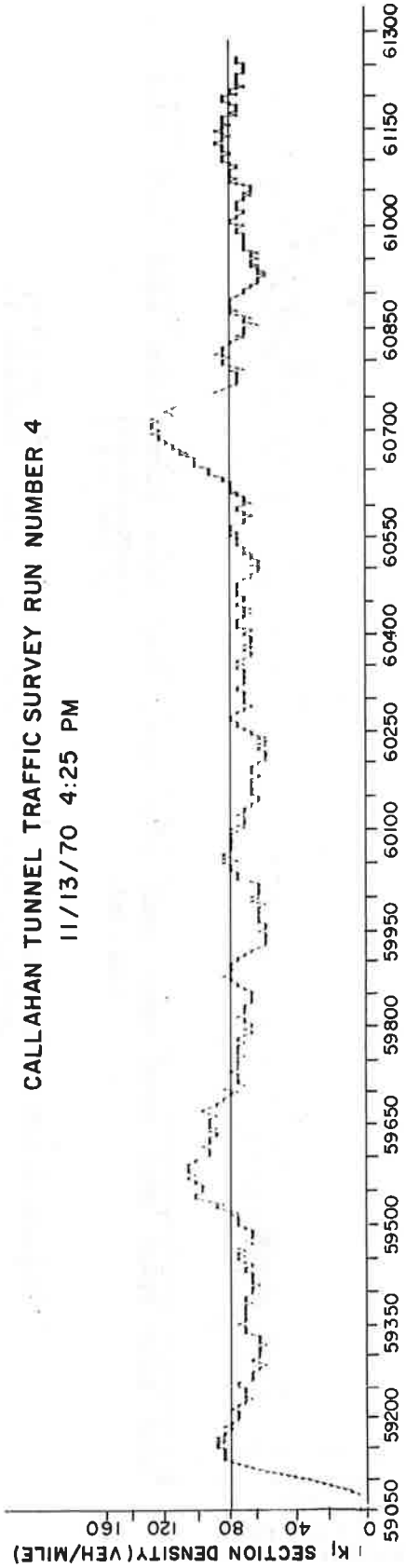


Figure 4.23. - Run #4: $k_i$, average vehicular density in the section between stations 2 and 3 vs. time.

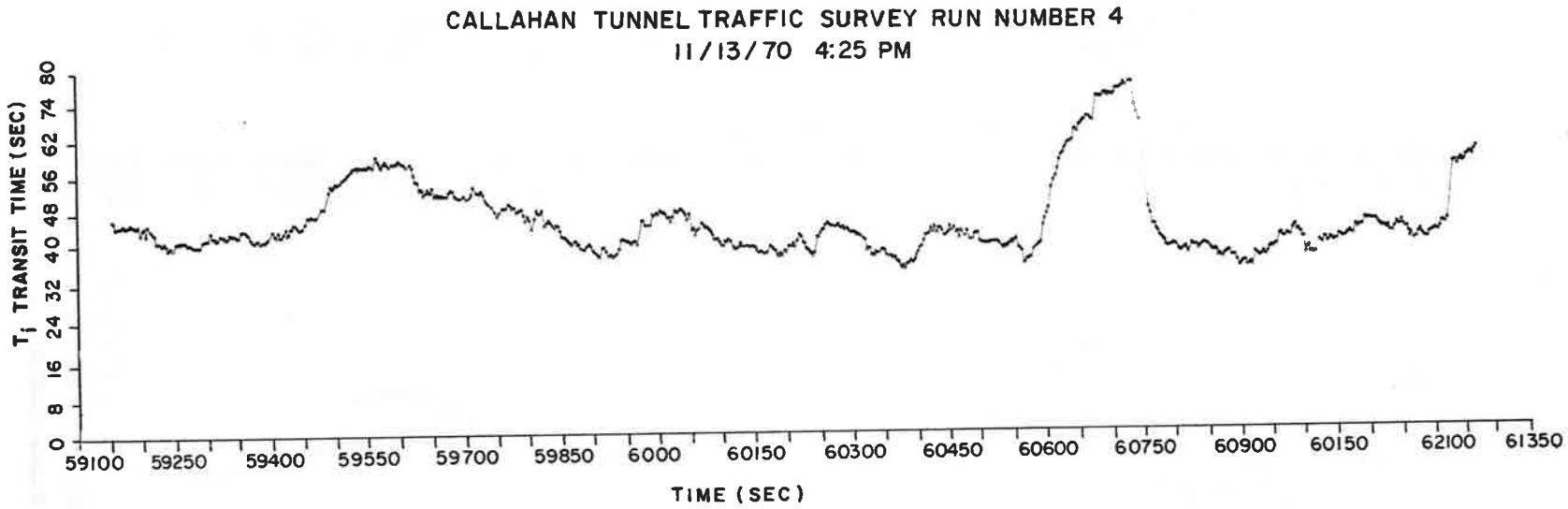


Figure 4.24. - Run #4: $T_i$, transit time of a vehicle travelling from stations 2 to 3 vs. middle of transit time.

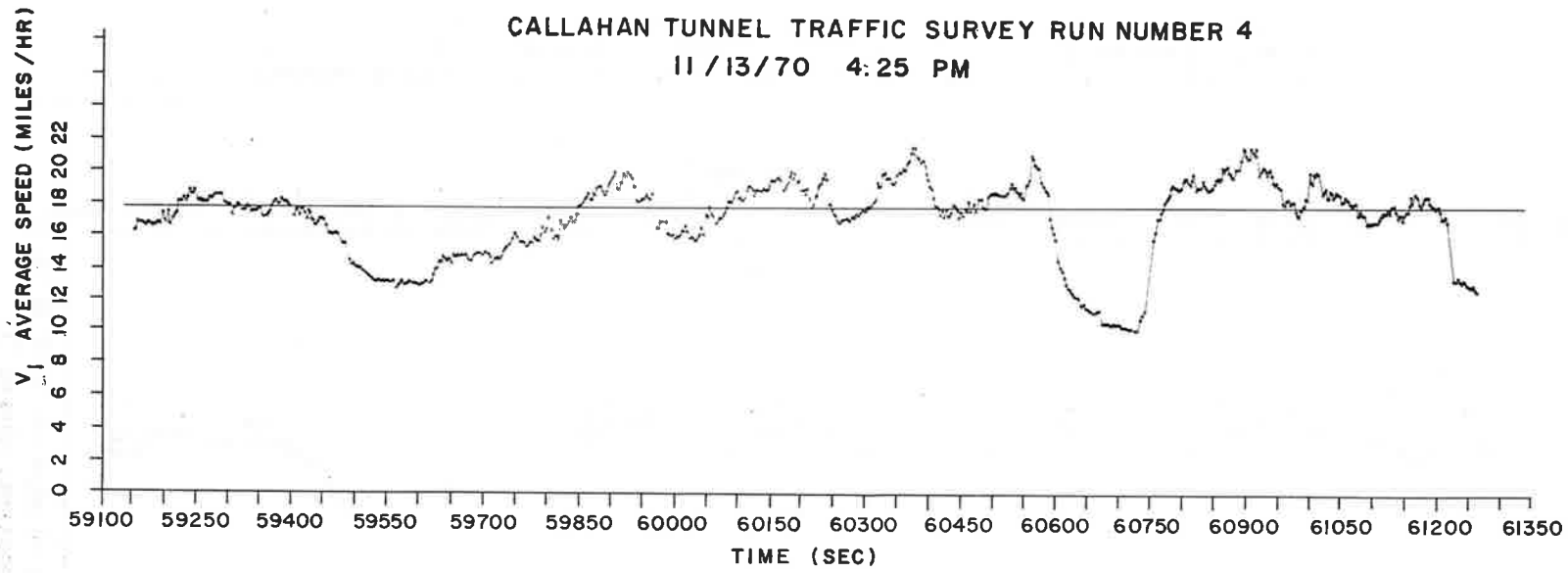


Figure 4.25. - Run #4: $V_i$, average speed of a vehicle in transit between stations 2 and 3 vs. the middle of the transit time.

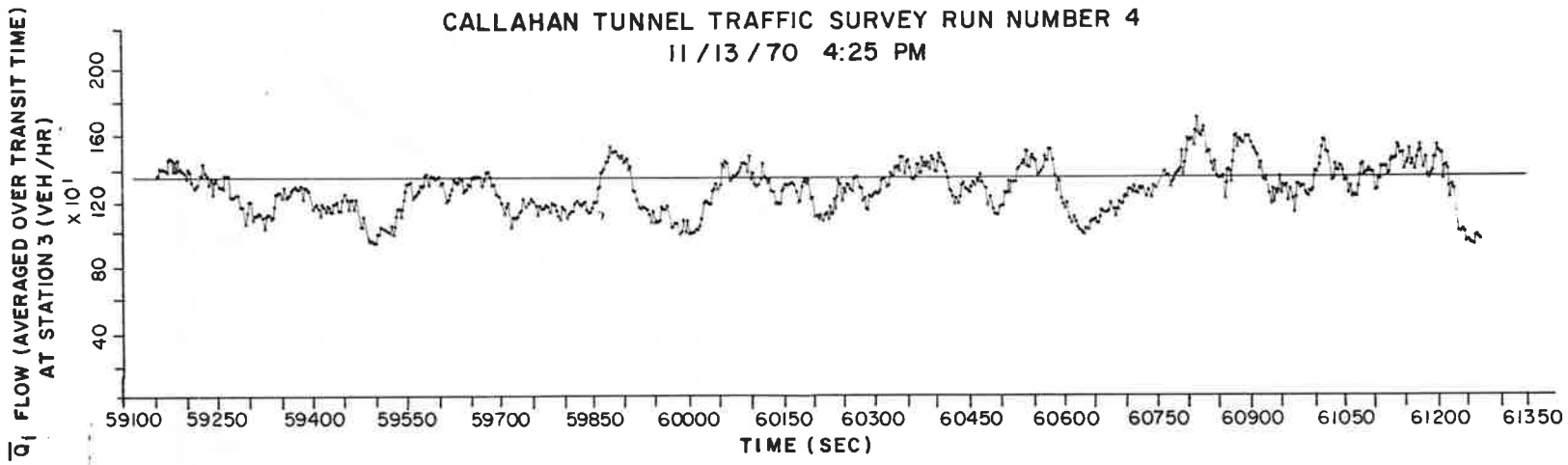


Figure 4.26. - Run #4: $Q_i$, flow at station 3 averaged over the transit time of a vehicle vs. the middle of the transit time.

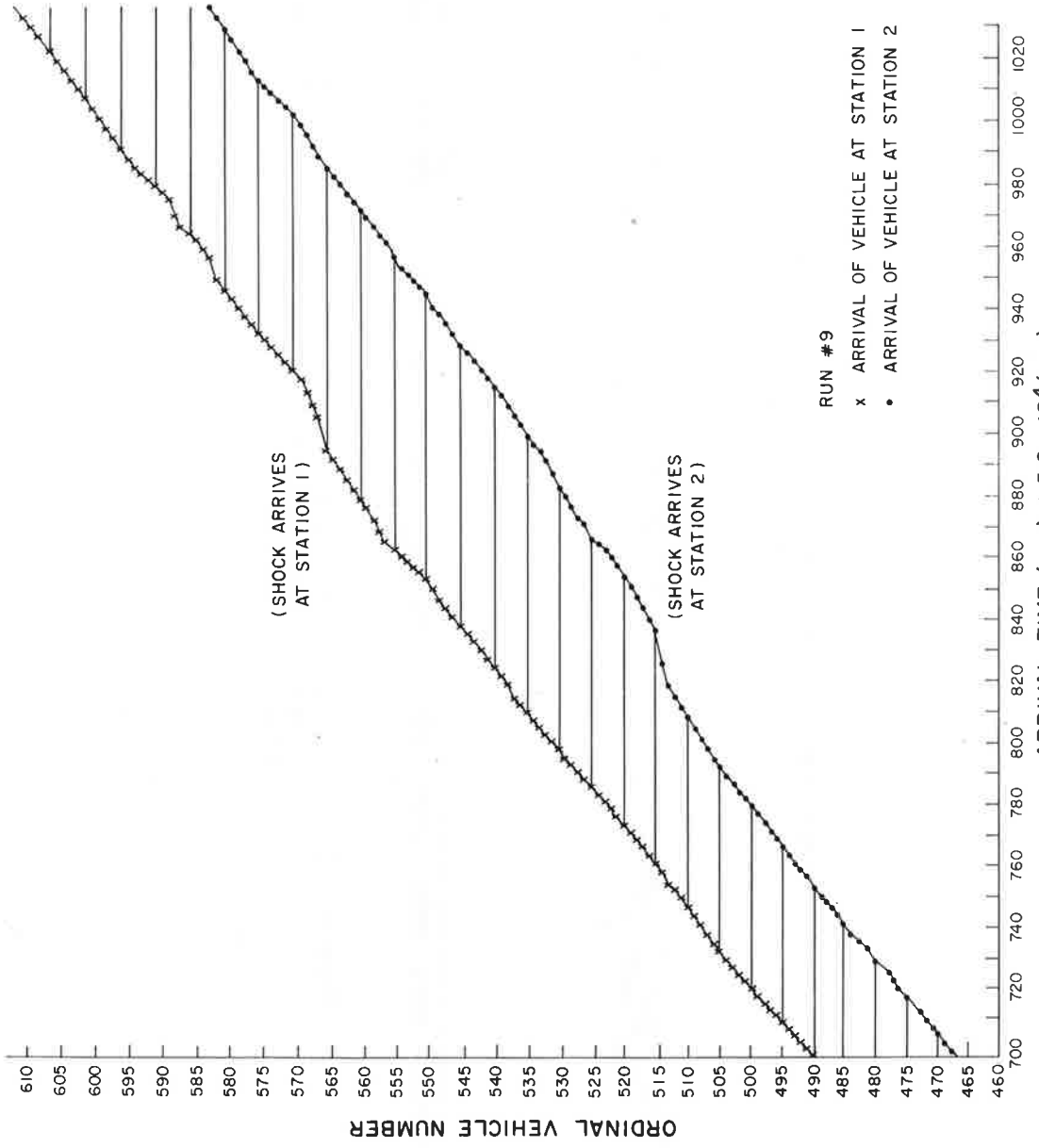


Figure 4.27a.- Run #9: Arrival times of vehicles at station 1 and 2 vs. ordinal vehicle number (time from 59,700 sec. to 60,030 sec.)

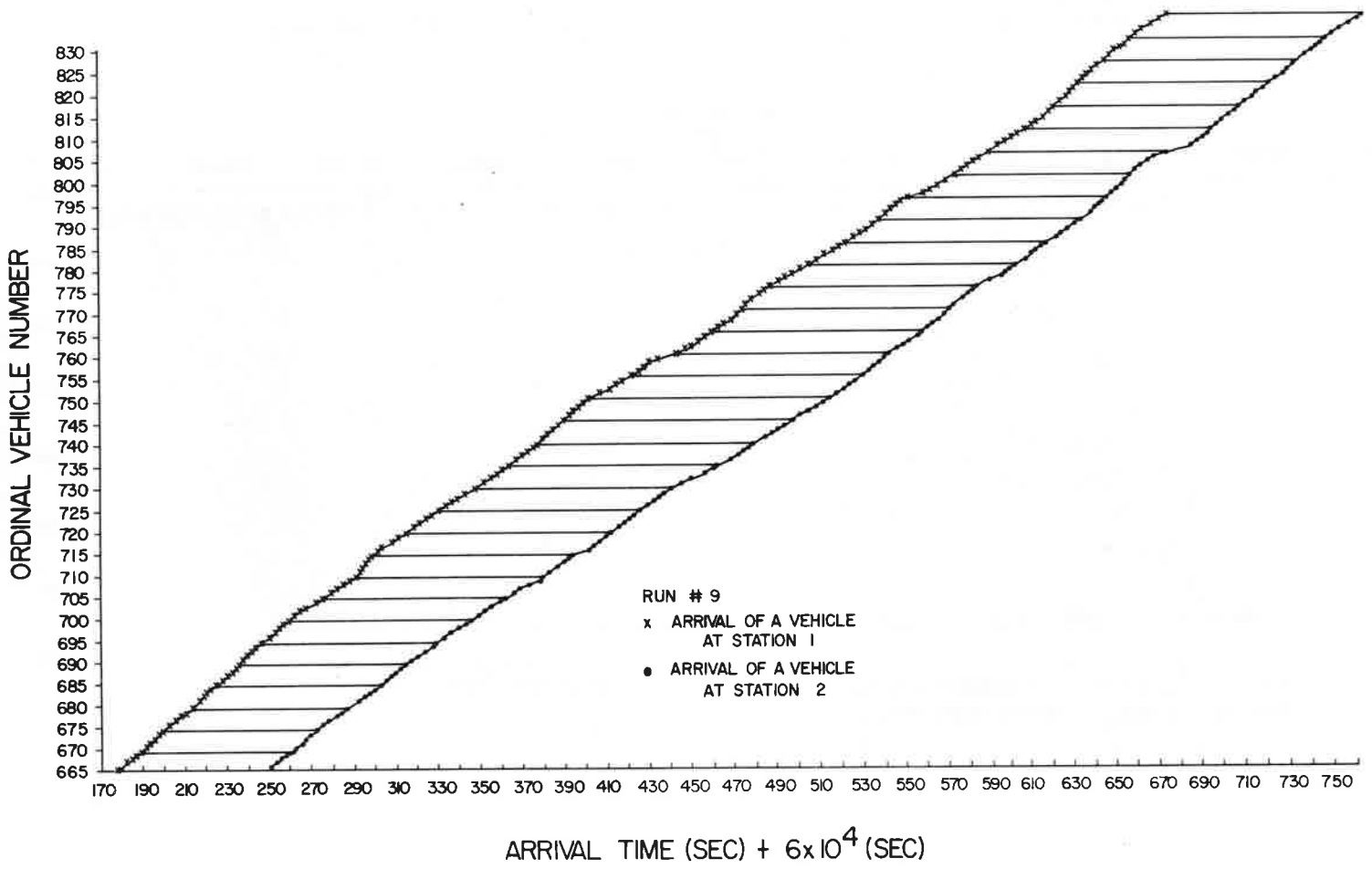


Figure 4.27b.- Run #9: Arrival times of vehicles at station 1 and 2 vs. ordinal vehicle number (time from 60,170 sec. to 60,760 sec.)

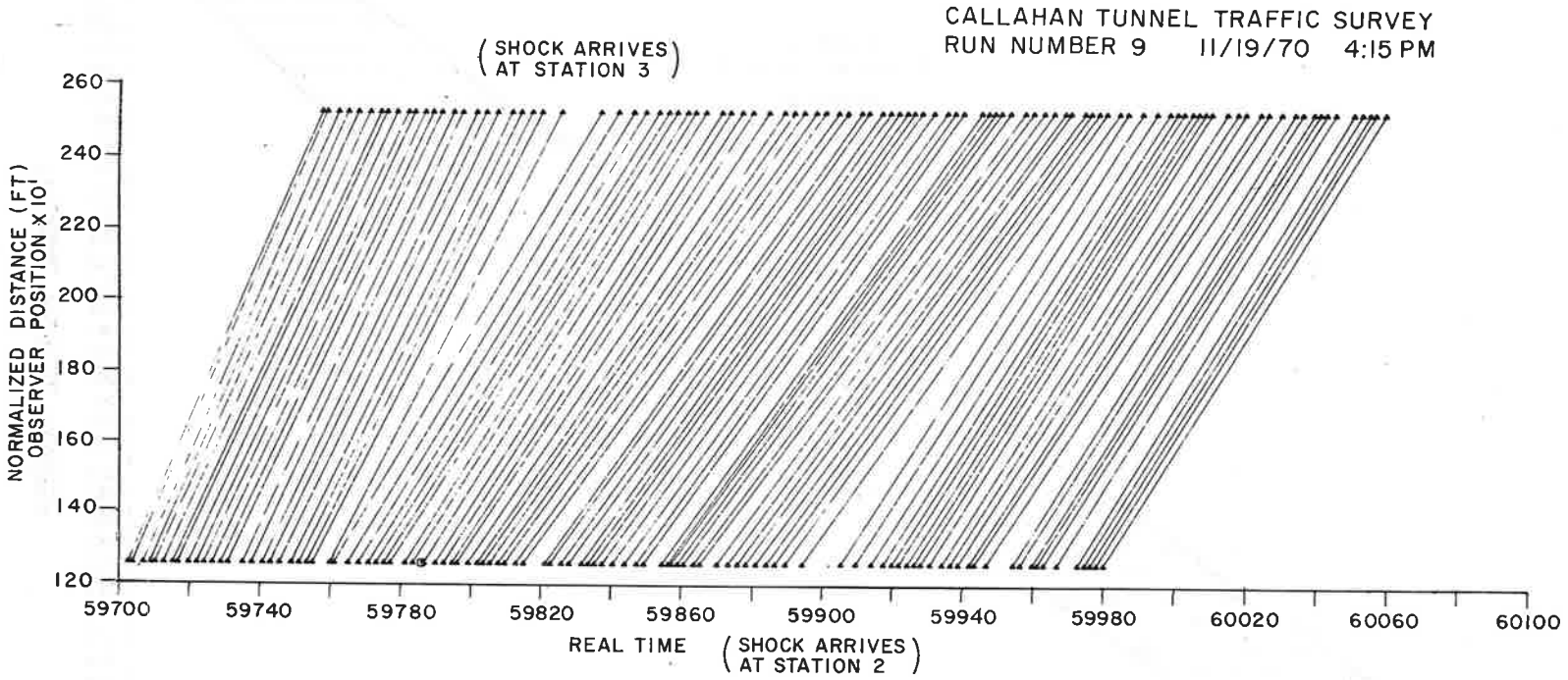


Figure 4.28a. - Run #9: Space vs. time diagram of vehicle passing through stations 1 and 2 (time from 59,700 sec. to 60,060 sec.)

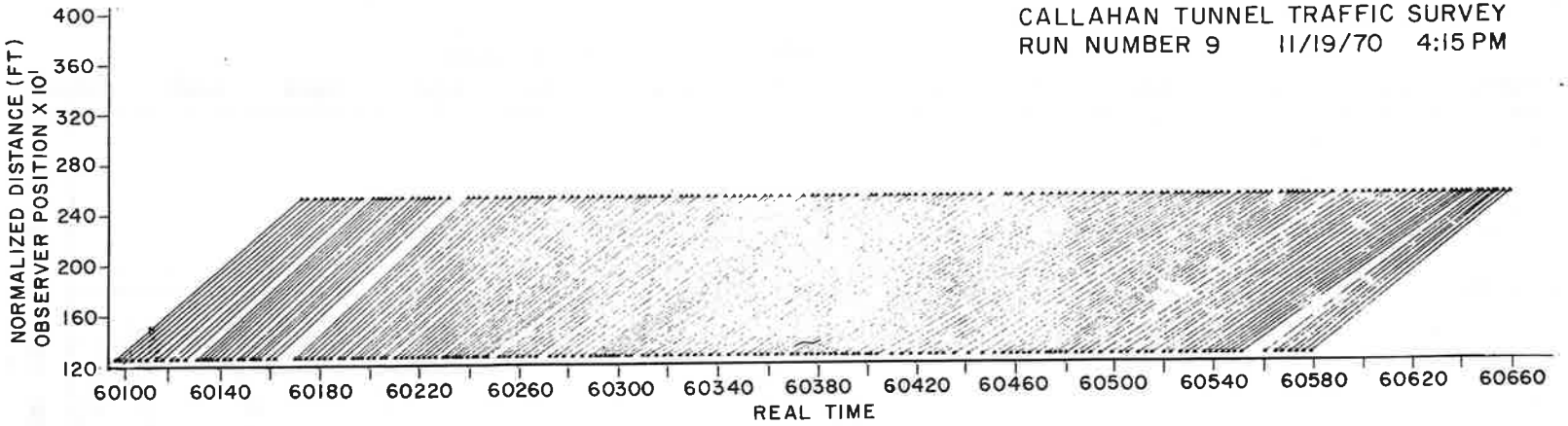


Figure 4.28b. - Run #9: Space vs. time diagram of vehicles passing through stations 1 and 2 (time from 60,100 sec. to 60,660 sec.)

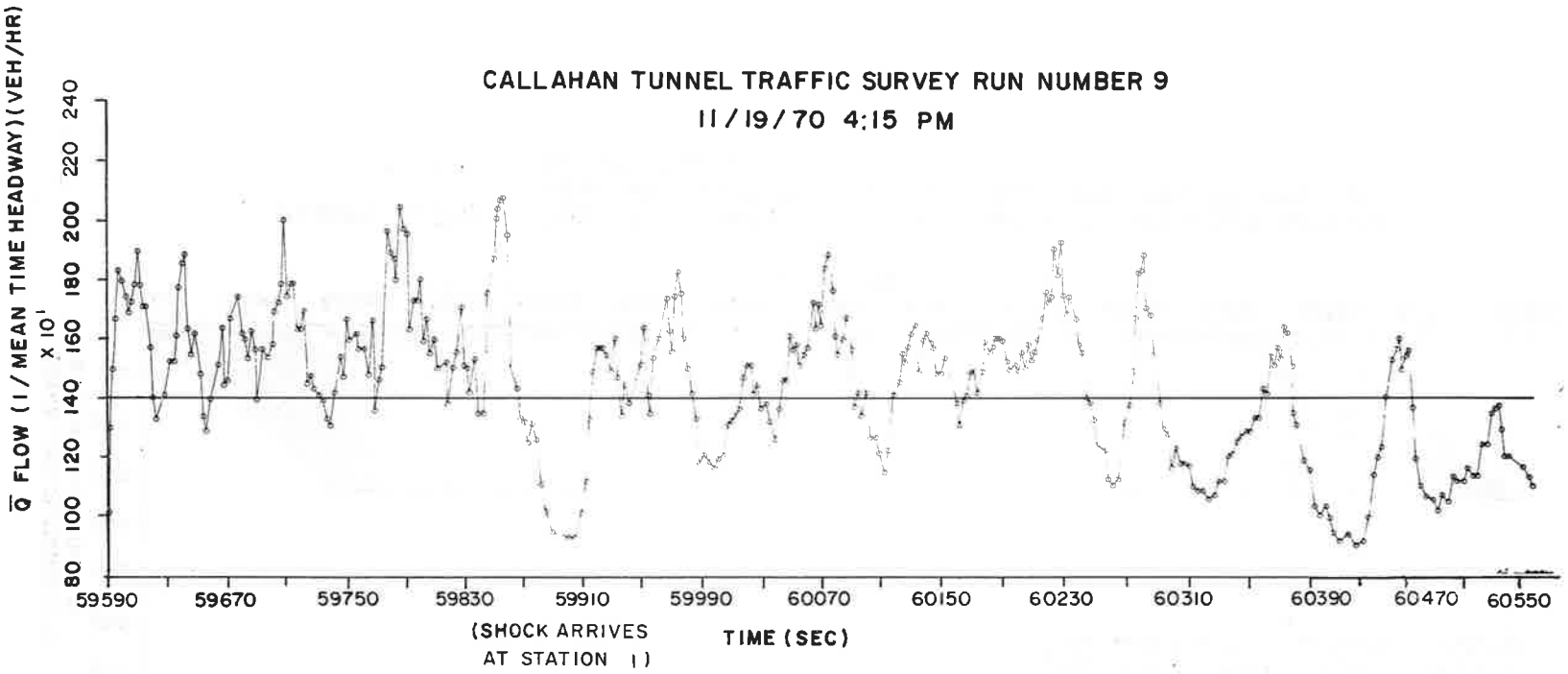


Figure 4.29a. - Run #9: $\bar{Q}$, Vehicular flow (1/mean time headway averaged over 7 vehicles), vs. time. Station 1.

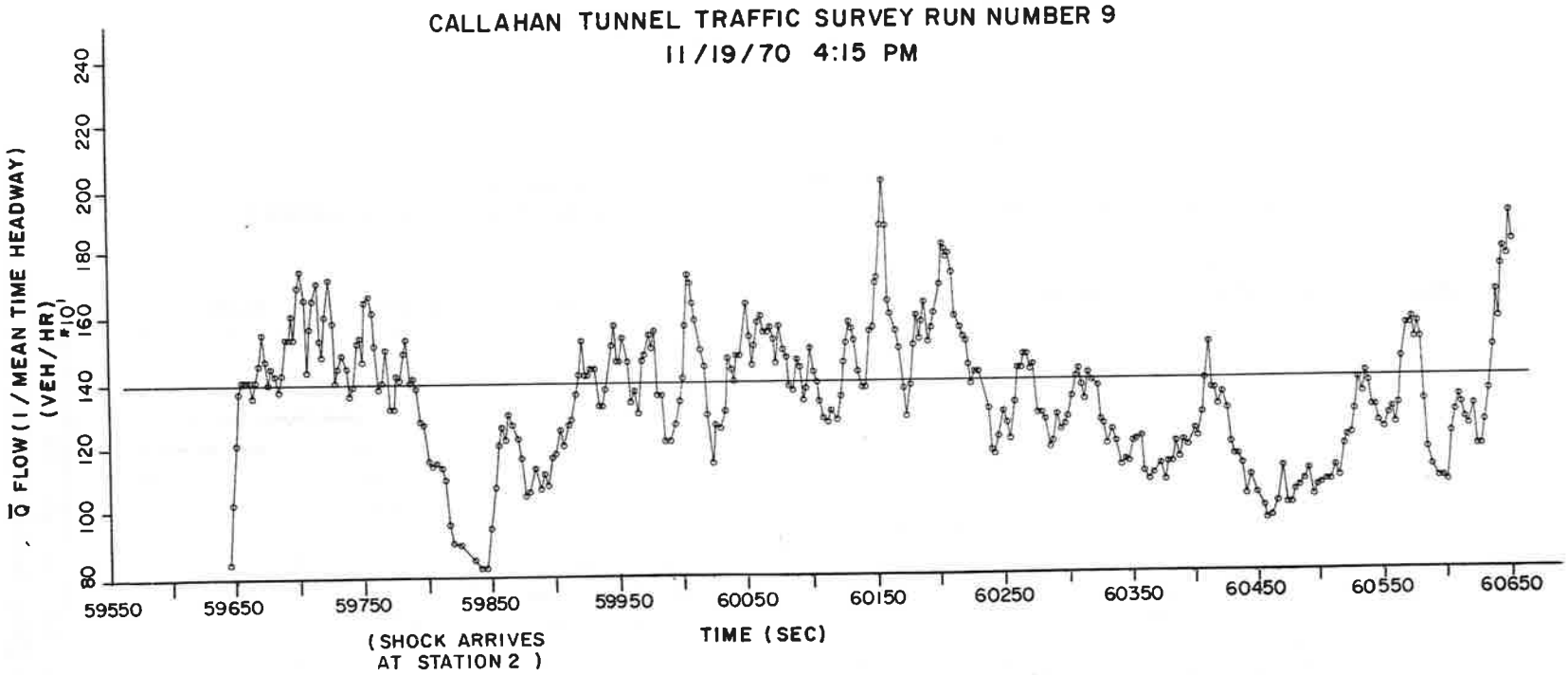


Figure 4.29b. - Run #9: $\bar{Q}$, Vehicular flow (1/mean time headway averaged over 7 vehicles), vs. time. Station 2.

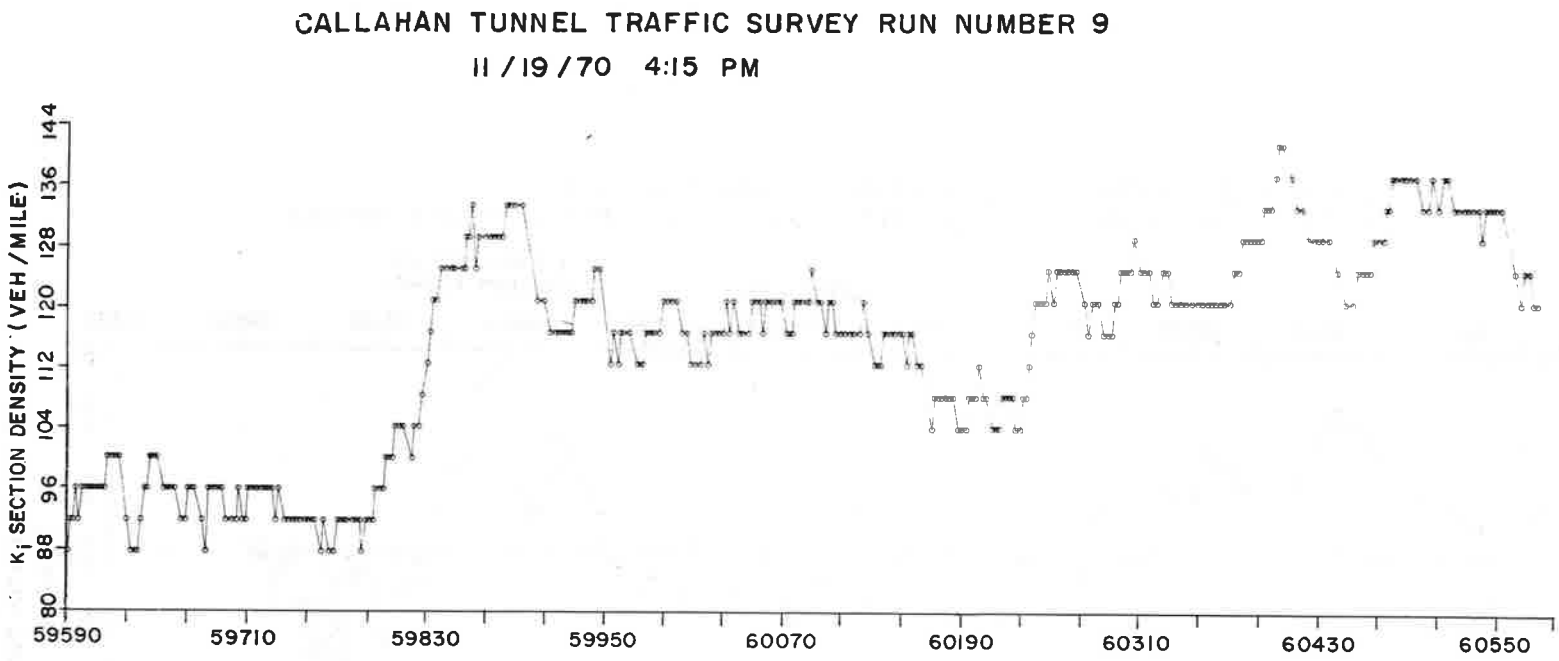


Figure 4.30. - Run #9: $K_i$, average vehicular density in the section between stations 1 and 2 vs. time.

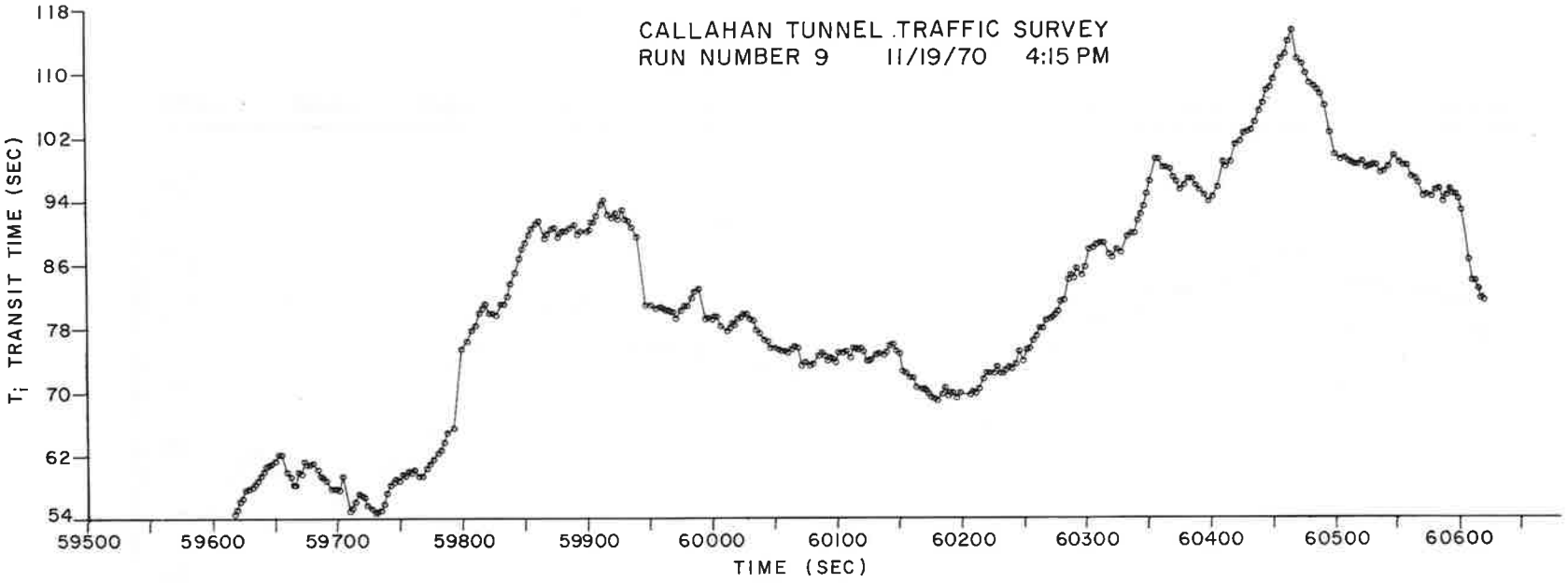


Figure 4.31. - Run #9: $T_i$, transit time of a vehicle travelling from stations 1 to 2 vs. the middle of the transit time.

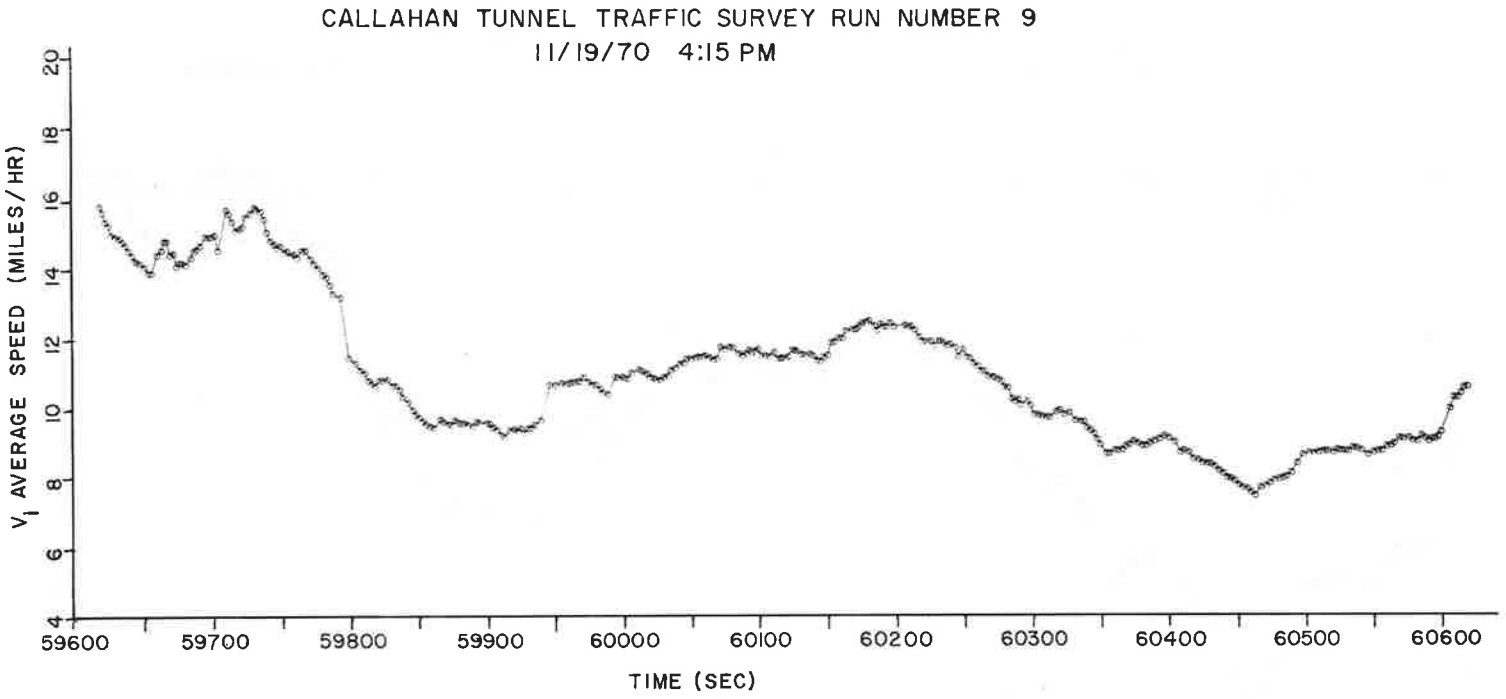


Figure 4.32. - Run #9: $V_i$, average speed of a vehicle in transit from stations 1 to 2 vs. the middle of the transit time.

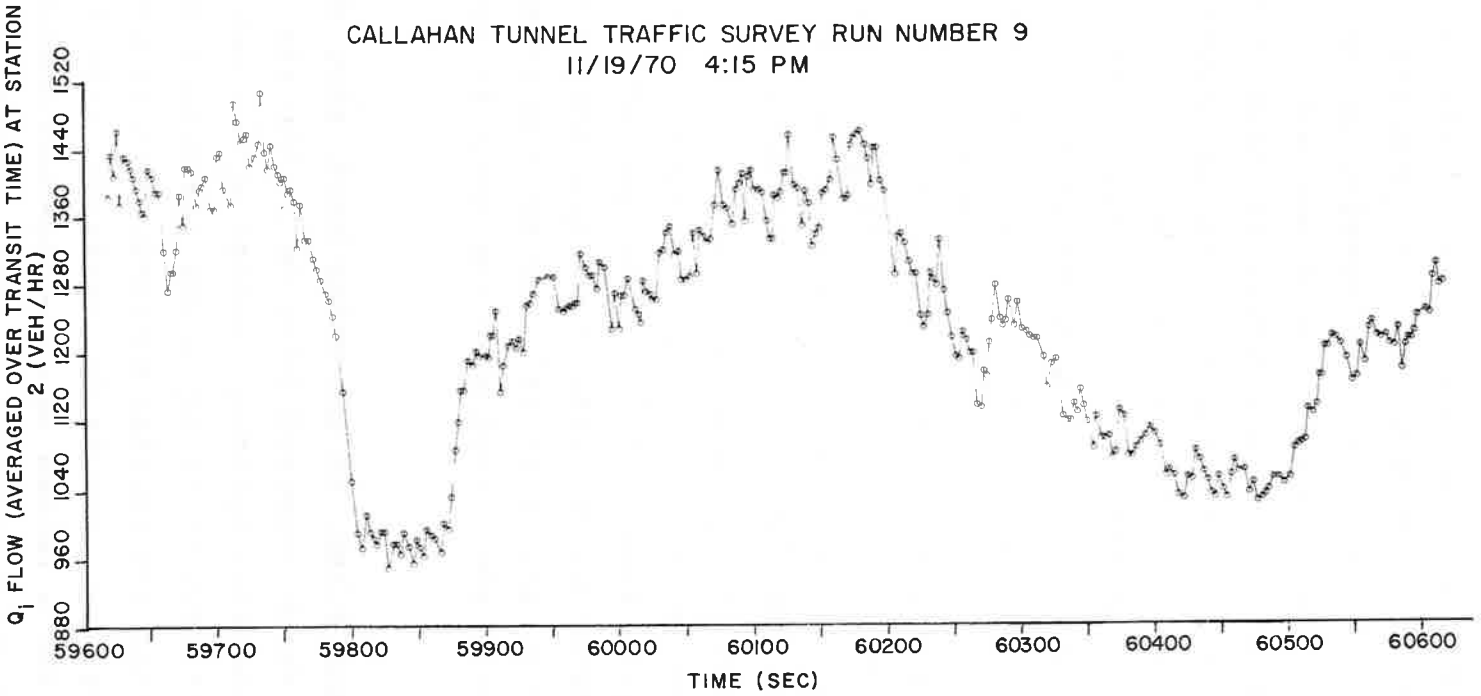


Figure 4.33. - Run #9: $Q_i$, flow at station 2 averaged over the transit time of a vehicle vs. the middle of the transit time.

Figure 4.27a shows that a slowdown reached station 2, the downstream station, at 59,822 sec. (at which time vehicle number 514 arrived) and travelled upstream reaching station 1 some 70 seconds later at 59,892 sec. (at which time vehicle number 565 arrived). The speed of the slowdown wave through the section was 18.1 feet/sec., (12.3 mph), and the density in the section during the passage of the wave rose almost one and a half times. A measure of the strength of this slowdown is obtained by using the above data, the observation that the maximum number of vehicles in the section was 32, the length of the section (1265 feet), and a computed jam density of 212.9 vpm. A stoppage width of 436 feet containing approximately 18 vehicles is obtained, and a "delay time" of 24 seconds is calculated from this width and the shock speed. These are about the same values as calculated for the shock wave in run number 4. In both cases the shock covers a span of several hundred feet effecting about 18 vehicles for about 25 seconds and causing a 50 percent increase in density in the section. The consequent loss of speed and drop in the flow due to this shock are shown in Figures 4.29 - 4.33.

First, as before, we show a space time representation of the slowdown wave, Fig. 4.28a. The slowdown period is seen to be pretty well bracketed by two sets of steeper-sloped parallel lines on either side of it, which indicate the faster speeds of the vehicles outside the period when the shock is present.

Figures 4.27b and 4.28b, on the other hand, show the general congestion build-up which occurred later on in the run. This is called a general congestion build-up instead of a shock phenomenon because there doesn't seem to be any clear indication of a return to normal density after the initial build-up. It is possible that a successive series of shocks is occurring, with insufficient time between shocks for a return to non-congested conditions. The shocks shown here may have occurred in rapid succession over an

extended period of time because of the particular configuration and the relationship of this section to the rest of the tunnel. The section must accept a high flow of speeding vehicles from the section immediately preceding it. If this section and the next section downstream cannot handle the high speeds and high flows from the downgrade, the vehicles will be forced to slow down, some quite abruptly. Such unstable driving conditions, high traffic densities and abrupt slowdowns might very well lead to the occurrence of a quick succession of shock waves postulated to cause the congested conditions observed here.

In the next set of figures 4.29 through 4.33, the flow, density, transit time and speeds are plotted as a function of time. In Figures 4.29a and 4.29b the flow, as the reciprocal of the mean headway time averaged over seven vehicles, is shown as a function of time at stations 1 and 2. Around the time 59,820 sec., the arrival of a shock is quite apparent and appears as a sharp drop in the flow of vehicles at that time (Figure 4.29a). The propagation of the shock from station 2 to station 1 is seen some 70 seconds later at time 59,890 sec. at station 1 (Figure (4.29b).

Figure 4.30 shows the density in the section as a function of time. The dramatic rise in density around 59,820 sec. signals the onset of the slowdown. The density recovers, dropping from around 136 vpm to 120 vpm, after the shock has passed but is still much higher than it was before the shock appeared. The density

begins to climb again around 60,230 sec. as the general congestion phenomenon sets in and remains high until the end of the run.

Figure 4.31 shows the corresponding transit times. There is a sharp rise in the time it takes a vehicle to cross the section during the time the shock is passing through. The transit time increases again as the traffic becomes heavy, (see Figure 4.30) around the time 60,230 sec., though at a more gradual pace and over a longer period of time. The transit times do come down somewhat toward the end of the run but are still relatively quite high, indicating that the congestion is still present.

Figure 4.32 shows the vehicular speeds in the section. The speeds drop some 40 percent from 16 mph to 9 and 10 mph when the shock arrives. The speeds increase again to about half of what they were before the shock, and then deteriorate even further as the density builds up to the high values shown in Figure 4.30.

Finally, we show another flow versus time curve (similar to Figure 4.29b), but this time the flow has been averaged over the transit time. It is very interesting to observe that the effects of the slowdown and congestion are shown even more dramatically here than in Figure 4.29b. In Figure 4.33 the integration time is longer than in Figure 4.29, and the curve is smoothed out, but the effect is to accentuate and dramatically highlight the loss in throughput rather than diminish it. Two very distinct flow-derogations stand out in this figure, the first due to the shock and the second, later on in the run, due to the congestion.

There are many different types of averages that one can use and this example, together with the example of run 4 discussed previously, points out the difficulty of knowing a priori which type best illustrates the physical phenomenon and which will be most efficient as accurate delineators of conditions which should activate a traffic control system. Before such a control system is set up, further thought must be given to this averaging choice.

### 4.3.4 Run Number 14 - End Section, Last 300 Feet

The next set of figures, 4.34 through 4.42, shows the occurrence of a slowdown wave at the end of the tunnel, between station $3_a$ and the exit portal, $B_2$, some 307 feet downstream.

Figure 4.34 shows the arrival time of vehicles at stations $3_a$ and $B_2$ as a function of the particular vehicle at these stations, around the time of the slowdown. The slowdown, orginiating from a toll booth back-up at the exit, reached station $B_2$ at the time 58,460 sec. and continued to travel upstream reaching station $3_a$ some 24 seconds later at time 58,484 sec. The wave thus travelled the 307.3 feet in 24 seconds with an average speed of 12.8 feet/sec. (8.7 mph), passing vehicle number 316 near the exit portal $B_2$, and vehicle number 329 at station $3_a$, as can be seen in the figure. An idea of the severity of the slowdown is obtained from the shock width: Using the observation that the density rose to 1.6 times its normal value when the wave passed and that the jam density is 223.4 vpm, we obtain a shock width of 115.26 feet within which there are 4.9 vehicles. The *delay time*, $w/V_s$ is 9.0 seconds, where $V_s$ is the shock speed. The stoppage here is shorter and the shock less severe than those which occurred in the beginning and middle sections, discussed above.

Figure 4.35 shows the slowdown on a space time diagram and Figure 4.36 shows the flow as a function of time. It was found to be difficult to detect the lowering of flow caused by the passage of the slowdown wave at the two stations by looking at flows averaged over some number of vehicles as has been done previously. However, this lowering of the flow became evident when we averaged the flow over time (10 second intervals with running shifts of 2 seconds) as seen in Figures 4.36a and b. This is due to the ability of seeing very low or zero flows when the slowdown is averaged over time, as the stoppage or slowdown lasts for some finite period of time. It is worthwhile to emphasize

here that the use of one or another type of average in no way affects the reality of the physical phenomenon. A slowdown exists or it doesn't exist, independently of whether the computer calculates vehicle or time averages. The ability to detect the presence of the phenomenon, however, is a function of the averaging used, and a correct choice is a non-trivial consideration.

Figure 4.37 shows the density plotted as a function of time for the duration of the whole run. Beginning at about time 58,240 sec., a number of above average densities are sustained and finally, at around 58,460 sec. there is a sharp rise in the density indicating the presence of the stoppage phenomenon depicted in the preceding graphs. The interesting point to note in this graph is the occurrence of the above average densities preceding the shock. This suggests that, in addition to pulses of high flow triggering a shock wave as discussed previously, a sustained high density situation may also help trigger the shock and produce wave growth.

Finally, the relationship between the traffic flow parameters is shown in Figures 4.38 through 4.41, in which the build-up in the number of vehicles in the section is related to the increase in the time it takes a vehicle to cross the section, to the drop in vehicle speeds and to the decrease in vehicular flow during the time the wave crosses the section.

### 4.3.5 Run Number 15- End Section, Last 300 Feet

In this final section on slowdown phenomena another slowdown wave is shown originating from the exit toll booths and travelling upstream to the exit portal ($B_2$) and then to station $3_a$, 307 feet further upstream. This is similar to run number 14 just preceding, except the slowdown was less pronounced. The wave passed vehicle number 77 and arrived at time 60,813 sec. at the exit portal, $B_2$, then passed vehicle number 92 reaching station $3_a$ some 33 seconds later at time 60,846 sec. (Figures 4.42 and 4.43). The wave traveled relatively slowly at 9.3 feet/sec. (6.4 mph), and probably did not cause an actual stoppage.

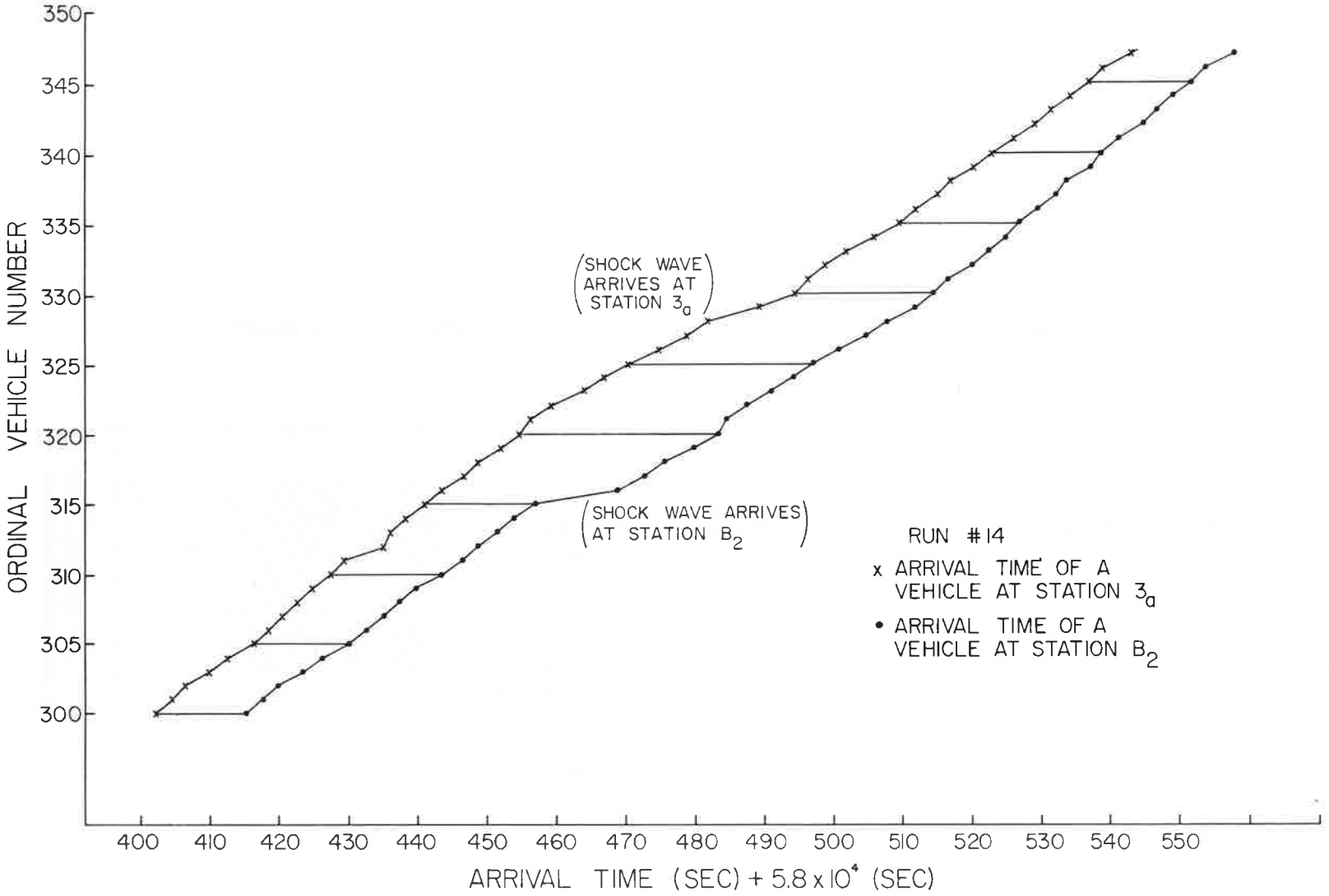


Figure 4.34.- Run #14: Arrival times of vehicles at stations $3_a$ and $B_2$ vs ordinal vehicle number around the time interval when a slow down wave occurred.

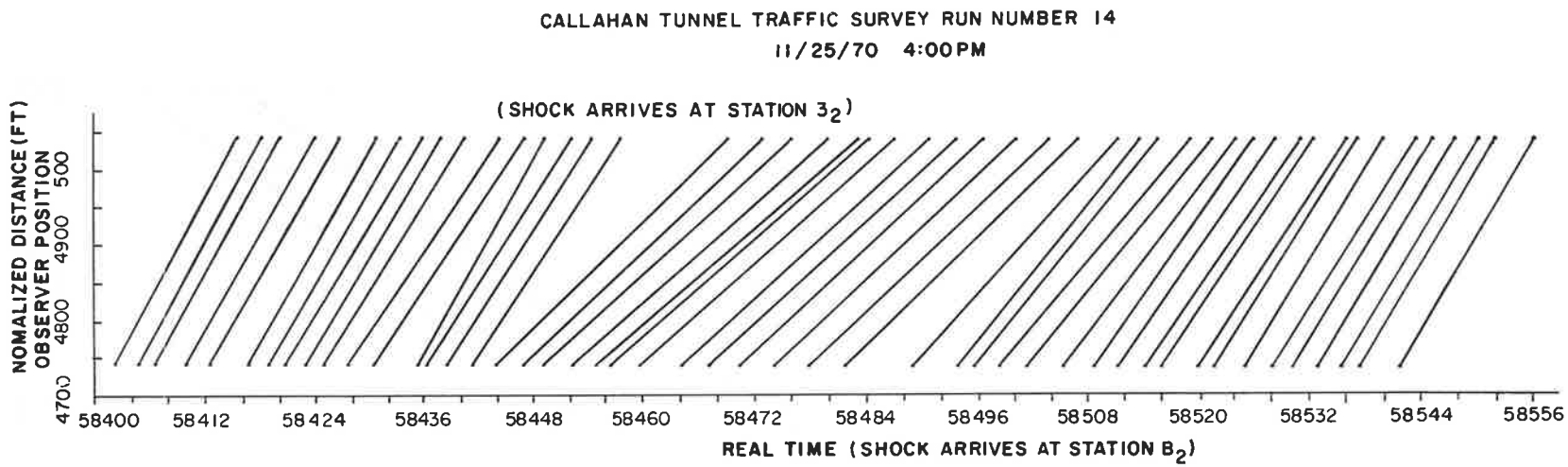


Figure 4.35. - Run #14: Space vs. time diagram of vehicles passing through stations $3_a$ and $B_2$.

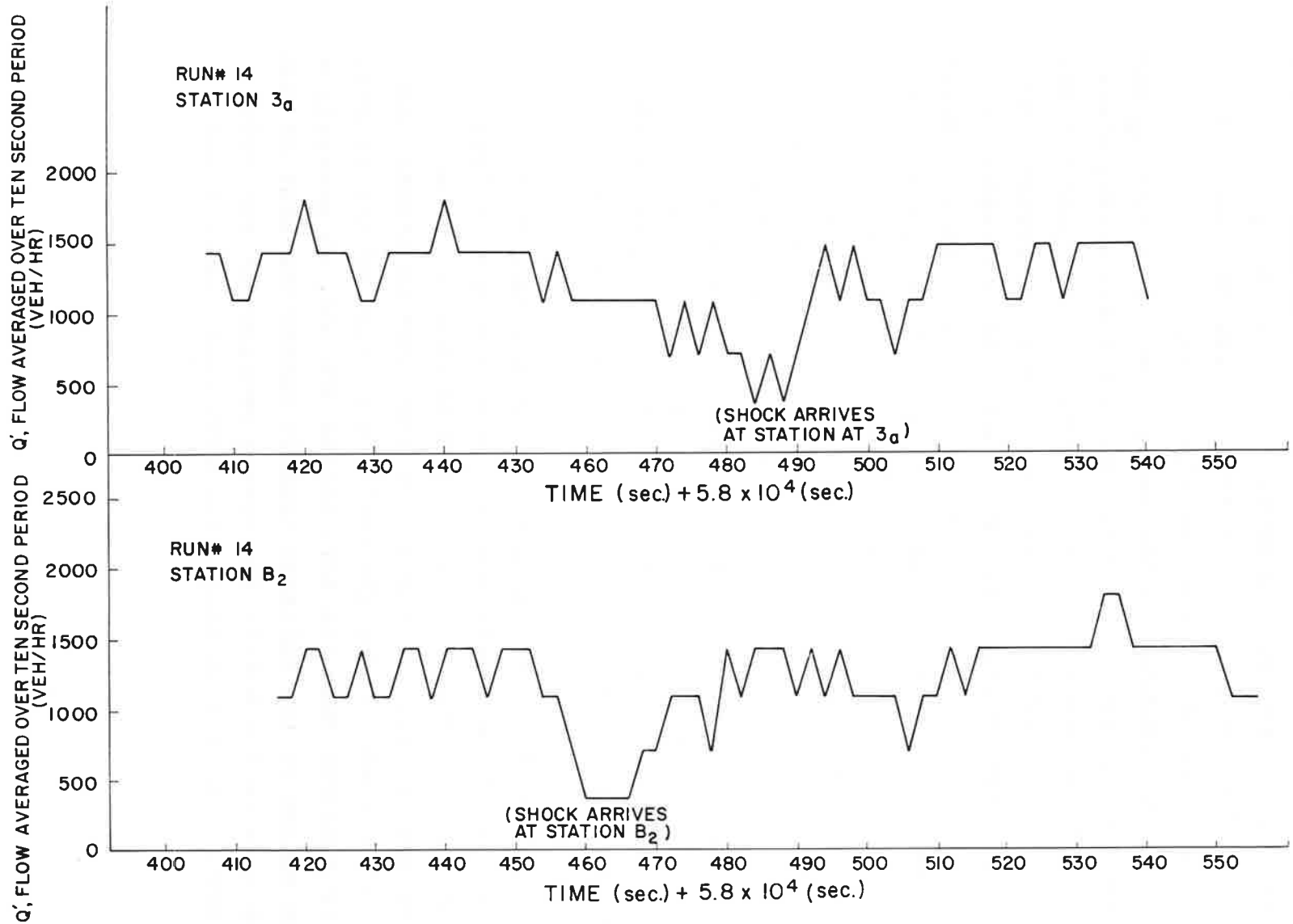


Figure 4.36a and b.- Run #14: Q', vehicular flow averaged over ten second period vs. time.
(a) station $3_a$
(b) station $B_2$

It had a relatively short width of 81 feet within which were only 3.4 vehicles on the average. A maximum possible delay time of 8.7 seconds would have occurred if the vehicles were stopped since the shock took this amount of time to pass.

The low flows produced by the wave, first at station $B_2$ and then at station $3_a$, are shown in Figures 4.44a and 4.44b, where flow (running 10 second averages) has been plotted against time. The traffic density for the entire run is shown in Figure 4.45, which for this weak shock, shows no abrupt rise, so evident in the previous slowdowns; instead its presence is recognized mainly by its longer time duration relative to several other occurring high, but short duration densities. That the wave growth is quite real, however, is evident from the next set of figures 4.46 through 4.48, where the rise in the number of vehicles in the section as the shock passes, stands out well (Figure 4.46). The concurrent sharp rise in transit time (Figure 4.47) and the associated drop in vehicle speed (Figure 4.48) also show the effects of the wave. Figure 4.49 shows, though less obviously, the reduction in flow (averaged over the transit time) when the shock is present.

A final comment is that this shock and the similar one measured in run 14 taken near the exit portal were much less severe than the ones observed in comparable runs in the middle sections of the tunnel. This plus the fact that no shocks were observed in run number 8 for the full end section of the tunnel, leads us to conclude that the toll booths are not, in general, a bottleneck source at the Callahan tunnel; rather the seat of congestion appears to lie within the center sections of the tunnel as discussed previously in connection with runs number 9 and 4.

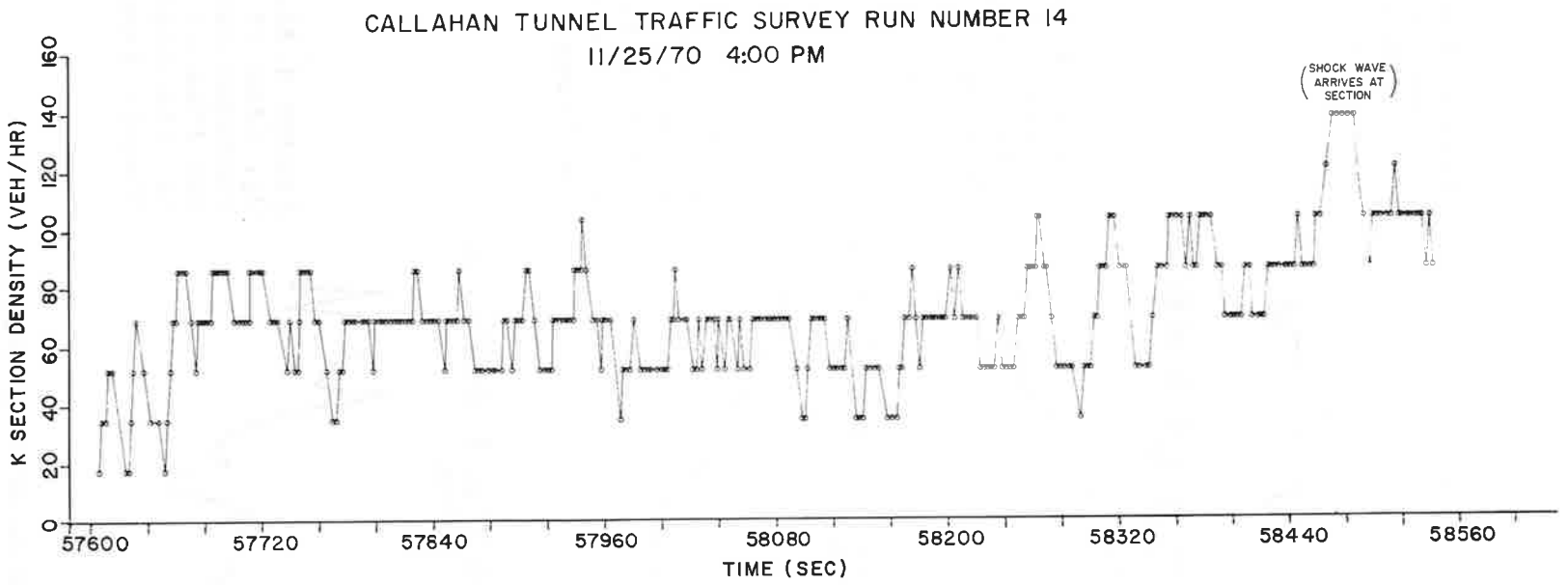


Figure 4.37. - Run #14: $K_i$, average vehicular density in the section between stations $3_a$ and $B_2$ vs. time for the time period of the entire run.

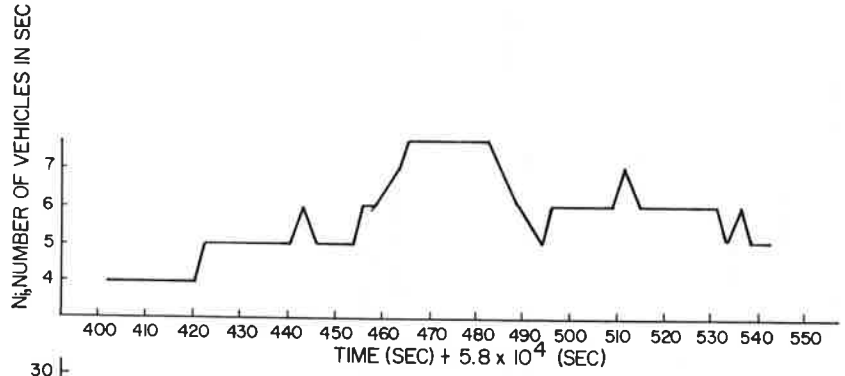


Figure 4.38.- Run #14: $N_i$, number of vehicles in the Section between stations $3_a$ and $B_2$ vs. time.

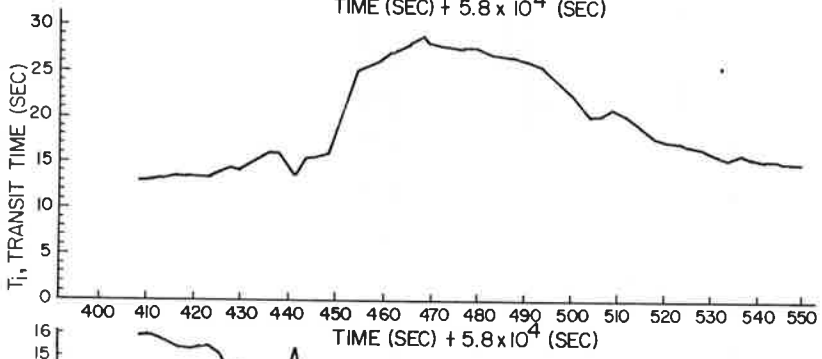


Figure 4.39.- Run #14: $T_i$ transit time of a vehicle travelling from stations $3_a$ to $B_2$ vs. the middle of the transit time.

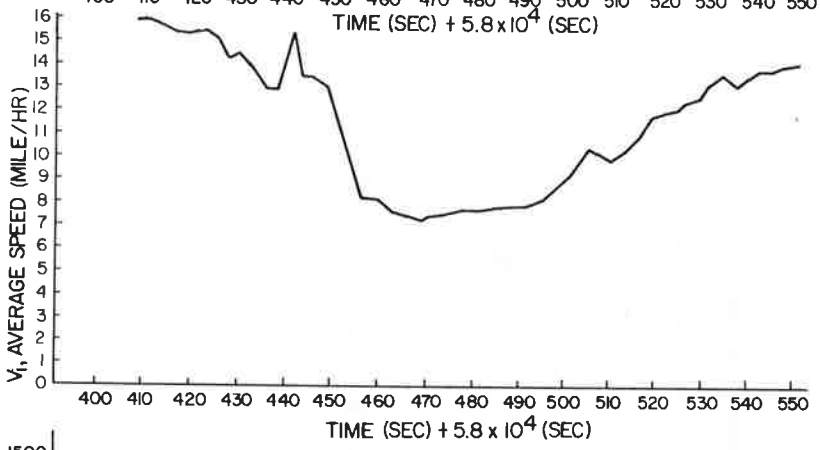


Figure 4.40.- Run #14: $V_i$ average speed of a vehicle in transit between stations $3_a$ and $B_2$ vs. the middle of the transit time.

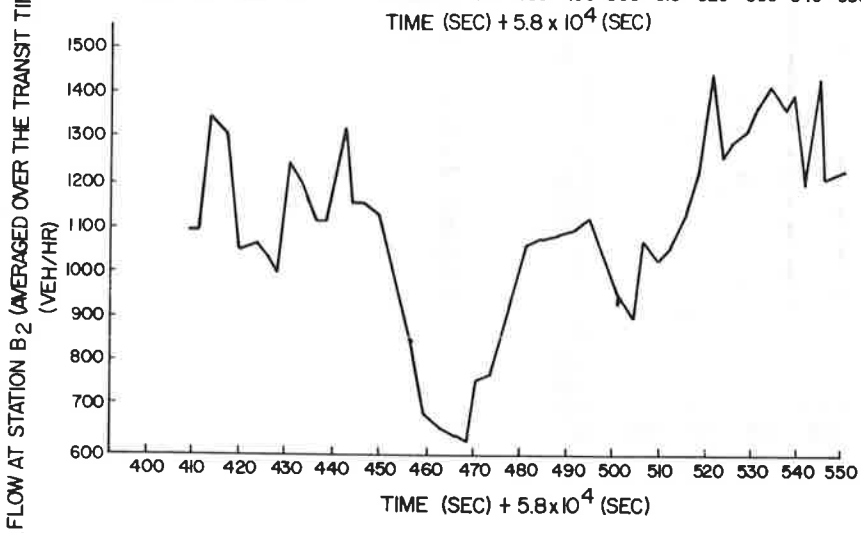


Figure 4.41.- Run #14: $Q_i$, flow at station $B_2$ averaged over the transit time of a vehicle vs. the middle of the transit time.

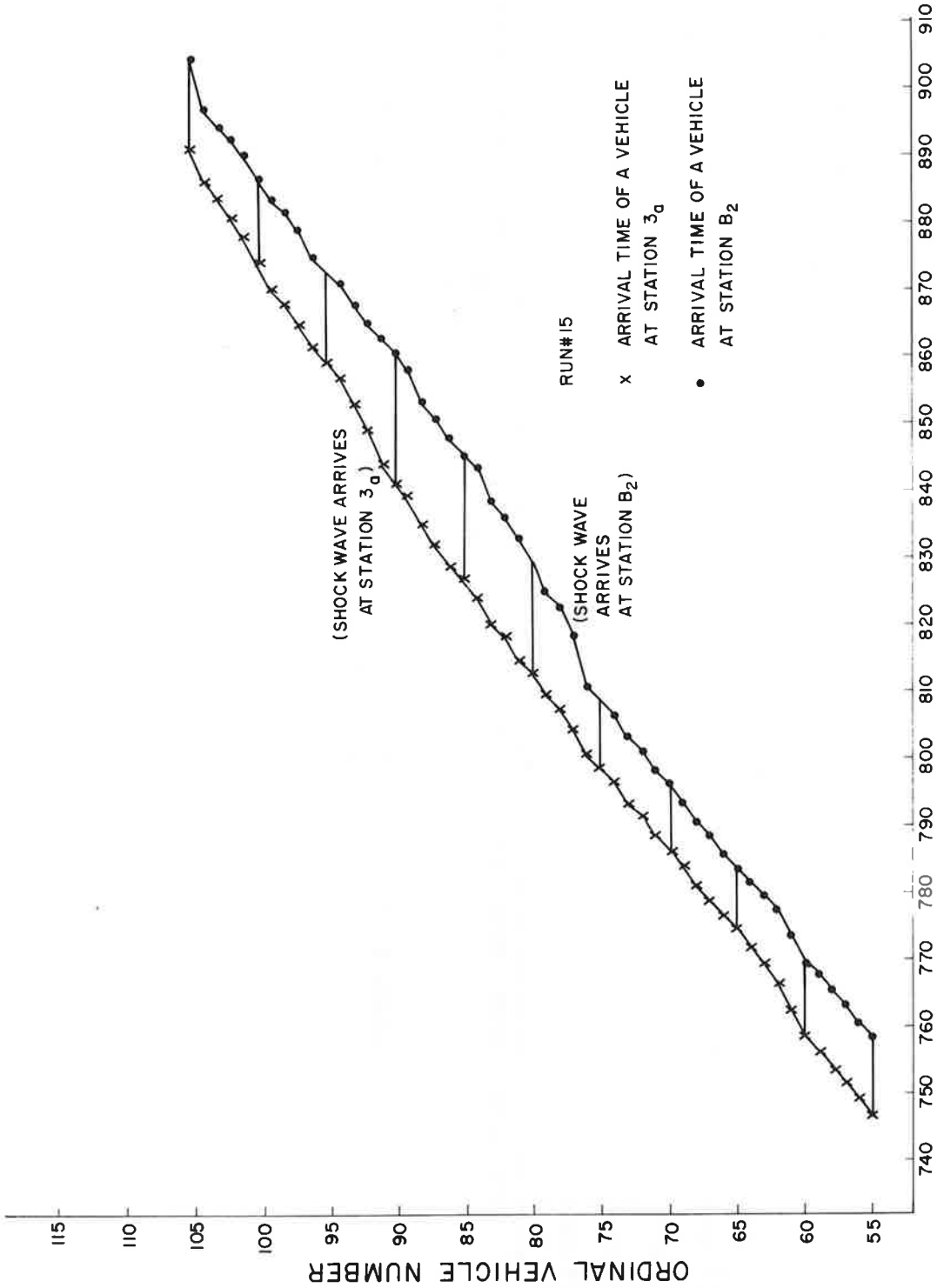


Figure 4.42.- Run #15: Arrival times of vehicles at stations $3_a$ and B2 vs. ordinal vehicle number around the time interval when a slow down wave occurred.

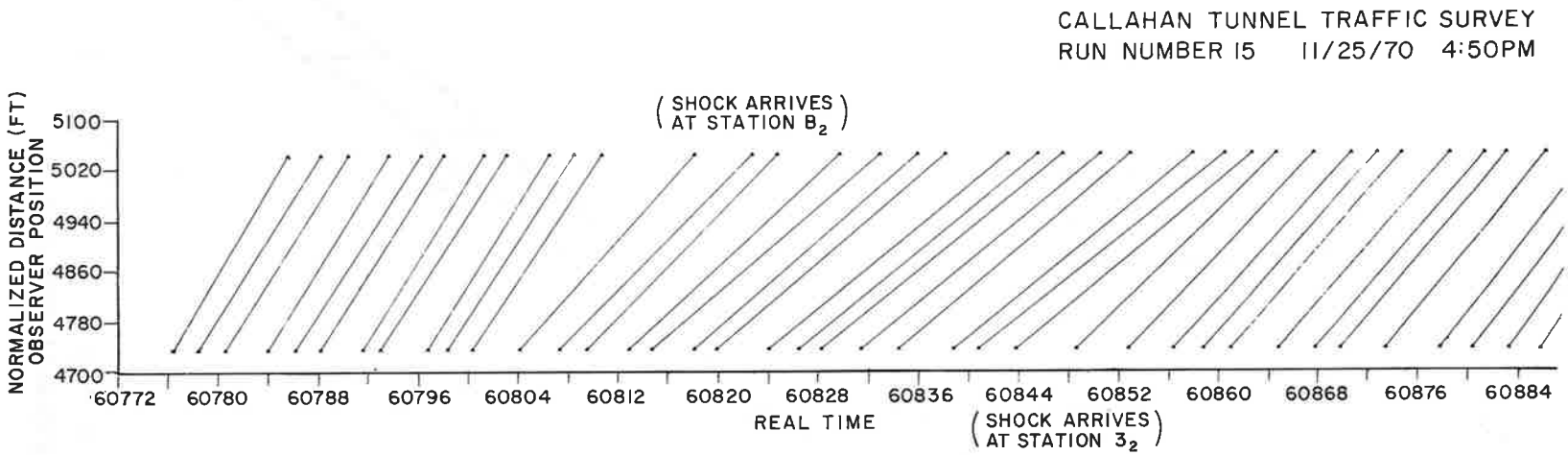


Figure 4.43. - Run #15: Space vs. time diagram of vehicles passing through stations $3_a$ and $B_2$.

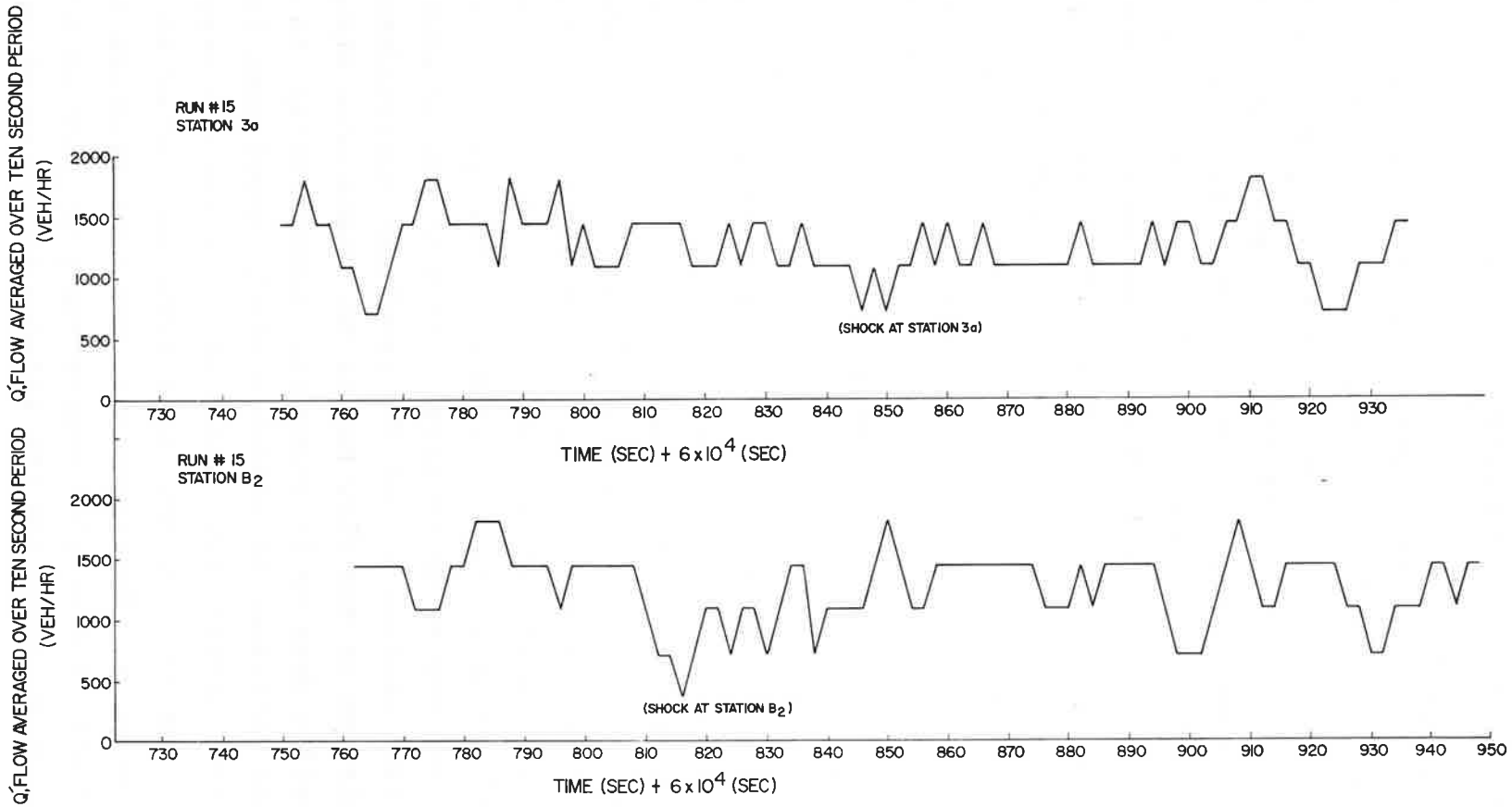


Figure 4.44a and b.- Run #15: Q' vehicular flow averaged over ten second period vs. time.
(a) station $3_a$ (b) station $B_2$

## 4.4 TRAFFIC FLOW WITH AND WITHOUT SHOCKS

### 4.4.1 Introduction

In previous paragraphs vehicular flow and speed were plotted as a function of density (Q-K and V-K curves) for an entire observation run. Some of these runs contained noticeable slowdown or wave growth phenomena and these phenomena were discussed separately in paragraph 4.3. Now we would like to present a picture of the flow and speed as a function of density when all data points associated with the slowdown wave have been removed, illustrating relatively steady unperturbed traffic flow. The curves containing all the data points are shown here also for comparison (even though they have been shown before). The purpose of displaying the Q-K and V-K relations with and without the slowdown, is to show what happens to the flow-density (and speed-density) curve when the perturbing slowdown wave is prevented from occurring.

The usual picture of flow increasing from zero at zero density to a maximum value, and then decreasing to zero again as jam concentration is approached, presupposes a single-valued relationship between flow and density. Section 2 showed that this cannot be strictly true due to the further dependence of the traffic flow on the time rate of change of density. In fact, for densities above some critical value where the flow is expected to be maximum, the difference between the usual Q-K relation and the actual one may be quite large. This is due to acceleration asymmetry (see Section 2) and the resultant multivaluedness of the Q-K relation as the flow begins to depend more strongly on how the traffic density is changing. Specifically, in Section 3 we presented experimental evidence which showed that for any given density, higher flows and greater speeds are associated with increasing density, and lower flows and slower speeds with decreasing density. Unfortunately, the same evidence could not be obtained with the simpler measurements of flow in the Callahan tunnel, though we could see the effects of the shock on the overall Q-K relation quite clearly. The presence of a growth wave or

shock in the traffic stream adds a number of both high and low density points not present when shocks are absent. Associated with the additional high density points are low traffic flows, as might be expected. Associated with the additional lower density points are also low traffic flows which occur soon after the onset of the shock when the density has not yet had time to build up in the section. These lower flows result when the first few vehicles which come in contact with the shock are slowed down. Since the number of vehicles in the section when the $i^{th}$ vehicle first enters, $N_i$ remains the same, but $T_i$, the transit time of the $i^{th}$ vehicle is increased when the vehicle strikes the shock entering the section, the measured flow $Q_i = N_i/T_i$ will be reduced.

These results are presented in Figures 4.50 through 4.73.

### 4.4.2 Data With And Without Shocks

In run number 9 taken in the first half of the middle section between stations 1 and 2, two periods of slowdown phenomena were found (see paragraph 4.3.3). The Q-K curves with these slowdown waves present are shown in Figures 4.50a and 4.50b. Figures 4.51a and b show the curve with the first slowdown wave removed, and Figures 4.52a and b with both removed. Inspection of the figures shows that the additional data points due to the shocks are generally points of higher density and lower flow as expected, and points of lower flow and lower density occurring soon after the arrival of the shock and causing a time delay of the first few vehicles.

The V-K curves are shown in Figures 4.53 through 4.55. The additional data points associated with the period when the growth wave was present depict the higher density, lower speed traffic resulting from the interaction of the wave with the traffic stream.

Both the Q-K and V-K curves show higher flows and higher speeds when the shocks have been removed which is particularly noticeable when both shocks have been removed, (Figures 4.52 and 4.57). In fact, when both shocks are removed a very significant

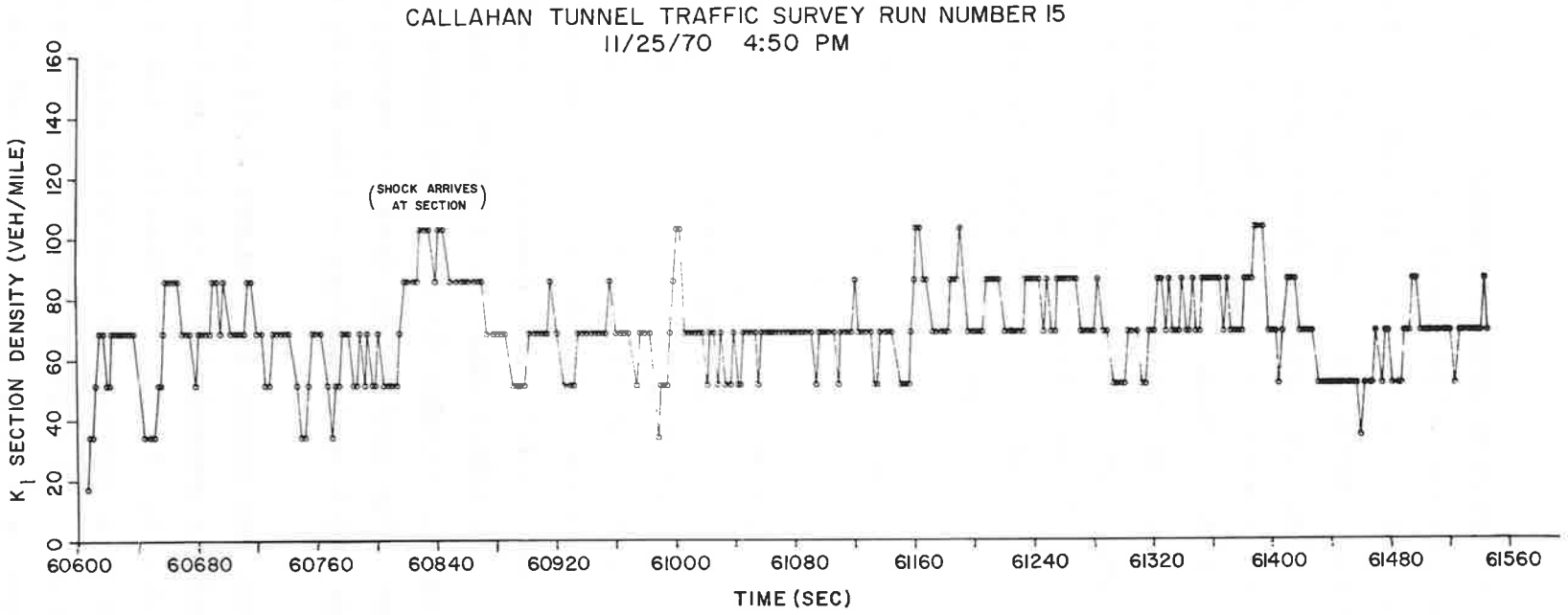


Figure 4.45. - Run #15: $K_i$, average vehicular density in the section between stations $3_a$ and $B_2$ vs. time period of the entire run.

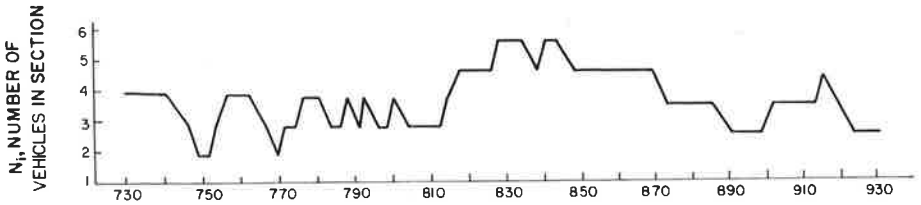


Figure 4.46.- Run #15: $N_i$, number of vehicles in the section between stations $3_a$ and $B_2$ time.

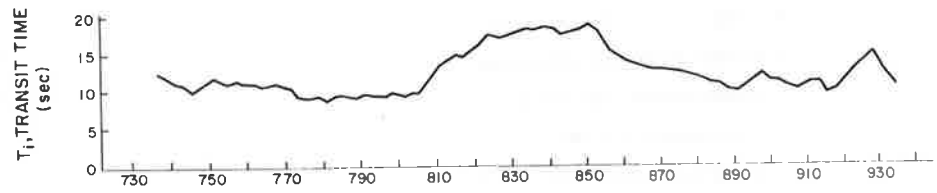


Figure 4.47.- Run #15: $T_i$, transit time of a vehicle travelling from stations $3_a$ to $B_2$ vs. the middle of the transit time.

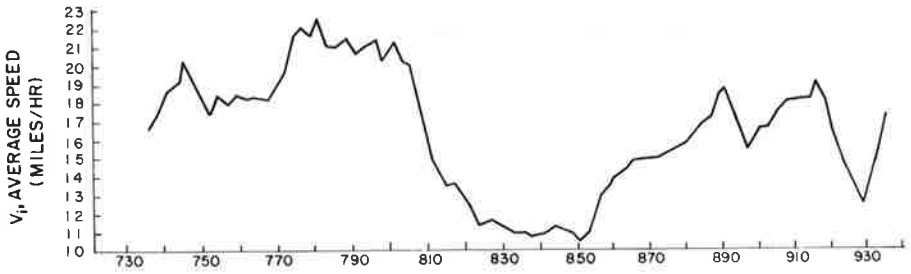


Figure 4.48.- Run #15: $V_i$, average speed of a vehicle in transit between stations $3_a$ and $B_2$.

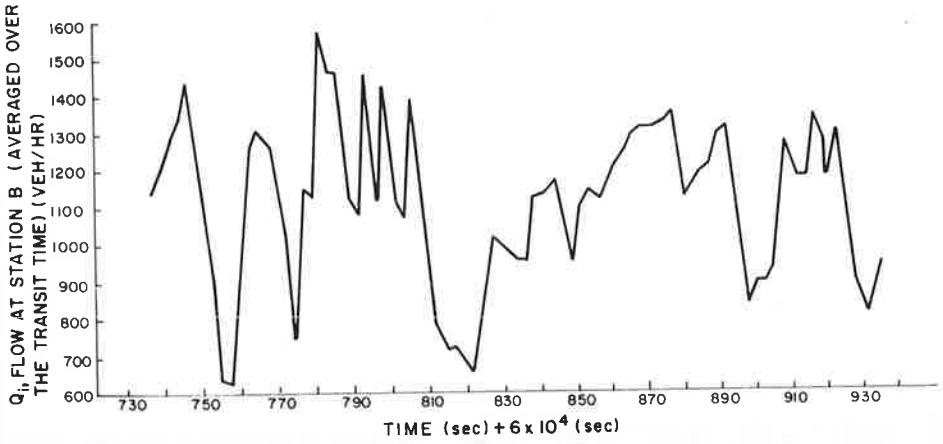


Figure 4.49.- Run #15: $Q_i$, flow at station $B_2$ averaged over the transit time of a vehicle vs. the middle of the transit time.

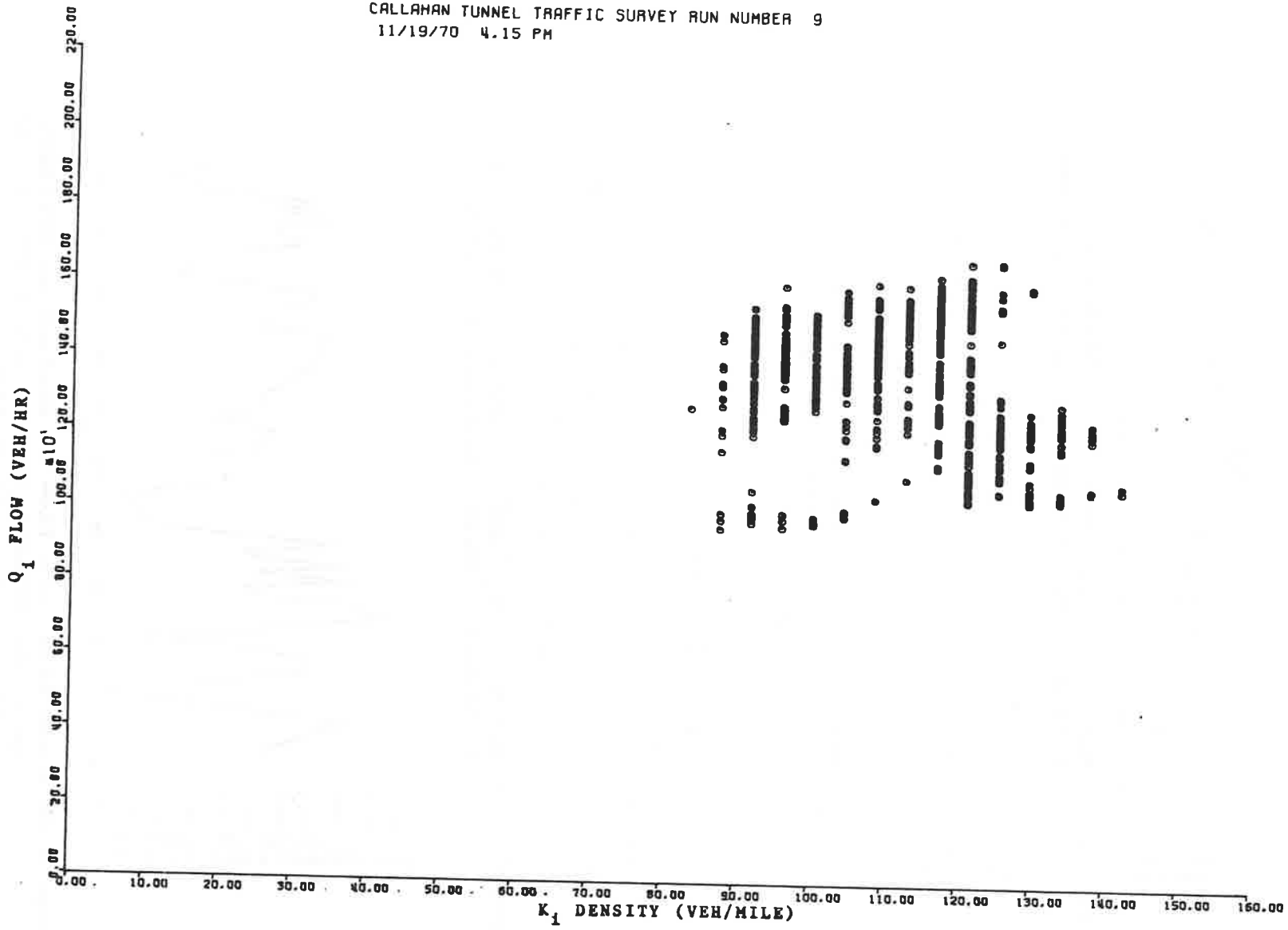


Figure 4.50a.- Run #9: Flow averaged over the transit time, $Q_i$, vs. average section density, $K_i$. Stations 1 to 2. Distance of 1265 ft. Slow down data included.

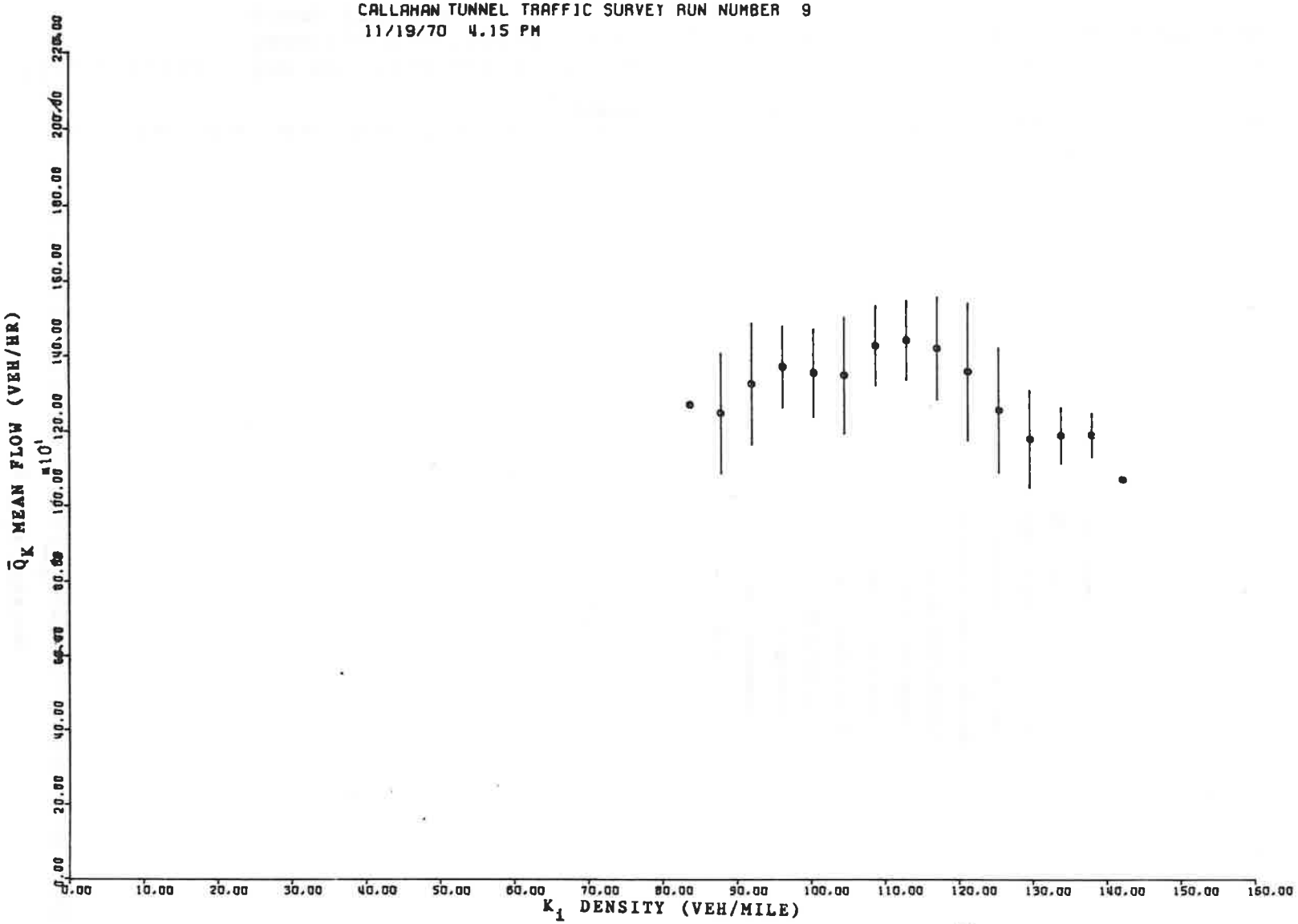


Figure 4.50b.- Run #9: Mean flow for a given section density, $\bar{Q}_K$, vs the density, $K_i$, stations 1 to 2. Distance of 1265 ft. Slow down data included.

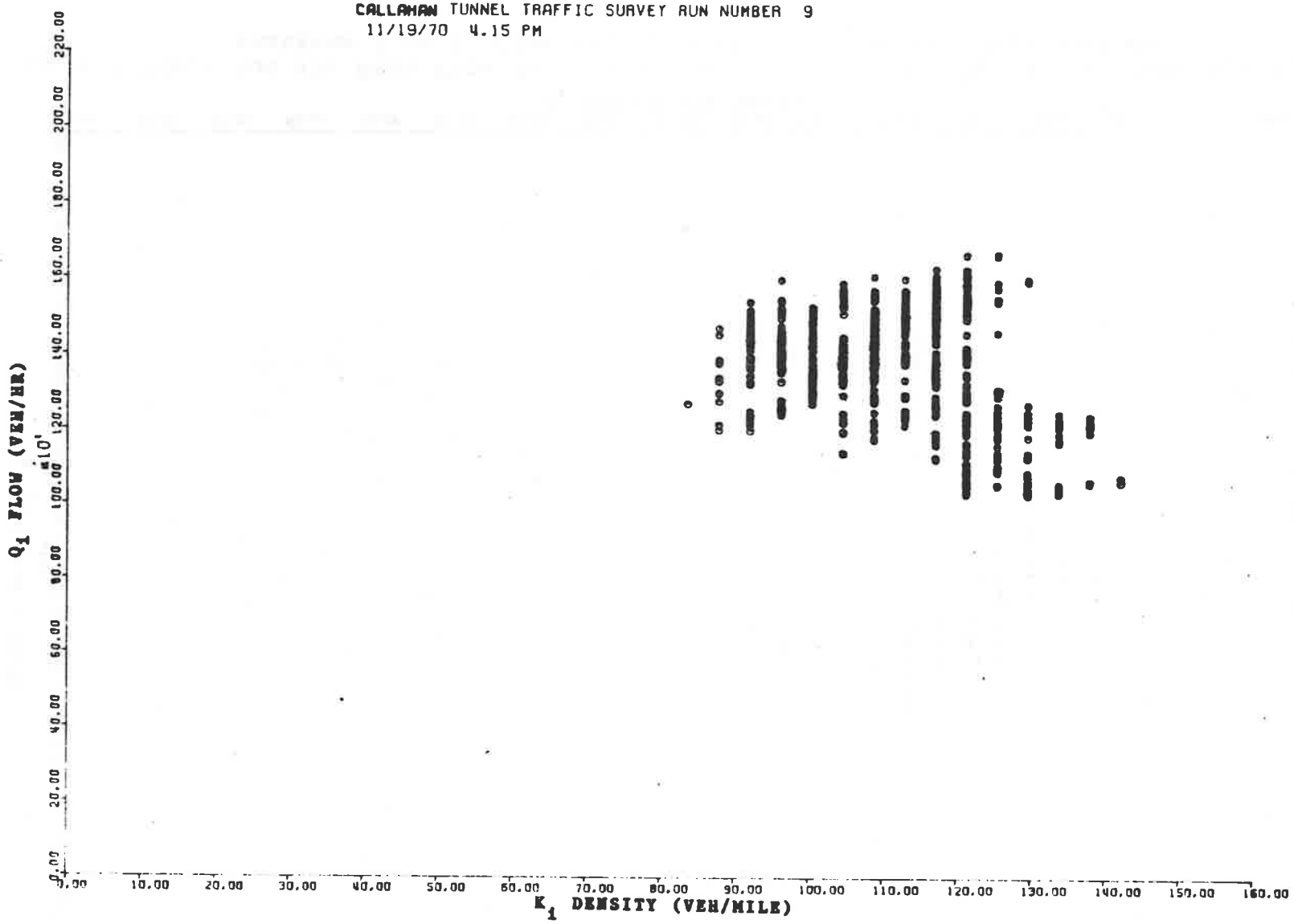


Figure 4.51a.- Run #9: Flow averaged over the transit time, $Q_i$, vs average section density, $K_i$. Stations 1 to 2. Distance of 1265 ft. First slow down group removed.

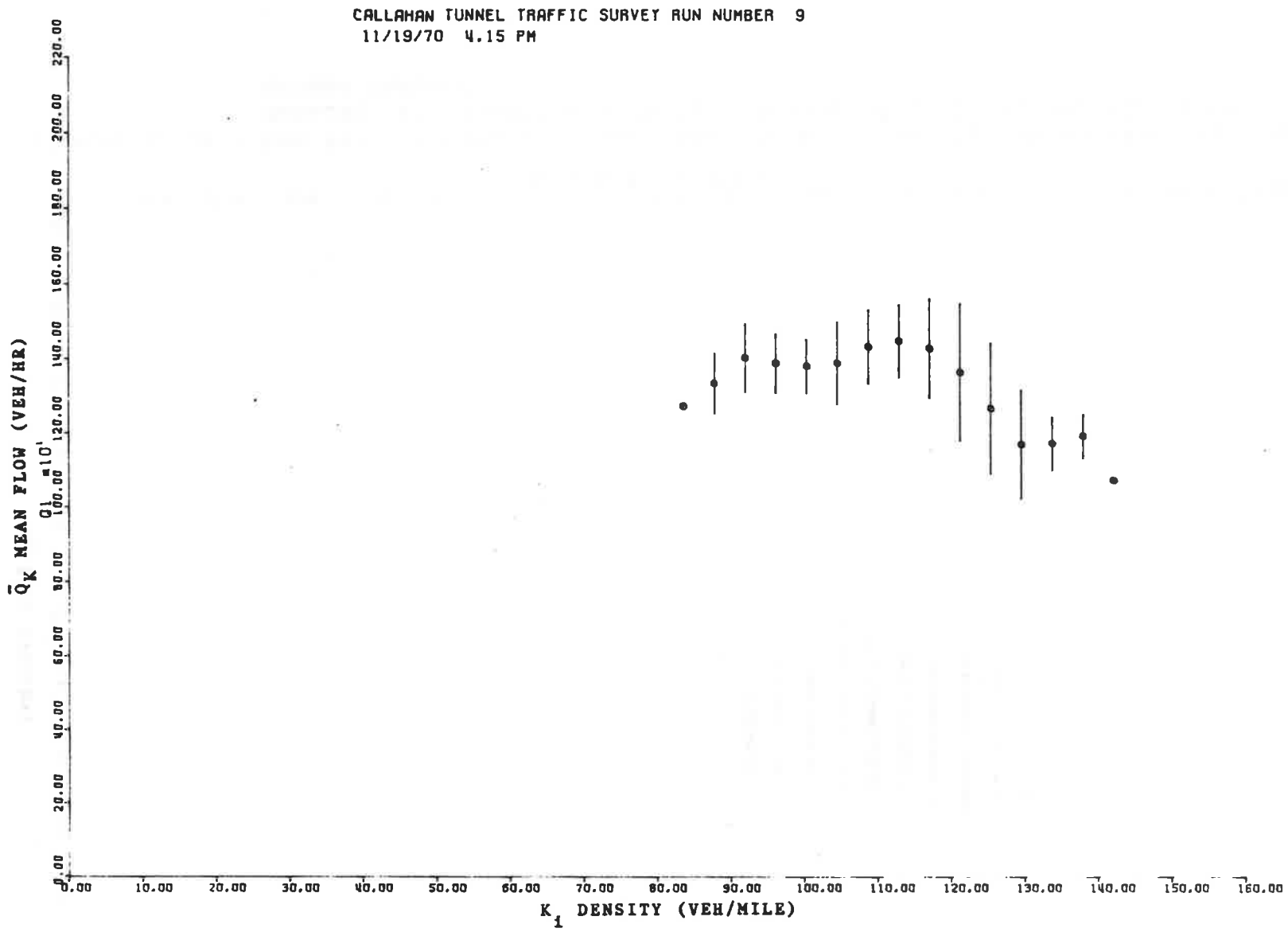


Figure 4.51b.- Run #9: Mean flow for a given section density, $\bar{Q}_K$, vs the density, $K_i$. Stations 1 to 2. Distance of 1265 ft. First slow down group removed.

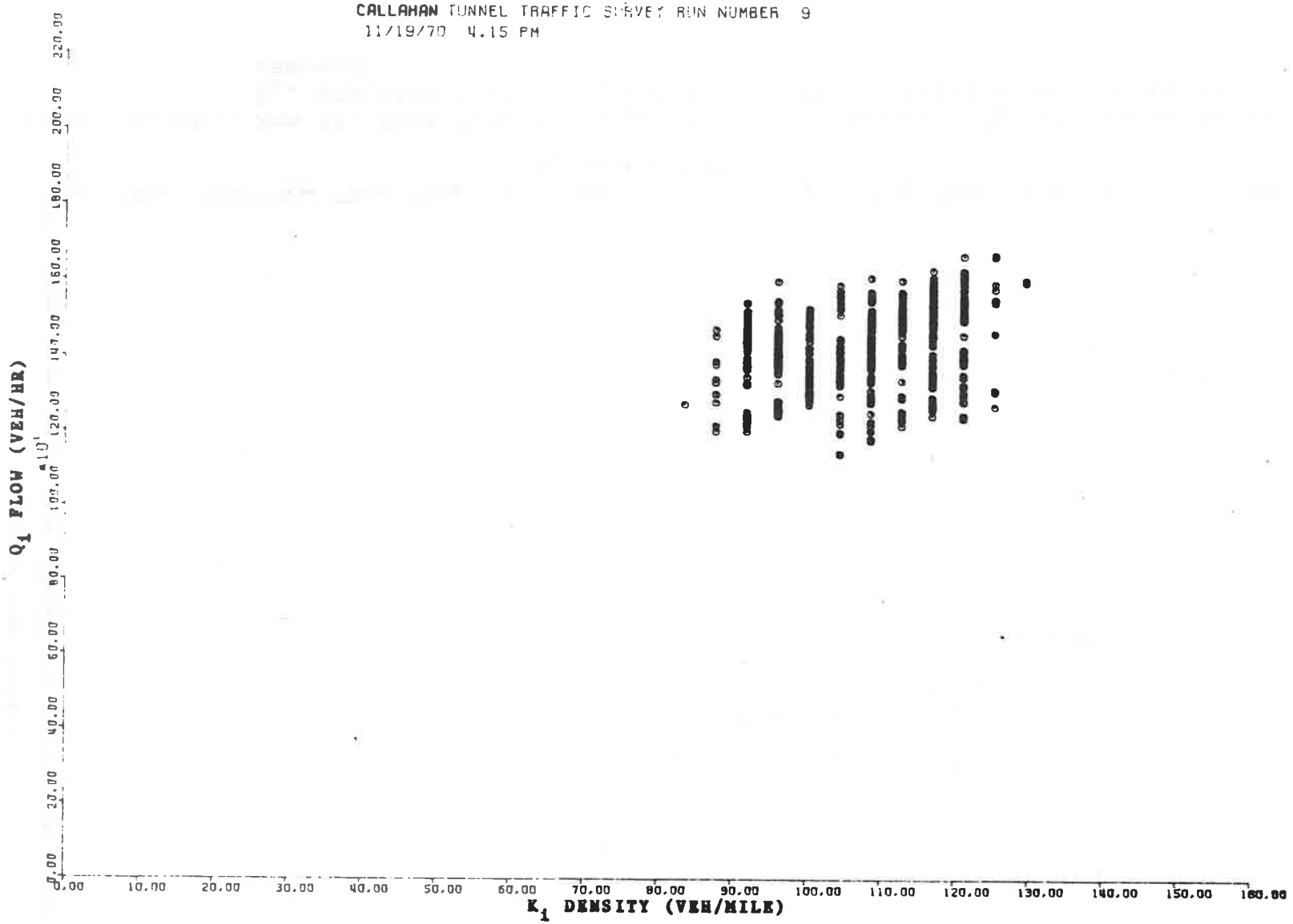


Figure 4.52a.- Run #9: Flow averaged over the transit time, $Q_i$, vs average section density, $K_i$. Stations 1 to 2. Distance of 1265 ft. Two slow down groups removed.

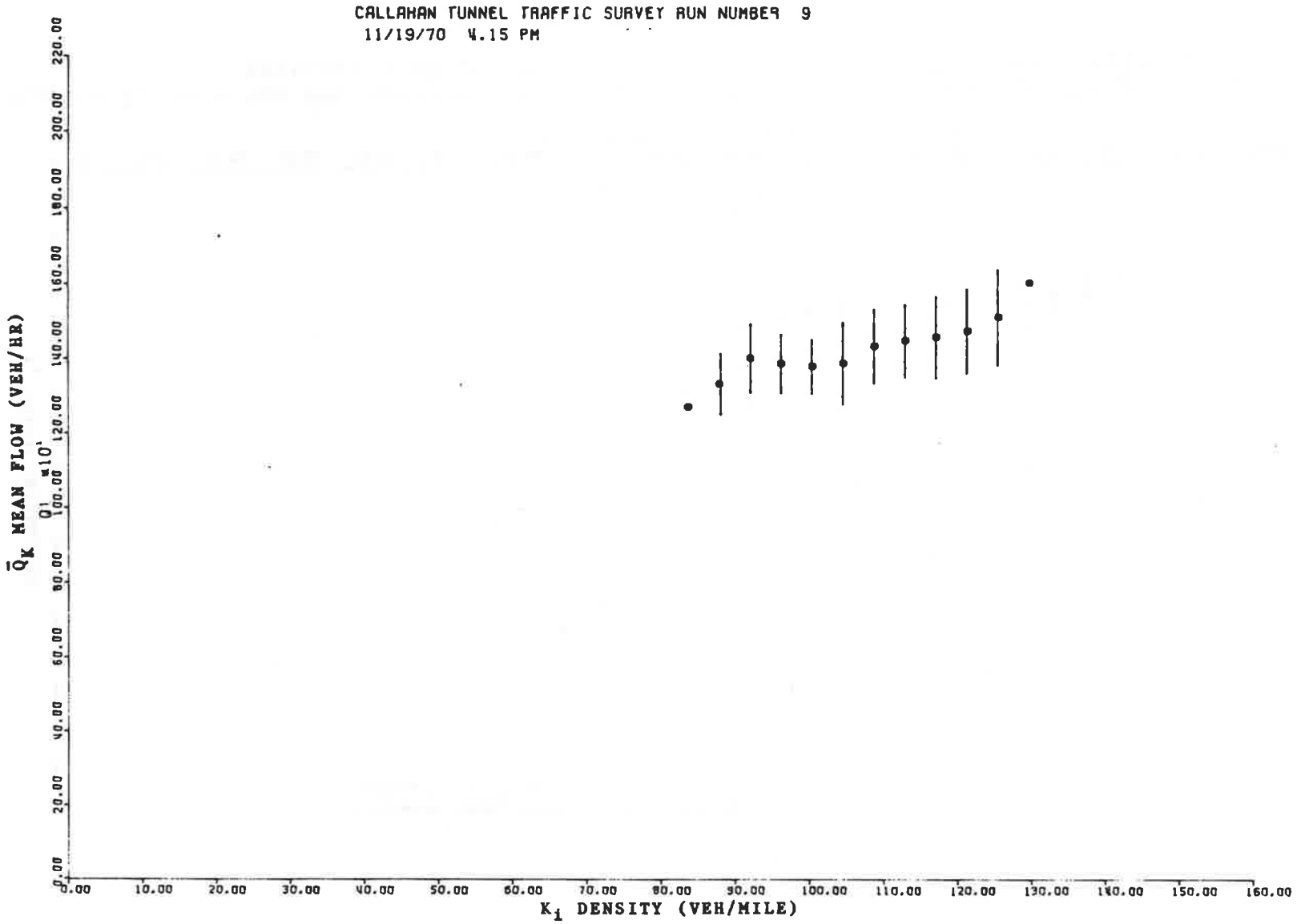


Figure 4.52b.- Run #9: Mean flow for a given section density, $\bar{Q}_K$, vs. the density, $K_i$. Stations 1 to 2. Distance of 1265 ft. Two slow down groups removed.

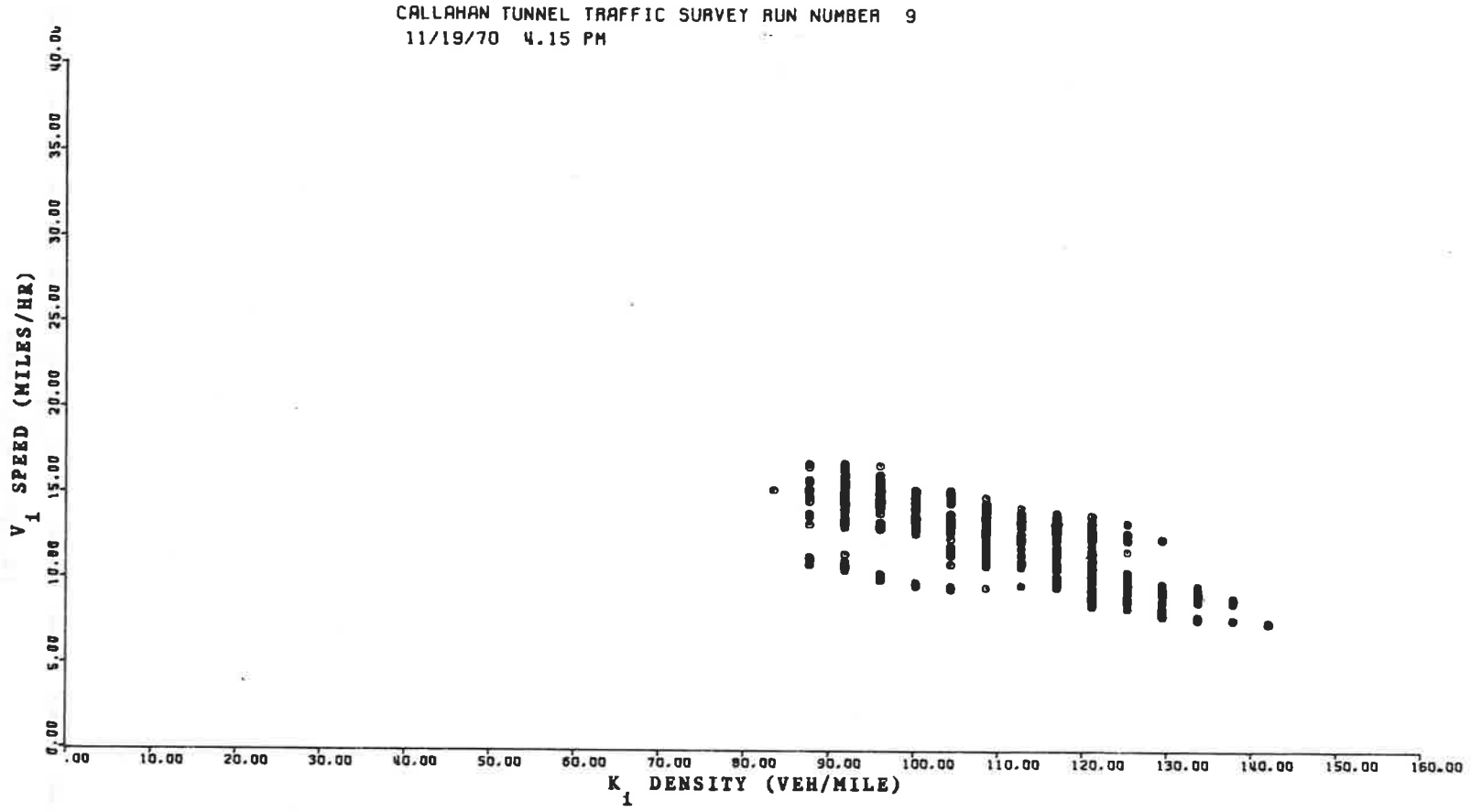


Figure 4.53a.- Run #9: Average speed over a section, $V_i$, vs section density, $K_i$, stations 1 to 2. Distance of 1265 ft. Slow down data included.

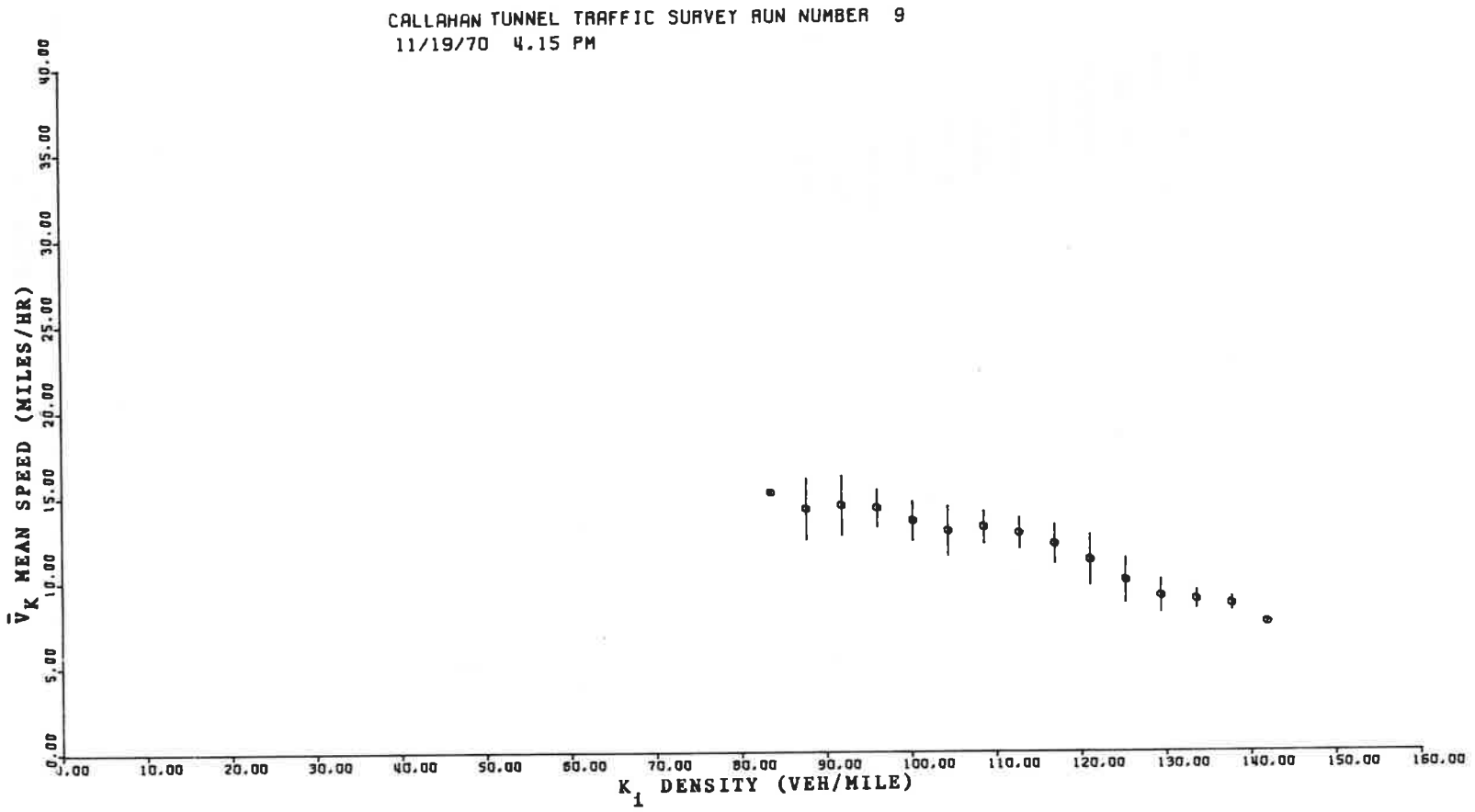


Figure 4.53b.- Run #9: Mean speed for a given density, $\bar{V}_K$, vs the density, $K_i$, stations 1 to 2. Distance of 1265 ft. Slow down data included.

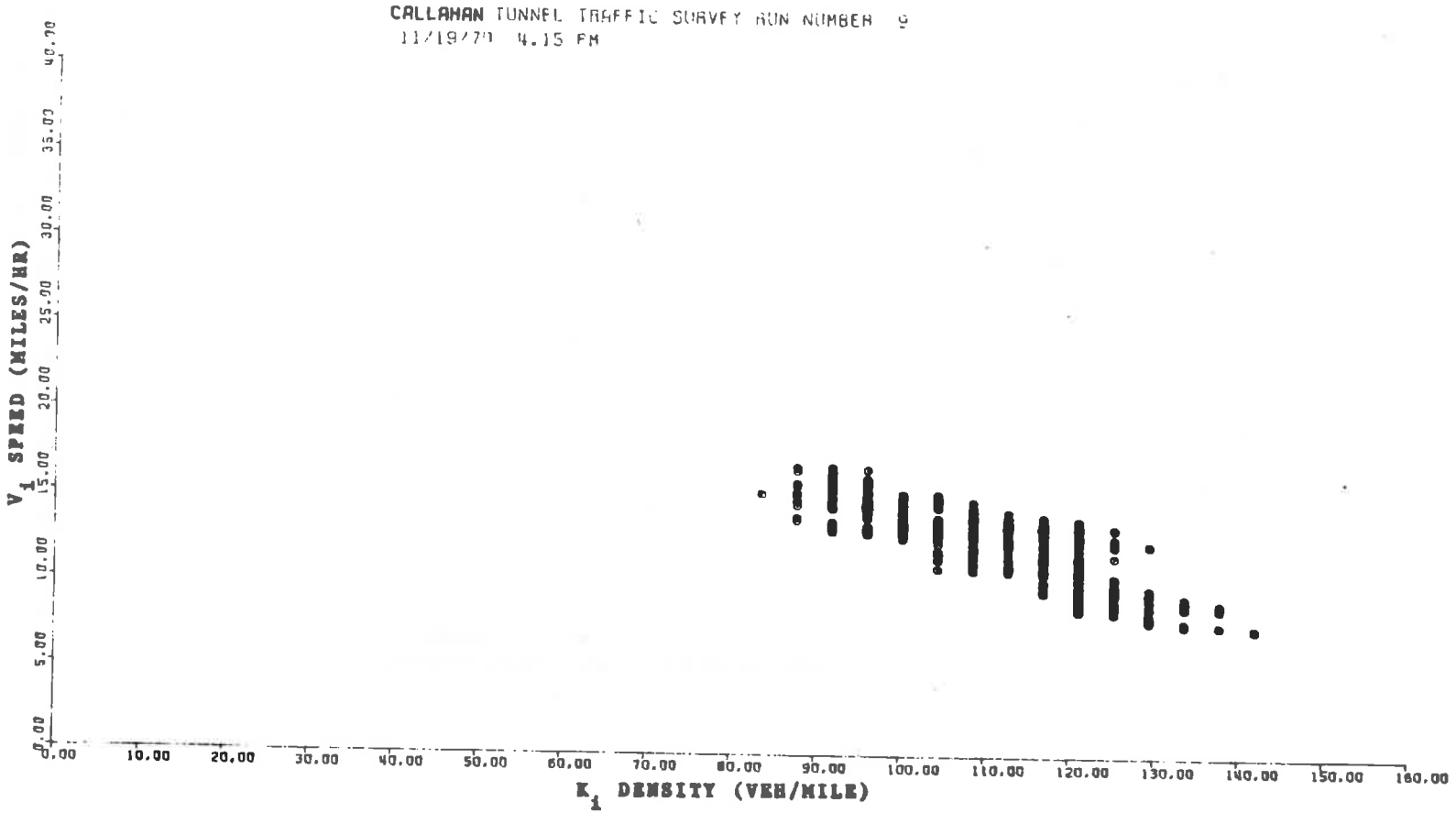


Figure 4.54a.- Run #9: Average speed over a section, $V_i$, vs section density, $K_i$, stations 1 to 2. Distance of 1265 ft. First slow down group removed.

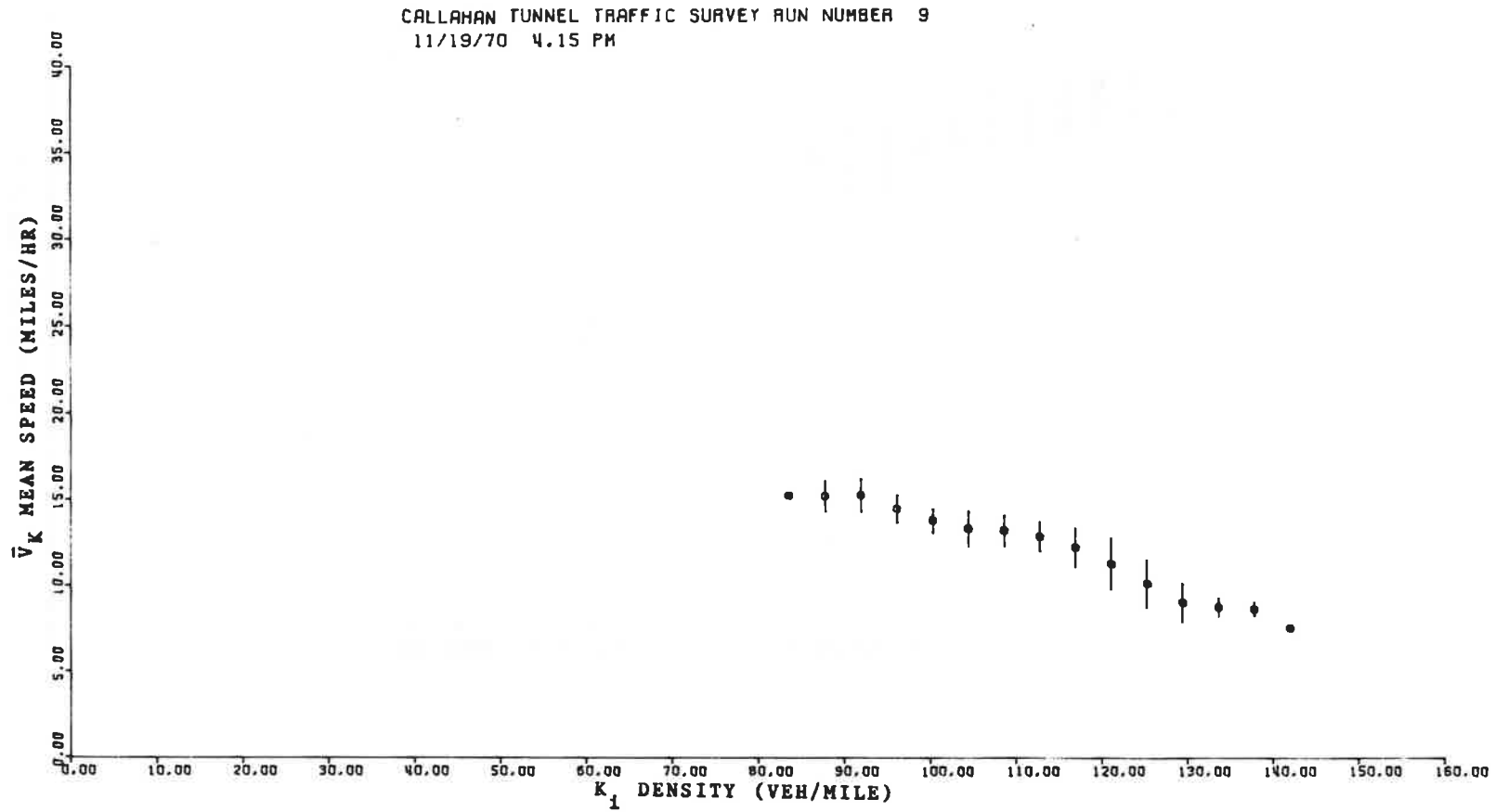


Figure 4.54b.- Run #9: Mean speed for a given density, $\bar{V}_K$, vs the density, $K_i$, stations 1 to 2. Distance of 1265 ft. First slow down group removed.

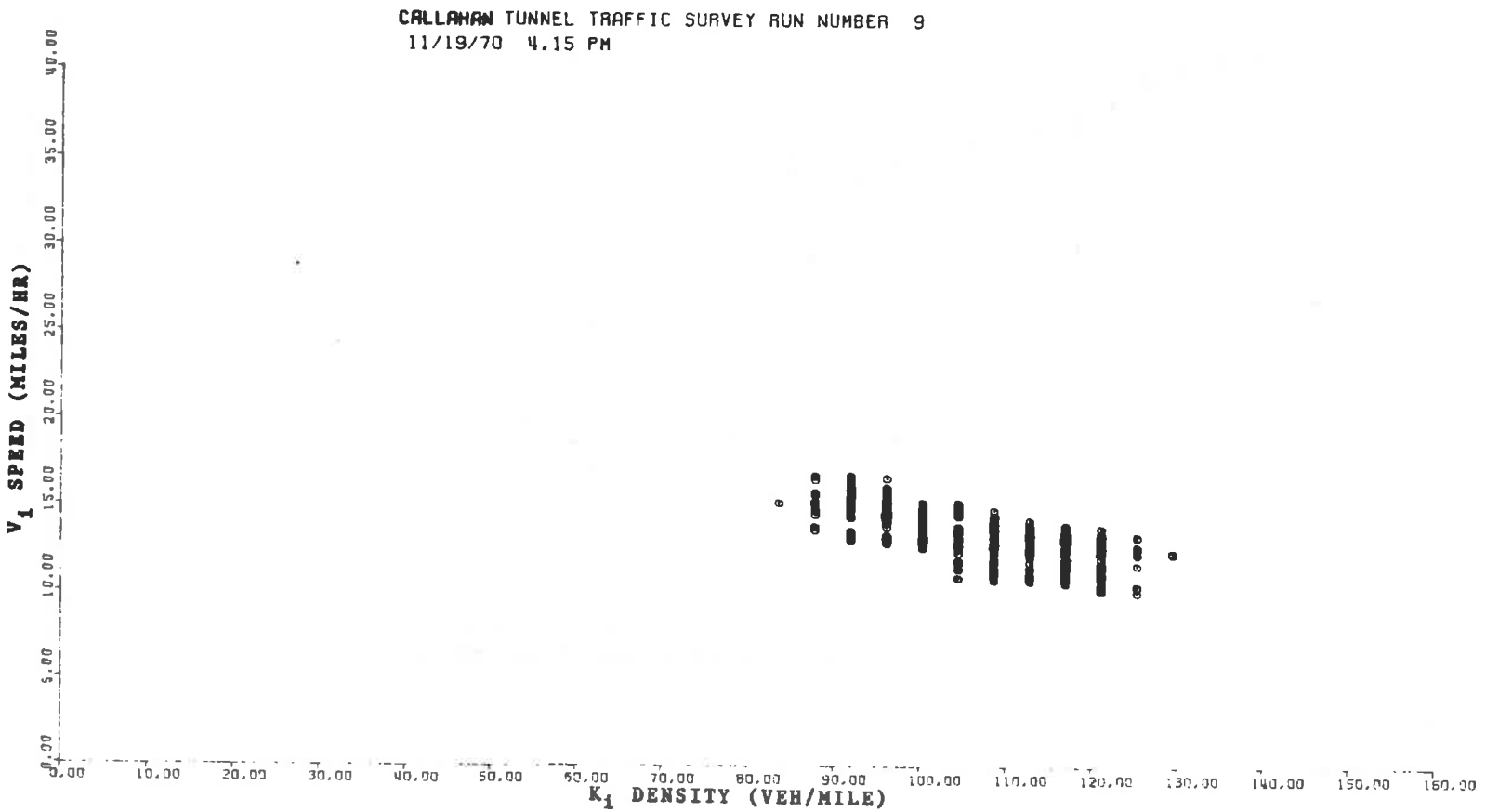


Figure 4.55a.- Run #9: Average speed over a section, $V_i$, vs section density, $K_i$. Stations 1 to 2. Distance of 1265 ft. Two slow down groups removed.

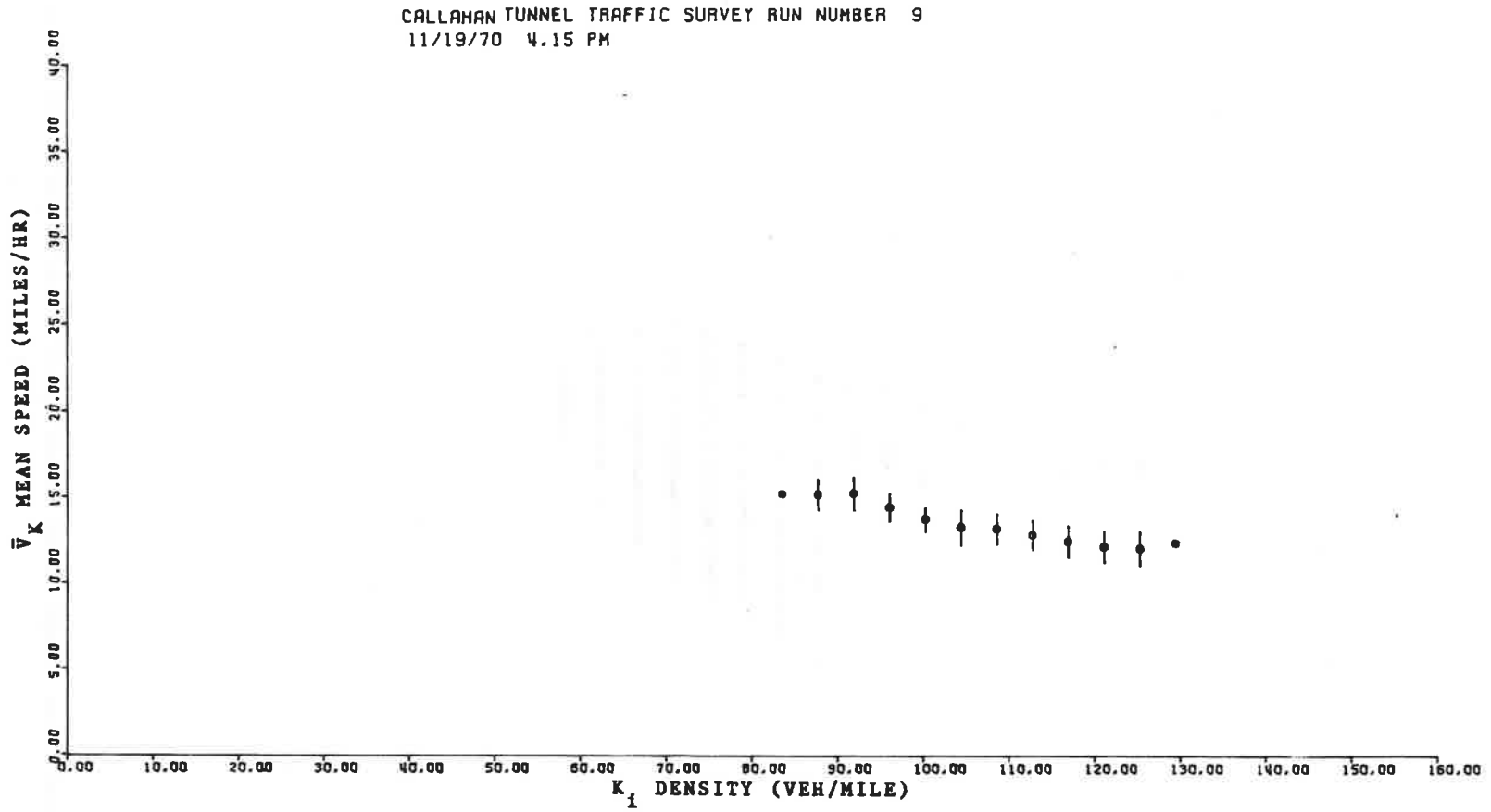


Figure 4.55b.- Run #9: Mean speed for a given density $\bar{V}_K$, vs the density $K_i$, stations 1 to 2. Distance of 1265 ft. Two slow down groups removed.

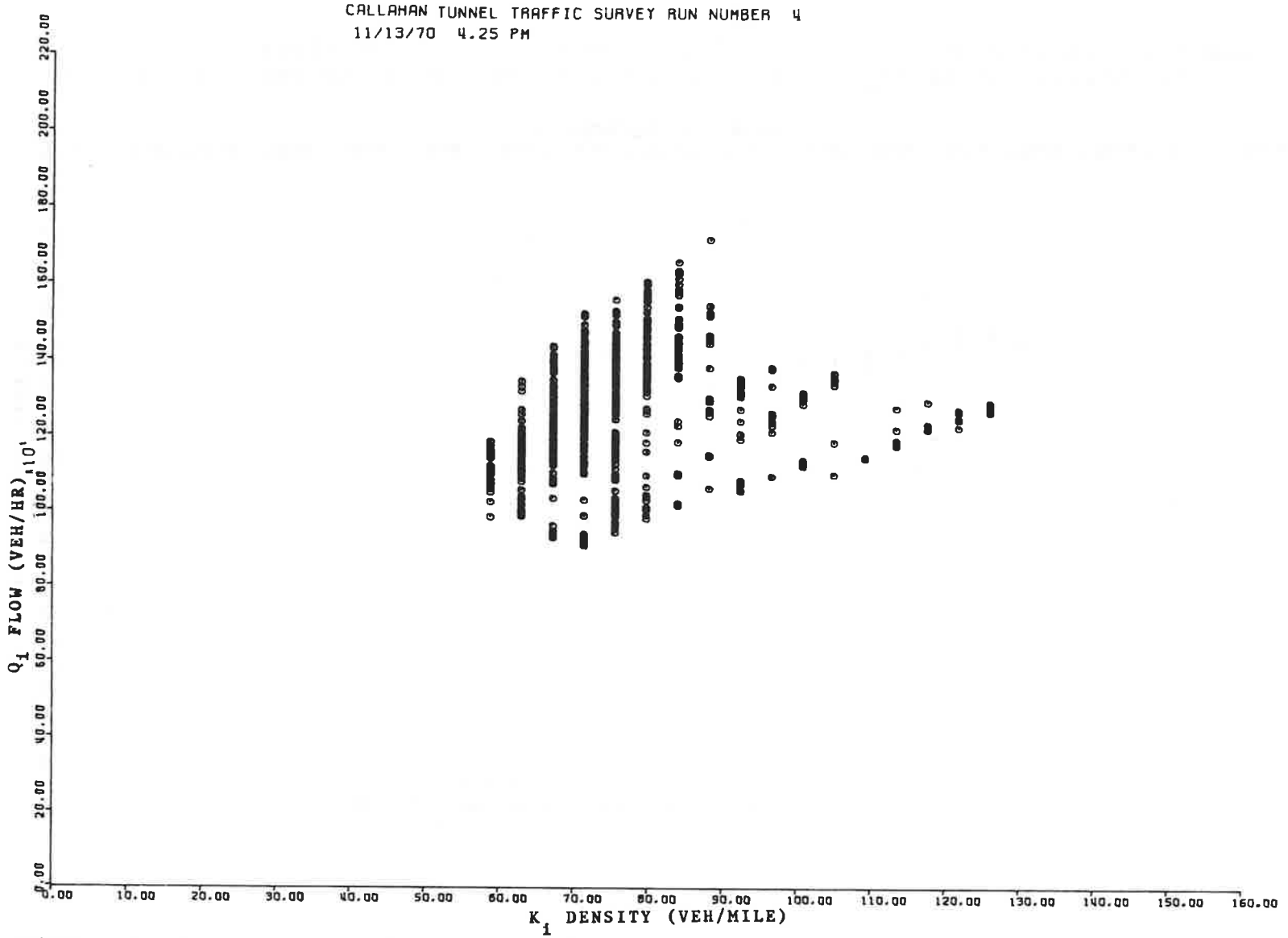


Figure 4.56a.- Run #4: Flow averaged over the transit time, $Q_i$, vs average section density, $K_i$, stations 2 to 3. Distance of 1260 ft. Slow down data included.

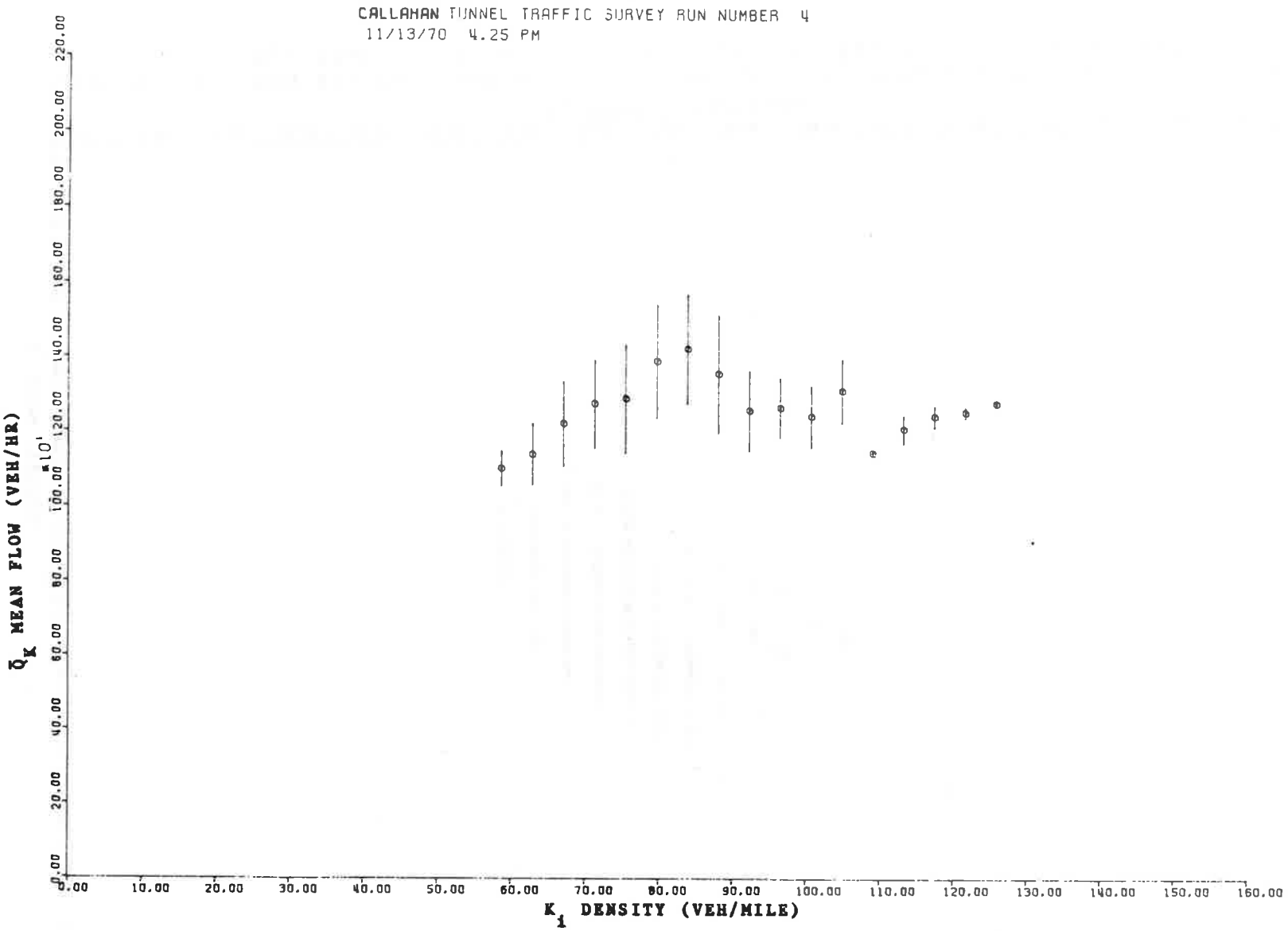


Figure 4.56b.- Run #4: Mean flow for a given section density, $\bar{Q}_K$, vs the density, $K_i$, stations 2 to 3. Distance of 1260 ft. Slow down data included.

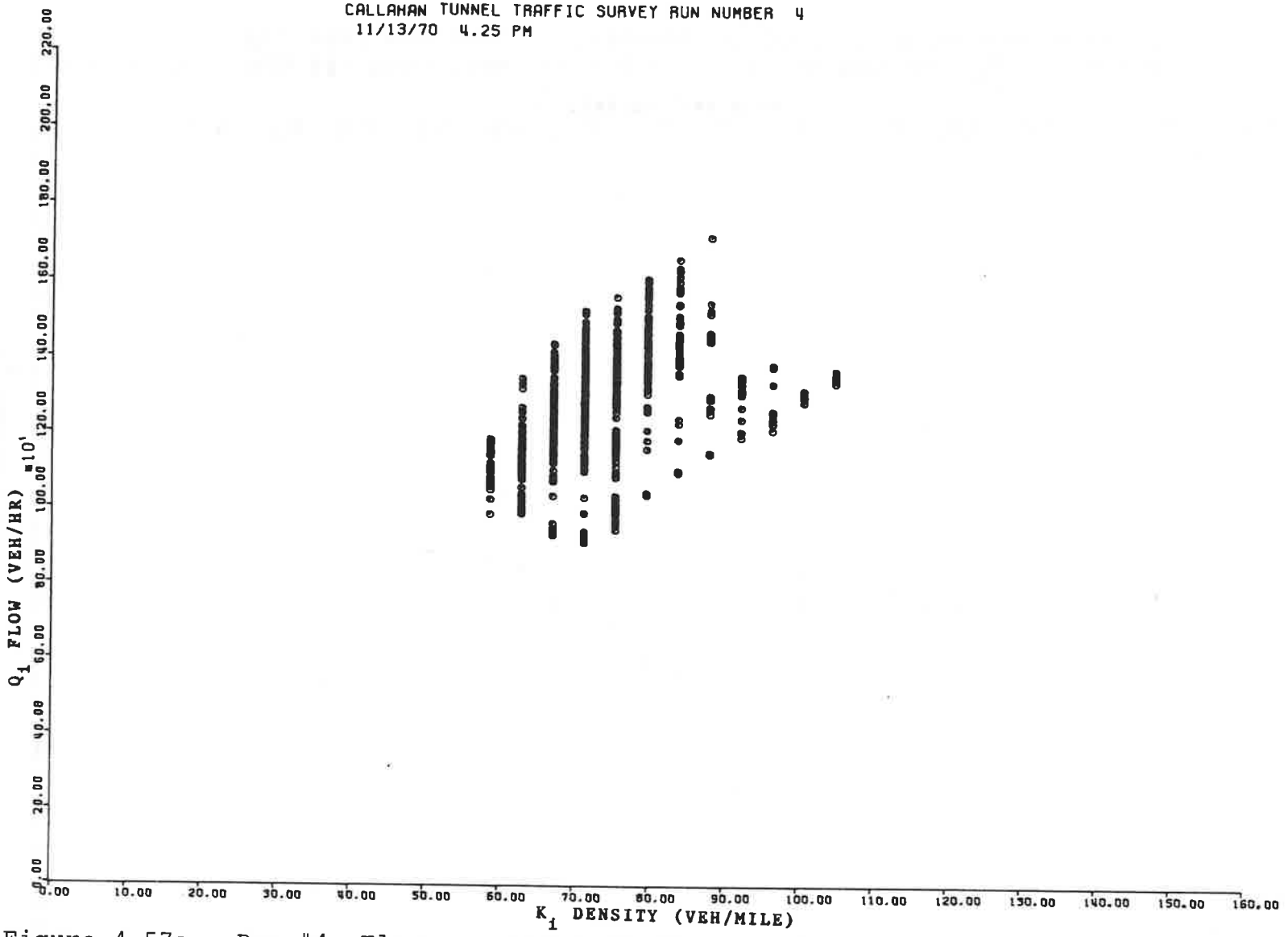


Figure 4.57a.- Run #4: Flow averaged over the transit time, $Q_i$, vs average density, $K_i$. Stations 2 to 3. Distance of 1260 ft. Slow down group removed.

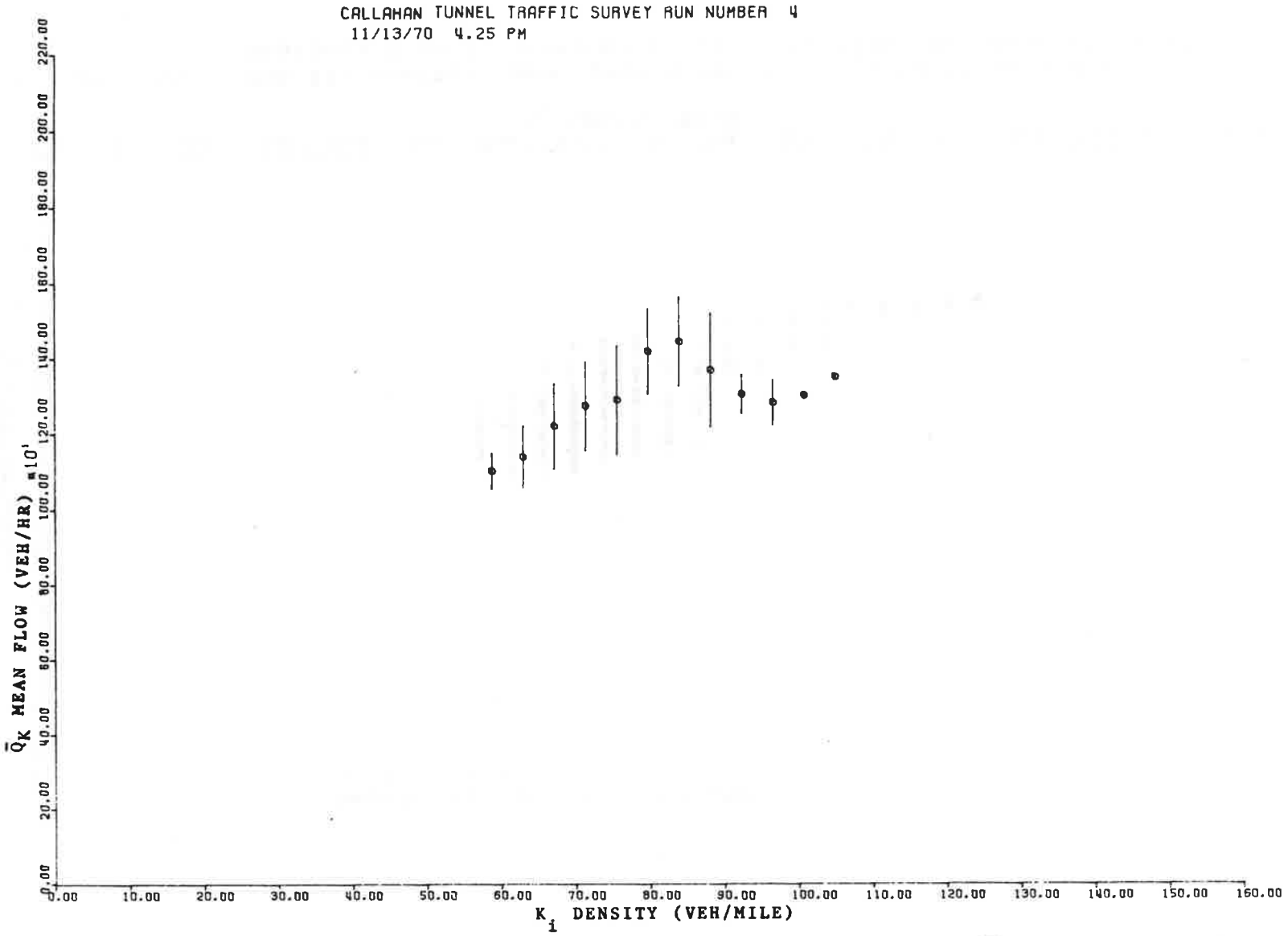


Figure 4.57b.- Run #4: Mean flow for a given section density, $\bar{Q}_K$, vs the density, $K_i$, stations 2 to 3. Distance of 1260 ft. Slow down group removed.

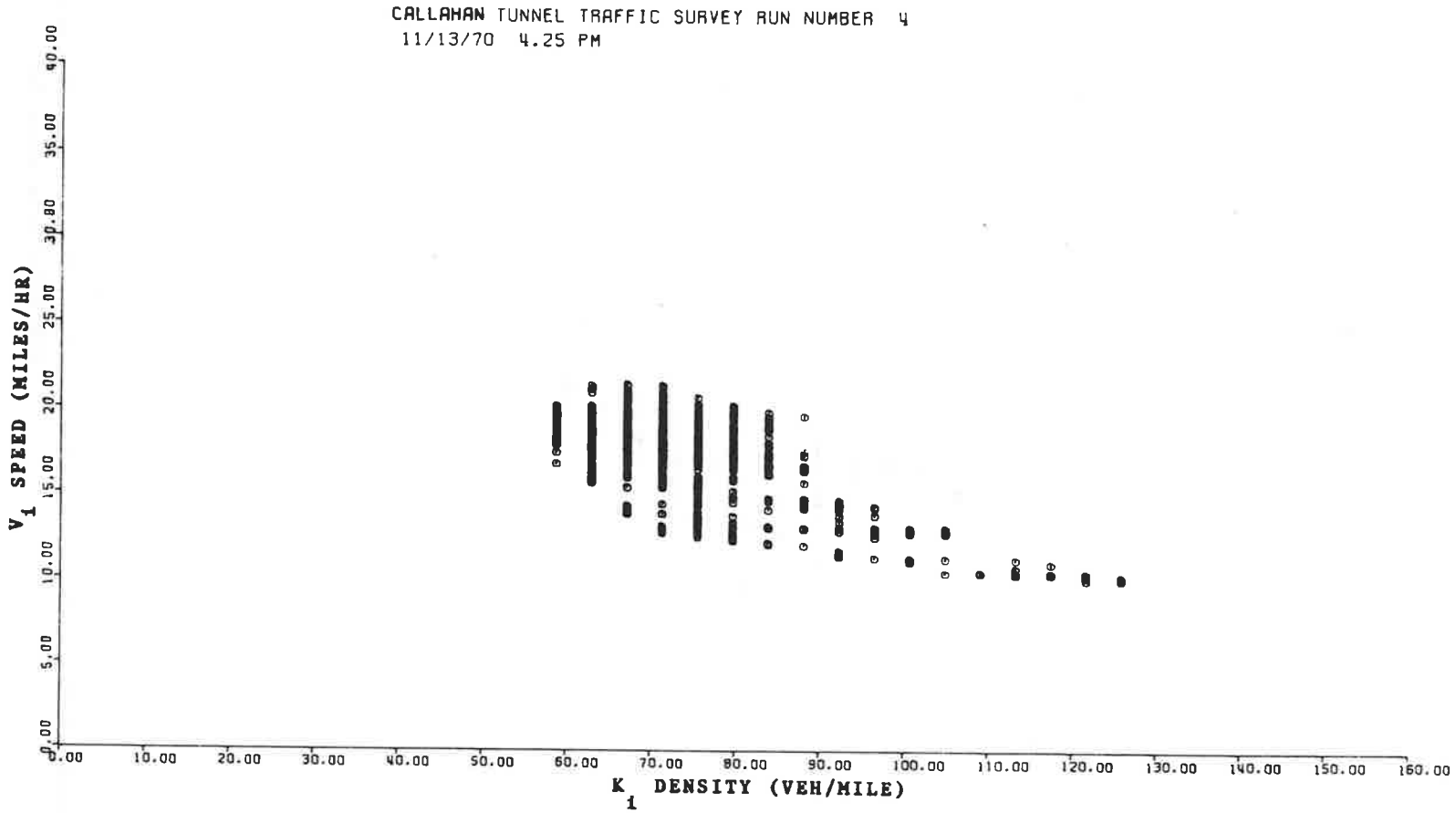


Figure 4.58a.- Run #4: Average speed over a section, $V_i$, vs section density, $K_i$. Stations 2 to 3. Distance of 1260 ft. Slow down data included.

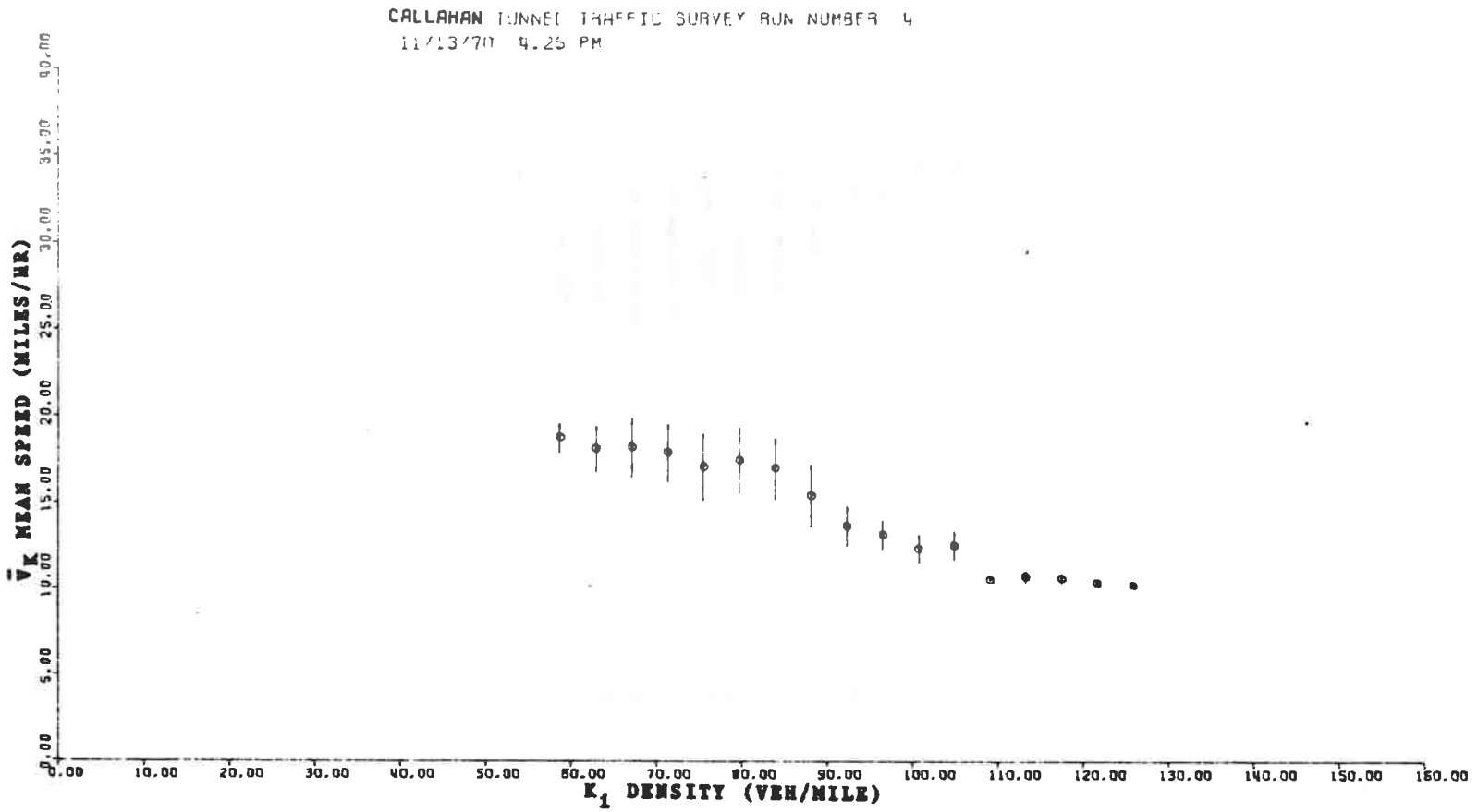


Figure 4.58b.- Run #4: Mean speed for a given density, $\bar{V}_K$, vs section density, $K_i$, stations 2 to 3. Distance of 1260 ft. Slow down data included.

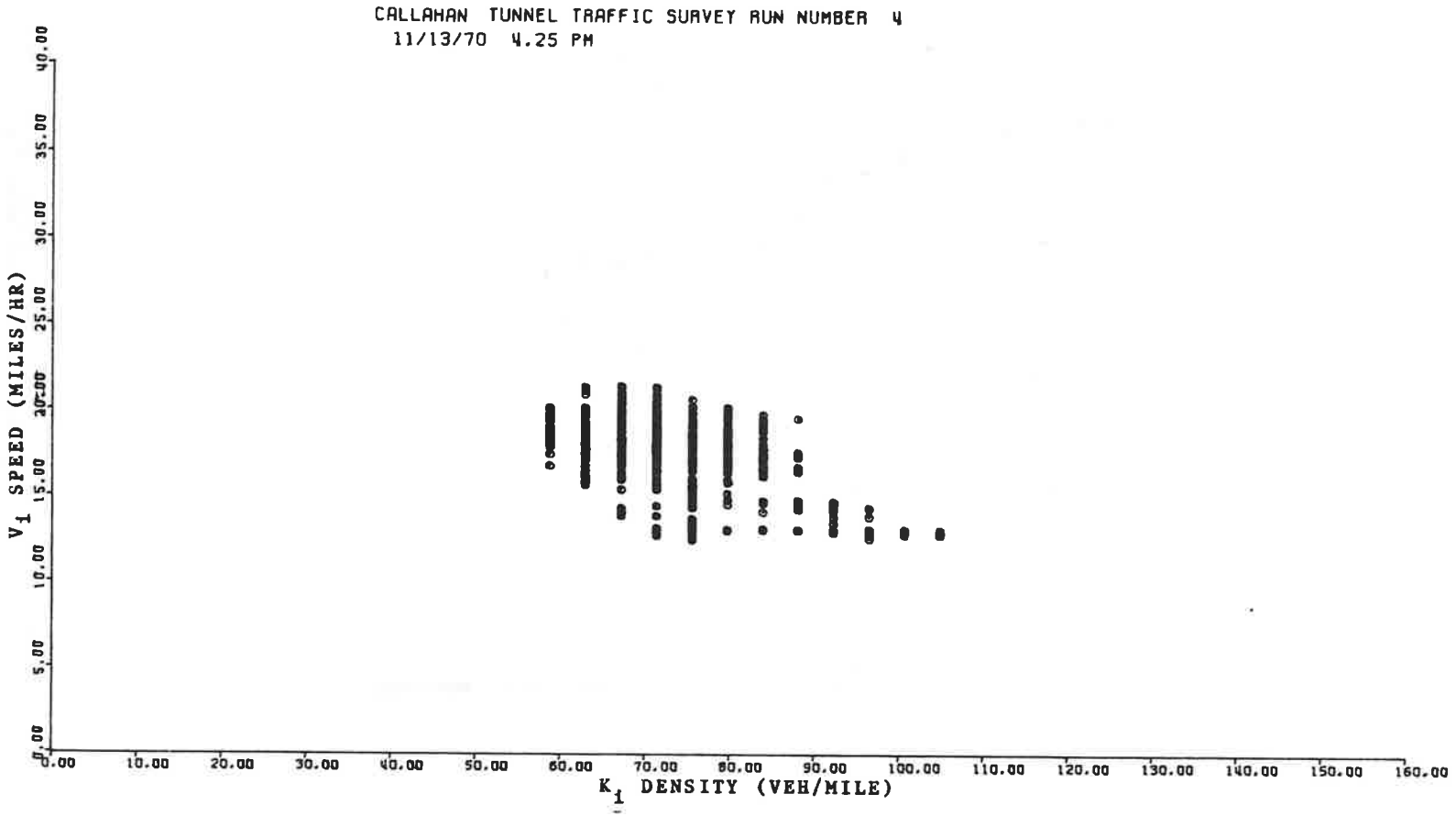


Figure 4.59a.- Run #4: Average speed over a section $V_i$, vs section density, $K_i$. Stations 2 to 3. Distance of 1260 ft. Slow down group removed.

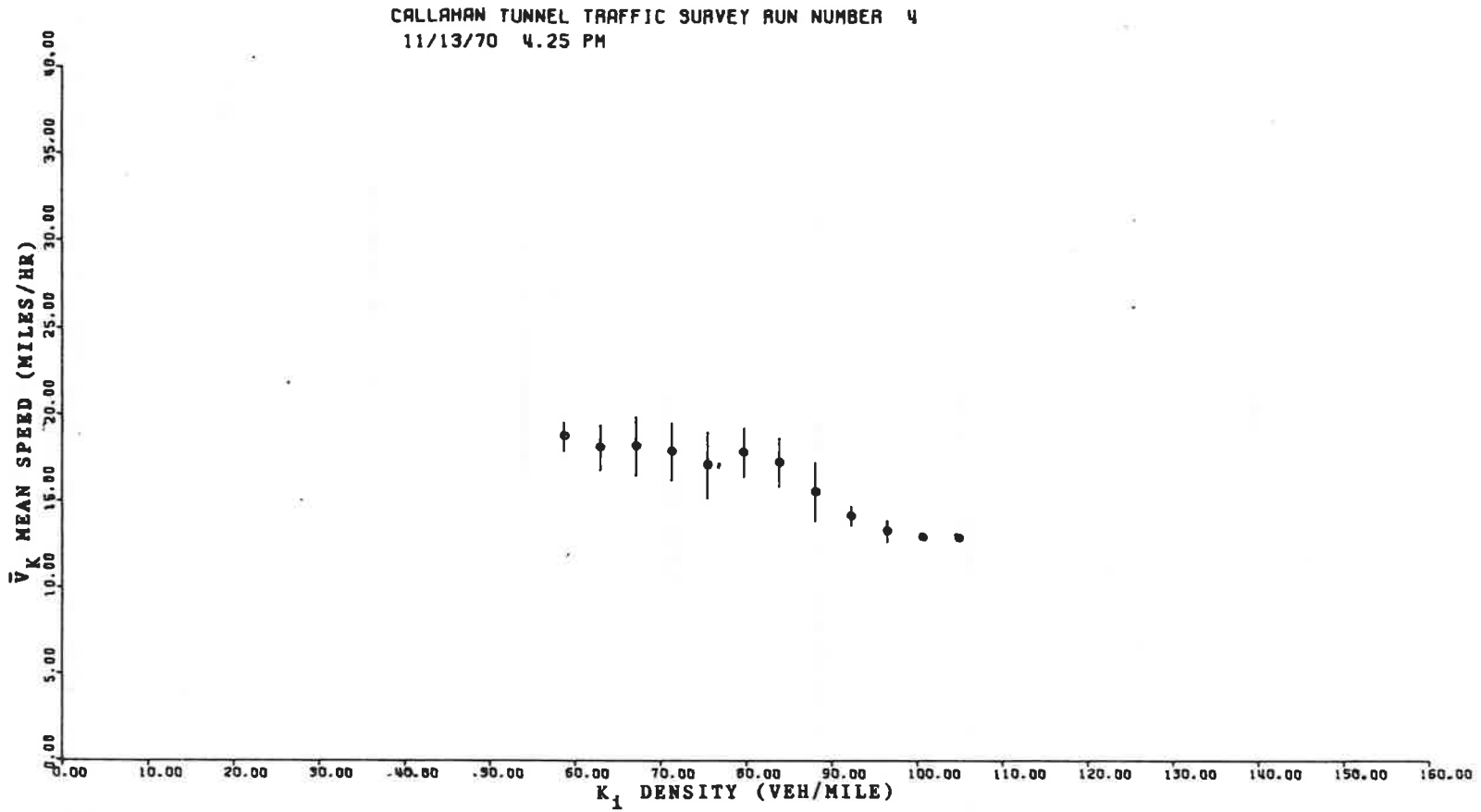


Figure 4.59b.- Run #4: Mean speed for a given density, $\bar{V}_K$, vs section density, $K_i$, stations 2 to 3. Distance of 1260 ft. Slow down group removed.

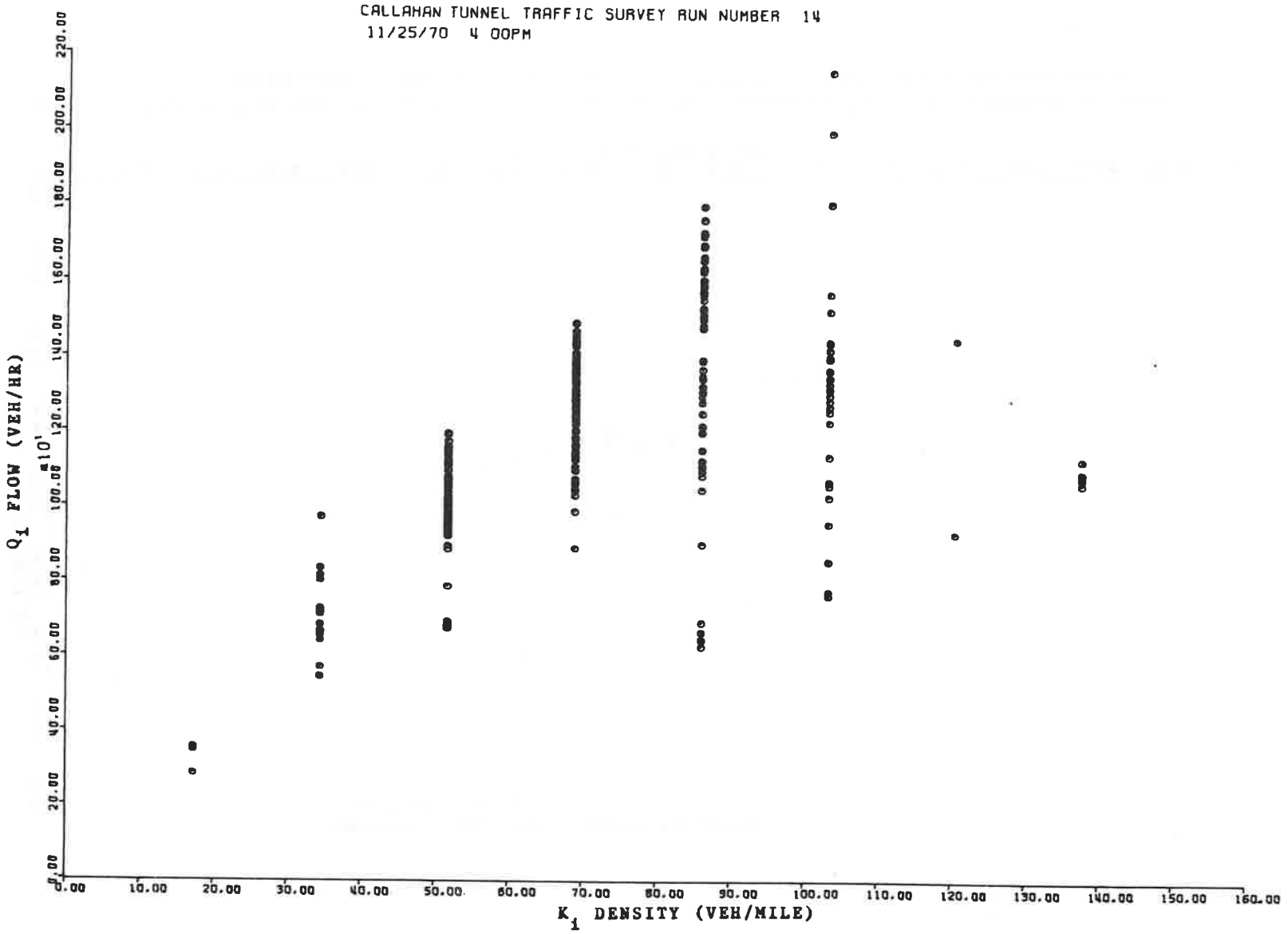


Figure 4.60a.- Run #14: Flow averaged over the transit time, $Q_i$, vs average section density, $K_i$. Stations $3_a$ to $B_2$. Distance of 307.3 ft. Slow down data included.

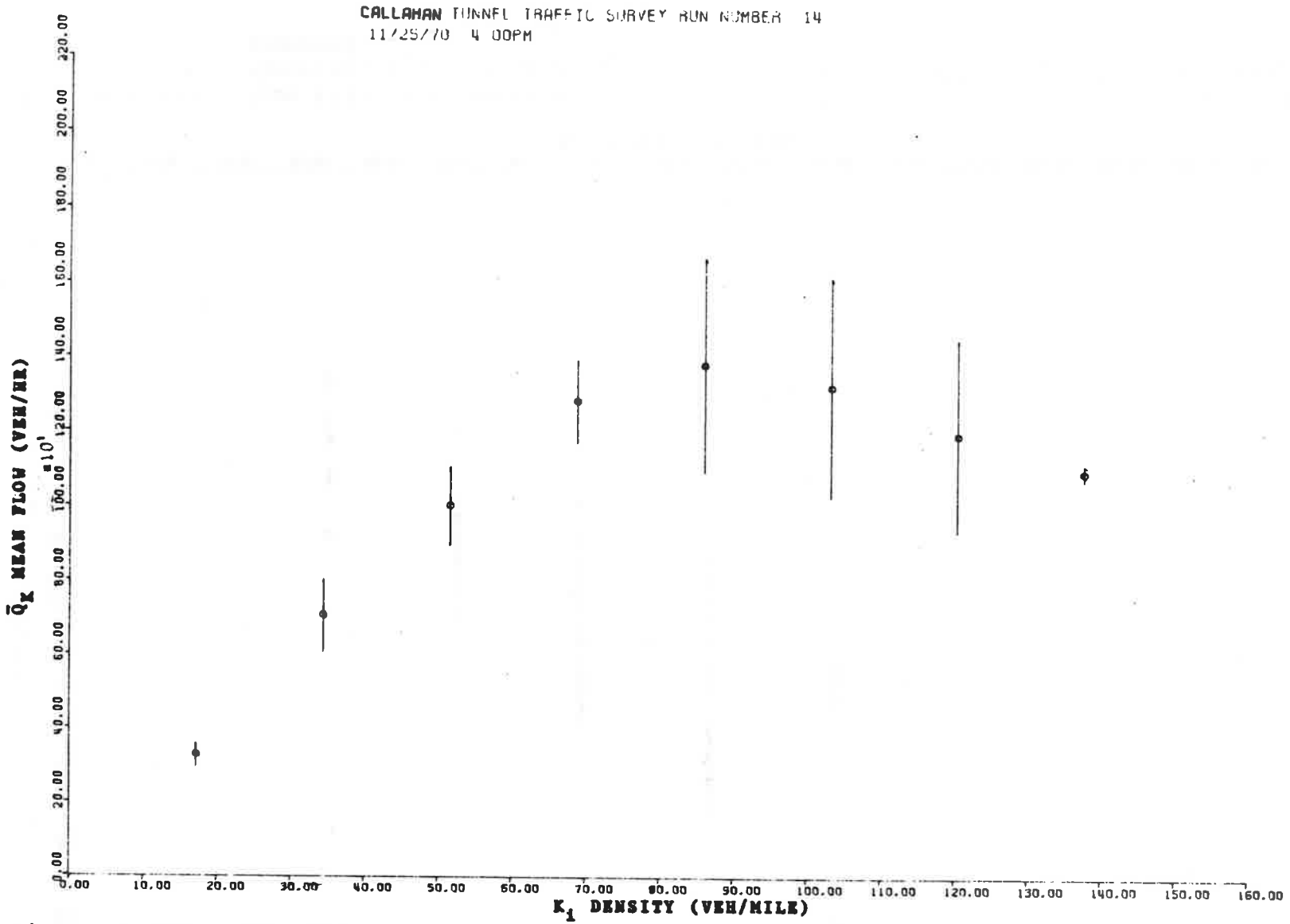


Figure 4.60b.- Run #14: Mean flow for a given section density, $\bar{Q}_K$, vs the density, $K_i$. Stations $3_a$ to $B_2$. Distance of 307.3 ft. Slow down data included.

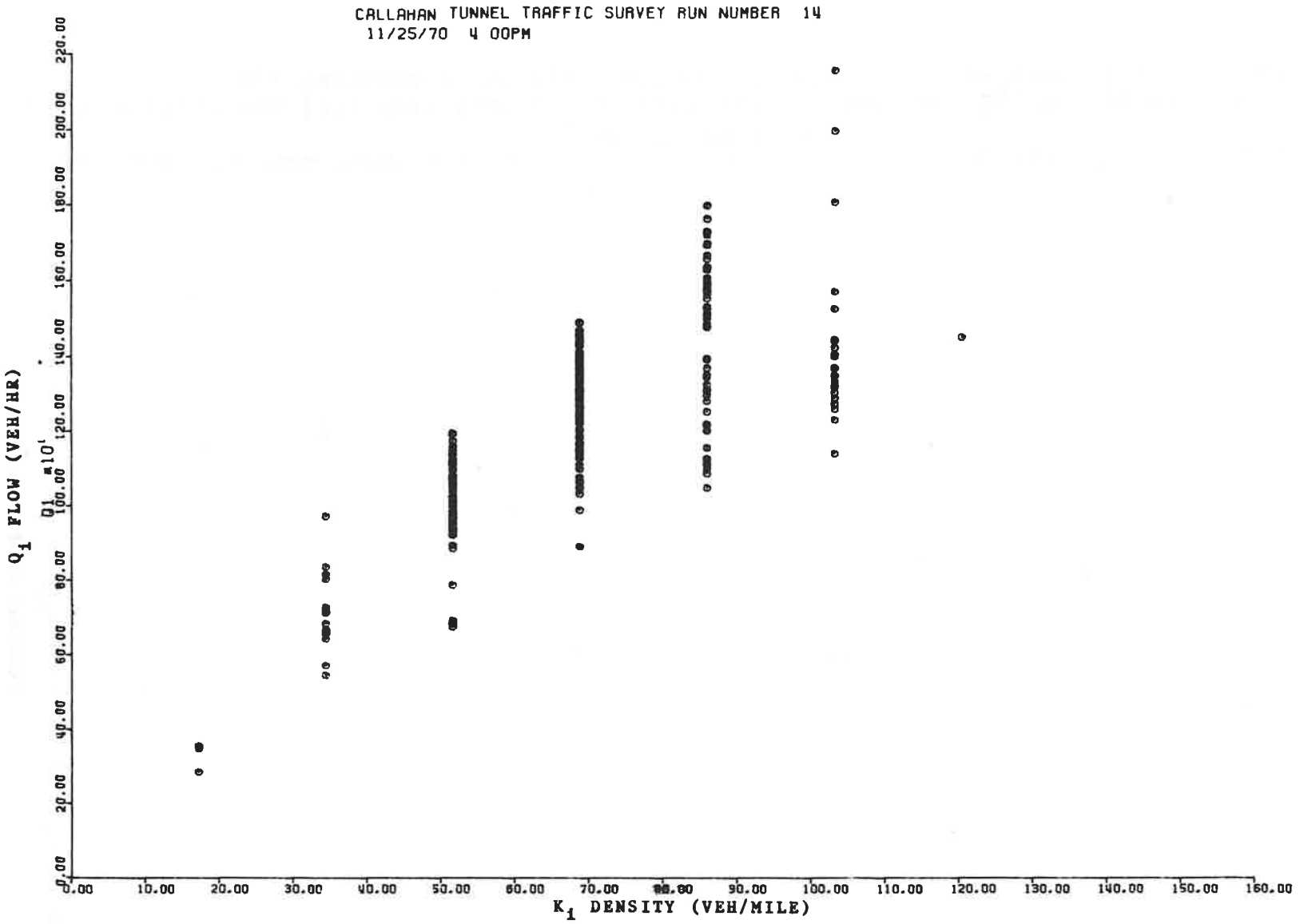


Figure 4.61a.- Run #14: Flow averaged over the transit time, $Q_i$, vs average section density, $K_i$. Stations $3_a$ to $B_2$. Distance of 307.3 ft. Slow down group removed.

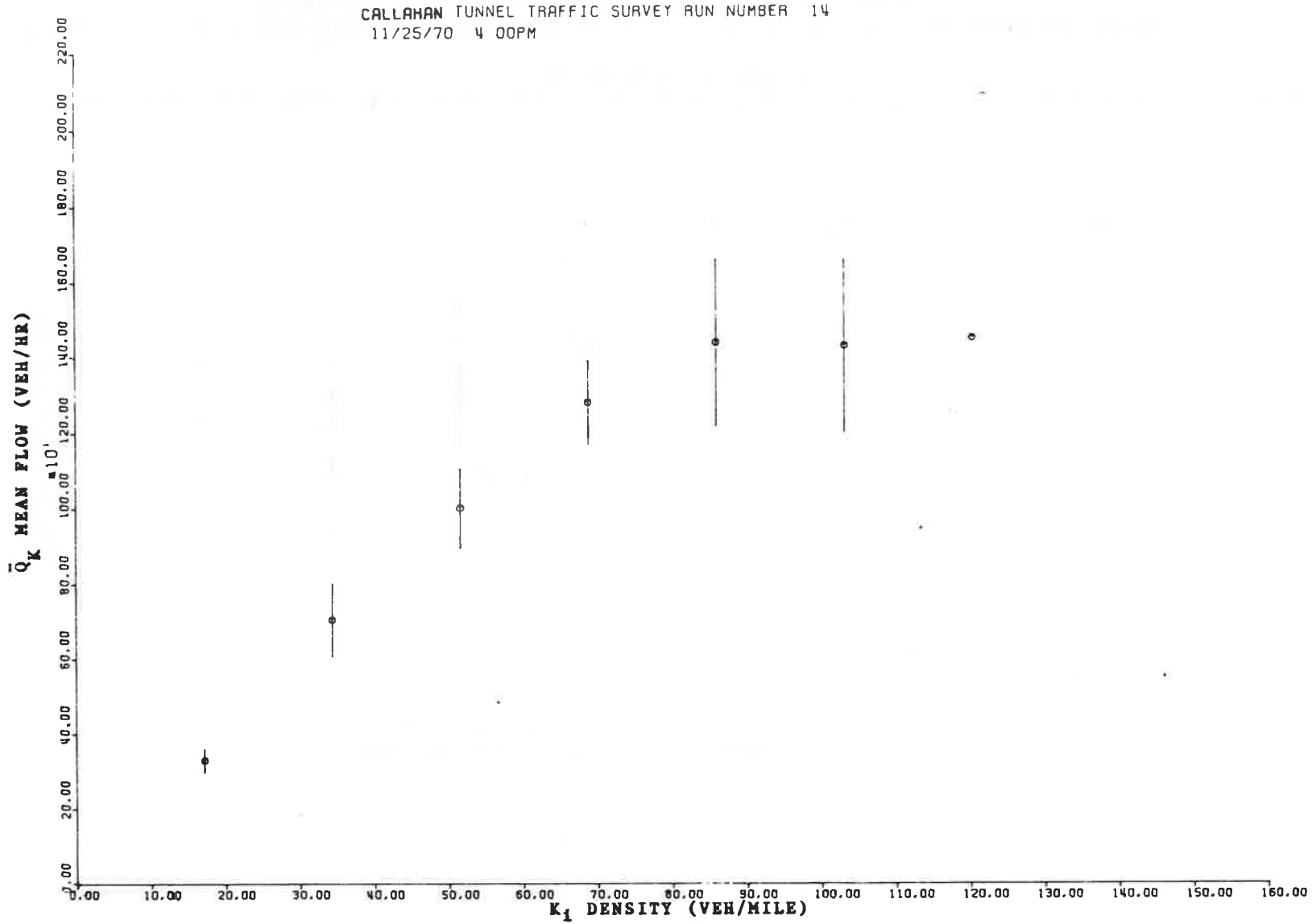


Figure 4.61b.- Run #14: Mean flow for a given section density, $\bar{Q}_K$, vs the density, $K_i$, stations $3_a$ to $B_2$. Distance of 307.3 ft. Slow down group removed.

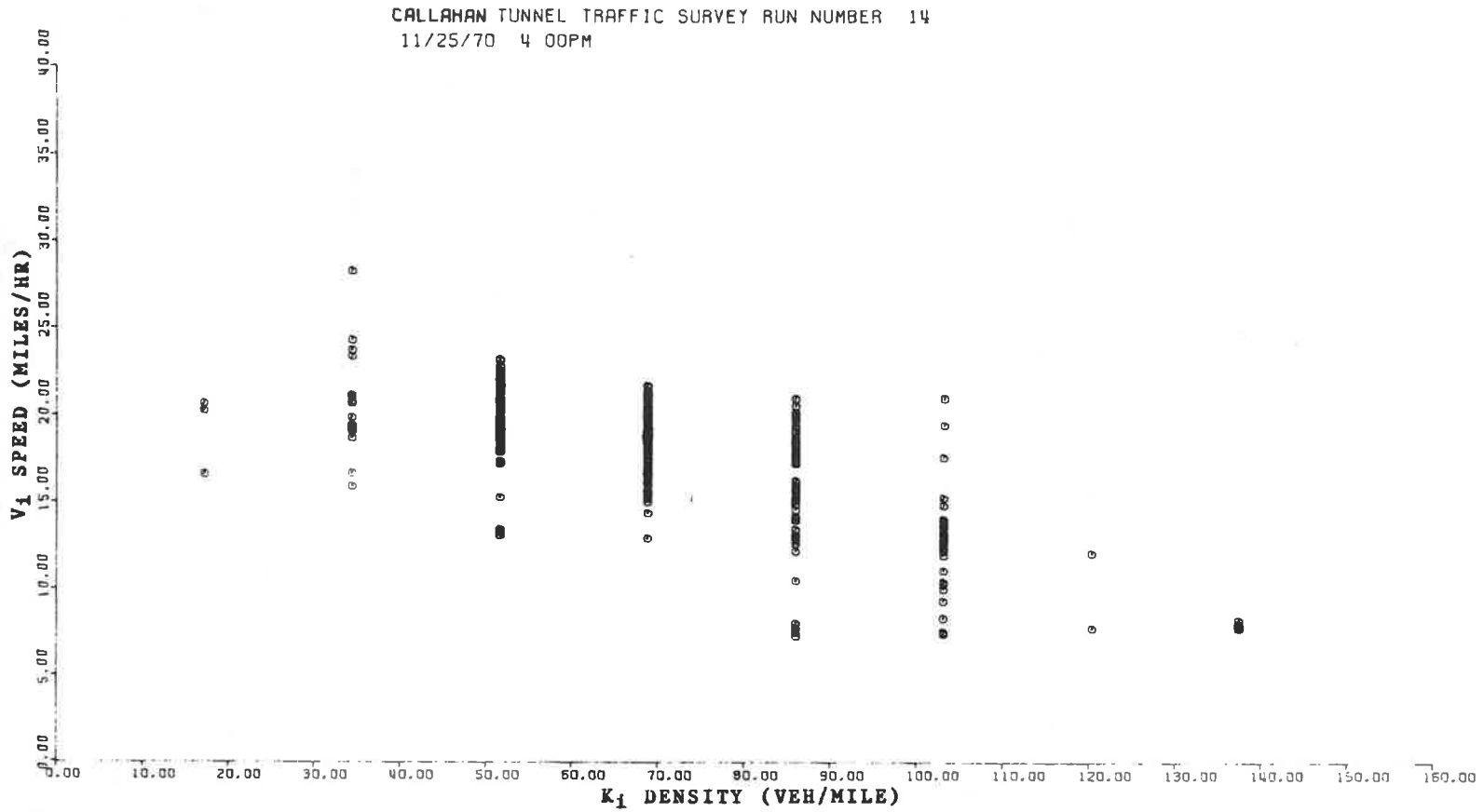


Figure 4.62a.- Run #14: Average speed over a section, $V_i$, vs section density, $K_i$, stations $3_a$ to $B_2$. Slow down data included.

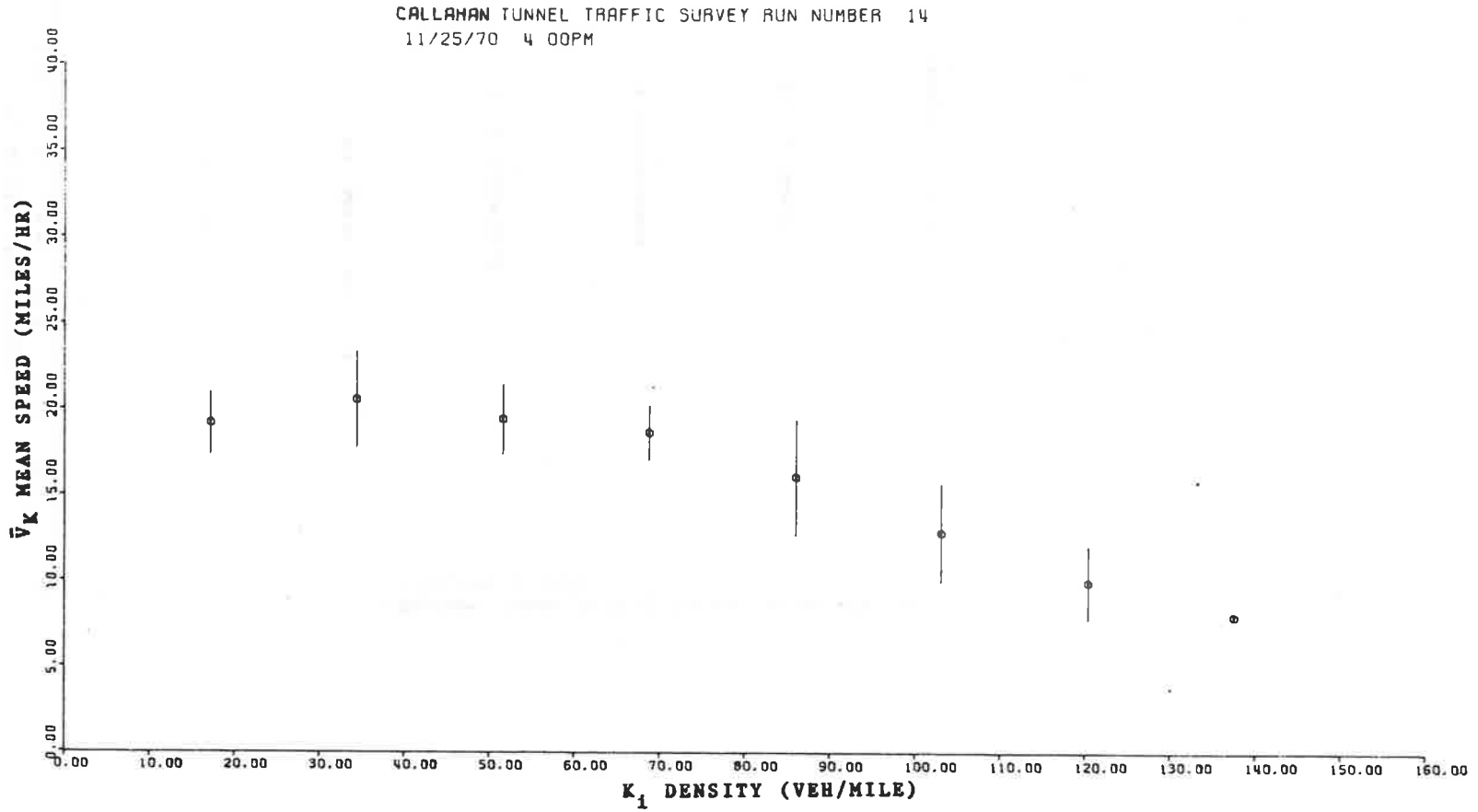


Figure 4.62b.- Run #14: Mean speed for a given density, $\bar{V}_K$, vs section density, $K_i$, station $3_a$ to $B_2$. Distance of 307.3 ft. Slow down data included.

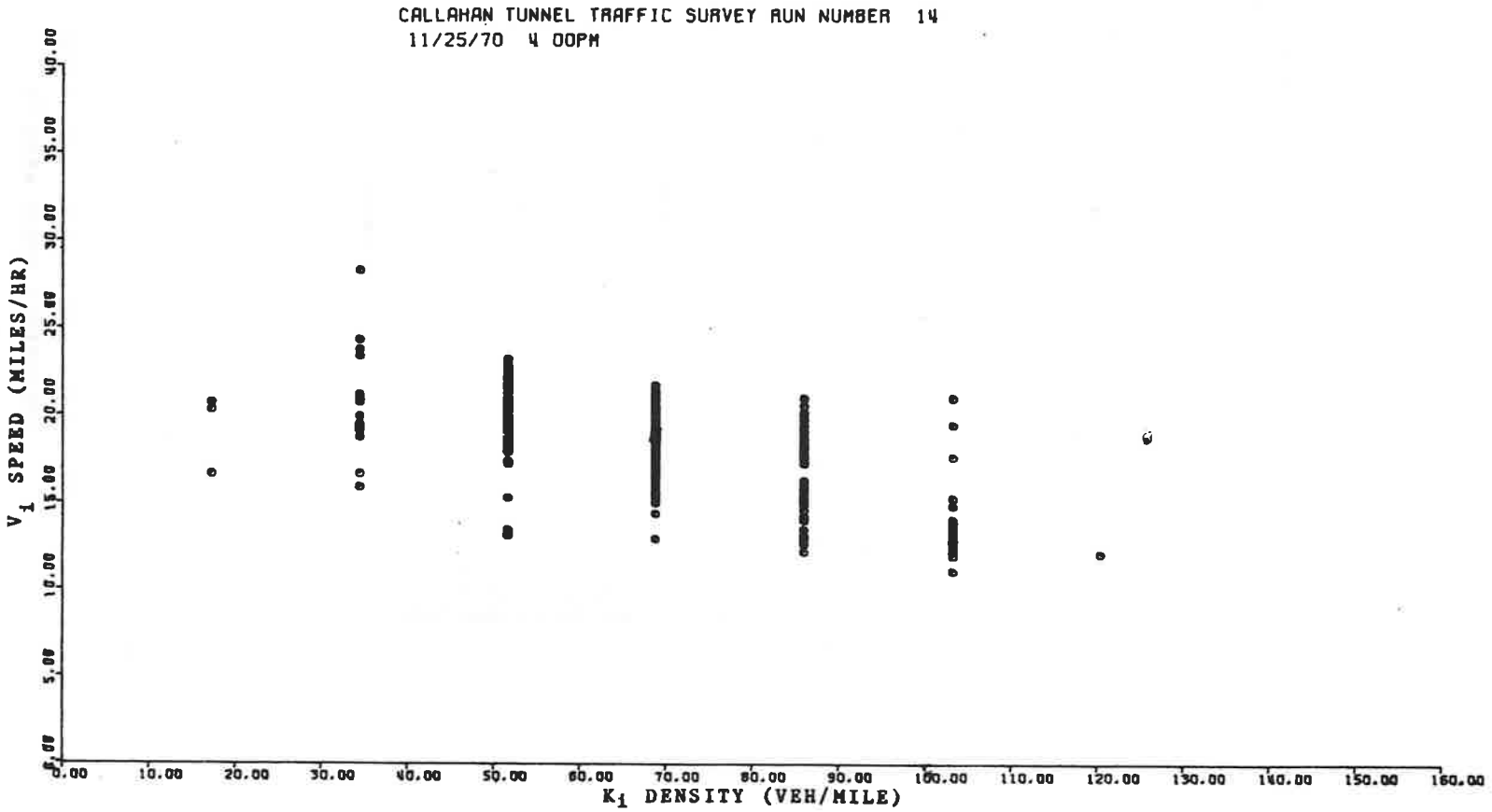


Figure 4.63a.- Run #14: Average speed over a section, $V_i$, vs section density, $K_i$, stations $3_a$ to $B_2$. Slow down group removed. Distance of 307.3 ft.

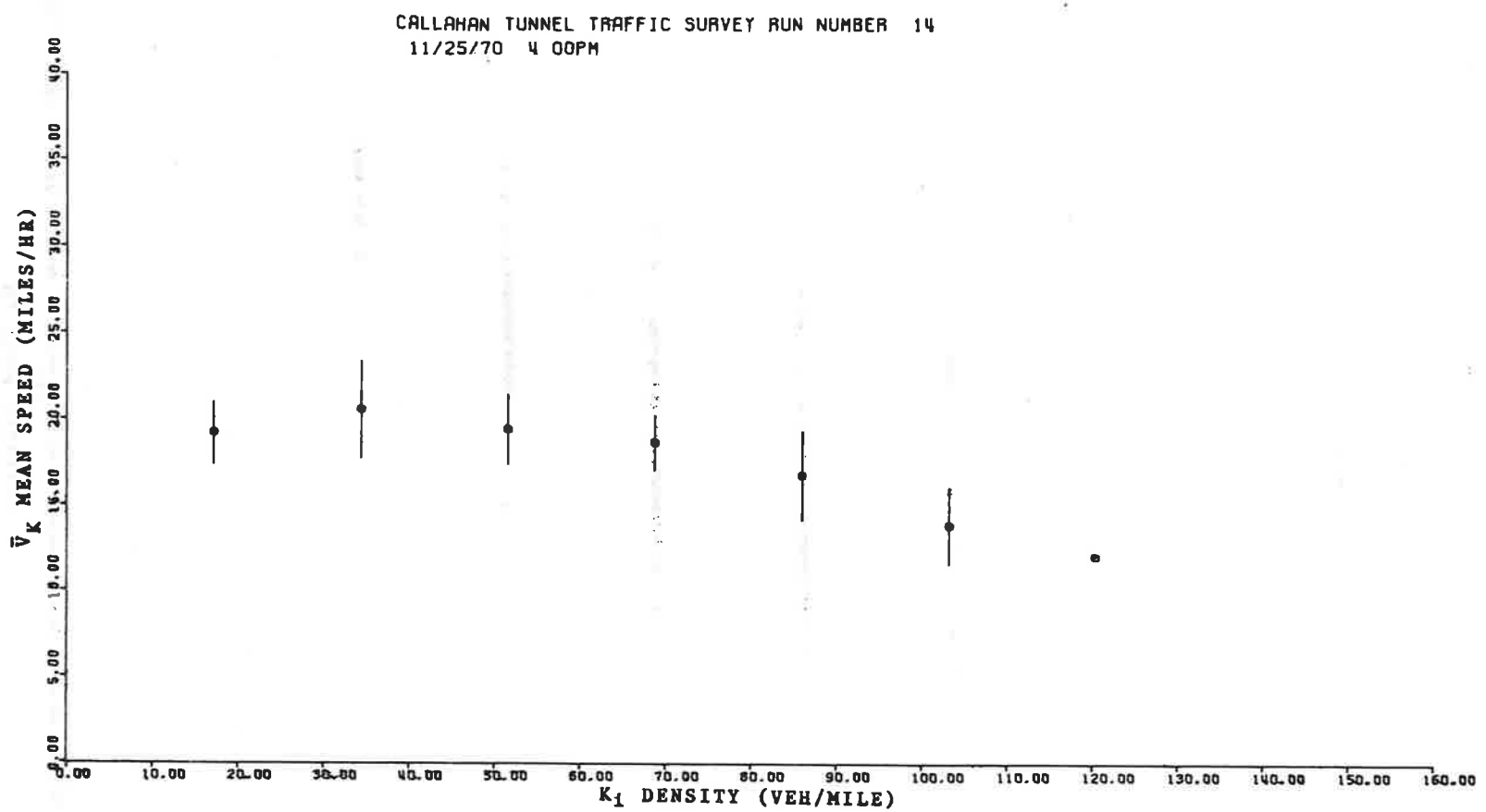


Figure 4.63b.- Run #14: Mean speed for a given density, $\bar{V}_K$, vs section density, $K_i$. Station $3_a$ to $B_2$. Distance of 307.3 ft. Slow down group removed.

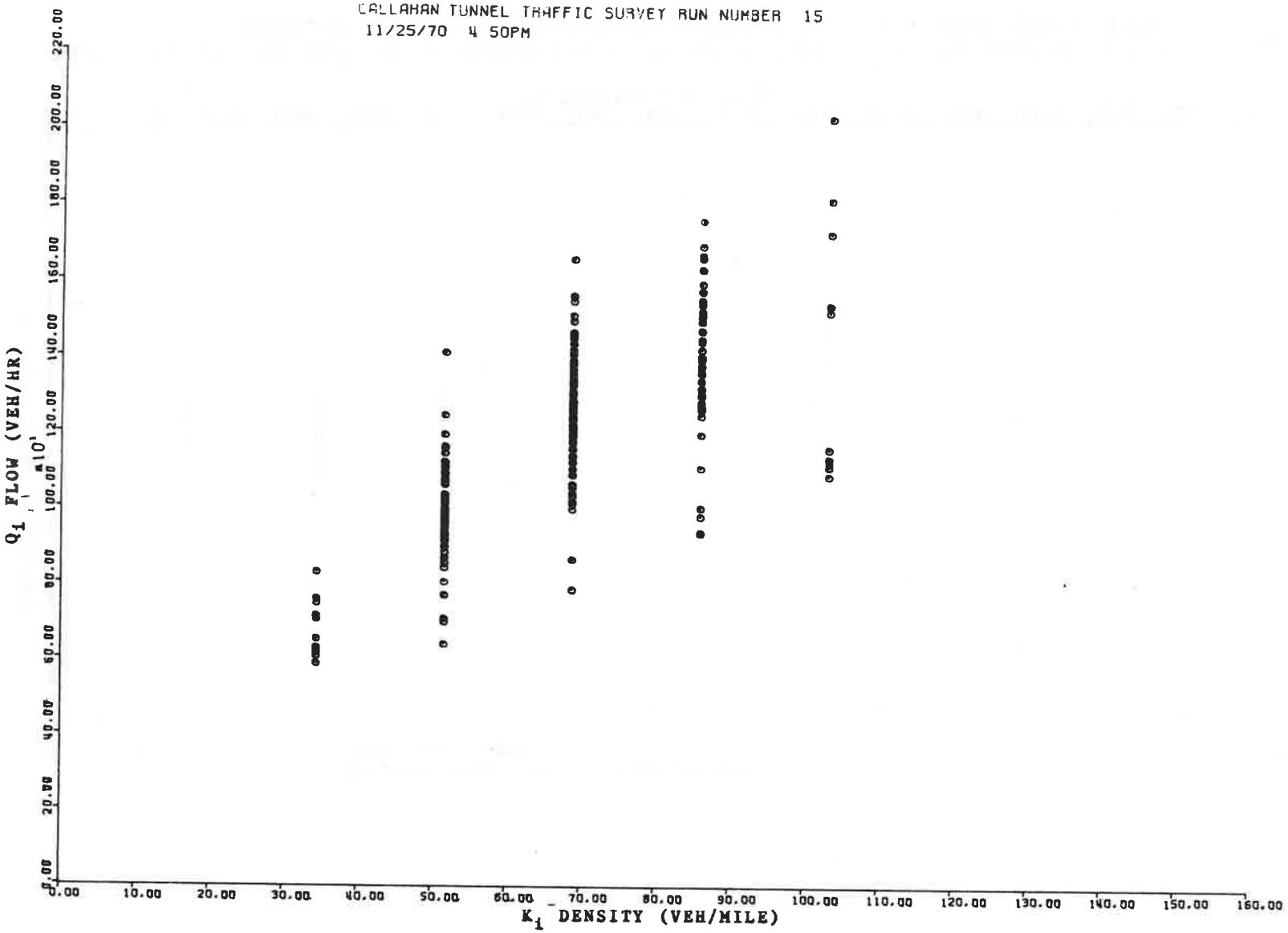


Figure 4.64a.- Run #15: Flow averaged over the transit time, $Q_i$, vs average section density, $K_i$. Station $3_a$ to $B_2$. Distance of 307.3 ft. Slow down data included.

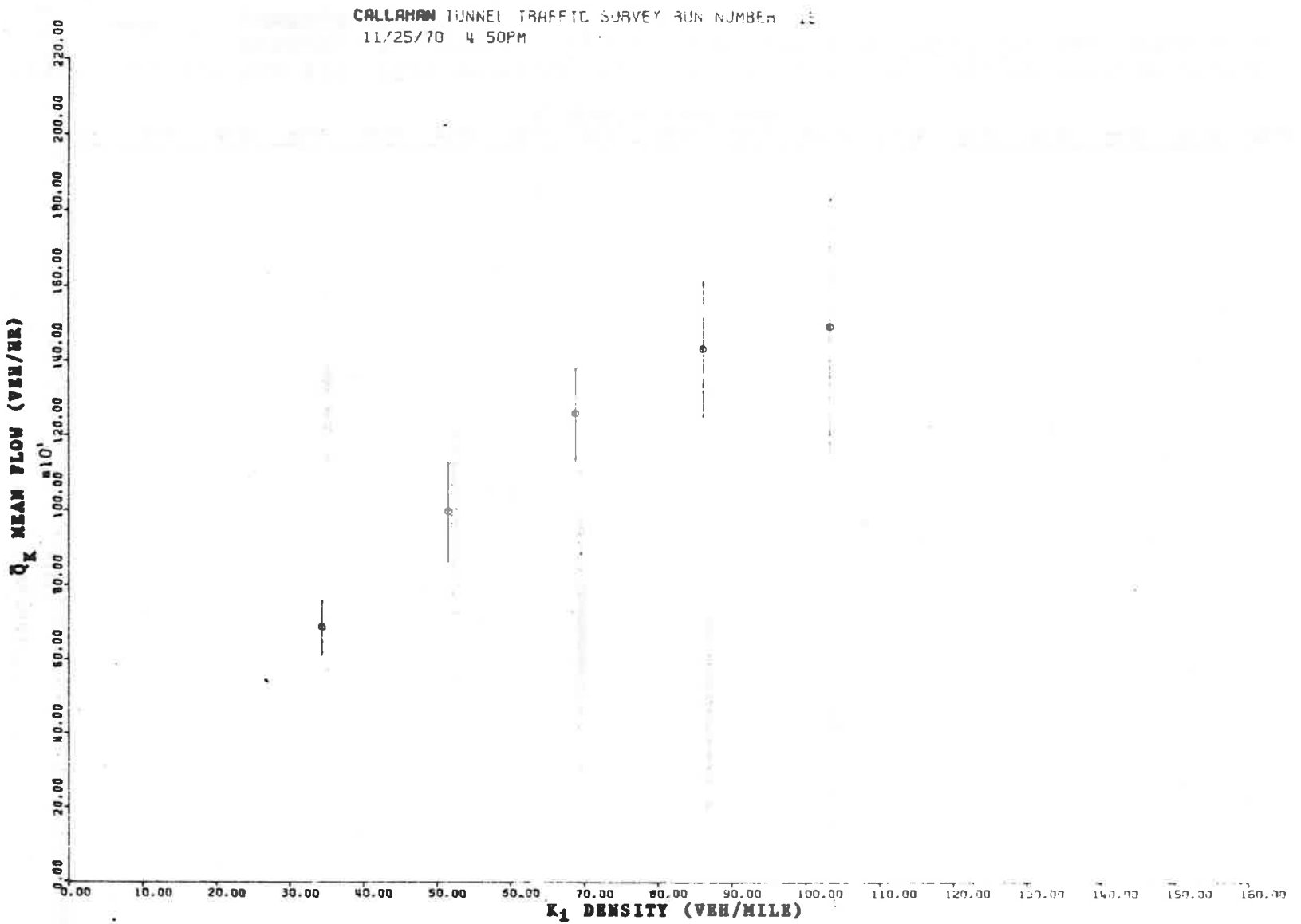


Figure 4.64b.- Run #15: Mean flow for a given section density, $\bar{Q}_K$, vs the density $K_i$, stations $3_a$ to $B_2$. Slow down data included.

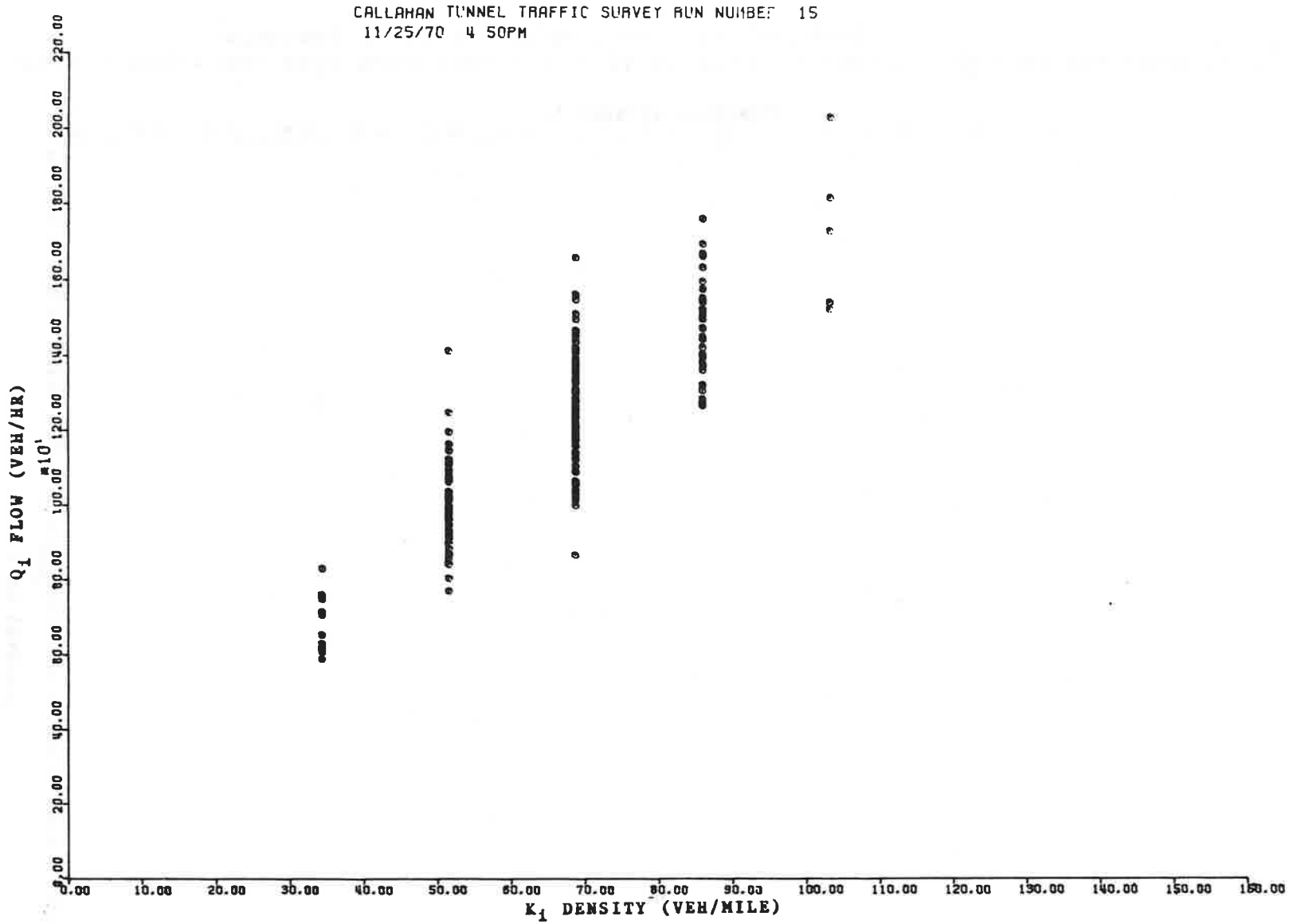


Figure 4.65a.- Run #15: Flow averaged over the transit time, $Q_i$, vs average section density, $K_i$, station $3_a$ to $B_2$. Distance of 307.3 ft. Slow down group removed.

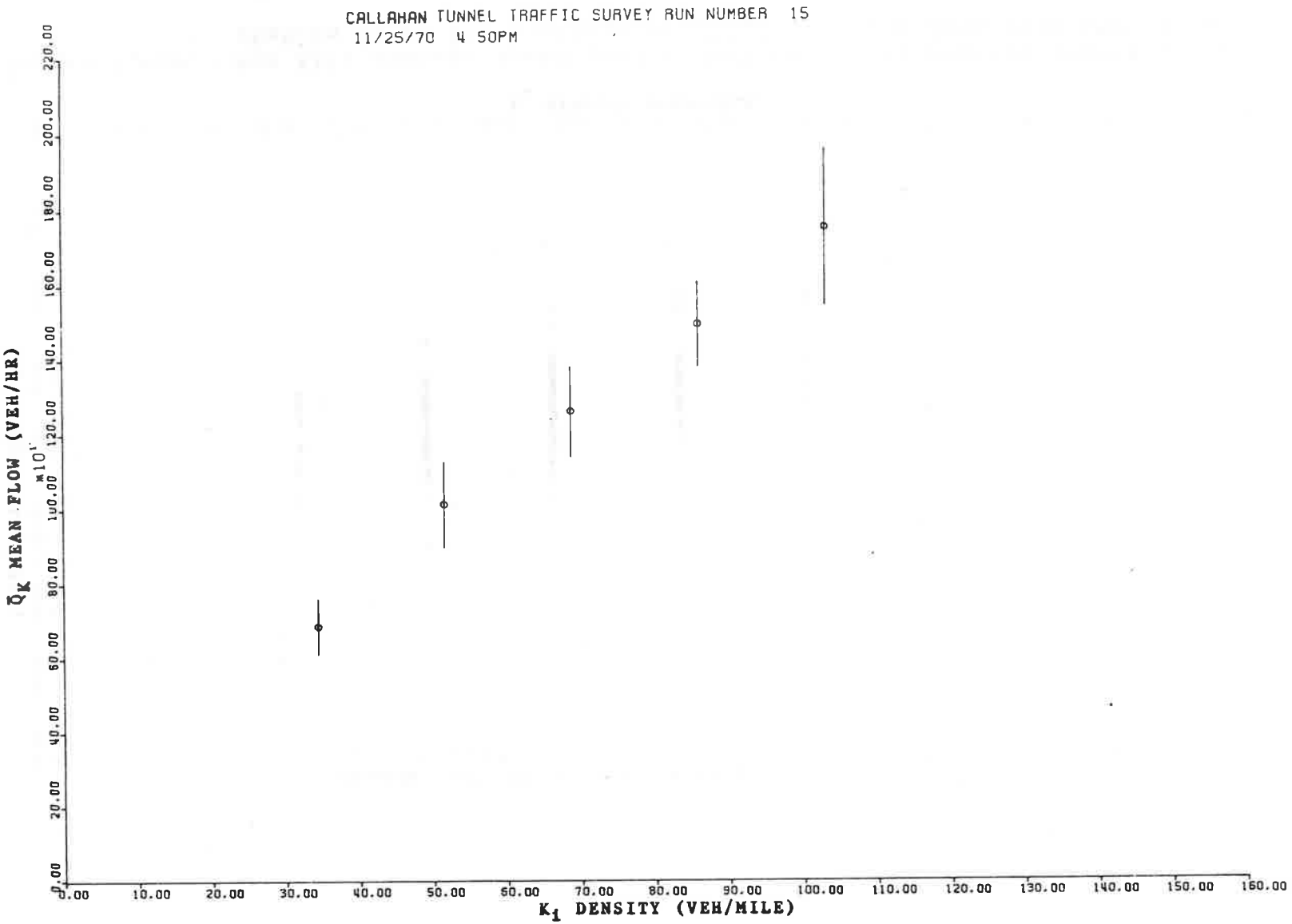


Figure 4.65b.- Run #15: Mean flow for a given section density, $\bar{Q}_K$, vs the density, $K_i$. Stations $3_a$ to $B_2$. Slow down group removed.

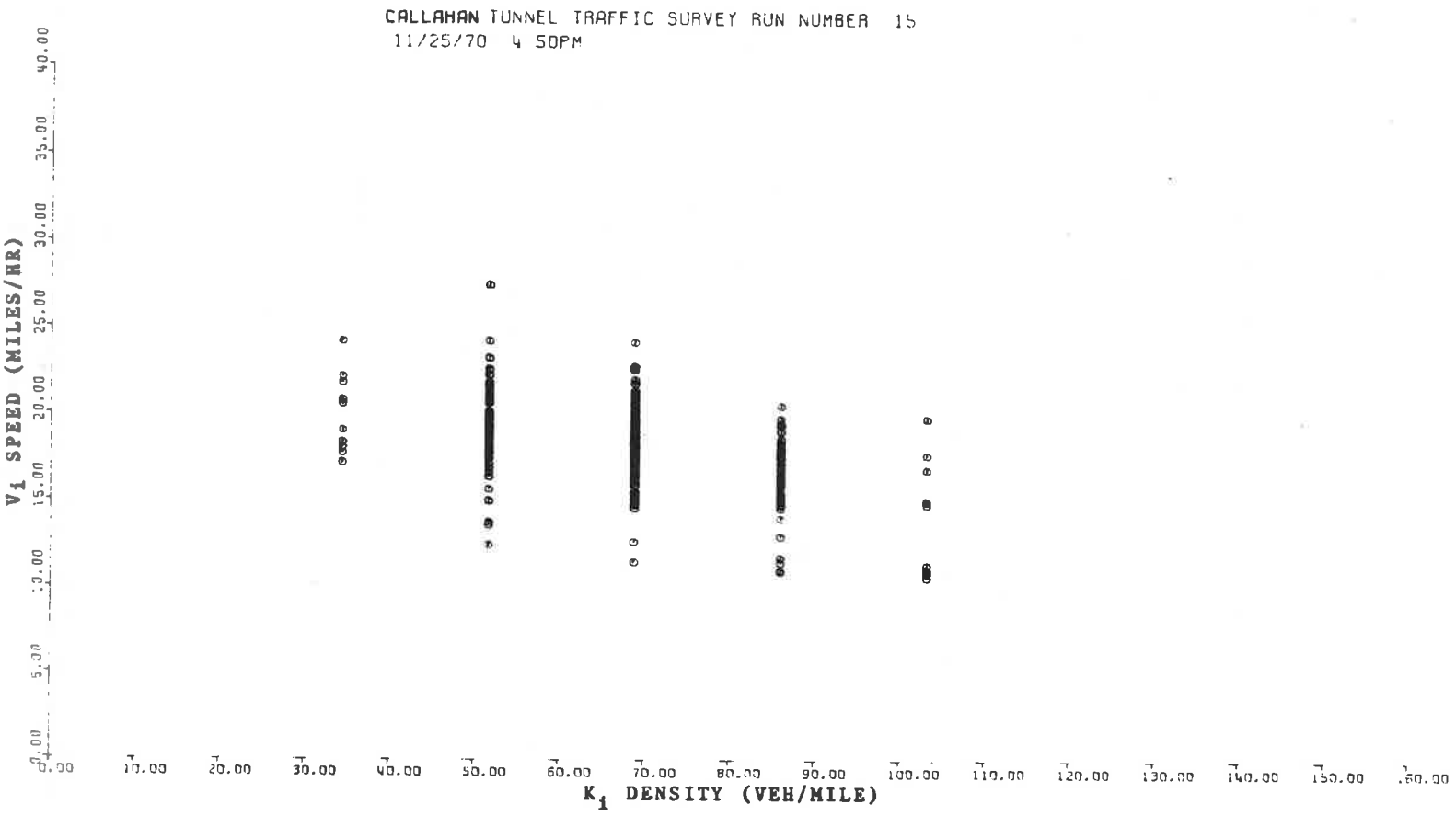


Figure 4.66a.- Run #15: Average speed over a section, $V_i$ vs section density, $K_i$, station $3_a$ to $B_2$. Distance of 307.3 ft. Slow down data included.

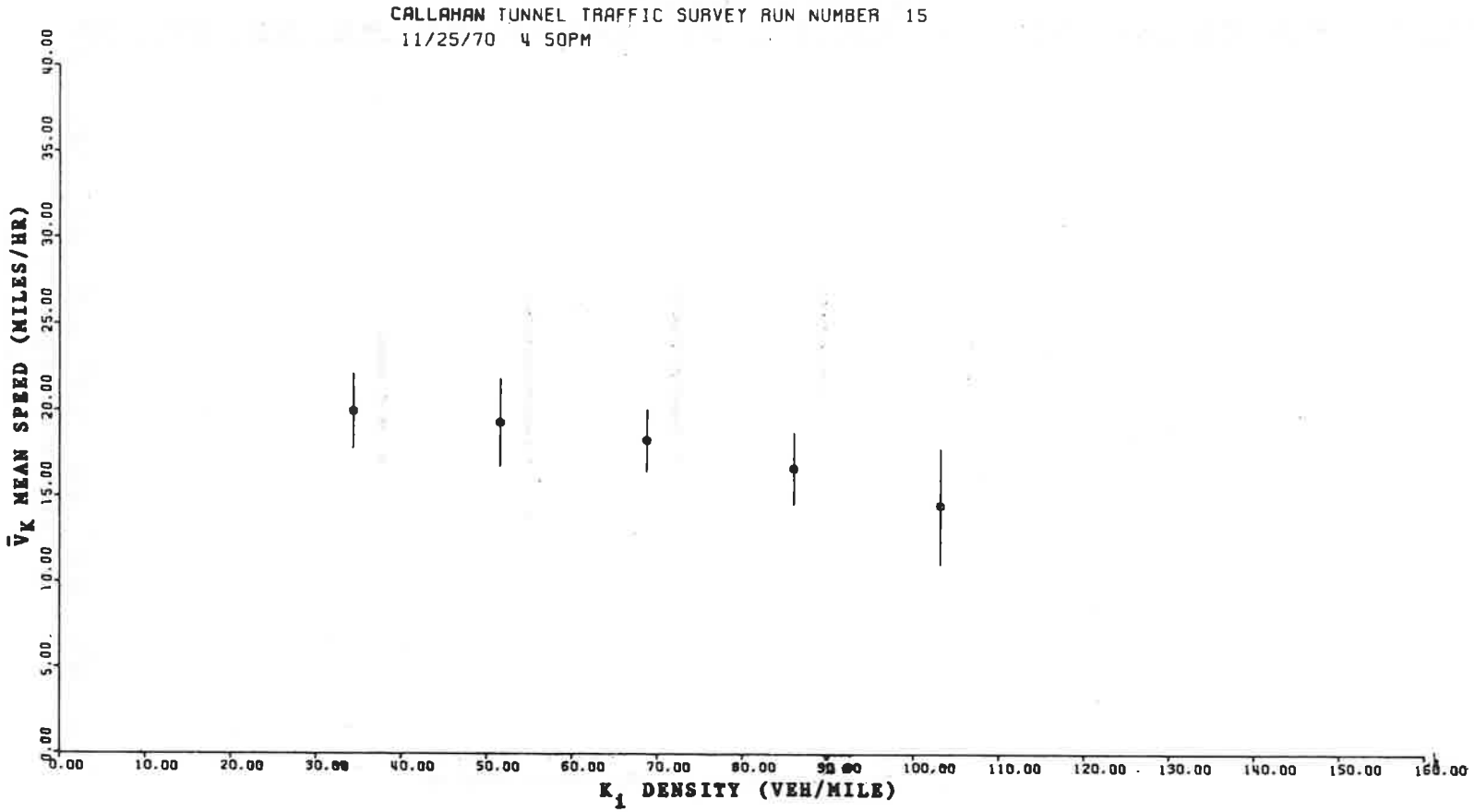


Figure 4.66b.- Run #15: Mean speed for a given density, $\bar{V}_K$, vs section density, $K_i$ station $3_a$ to $B_2$. Distance of 307.3 ft. Slow down data included.

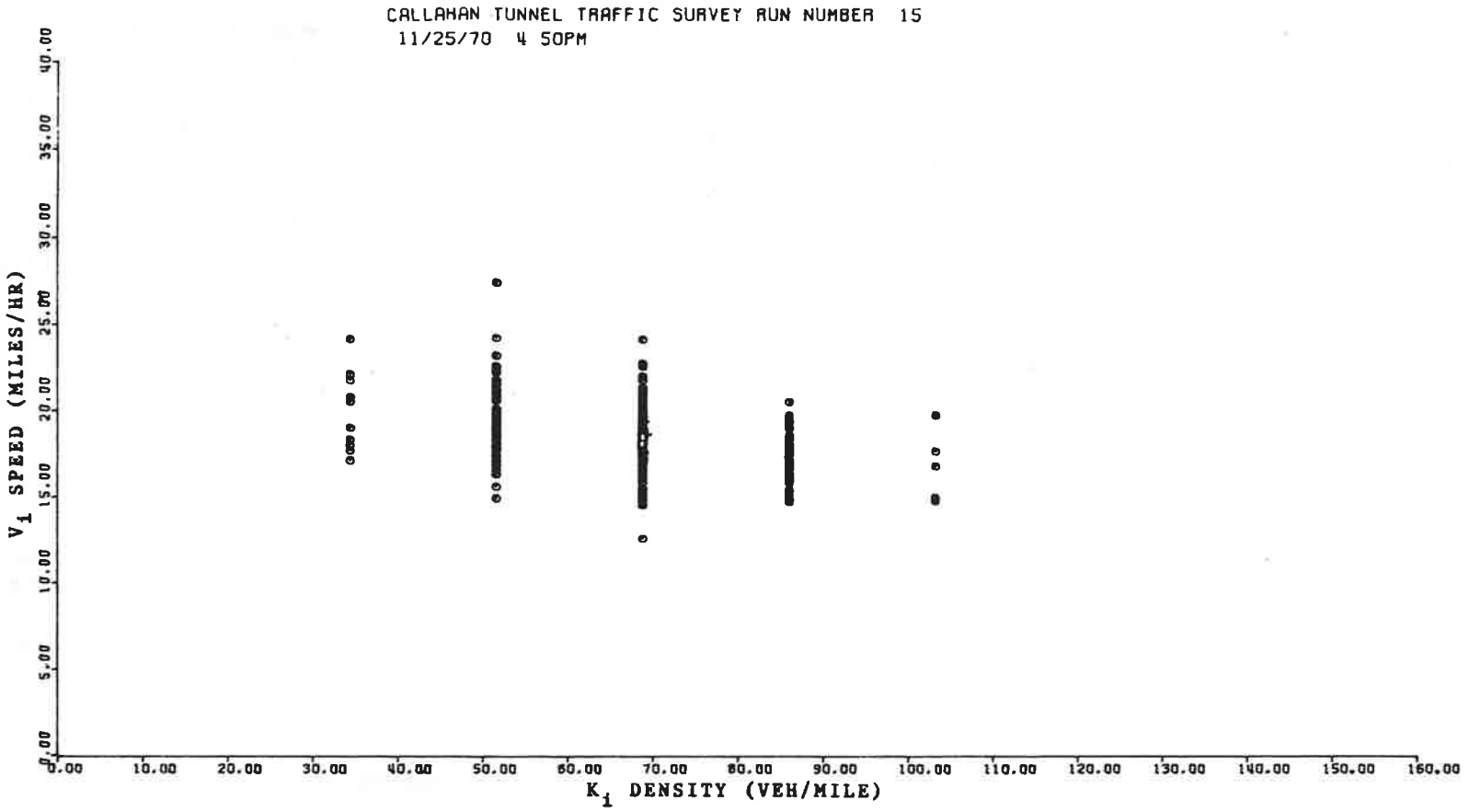


Figure 4.67a.- Run #15: Average speed over a section, $V_i$, vs section density, $K_i$, station $3_a$ to $B_2$, Distance of 307.3 ft. Slow down group removed.

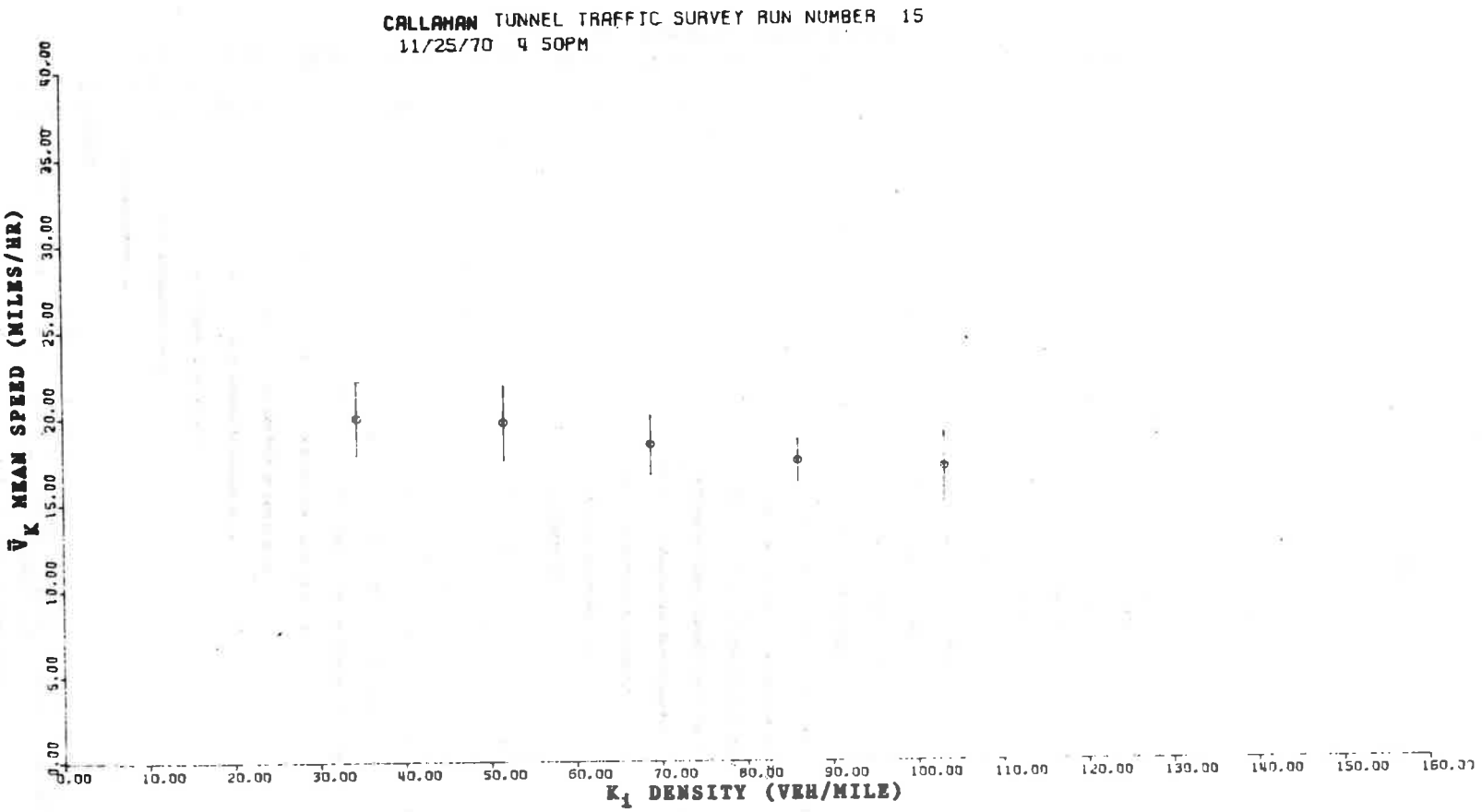


Figure 4.67b.- Run #15: Mean speed for a given density, $\bar{V}_K$, vs section density $K_i$, station $3_a$ to $B_2$. Distance of 307.3 ft. Slow down group removed.

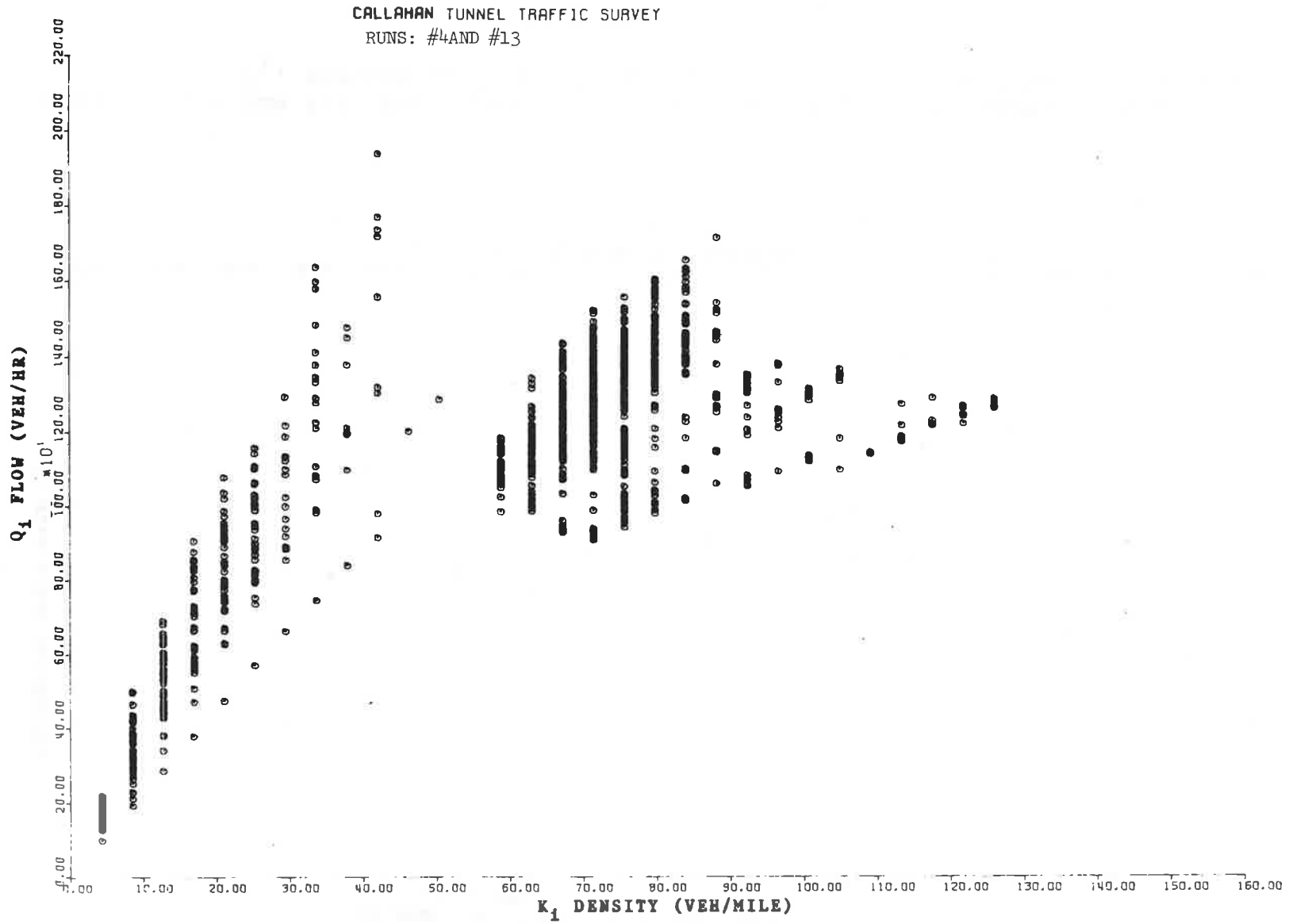


Figure 4.68a.- Runs #4 and #13 together: Flow averaged over the transit time, $Q_i$, vs average section density, $K_i$. Stations 2 to 3. Distance of 1260 ft. Slow down data included.

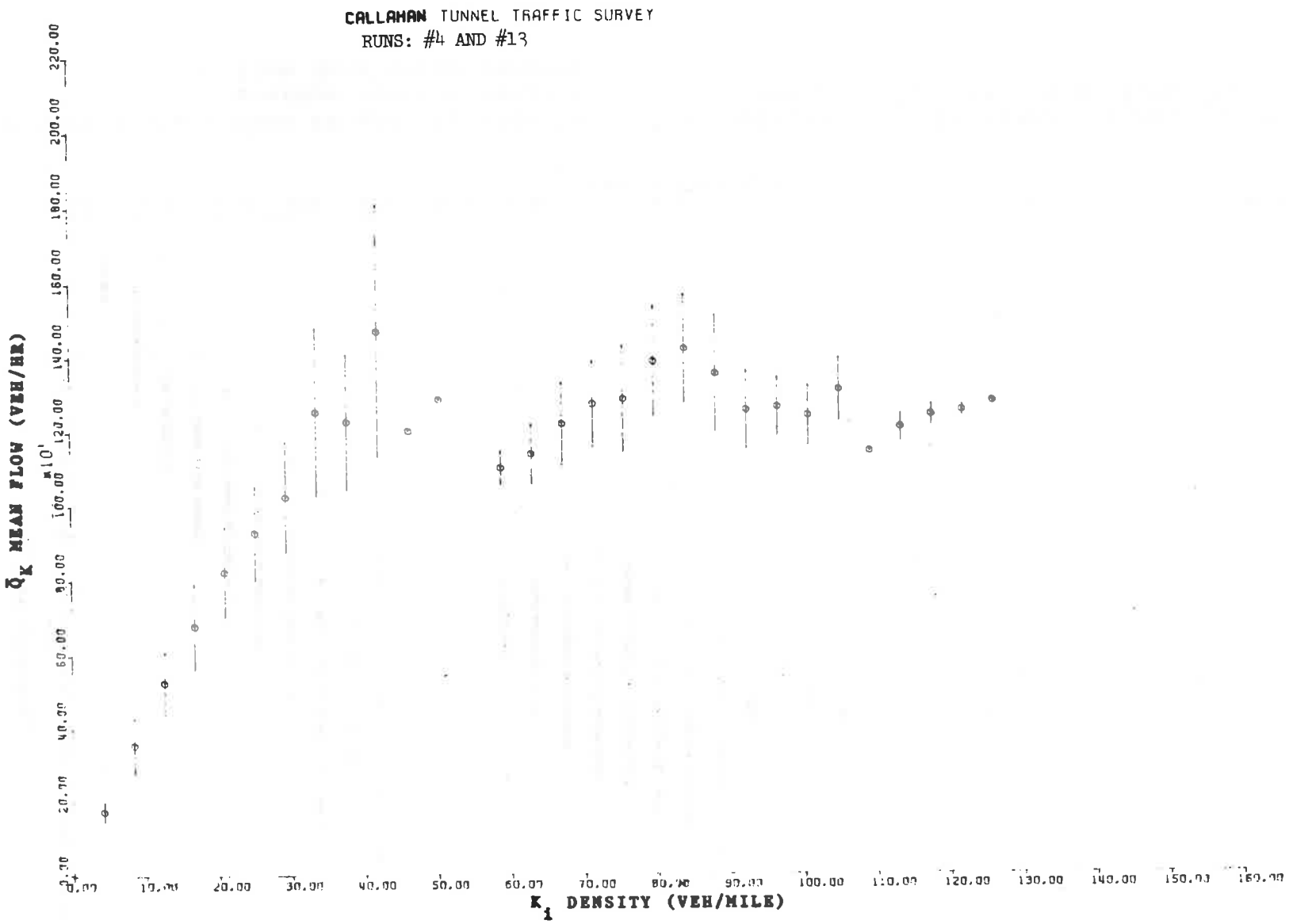


Figure 4.68b.- Runs #4 and #13 together: Mean flow for a given section density, $\bar{Q}_K$, vs the density $K_i$. stations 2 to 3. Distance of 1260 ft. Slow down data included.

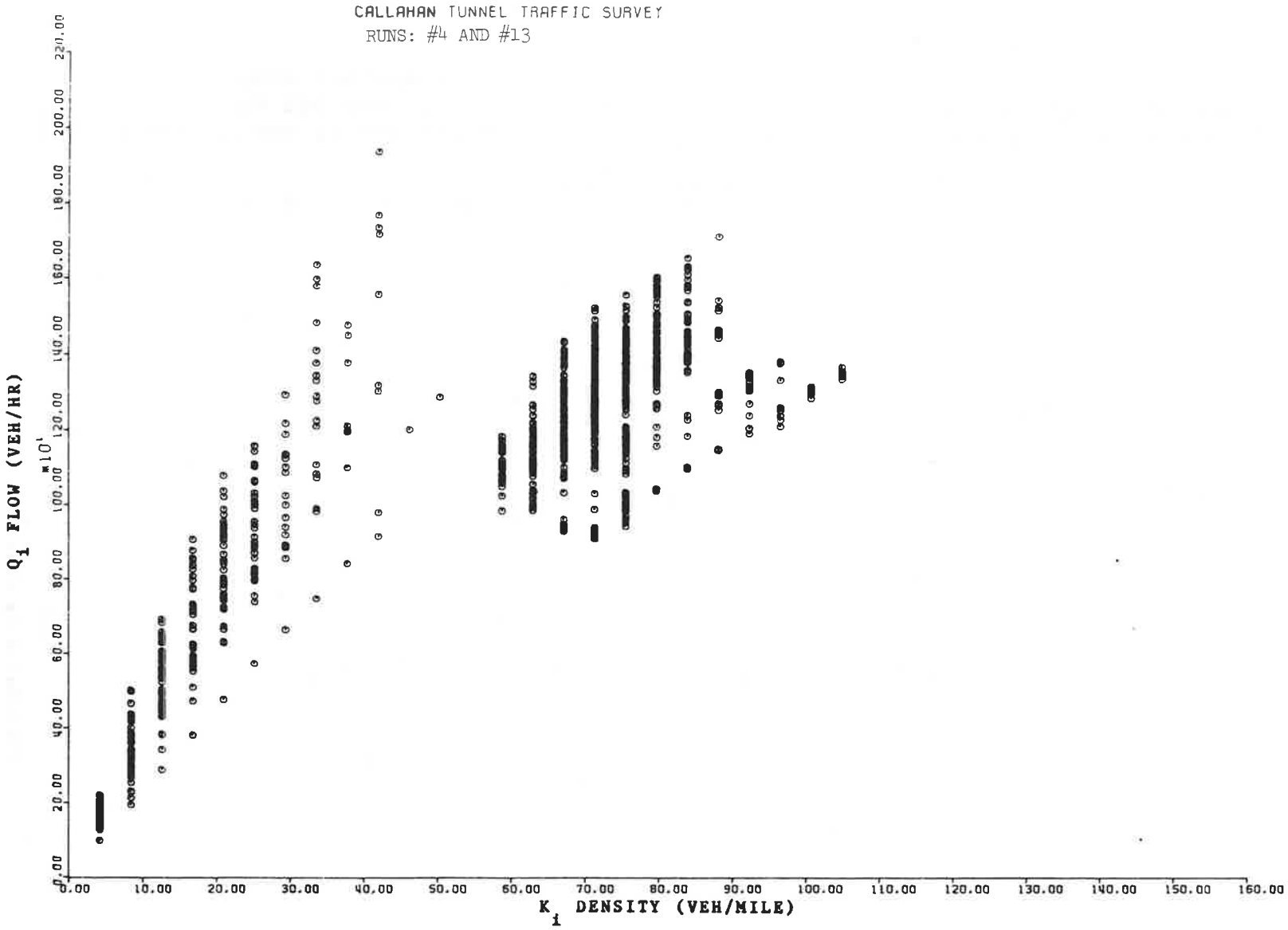


Figure 4.69a.- Runs #4 and #13 together: Flow averaged over the transit time, $Q_i$, vs average section density, $K_i$. Stations 2 to 3. Distance of 1260 ft. Slow down group removed.

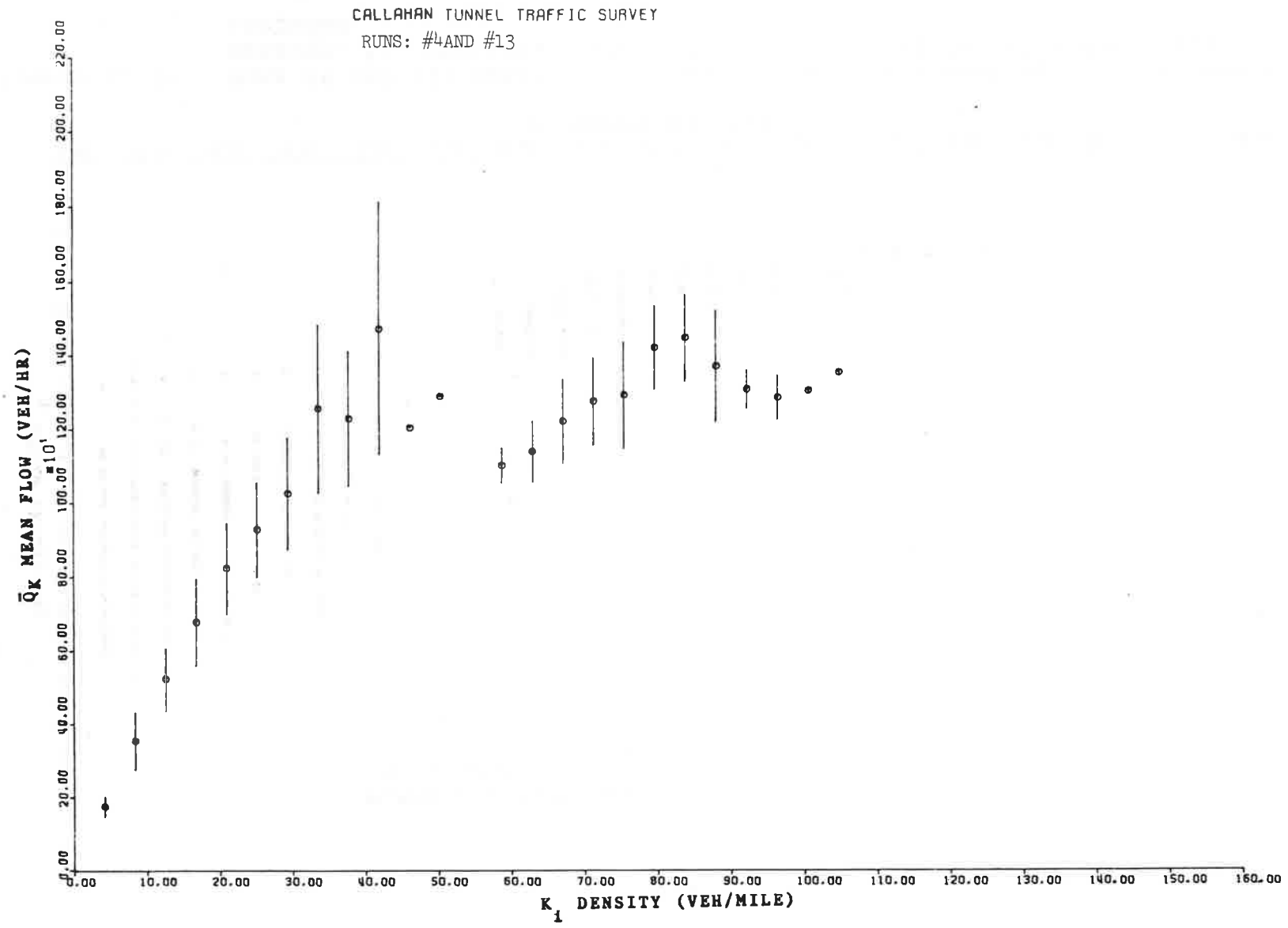


Figure 4.69b.- Runs #4 and #13 together: Mean flow for a given section density, $\bar{Q}_K$, vs the density, $K_i$. Stations 2 to 3. Distance of 1260 ft. Slow down group removed.

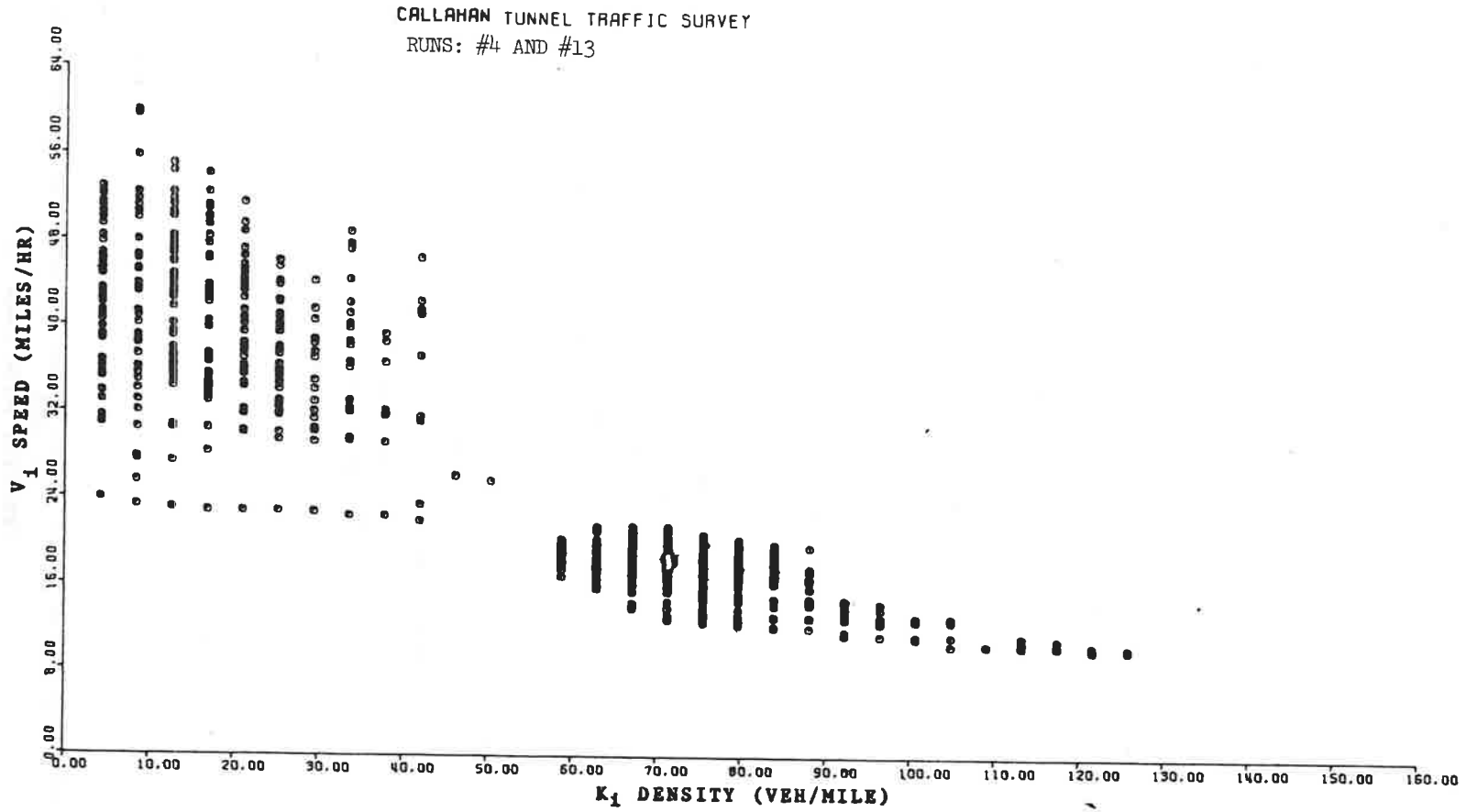


Figure 4.70a.- Runs #4 and #13 together: Average speed over a section, $V_i$, vs section density, $K_i$. Stations 2 to 3. Distance of 1260 ft. Slow down data included.

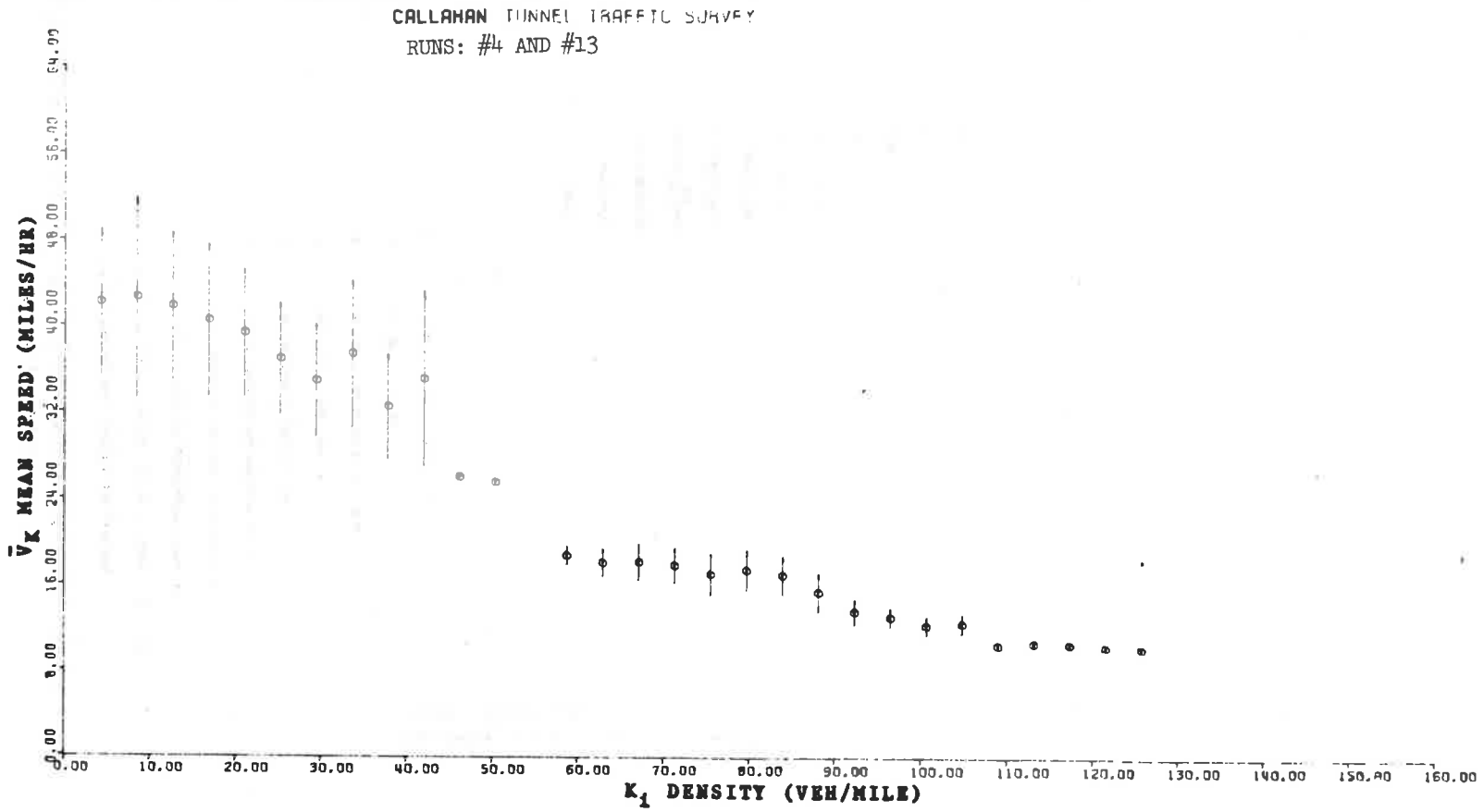


Figure 4.70b.- Runs #4 and #13 together: Mean speed for a given density, $\bar{V}_K$, vs section density, $K_i$. Stations 2 to 3. Distance of 1260 ft. Slow down data included.

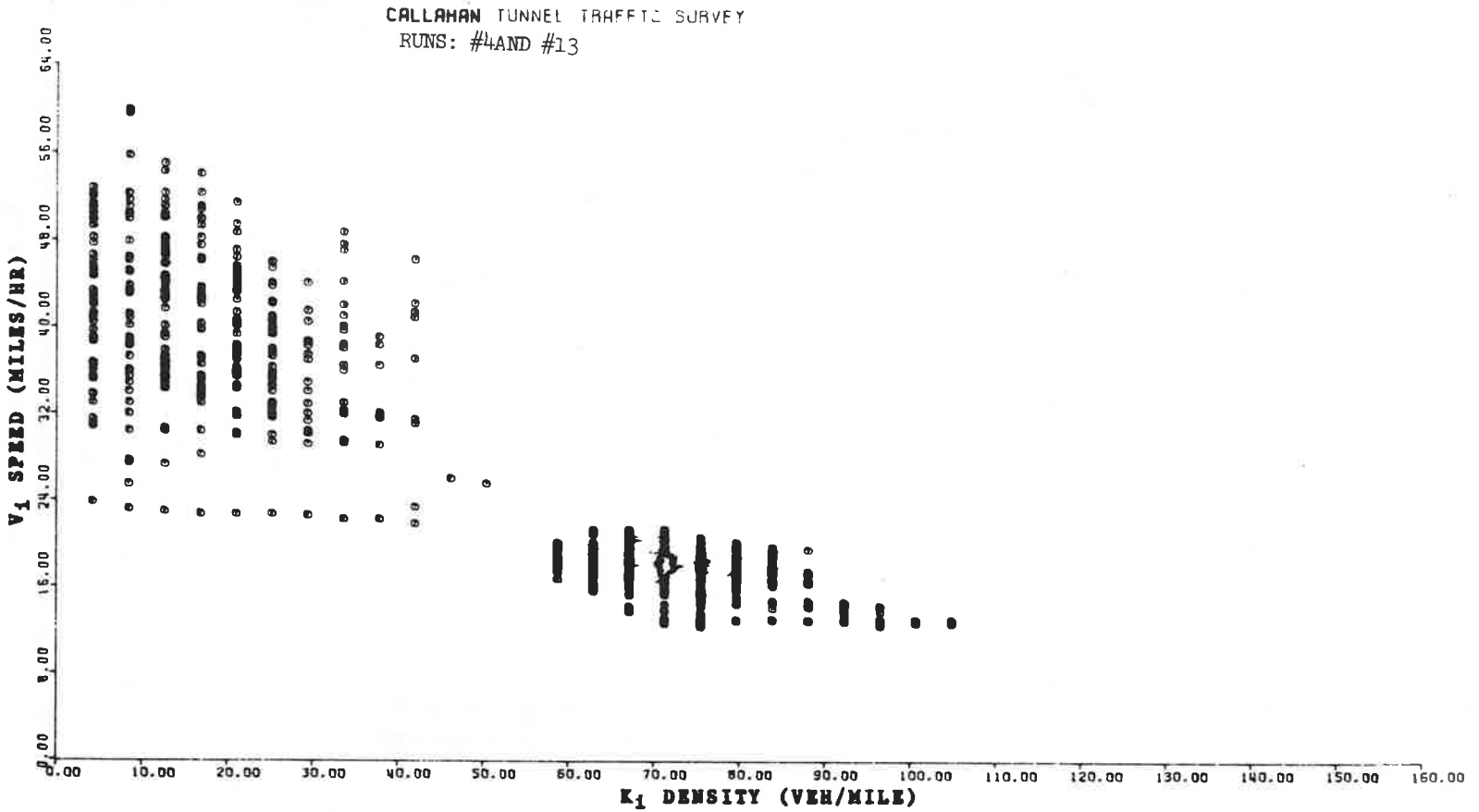


Figure 4.71a.- Runs #4 and #13 together: Average speed over a section $V_i$, vs section density, $K_i$. Stations 2 to 3. Distance of 1260 ft. Slow down group removed.

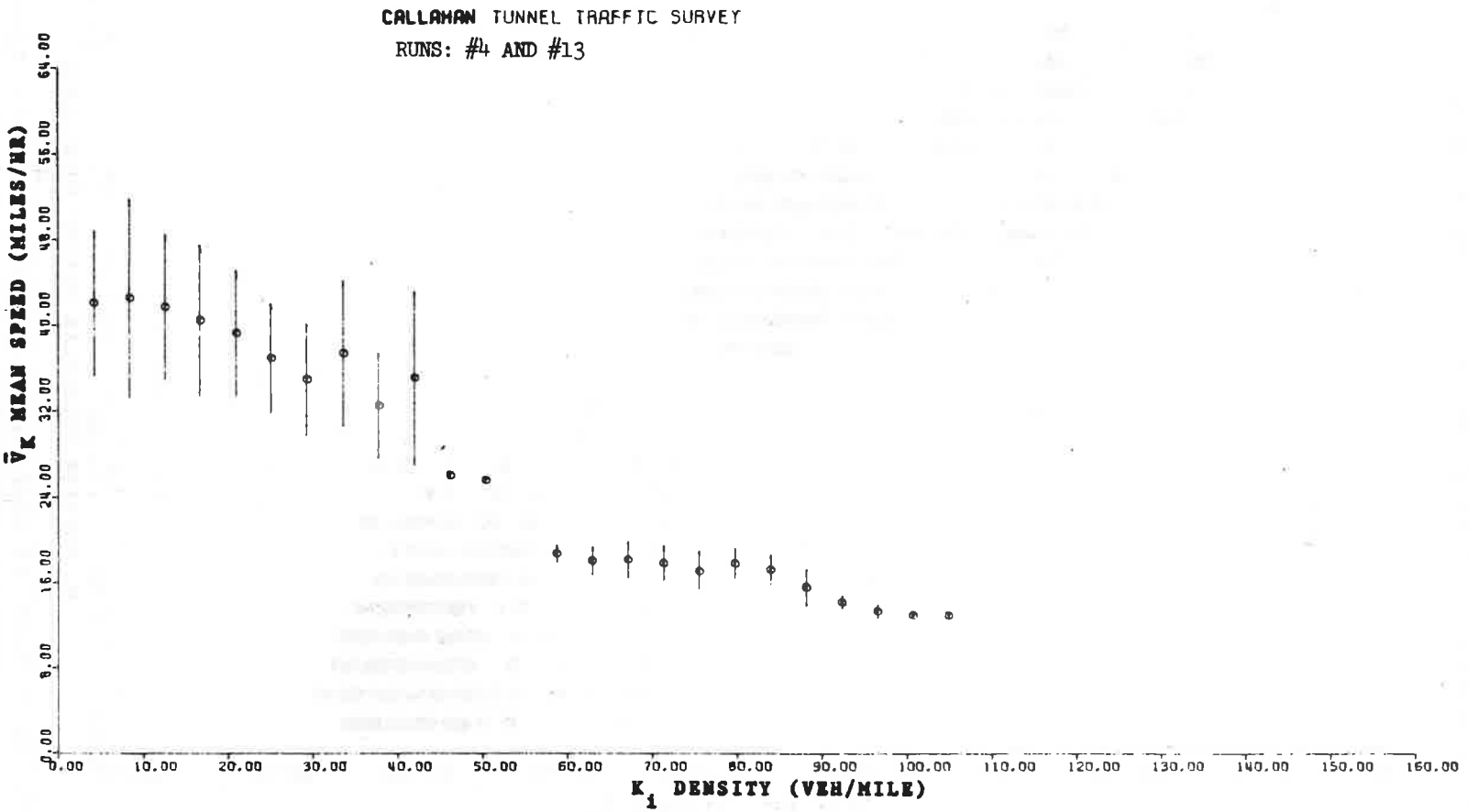


Figure 4.71b.- Runs #4 and #13 together: Mean speed for a given density $\bar{V}_K$, vs section density, $K_i$. Stations 2 to 3. Distance of 1260 ft. Slow down group removed.

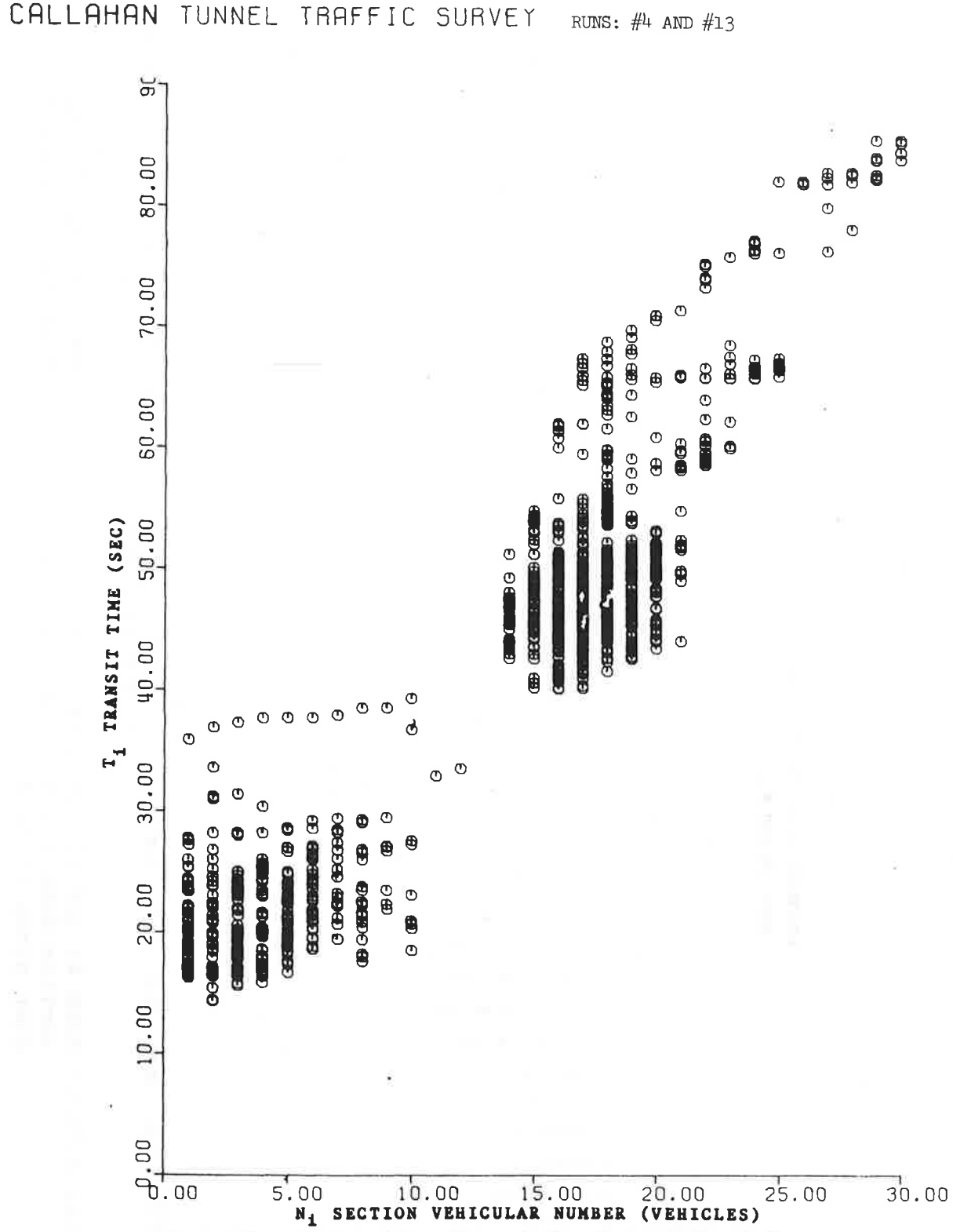


Figure 4.72a.- Runs #4 and #13 together: Transit time, $T_i$ vs section vehicular number, $N_i$. Stations 2 to 3. Distance of 1260 ft. Slow down data included.

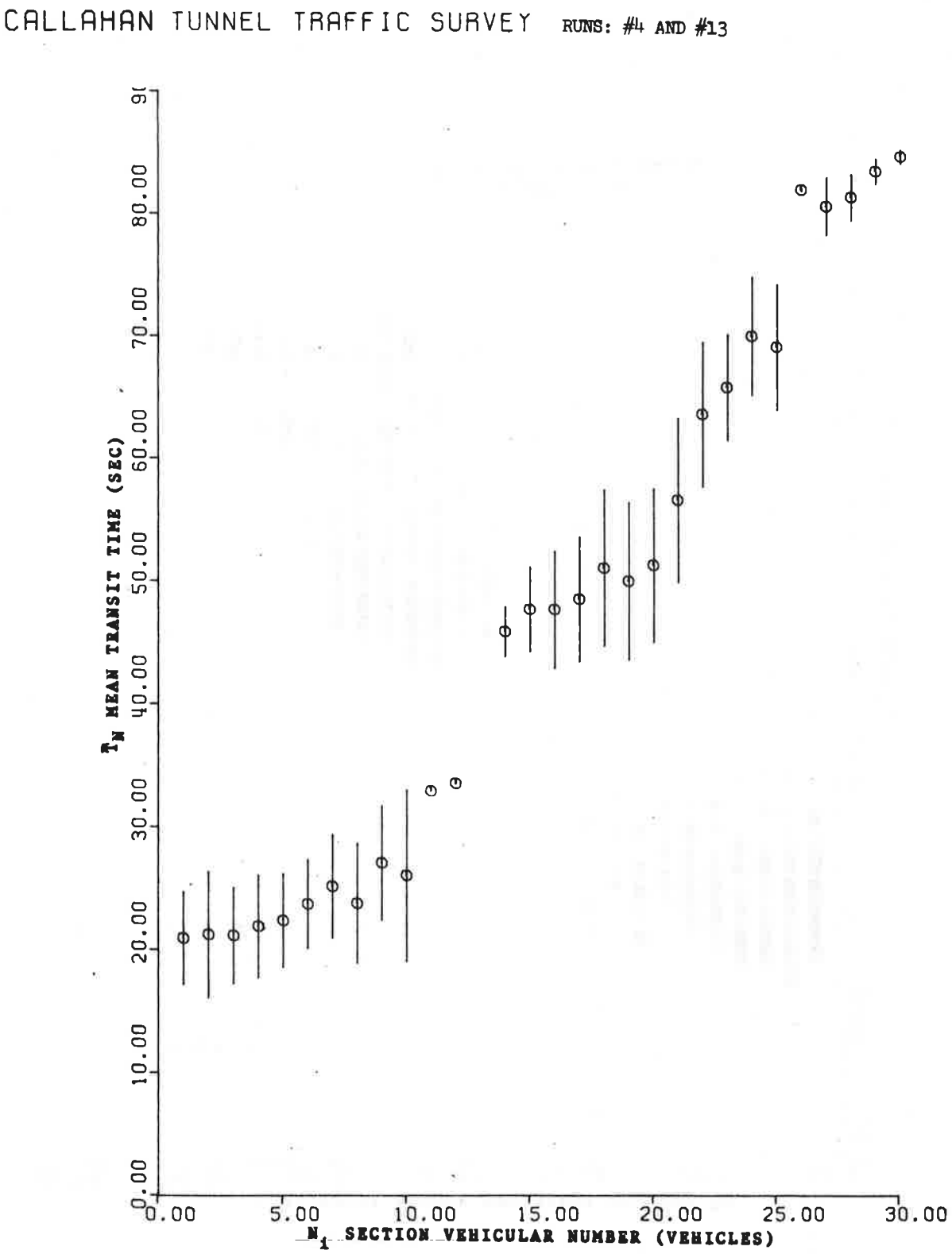


Figure 4.72b.- Runs #4 and #13 together: Mean of transit time, $\bar{T}_N$, (for a given section vehicular number) vs the section number $N_i$. Stations 2 to 3. Distance of 1260 ft. Slow down data included.

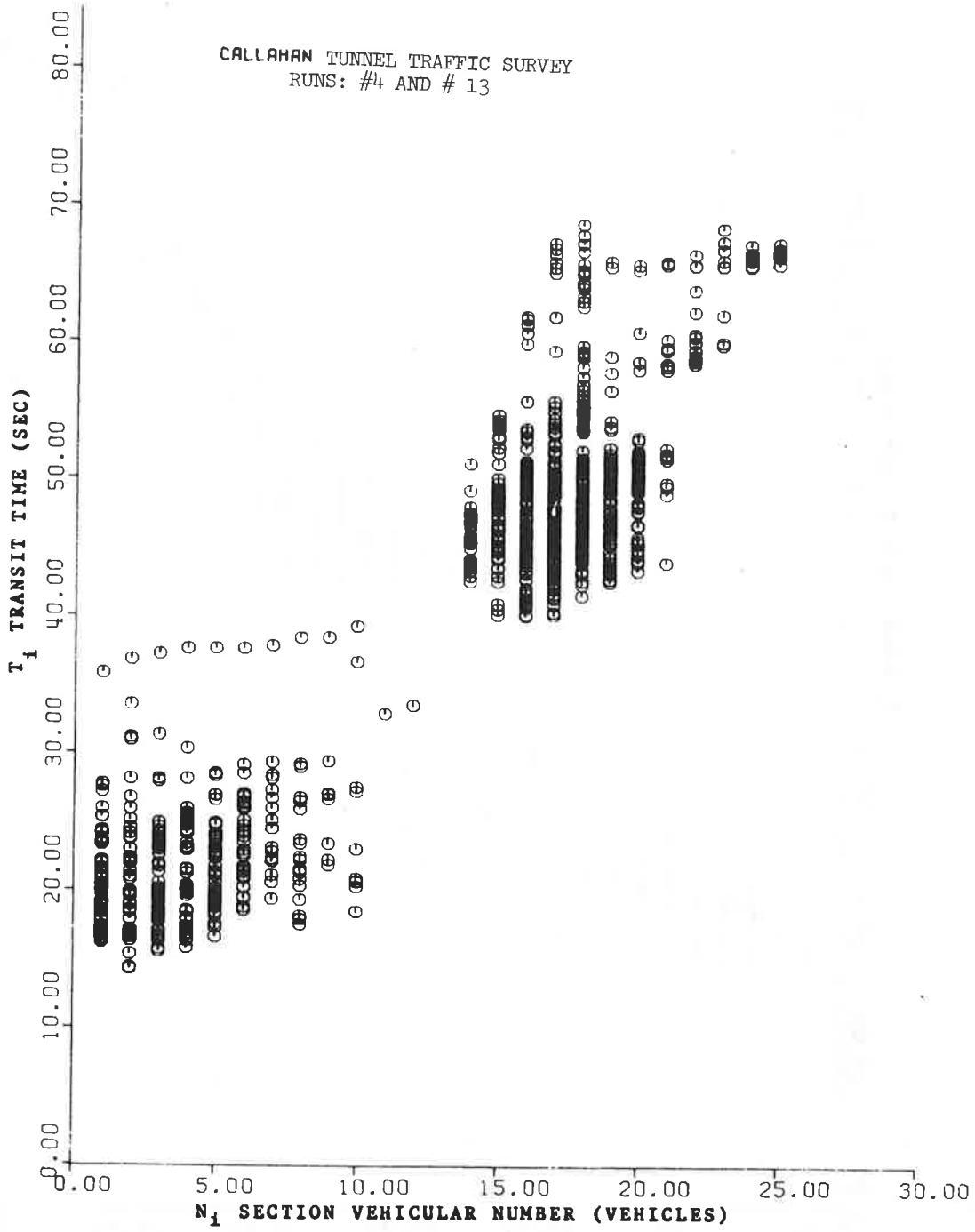


Figure 4.73a.- Runs #4 and #13 together: Transit time, $T_i$, vs section vehicular number, $N_i$. Stations 2 to 3. Distance of 1260 ft. Slow down group removed.

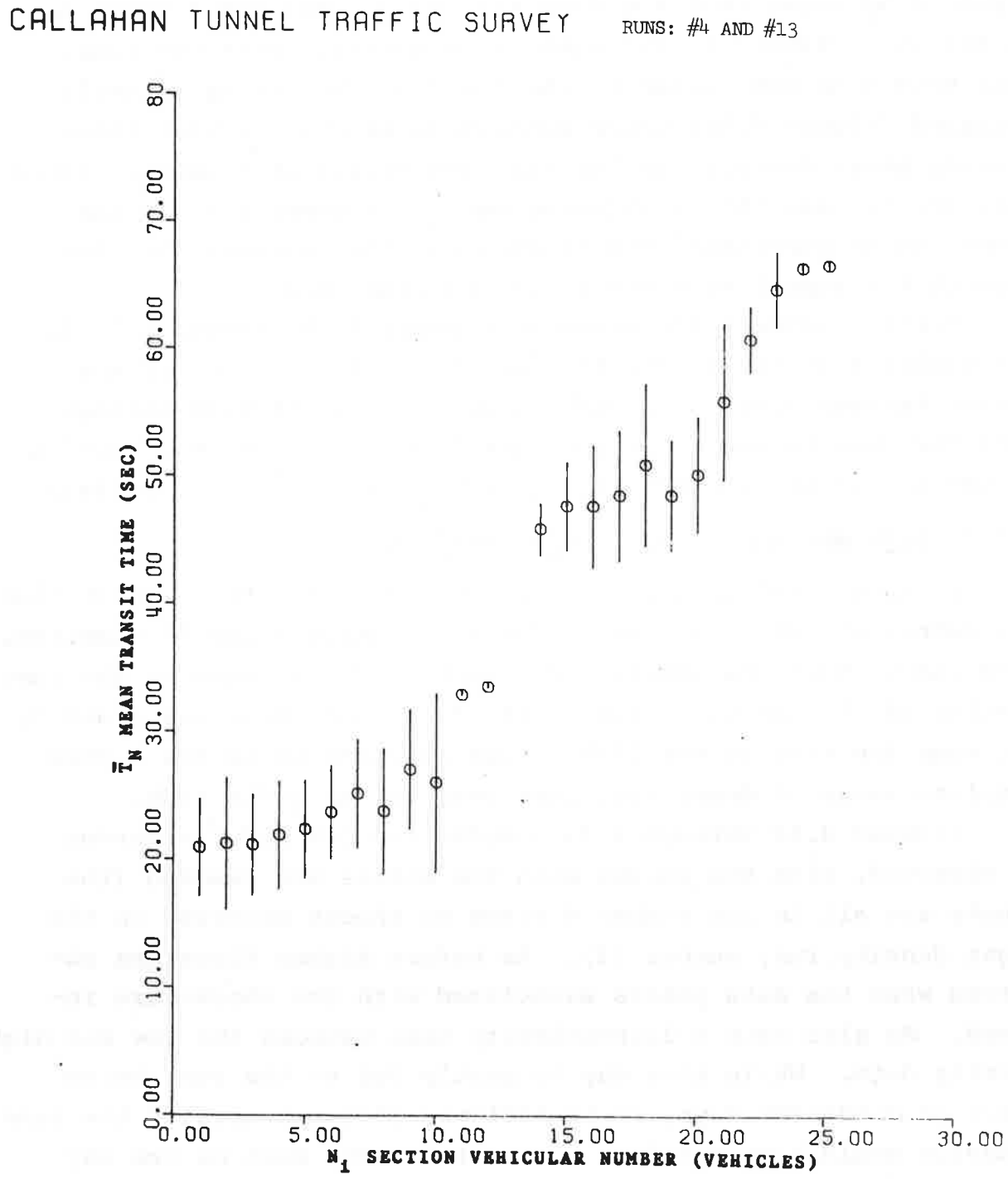


Figure 4.73b.- Runs #4 and #13 together: Mean of transit time, $\overline{T}_N$, (for a given section vehicular number) vs the section number, $N_i$. Stations 2 to 3. Distance of 1260 ft. Slow down group removed.

change in the type of traffic flow can be expected in this section. Figure 4.52 shows that the flow has not yet reached a maximum, rather it continues to increase, as congestion does not form. This should be contrasted to the traffic behavior as actually measured (Figure 4.50) where congestion is evident with flows already going downhill rather than continuing to increase. Since this section was the troublesome one it appears that if the waves can be prevented from growing in this section, the flow through the tunnel as a whole will be increased.

Similar effects are shown in Figures 4.56 through 4.59 for run number 4 in the second half of the middle section of the tunnel between stations 2 and 3 ; and in Figures 4.60 through 4.67 for runs 14 and 15 in the last 300 feet of the end section of the tunnel between station $3_a$ and $B_2$ (near the exit portal).

### 4.4.3 High and Low Density Runs Combined

In this final section we show Q-K, V-K and T-N (transit time vs. number of vehicles) curves for runs number 4 and 13 combined, with and without the shocks. Run number 13 was taken in the same section of the tunnel as run number 4, between stations 2 and 3, but when the traffic was light, thus allowing us to see a more complete range of densities, from very low to quite high.

Figures 4.68 through 4.71 compare the Q-K and V-K curves as observed, with the curves when the shocks are removed (the shocks are all in run number 4 since no shocks occurred in the light density run, number 13). As before higher flows are observed when the data points associated with the shocks are removed. We also note a discontinuity here between the low and high density data. While this may be partly due to the runs being taken on different days, it is believed that essentially the same behavior would have resulted had we taken the data on one day sufficiently long to allow the gathering of data on both the high and low density traffic. This observed break in the flow around "maximum flow" is believed to be real and due to the fact that

flow is not a single-valued function of the density as has been discussed before.

Finally Figures 4.72 and 4.73 show a plot of transit time versus number of vehicles in the section. The tangent to the curve extended from the origin gives a "section number,"(Ref. 20), corresponding to the "maximum flow", which is about 1445 vph without the shock and 1400 vph with the shock. In general longer transit times are apparent when shocks are present than when they are not. From these figures it is obvious that if we could have prevented the shock from propagating upstream into the oncoming traffic, we would have increased the traffic flow and would have reduced the time required for vehicles to drive through the tunnel, often substantially.

## SECTION 5
## HIGHLIGHTS OF STUDY

In the theoretical portion of this investigation a method was developed to include a driver's finite time of reaction into the equation of motion of a traffic stream. It was argued that the predictions of this theory such as wave amplitude growth were more in accord with observation than predictions of shock discontinuities of the classical, instantaneous, theories of collective traffic flow.

It was also argued that there is a necessity to include the functional dependence of traffic flow on the dynamic as well as on the static traffic situation. This was done by developing equations of motion of traffic in which the flow was a function not only of the density itself, but also of the time rate of change of the density. Experimental evidence confirms this dynamic dependence of the flow; it also confirms an assumed asymmetry of acceleration response due to a changing and dynamic traffic density.

In the experimental portion of this investigation a study was made of slowdown wave phenomena in the Holland and Callahan tunnels. The data for the two tunnels was gathered with quite different instrumentation; the data for the Callahan tunnel was obtained with inexpensive data taking equipment. It is felt that similar analysis on low budgets using the same or similar techniques and equipment may be made by non-highly trained personnel on different tunnel- or other single-lane roadways where an understanding of the traffic flow and associated slowdowns is necessary as a prelude to traffic flow modification.

Within the framework of using only simple data taking techniques and equipment, a number of different measures were used for determining the effects of the slowdown and the resultant deterioration of the traffic. These were such wave parameters as "shock width," and "shock time," and such vehicular flow parameters as the vehicular speed, transit time, density and different

flow averages. We feel that these *measures* together with the graphical display, afforded a good understanding of the traffic flow both under normal and under deteriorating conditions. Measures of predictability of the slowdown phenomena also emerged.

For the specific Callahan roadway, using these techniques, it was possible to establish which are the bottleneck sections in the tunnel, and what are the associated section densities, speeds, flows and capacities. The first quarter of the tunnel had the highest capacity, highest speeds and least congestion. The average peak hour speeds were 23 miles per hour and the average peak hour densities, 58 vehicles per mile. By contrast the second quarter had the lowest capacity, slowest speeds and greatest congestion. The average speeds here dropped to 12 miles per hour and the densities increased to 110 vehicles per mile. The complete profile was summarized in Section 4.2.7 and it confirmed the existence in the Callahan of a severe bottleneck beyond the downgrade section. However, the installation of a system to modify the traffic flow in the tunnel by preventing the widely disparate speeds and densities measured in the different tunnel sections from occurring, will help prevent the formation of bottlenecks and hence will reduce the number and severity of shocks due to the bottlenecks. Such a system will increase the tunnel's throughput and decrease the congestion around the entrances to the tunnel as more vehicles are serviced in shorter time; it should also decrease the amount of vehicle breakdowns and vehicle pollutants in the tunnel because of fewer necessary acceleration and deceleration maneuvers.

It is hoped that the theoretical and experimental programs presented here lead to a clearer understanding of traffic flow and its control for the benefit of both the driver and the environment.

## REFERENCES


1. Lighthill, M. J. and Whitham, G. B.: On Kinematic Waves II, A Theory of Traffic Flow on Long Crowded Roads. Proceedings of the Royal Society, London, Series A, Vol. 229, No. 1178, 1955.

2. Richards, P. I.: Shock Waves on the Highway. Operations Research, Vol. 4, No. 1, Feb. 1956.

3. Newell, G. F.: Theories of Instability in Dense Highway Traffic. Journal of the Operations Research Society of Japan, No. 5, 1962.

4. Pipes, L. A. Topics in the Hydrodynamic Theory of Traffic Flow. Transportation Research, Vol. 2, 1968.

5. Prigogine, I. and Andrews, F. C.: A Boltzmann-like Approach for Traffic Flow. Operations Research, Vol. 8, 1960.

6. Prigogine, I., Herman, R., and Anderson, R.: Further Developments in the Boltzmann-like Theory of Traffic Flow. Proceedings of the Second International Symposium on the Theory of Traffic Flow, London, June 1963.

7. Prigogine, I., Herman, R., and Anderson, R.: Local Steady State Theory and Macroscopic Hydrodynamics of Traffic Flow. Proceedings of the Third International Symposium on the Theory of Traffic Flow, New York, 1965.

8. Balescu, R., Progogine I., Herman, R., and Anderson, R.: Statistical Hydrodynamics of Traffic Flow. Proceedings of the Third International Symposium on the Theory of Traffic Flow, New York, 1965.

9. Prigogine, I.: A Boltzmann-like Approach to the Statistical Theory of Traffic Flow. Proceedings of the First International Symposium on the Theory of Traffic Flow, Michigan, Dec. 1959.

10. Anderson, R.L., Herman, R., and Prigogine, I.: On the Statistical Distribution Function Theory of Traffic Flow. Operations Research, Vol. 10, 1962.

11. Herman, R. and Rothery, R. W.: Car Following and Steady State Flow. Proceedings of the Second International Symposium on the Theory of Traffic Flow, London, June 1963.

12. Gazis, D. C., Herman, R., and Rothery, R. S.: Nonlinear Follow-The-Leader Models of Traffic Flow. Operations Research, Vol. 9, No. 4. July-Aug. 1961.

13. Newell, G. F.: Non Linear Effects in the Dynamics of Car Following. Operations Research, Vol. 9, No. 2, 1961.

14. Gazis, D. C., Herman, R., and Potts, R. B.: Car-Following Theory of Steady-State Traffic Flow. Operations Research, Vol. 7, No. 4, July-Aug. 1959.

15. Pipes, L. A.: Car-Following Models and the Fundamental Diagram of Road Traffic. Transportation Research, Vol. 1, 1967.

16. Gazis, D. C., Herman, R., and Rothery, R. W.: Analytical Methods in Transportation: Mathematical Car-Following Theory of Traffic Flow. Journal of the Engineering Mechanics Division, EM 6, Dec. 1963.

17. Herman, R., and Gardels, K.:Vehicular Traffic Flow, Scientific American, Dec. 1963.

18. Foote, R. S.: Urban Systems Requirements for Physical Measurements, Instrument Society of America, Preprint Number 16. 1-1-66, Oct. 1966.

19. Drew, D. R.: Traffic Flow Theory and Control, McGraw-Hill Book Company, New York, 1968. Ch. 16.

20. Edie, L. C., and Foote, R. S.: Experiments on Single-Lane Flow in Tunnels. Proceedings of the First International Symposium on the Theory of Traffic Flow, Michigan, 1959.

21. Herman, R.: Theoretical Research and Experimental Studies in Vehicular Traffic. Proceedings of the Australian Road Research Board, Vol. 7, Part 1, 1966.

22. Carter, Jr., A. A., Hess, J. W., Hodgkins, E. A., and Raus, J.: Highway Traffic Surveillance and Control Research, Proc. of the IEEE, April 1968.

23. Gazis, D. C., and Edie, L. C.: Traffic Flow Theory, The Status of Transportation, Proc. of the IEEE, April 1968.

24. Newell, G. F.: Instability in Dense Highway Traffic, A Review. Proceedings of the Second International Symposium on the Theory of Traffic Flow, London, June 1963.

25. Courant and Hilbert: Methods of Mathematical Physics, Vol. 2, Interscience Publishers, New York, 1966, pp. 147-153.

26. Foote, R. S., and Crowley, K. W.: Density-Speed-Flow Dynamics in Single-Lane Traffic Flow. Proceedings of the Third International Symposium on the Theory of Traffic Flow, New York, 1965.

27. Foote, R. S., and Crowley, K. W.: Developing Density Controls for Improved Traffic Operations. Highway Research Board, Record 154, 1967.

28. Edie, L. C., Foote, R. S., Herman, R., and Rothery, R.: Analysis of Single Land Traffic Flow, Traffic Engineering, Jan. 1963.

29. Edie, L. C., and Bavarez, E.: Generation and Propagation of Stop-Start Traffic Waves. Proceedings of the Third International Symposium on the Theory of Traffic Flow, New York, June 1965.

30. Gafarian, A. V., Lawrence, R. L., Munjal, P. K., and Pahl, J.: An Experimental Validation of Various Methods for Obtaining Relationships Between Traffic Flow, Concentration and Speed on Multi-Lane Highways, Final Report: Analytical Models of Unidirectional Multi-Lane Traffic Flow, Vol. II System Development Corporation, Santa Monica, Calif. 15 Feb. 1970. TM-3858/022/00.

31. Greenberg, I.: An Analysis of Traffic Over a Length of Roadway, The New York Port Authority, Tunnel and Bridges Research Section, 111 Eighth Avenue, New York 11, New York, April 1962.

## ADDITIONAL REFERENCES FOR TUNNEL STUDY

32. Greenberg, I.: A Relationship Between Travel Time and Traffic Density, Tunnels and Bridges Research Division Report (TBR), April 1962.

33. Crowley, K. W.: Classification of Vehicles by Length, TBR 2-63, April 1963.

34. Foote, R. S.: Single Land Traffic Flow Control, TBR 5-63, May 1963.

35. Daou, A.: On Flow Within Platoons, TBR 6-64, May 1964.

36. Duckstein, L.: Control of Traffic in Tunnels to Maximize Flow, TBR 5-65, Sept. 1965.

37. White, C. F.: A Tunnel Traffic Control and Surveillance System, Ibid, Oct. 1966.

38. Foote, R. S.: Instruments for Road Transportation, TBR 2-68, March 1968.

39. Bennett, B. T., Gazis, D. C., Edie, L. C., and Foote R. S.: Control of the Lincoln Tunnel Traffic by an on-line Digital Computer, IBM Research RC 2218, Sept. 1968.

40. Gazis, D. C., and Foote, R. S.: Surveillance and Control of Tunnel Traffic by an on-line Digital Computer, Ibid RC 2358, Jan. 1969.

41. Foote, R. S.: Surveillance and Measurements for Urban Arterials, TBR 5-69, May 1969.

42. Gazis, D. C., and Foote, R. S.: Calibration and Correction of Magnetic Loop Detectors, IBM Research RC 2520, June 1969.

43. Foote, R. S.: Bridging the Gap Between Theory and Practice, TBR 6-69, Sept. 1969.

44. Cunningham, R. F., and White, C. F.: Vehicular Tunnel Traffic Flow Control, TBR 7-69, Oct. 1969.

45. Kahn, D.: Traffic Flow Systems a Review and Program for the Transportation Systems Center. June 1, 1970.